Regulation of APOBEC3 activity and HIV-1 replication by P-body associated proteins

Phalora, Prabhjeet

Awarding institution:
King's College London

Regulation of APOBEC3 activity and HIV-1 replication by P-body associated proteins

Submitted by

Prabhjeet Kaur Phalora

To King's College London for the degree of

Doctor of Philosophy

Department of Infectious Diseases, King's College London
School of Medicine, London, SE1 9RT

September 2011

The work presented in this thesis is my own

Prabhjeet Phalora

ABSTRACT

The APOPEC3 family of cytidine deaminases play an important role in host mediated antiviral defence against retroelements, including HIV-1. Although much has been discerned regarding the anti-viral nature of these proteins, their cellular function, as well as mechanisms of functional regulation and cellular co-factors, remains poorly defined. To address this, several cellular proteins that interact with APOBEC3G (A3G) have now been identified. The most intriguing of these are the Argonaute proteins, as the interaction is at least partially resistant to RNase treatment. The Argonautes are integral components of RISC, which is involved in miRNA mediated translational repression and mRNA decay. Components of this pathway, as well as A3G and silenced mRNAs have been shown to localise to discrete cytoplasmic foci termed mRNA Processing (P) Bodies. These foci have very recently been implicated in influencing viral life cycles. However, the functional relevance of the interaction with the Argonaute proteins and localisation to P-bodies, to APOBEC3 anti-viral and cellular activity is currently unknown and therefore was investigated in more detail.

It has been found that the ability of the APOBEC3 proteins to interact with Argonaute 2 does not closely correlate with their anti-viral phenotypes. Further, knockdown of Argonaute 2 did not impact upon APOBEC3 mediated viral inhibition, suggesting that this cellular protein is not required for this process. Conversely, the role of APOBEC3 proteins in the regulation of cellular RNA was also examined. However, the APOBEC3 proteins did not specifically affect the post-transcriptional regulatory pathways of miRNA mediated repression, siRNA mediated silencing or ARE mediated decay. Localisation of APOBEC3 proteins to mRNA Processing bodies, on the other hand, does correlate with their anti-viral activities, implying that subcellular localisation may be important for viral inhibition. However, depletion of P-bodies through knockdown of DDX6 and Lsm1, did not affect APOBEC3 restriction of HIV-1 or replication of HIV-1 in general. In sum, P-body associated proteins do not appear to regulate APOBEC3 anti-viral activity and thus may be more relevant to an as yet unidentified cellular function of this protein family.

ACKNOWLEDGEMENTS

First and foremost I would like to express my sincerest gratitude to my supervisor Michael Malim for his continued advice, support and insight. It has been a tremendous learning experience and I am incredibly grateful for all that he has taught me.

I am immensely indebted to Chad Swanson for his time, encouragement and invaluable guidance throughout the course of this work.

I am also grateful to past and present members of the Malim lab including Luis Apolonia, Shetal Arjan, Flavia Autore, Helene Bauby, Julien Bergeron, Kate Bishop, Kieran Gillick, Caroline Goujon, Hendrik Huthoff, Fransje Koning, Carol McHattie, Stelios Papaioannou, Torsten Schaller and Valerie Wicksey. In particular I would like to thank Nathan Sherer and Sarah Gallois-Montbrun from whom I have learnt a great deal. It has been a real priviledge to work alongside not just such talented scientists but also such wonderful people.

I would also like to acknowledge everyone in the Departments of Immunology and Infectious Diseases for providing such a friendly and supportive working environment. In particular, the labs of Juan Martin-Serrano and Stuart Neil have provided much appreciated advice and reagents. I would like to say a special thank you to Monica Agromayor, Jeremy Carlton and Bethan McDonald for all their help and encouragement.

Most of all I wish to thank my amazing family and friends, especially my parents, for their overwhelming love and support.

TABLE OF CONTENTS

LIST OF FIGURES

LIST OF TABLES

ABBREVIATIONS

AAV	adeno-associated virus
AID	activation induced deaminase
AIDS	acquired immunodeficiency syndrome
agm	African green monkey
Ago	Argonaute
AMD	AU rich element mediated decay
APOBEC	apolipoprotein B mRNA editing enzyme polypeptide like
ARE	AU rich element
ARE-BP	ARE binding protein
AU	adenosine and uridine
bp	base pairs
BSA	bovine serum albumin
CA	Capsid
CD4	cluster of differentiation 4
CDM	cytidine deaminase motif
cDNA	complementary deoxyribonucleic acid
Co-Ip	co-immunoprecipitation
Cox-2	cyclooxygenase 2
cpz	chimpanzee
Cyp	Cyclophilin
DMEM	Dulbecco's modified Eagle medium
dNTP	2'-deoxy nucleotide 5'-trisphosphate
EBV	Epstein Barr virus
EDTA	ethylenediaminetetraacetic acid
EIAV	equine infectious anaemia virus
ELISA	enzyme linked immunosorbent assay
Env	Envelope glycoprotein
ER	endoplasmic reticulum
FACS	fluorescence activated cell sorting
FCS	foetal calf serum
FLIM	fluorescence lifetime imaging microscopy
Fv1	Friend virus susceptibility 1
FRET	fluorescence resonance energy transfer
FXR1	fragile X mental retardation protein 1
Gag	Group specific antigen
GFP	green fluorescent protein
gor	gorilla
gRNA	genomic RNA
HA	haemagglutinin
HAART	highly active anti-retroviral therapy
HBV	hepatitis B virus
HCHO	formaldehyde
HCMV	human cytomegalovirus
HCV	hepatitis C virus
HERV	human endogenous retrovirus
HIV	human immunodeficiency syndrome
HRP	horseradish peroxidase

HPV	human papilloma virus
HSV	herpes simplex virus
HSP90	Heat shock protein 90
HTLV	human T-cell lymphotropic virus
IAP	intracisternal A particle
Ig	immunoglobulin
IL	inter-leukin
IN	Integrase
kb	kilobase
kDa	kilo Dalton
LINE	long interspersed nucleotide element
LTR	long terminal repeat
MA	Matrix
mac	macaque
miRNA	micro RNA
MLV	murine leukemia virus
mRNA	messenger RNA
NC	Nucleocapsid
Nef	Negative factor
NES	nuclear export signal
NLS	nuclear localisation signal
NMD	nonsense mediated decay
nt	nucleotide
ORF	open reading frame
PABP	Poly A binding protein
PAZ	PIWI-Argonaute-Zwille
P-body	mRNA processing body
PBS	primer binding site/phosphate buffered saline
PCR	polymerase chain reaction
PEI	polyethylenimine
PFV	primate foamy virus
PIC	pre-integration complex
piRNA	PIWI-interacting RNA
PM	plasma membrane
Pol	Polymerase
PPT	polypurine tract
PR	Protease
PTC	premature termination codon
R	repeat
RDRP	RNA dependent RNA polymerase
RNAi	RNA interference
Rev	Regulator of expression of viral proteins
RISC	RNA induced silencing complex
RING	really interesting new gene
RNA	ribonucleic acid
RNP	ribonucleoprotein
rpm	rotations per minute
RPMI	Roosevelt Park Memorial Institute medium
RT	Reverse transcriptase
RTC	reverse transcription complex
SINE	short interspersed nucleotide element

siRNA	small interfering RNA
SIV	simian immunodeficiency virus
SDS	sodium dodecyl sulphate
SDS-PAGE	SDS-polyacrylamide gel electrophoresis
shRNA	small hairpin RNA
SRS	suppressor of RNA silencing
Tat	transactivator
TEMED	N, N, N', N'-tetra-methyl-ethylenediamine
TNF	tumour necrosis factor
TRIM	Tripartite motif
Tris	tris(hydroxymethyl)methylamine
TRBP	TAR RNA binding protein
tRNA	transfer RNA
TRPT	target primed reverse transcription
TTP	Tristetraprolin
U	unit/unique
Vif	Viral infectivity factor
VLP	virus like particle
Vpr	Viral protein R
Vpu	Viral protein U
VSV-G	vesicular stomatitis virus protein G
YFP	yellow fluorescent protein

CHAPTER 1

INTRODUCTION

1. INTRODUCTION

1.1 Introduction to retroelements

1.1.1 Retroviruses

Human immunodeficiency virus type-1 (HIV-1) is a lentivirus belonging to the retrovirus family. Retroviruses are distinguished by two unique steps in their life cycle. Firstly, the reverse transcription of their RNA genome into a DNA copy and secondly, the integration of this DNA into the genome of the infected host cell, thus establishing a provirus which enables the production of viral RNA and proteins. There are seven genera of retroviruses (alpha, beta, gamma, delta, epsilon, lenti and spuma viruses), classified according to several criteria including core morphology, genome organisation and site of viral assembly. Gammaviruses, such as murine leukaemia virus (MLV), are considered simple retroviruses as they only encode the *gag*, *pol* and *env* genes, whereas complex retroviruses, such as lentiviruses, harbour additional genes encoding accessory proteins that are essential for viral replication (Goff, 2001).

1.1.2 Retrotransposons

In addition to exogenous retroviruses, endogenous retroelements are also present in the genomes of eukaryotes. These are host encoded DNA sequences that are able to convert their DNA into an RNA intermediate, which is reverse transcribed, and thus duplicated before re-integration back into the genome.

Two main classes of retroelements have been delineated, containing either long terminal repeats (LTRs) at their 3' and 5' ends (LTR retrotransposons) or not (non-LTR retrotransposons). Examples of the former include the Ty elements in yeast, the intracisternal A particles (IAPs) and MusD elements in mice and the human endogenous retroviruses (HERVs) in humans. These retrotransposons are similar in structure to retroviruses as they encode a viral particle coat protein (Gag) as well as the enzymes necessary for reverse transcription (RT) and integration (IN) to facilitate autonomous retrotransposition. However they lack a functional envelope protein, which restricts their intercellular movement and means retrotransposition events are limited to the genome from which they originate.

The most well known non-LTR retroelements are the autonomous long interspersed nucleotide elements-1 (LINE-1s). LINE-1s contain two open reading frames, both of which are required for successful retrotransposition (Ostertag and Kazazian, 2001). The first of these, ORF1p (open reading frame-1p), encodes a nucleic acid binding protein which is able to form ribonucleoprotein complexes in both human and mouse cells (Doucet et al., 2010; Kulpa and Moran, 2005). It also possesses nucleic acid chaperone activity (Martin et al., 2005). The second, ORF2p (open reading frame-2p), has both endonuclease and reverse transcriptase enzymatic activity (Feng et al., 1996a; Moran et al., 1996). These elements retrotranspose through a process termed target primed reverse transcription (TPRT) whereby the nuclear genomic DNA is nicked by the ORF2p endonuclease, exposing a free 3' hydroxyl end. This is then used as the primer, and the RNA as the template, for reverse transcriptase to generate a cDNA copy of the LINE-1 transcript directly on the DNA. One strand is first integrated before it is used as the template for generation of the second strand. The LINE-1 elements have *cis* preference wherein they will preferentially act on the RNA which encodes them. However the non-autonomous SINE (short interspersed nucleotide elements) retrotransposons are able to hijack the LINE-1 machinery to promote their own replication which demonstrates that LINE elements are also able to work on sequences in *trans*. This has ensured the survival and success of SINEs as the human Alu element, originally derived from 7SL RNA, is believed to comprise up to 11% of the human genome (Kazazian, 2004).

LINE-1s are thought to comprise approximately 17% of the human genome, yet only 80 - 100 of these elements are currently active (Sassaman et al., 1997). The potential for retrotransposition to cause serious genetic mutation via these gene insertion events is immense and potentially problematic for the stability of the genome. Disease induced mutations, including cancers, have been documented, (Boissinot et al., 2001; Kazazian, 2004) and Alu retrotransposition events account for almost 0.3% of all human genetic diseases [reviewed in (Cordaux and Batzer, 2009)]. In defence, cellular control mechanisms have been established to limit the deleterious effects of these mobile elements. Transcriptional inactivation by DNA methylation is one such mechanism (Hata and Sakaki, 1997), as is utilisation of the RNAi pathway whereby small interfering RNAs produced from bi-directional transcription are used to silence the encoded transcripts. Knockdown of Dicer, the enzyme responsible for biogenesis of

these small non-coding RNAs, leads to an increase in retrotransposition events in both human cultured cells and mouse embryos (Svoboda et al., 2004; Yang and Kazazian, 2006). Finally, cellular proteins may also mediate suppression of retrotransposon activity. One such group of proteins are the APOBEC3 family of cytidine deaminases whose members have been implicated in the inhibition of both LINE-1 and Alu retrotransposition [reviewed in (Chiu and Greene, 2008)]. The inhibitory effect of these proteins can be extended to other retroelements, as well as other viruses and this will be discussed in greater depth in subsequent sections.

1.2 Introduction to HIV-1

1.2.1 Origin of HIV-1

In 1983, HIV-1 was isolated and a year later identified as the causative agent of acquired immunodeficiency syndrome (AIDS) (Barre-Sinoussi et al., 1983; Gallo et al., 1984). Worldwide, HIV-1 has caused approximately 25 million deaths and in 2008 33 million people were estimated to be infected, with the majority of the disease burden in sub-saharan Africa (UNAIDS, 2009). HIV-1 arose as a result of a cross-species zoonosis, transmitted from chimpanzees to humans on three separate occasions, giving rise to the three different HIV-1 lineages, M (cause of the global AIDS pandemic), N (which is restricted to Cameroon) and O (restricted to central-west Africa) (Gao et al., 1999; Keele et al., 2006; Van Heuverswyn et al., 2006). A fourth subtype, designated P, has also been reported and appears to be more closely related to simian immunodeficiency virus (SIV) from gorillas (SIVgor), which may also be the source of group O (Van Heuverswyn et al., 2006). A related yet distinct virus, termed HIV-2, primarily found circulating in West Africa gives a similar disease phenotype to HIV-1 but with slower progression (Clavel et al., 1986). This virus is thought to have arisen in humans from multiple cross species transmission events of SIV from sooty mangabeys (SIVsm). In general, SIVs do not cause disease in their natural hosts, but it has recently been shown that infected wild chimpanzees may be subject to increased mortality and AIDS-like immunopathology (Keele et al., 2009).

1.2.2 HIV-1 pathogenesis

HIV-1 disease and progression to AIDS is characterised by a severe depletion of activated CD4+ T cells, which are the primary targets of productive HIV-1 infection *in vivo*. Specifically it is mucosal CD4+ memory T cells which are primarily targeted and the virus is then able to spread as these cells migrate through lymphoid tissues. Viral dissemination is also facilitated by dendritic cells. Although these cells cannot be productively infected, due to an inherent block to viral replication, they do express CD4 and can capture virus on their surface and present it to CD4+ T cells. This is reflected in the fact that lymph nodes contain 5 – 10 fold more infected cells than the peripheral blood. The acute stage of HIV-1 infection is also associated with very high viral loads (Cohen and Fauci, 2001).

However, direct infection of CD4+ T cells does not appear to be the predominant cause of the depletion of these cells and progression to AIDS. A major contributory factor may in fact be general immune activation, which is associated with early HIV-1 infection. This results in increased frequencies of T cells displaying activating and memory markers, as well as increased pro-inflammatory cytokines and increased turnover of a number of other immune related cell types. This therefore provides a fresh pool of HIV-1 target cells to maintain the infection [reviewed in (Grossman et al., 2006)].

Following the initial or acute stages of infection, the viral load appears to stabilise and virus production is also levelled through rapid clearance by CD8+ cytotoxic T lymphocytes (CTLs). However the slow but steady decline of the CD4+ T cell population continues and after a number of years eventually falls below a critical threshold required for efficient cell mediated immune responses. This signifies the onset of AIDS and infected individuals are highly susceptible to infections by opportunistic pathogens, which often prove fatal (Cohen and Fauci, 2001).

The persistence of latently infected cells, those that harbour provirus but do not express viral proteins as they are in a resting state, represents a significant barrier to the clearance of the virus by both the immune system and anti-viral therapies.

1.2.3 HIV-1 therapeutics

There is currently no cure for HIV-1 and although there has been considerable investment in the development of a protective vaccine, this has so far proved an elusive goal. However, the virus can be controlled for an extended period of time through the use of combined antiviral drugs, referred to as highly active antiretroviral therapy (HAART). These drugs target different viral proteins, namely reverse transcriptase and protease, in combination, in an attempt to reduce the potential for the emergence of drug resistant strains. They also act to reduce viral loads thereby minimising the chances of generating resistance mutations. However, the mutagenic capacity of HIV-1 is immense due to the error prone nature of the reverse transcriptase enzyme, which causes 3.4×10^{-5} nucleotide changes per site per replication cycle, and its ability to induce recombination of the viral genome (Freed and Martin, 2001). Thus the identification of new drug targets is an area of intense research and drugs that interfere with viral entry and integration have also now been developed. However, targeting cellular proteins may be a more attractive route since they are less likely to mutate and thus contribute to drug resistance. Two types of cellular proteins may make ideal drug targets. Firstly those that are utilised by the virus in order to complete its life cycle and thus are necessary for virus replication. Numerous examples have now been documented, such as Cyclin T, LEDGF and the ESCRT proteins and these will be discussed in more detail in the ensuing sections. The second class of proteins are those that act to inhibit virus replication, so called restriction factors, that form part of the innate (or intrinsic) immune defence system (see section 1.6). Mechanisms to enhance or mimic the activity of these proteins may significantly aid natural immune responses to viral infection. Therefore the need to thoroughly understand the relevance of these proteins for viral replication and more importantly, how perturbing these proteins may affect cellular functioning is paramount and will dramatically contribute to future attempts to control HIV-1 and other viruses.

1.3 HIV-1 genome organisation

HIV-1 has a diploid genome, comprised of two 9 kb long positive sense, single stranded RNA molecules. Akin to most cellular mRNAs, these RNAs are both capped at their 5' end and polyadenylated at their 3'end.

The RNA genome contains several *cis* acting elements that are essential for the successful replication of the virus and production of infectious progeny virions (Figure 1.1A). These include the Ψ packaging signal for virion incorporation, the primer binding site (PBS) for initiation of reverse transcription, the polypurine tract (PPT) for plus strand DNA synthesis, the Rev response element (RRE) involved in nuclear export and the transactivating response region (TAR) involved in transcription elongation (Freed and Martin, 2001).

The resulting mRNA transcript encodes for fifteen proteins produced from nine open reading frames. The group specific antigen (*gag*), polymerase (*pol*) and envelope (*env*) genes are common to all retroviruses (Figure 1B). However, being a complex retrovirus, HIV-1 also encodes six additional genes, for the regulatory proteins Tat and Rev and the accessory proteins, Vif, Vpr, Vpu and Nef [reviewed in (Swanson and Malim, 2008)] (Figure 1C). The varying and essential functions of these genes will be outlined in the following sections.

The genomic RNA is used as the template for reverse transcription, whereby a DNA copy is produced that is subsequently integrated into the host genome, termed the provirus. This provirus is transcribed by host cellular machinery to produce RNA transcripts that are either translated to produce viral proteins or else packaged into nascent virions, thus initiating the next round of infection. The establishment of the provirus confers several advantages to HIV-1 and other retroviruses to secure their successful propagation. It not only ensures that viral gene products are continually produced throughout the lifetime of the cell but also allows for vertical transmission of the virus through the germline (Goff, 2001).

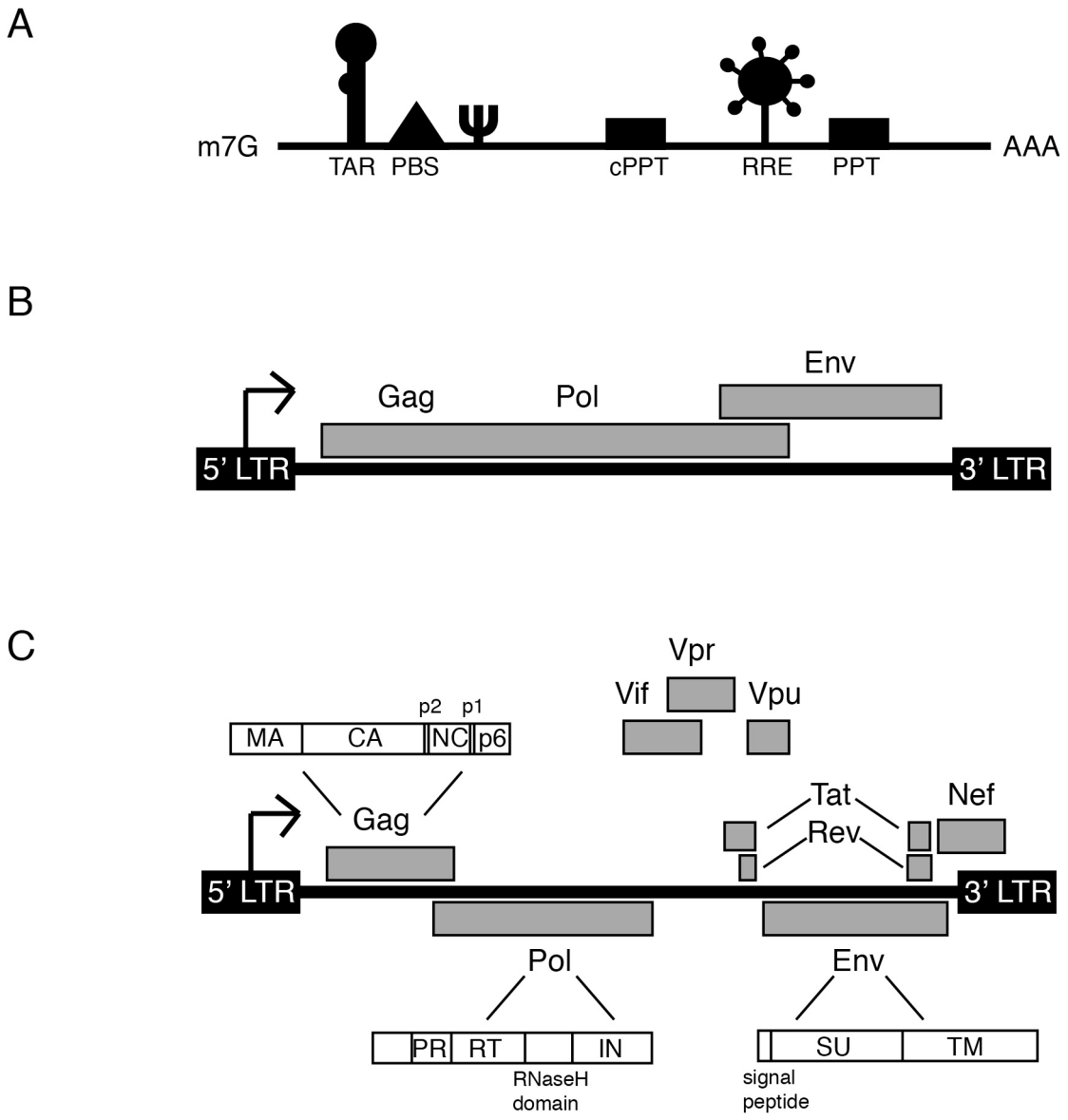

Figure 1.1: Genetic organisation of HIV-1 and MLV.

A. Schematic diagram of the HIV-1 RNA genome, displaying several *cis* acting elements including the transactivating response (TAR) stem loop structure, the primer binding site (PBS), the Ψ packaging signal, the Rev response element (RRE) and the polypurine tract (PPT), as well as an additional central PPT (cPPT). Adapted from (Freed and Martin, 2001). **B.** The genome of the simple gammaretrovirus, murine leukaemia virus (MLV), encodes the Gag, Pol and Env proteins. Adapted from (Freed and Martin, 2001). **C.** The complex retrovirus, HIV-1, additionally encodes the accessory proteins Vif, Vpr, Vpu, and Nef and the regulatory proteins Tat and Rev. The Gag polyprotein is cleaved to generate the Matrix (MA), Capsid (CA), spacer protein 2 (p2), Nucleocapsid (NC), spacer peptide 1 (p1) and p6. Pol is synthesised as a Gag-Pol polyprotein by ribosomal frameshift and is cleaved to generate the viral Protease (PR), Reverse transcriptase (RT) and Integrase (IN) proteins. The Env protein contains an N-terminal signal peptide sequence and is cleaved to generate the gp120/Subunit (SU) and gp41/Transmembrane (TU) proteins. Adapted from (Swanson and Malim, 2008).

1.4 HIV-1 life cycle

1.4.1 Overview

To ensure the production of infectious progeny virions, HIV-1 must first successfully complete its life cycle within the host cell. There are numerous steps involved in this pathway, starting with attachment and entry into the target cell, followed by uncoating of the viral core, reverse transcription of the RNA genome into a DNA form, integration, transcription, nuclear export of the mRNA, translation in the cytoplasm, assembly of viral particles, budding and release (Figure 1.2). Along this pathway, HIV-1, like all obligate intracellular pathogens, will encounter numerous host proteins. The limited genetic repertoire of the virus means that it is dependent on some of these cellular proteins to facilitate its propagation. Although several of these factors have been independently identified and characterised, recent whole genome screens, based on high throughput RNA interference (RNAi) technology, have unearthed a multitude of proteins and pathways that are utilised by HIV-1 (Brass et al., 2008; Konig et al., 2008; Yeung et al., 2009; Zhou et al., 2008). Between them, these screens listed over one thousand genes that are necessary for optimal viral replication. However, only 34 genes were replicated in two or more of the reports and some known factors were not found. This emphasises the need for many of these factors to be independently verified in more than one type of system and cell line (Pache et al., 2011). Nevertheless, these screens have proven extremely useful in highlighting previously unknown cellular factors on which HIV-1 appears to be dependent such as the nuclear pore machinery, the transcription related mediator complex and the NFkβ complex.

The following sections will outline in greater detail the various steps of the HIV-1 life cycle with the known cellular proteins required by the virus described at the relevant stages.

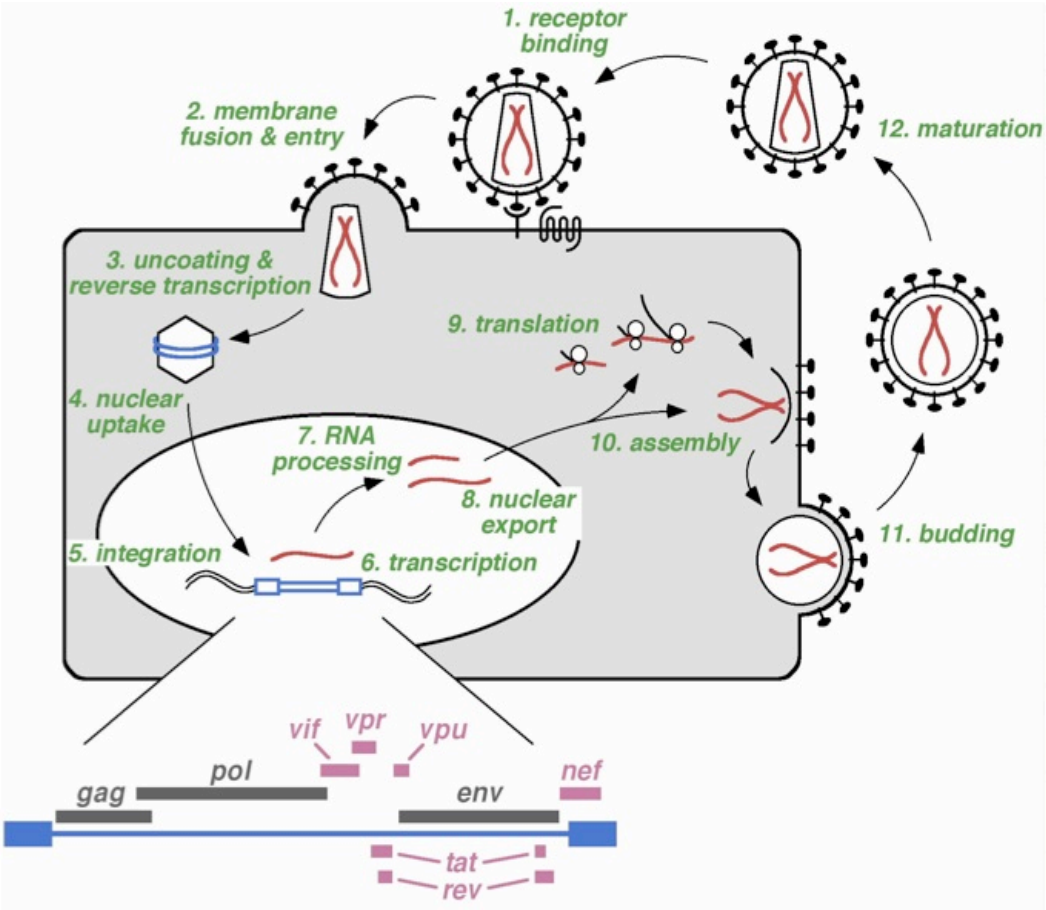

Figure 1.2: HIV-1 life cycle.

HIV-1 binds to the CD4 receptor on the surface of the target cell in association with either the CXCR4 or CCR5 chemokine co-receptors, via its gp120 envelope protein expressed on the viral surface. Membrane fusion occurs and the viral core is released into the target cell. It then undergoes a process termed uncoating before the initiation of reverse transcription. The viral RNA genome is converted to a double stranded DNA form and enters the nucleus to integrate into host chromosomal DNA, thus establishing the provirus. The provirus is transcribed and translated akin to cellular genes. The viral proteins and genomic RNA accumulate at the plasma membrane for the assembly of new viral particles which upon formation bud from the infected cell. The virion is of an immature form and must undergo a process of maturation, whereby the spherical core condenses into a conical structure, in order to generate a mature infectious virion.

1.4.2 Attachment and entry

Unlike some enveloped viruses, which are dependent upon an acidic environment for entry via endocytosis, HIV-1 enters its target cell through direct fusion of the viral envelope and plasma membrane in a pH independent manner. Cells express numerous receptors on their surface, which provide a link between the intracellular and intercellular compartments. One such receptor, CD4, a member of the immunoglobulin G (IgG) superfamily is utilised by HIV-1 for attachment and entry of its viruses. Cells which express this receptor, namely T helper cells, are thus prime targets for HIV-1 infection (Clapham et al., 1991; Maddon et al., 1986). Although CD4 is generally necessary for infection (CD4 independent entry has also been reported), it is not sufficient. This was concluded from two key observations. Firstly mouse cells engineered to express CD4 are still resistant to HIV-1 infection (Maddon et al., 1986) and secondly, only a subset of CD4+ cells are infected by HIV-1 in humans. This issue was eventually resolved through the identification of the chemokine co-receptors, CXCR4 (originally termed fusin) (Feng et al., 1996b) and CCR5 (Alkhatib et al., 1996; Deng et al., 1996; Dragic et al., 1996). Viral isolates are designated either X4 or R5 depending on whether they utilise CXCR4 or CCR5 as their co-receptor respectively. Primary viral isolates tend to be R5 tropic but in 50% of infected individuals, during the late stage of disease, viruses will mutate and switch from R5 to X4 tropism. This results in a massive depletion of CD4+ T cells and signifies decline into AIDS (Cohen and Fauci, 2001). There are also cases of viruses that are dual tropic (X4R5) and can use either co-receptor for entry. The fundamental role that these receptors play in infection is illustrated by a 32 base pair deletion in the CCR5 gene (CCR5Δ32), which is found in approximately 5 - 10% of Northern Europeans. This results in a truncated non-functional version of the protein that is not expressed at the cell surface (Liu et al., 1996; Samson et al., 1996). Accordingly, homozygotes for this mutation are resistant to HIV-1 infection and heterozygotes are afforded moderate protection and slower disease progression (Rowe, 1996). Although individuals with this mutation appear to be healthy, they may be more susceptible to other pathogens such as West Nile Virus (Glass et al., 2006).

The viral envelope (Env) protein mediates attachment to the cell surface receptors. This protein is initially synthesised in the endoplasmic reticulum (ER) as a membrane bound polyprotein precursor, termed gp160 and is subsequently transported to the Golgi where

it is cleaved by the cellular protease furin into the gp120 (Subunit, SU) and gp41 (Transmembrane, TM) subunits (Moulard and Decroly, 2000). These subunits are heavily glycosylated and remain non-covalently bound as they traffick to the cell surface where they are incorporated into virus particles as trimers. CD4 is first bound by the gp120 SU protein which contains variable loops within its structure that determine the tropism of the virus and are also essential for membrane fusion. This binding event instigates a conformational change in gp120, exposing binding sites allowing interactions with its chemokine co-receptor. Fusion of the viral and cellular membranes is then mediated by the gp41 TM protein which itself undergoes a conformational change exposing a hydrophobic domain at its N-terminal called the fusion peptide. This peptide penetrates the membrane of the target cell and orchestrates the fusion process, with gp41 adopting a six-helix bundle formation to maintain both membranes in close proximity. The generation of a fusion pore allows movement of the viral core into the cytoplasm of the infected cell and subsequent commencement of reverse transcription.

1.4.3 Uncoating

Following entry into the cytoplasm of the target cell, the viral core, consisting of the RNA genome and associated viral proteins, including Capsid (CA) and Nucleocapsid (NC), undergoes a poorly defined process termed uncoating. This is where viral and cellular components are either added or removed to form the reverse transcription complex (RTC). This is believed to be composed of the viral factors Reverse transcriptase (RT), Integrase (IN), Matrix (MA), NC, Vpr and the viral genome (Fassati and Goff, 2001), plus any host factors necessary for reverse transcription to take place, such as the $tRNA_{lys3}$ incorporated from the virus producer cell. The involvement of CA in this complex and its role in the subsequent translocation of the viral DNA into the nucleus is a matter of debate (Fassati and Goff, 2001; Yamashita et al., 2007; Zhou et al., 2011). Also, it is during this stage that the retroviral restriction factors Fv1 and Trim5α are thought to act (see section 1.6.1).

1.4.4 Reverse transcription

Formation of the RTC allows the initiation of reverse transcription, a defining event in the life cycle of all retroviruses. This is dependent on the *pol* encoded Reverse transcriptase (RT) enzyme. Pol is the most highly conserved region of the HIV-1 genome and it is initially produced as a Gag-Pol fusion peptide by ribosomal frame-shift, which is subsequently cleaved during maturation of the virion. RT harbours both RNA and DNA directed DNA polymerase activity as well as RNase H catalytic activity, which catalyses the degradation of RNA in RNA-DNA hybrids (Gilboa et al., 1979).

All retroviruses encapsidate host tRNAs to act as primers for initiation of reverse transcription. The exact one will differ for different viruses, but for HIV-1 this role is fulfilled by $tRNA_{lys3}$. This binds to the primer binding site (PBS) at the 5'end of the viral RNA, and DNA synthesis proceeds in a 3' to 5' direction. This generates a short fragment of minus strand DNA, termed minus strong stop, which encodes both the unique 5' (U5) and the repeat (R) regions. The RNA template, now contained within an RNA-DNA duplex, is then degraded by the RNase H capacity of RT. The strong stop DNA then translocates to the 3' end of the RNA, in what is known as first strand transfer, where it binds to the complimentary R region found at the 3' end. Synthesis of the minus strand of DNA is then continued up until the PBS. The RNA template is degraded along the way except at the polypurine tract (PPT), which is partially resistant to the RNase H activity of RT and therefore maintains a short section of an RNA-DNA hybrid. Lentiviruses also harbor a second PPT (cPPT), which is situated towards the centre of the genome (Charneau et al., 1992; Charneau and Clavel, 1991), and either one of these regions can act as the primer for generation of the plus strand of DNA (termed plus strong stop), which proceeds in a 5' to 3' direction. Strong stop DNA is used as the template for plus strand DNA synthesis, except at the PBS, where the $tRNA_{lys3}$ is used instead. RT degrades the $tRNA_{lys3}$ primer, which exposes the PBS at the 3' end and allows it to bind to the complementary site on the minus strand DNA, thus generating a circular intermediate form of DNA. This second strand transfer event allows elongation of the minus and plus strands to be completed through strand displacement. The final product is a linear, double stranded DNA molecule with identical long terminal repeat regions at each end containing the U3, R and U5 regions (Figure 1.3).

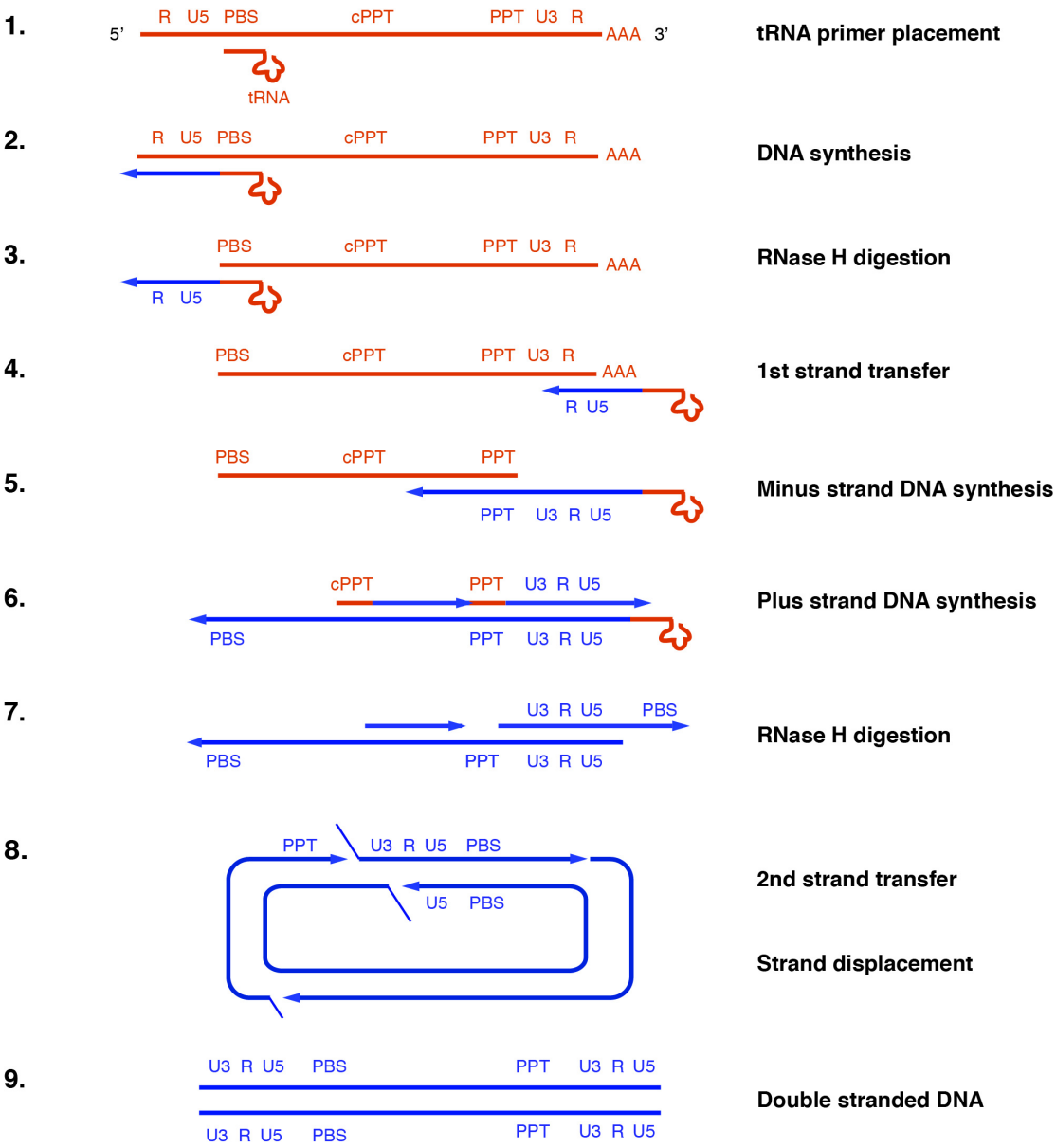

Figure 1.3: Reverse transcription.

Schematic diagram of reverse transcription. RNA is depicted in red and DNA in blue. 1. DNA synthesis is primed by binding of the cellular tRNA to the viral RNA at the primer binding site (PBS). 2. Reverse transcriptase catalyses extension of the primer to form minus sense DNA in an RNA-DNA duplex. 3. The RNase H activity of reverse transcriptase digests the RNA in this duplex resulting in single stranded DNA (minus strand strong stop DNA). 4. This DNA translocates to the 3' end of the viral RNA which is facilitated by binding of the complementary R sequences (1st strand transfer). 5. Elongation of minus strand DNA and degradation by RNase H digestion continues. 6. Plus strand DNA synthesis is initiated at the polypurine tract (PPT) or the central PPT (cPPT, unique to lentiviruses), both of which are resistant to RNase H digestion. 7. The U3, R and U5 regions in minus strand DNA are copied by reverse transcriptase to yield the complementary plus strand DNA (plus strand strong stop DNA). The tRNA primer is used as the template to reconstitute the PBS. The tRNA primer from minus strand and the PPT primers from plus strand DNA are removed by RNase H digestion. 8. Circularisation of the DNA strands occurs (second strand transfer) and the two long terminal repeat (LTR) sequences are generated by strand displacement. 9. Elongation of the plus and minus strands of DNA is continued to completion, generating linear double stranded DNA with two identical LTRs, which is competent for integration.

Although HIV-1 contains two copies of its RNA genome only one provirus is formed per infectious virion. However, both molecules of RNA may contribute to the production of the proviral DNA. The inherent poor processivity of RT means that it frequently switches between RNA templates during the reverse transcription process. It may also be forced to switch templates if one strand is damaged in any way. This means that a recombinant form of DNA can be produced in co-infected cells, which contributes to genetic diversity. Combined with the high error rate of RT, due to its lack of exonucleolytic proof reading capabilities, means that HIV-1 displays a very high level of sequence diversity even within isolates taken from the same infected individual. This provides the virus with greater flexibility in evading both the immune response and antiviral therapies.

1.4.5 Nuclear entry

In order to integrate into the host genome, the newly synthesised cDNA must first gain access to the nucleus. A unique property of lentiviruses is their ability to infect non-dividing cells, which means that active transport across a fully intact nuclear envelope is required (Lewis et al., 1992; Weinberg et al., 1991). Other retroviruses, such as the gammaretrovirus MLV, require mitosis to penetrate the nucleus and thus they are restricted to infecting cells in the process of cell division (Roe et al., 1993). Even before the completion of reverse transcription, various cellular and viral components will assemble on the DNA forming the pre-integration complex (PIC). The viral proteins, Vpr, IN and MA all contain putative nuclear localisation signals (NLS) and thus have been implicated in mediating the transport of the PIC through the nuclear pore. However, the role these proteins play in this process is controversial (Yamashita and Emerman, 2005). Matrix was originally believed to be involved in nuclear import of the PIC (Bukrinsky et al., 1993), but more recent work with tagged versions of this protein show that it does not localise to the nucleus (Depienne et al., 2000). Further, HIV-1 viruses with mutations in MA can still efficiently infect non-dividing macrophages (Reil et al., 1998). Although Vpr does not contain a canonical NLS, it does localise to the nucleus and its deletion reduces HIV-1 replication in non-dividing monocyte derived macrophages (Nitahara-Kasahara et al., 2007). The role of Integrase is similarly uncertain but mutations in this protein do appear to block nuclear entry (Gallay et al., 1997). Another viral element, the DNA flap, which is a discontinuous segment of DNA formed during reverse transcription, has also been implicated in nuclear entry (Zennou

et al., 2000) but its exact functional role is unclear and more recent data suggests that it does not influence this process (Limon et al., 2002).

The movement of the PIC is also most probably dependent on cellular factors. This includes the alpha and beta Importin pathways which serve to transport numerous cellular factors through the nuclear complex. More recently, the karyopherin Transportin 3 (TNPO3), in conjugation with several nuclear pore proteins, has been linked to nuclear entry of HIV-1 DNA from whole genome RNAi screens (Brass et al., 2008). These findings require further validation and so the mechanism of entry into the host nucleus and the precise requirements of this process have yet to be fully resolved.

1.4.6 Integration

Along with reverse transcription, integration of viral DNA into the genetic material of the host is a defining feature of all retroviruses. Not only does it ensure the continued production of viral gene products throughout the lifetime of the cell, it also enables the vertical transmission of viral DNA to daughter cells.

The integration reaction is catalysed by the viral Integrase protein (IN) (Bushman et al., 1990), which is produced as a cleavage product of the Gag-Pol precursor polyprotein. This 32 kDa protein has a N-terminal zinc binding domain (important for multimerisation), a central domain containing the catalytic core and a C-terminal DNA binding domain. It is responsible for two spatially and temporally distinct reactions that are essential for integration to occur. Firstly, in the cytoplasm, two nucleotides from the 3'end of both strands of DNA are removed, generating 3'OH recessed ends, in a process termed 3'end processing. In the nucleus, at the site of integration, these reactive hydroxyl ends attack phosphodiester bonds in the genomic DNA resulting in cleavage of the DNA at staggered sites. The 3'ends of the viral DNA are then ligated to the 5'O-phosphates of the host DNA, completing the strand transfer reaction. Cellular repair machinery then acts to fill in any gaps and remove any unpaired dinucleotides. The integrated proviral DNA has thus lost two nucleotides at its 3'end and is flanked by a 5 base pair duplication of the cellular target sequence as a result of the joining and repair process (Freed and Martin, 2001).

The linear proviral DNA is not the only form that the viral DNA can take in the nucleus. In fact, the formation of DNA circles by recombination (1 LTR circle) or by ligation of the two LTR ends or autointegration (2 LTR circles) can result in DNA species that are

aberrant dead end products for the virus. However, it has been reported that a small amount of transcription may take place from 2 LTR circles thus providing an alternative source of RNA if for some reason proviral integration is impaired (Wu and Marsh, 2001).

The involvement of cellular proteins, like at all stages of the HIV-1 life cycle, is essential for the integration process. Lens epithelium growth factor (LEDGF) is one such protein. It is tightly bound to chromatin throughout the cell cycle and tethers IN to chromatin thereby facilitating integration (Llano et al., 2006). This interaction appears to be specific to lentiviruses. Originally identified for MLV, the barrier to autointegration factor (BAF) is also required for efficient integration as it prevents suicidal autointegration events, though its exact mechanism of action is unclear (Chen and Engelman, 1998; Mansharamani et al., 2003).

For all retroviruses, integration does not occur randomly but is targeted to areas of the genome displaying certain characteristics. HIV-1 preferentially integrates into active transcription units whereas MLV prefers CpG islands and near the transcriptional start sites of actively transcribed genes (Wu et al., 2003). What determines these differences in integration patterns is not clear but has been attributed to both cellular and host factors. IN itself may be a contributory factor as HIV-1 chimeras containing the IN protein of MLV resulted in integration of the proviral DNA at sites reminiscent of MLV site preferences (Lewinski et al., 2006). LEDGF may also influence this process as cells depleted of this protein showed reduced integration at transcription start sites (Llano et al., 2006; Shun et al., 2007).

1.4.7 Transcription

The proviral DNA is recognised and processed analogous to host cellular DNA by the RNA polymerase II (RNA Pol II) enzyme. Transcription is initiated at the 5' LTR, which contains several *cis*-acting elements for the binding of positive and negative transcription factors that seek to control the level of viral transcription. The 5' LTR also facilitates the loading of RNA Pol II onto the DNA template. The processivity of RNA Pol II is poor, and so the majority of initial RNAs produced are short due to lack of elongation. Early, full-length transcripts encoding the viral gene products of Tat, Rev and Nef are synthesised however, albeit inefficiently. They are capped at their 5' end, polyadenylated at the 3' end and fully spliced before export into the cytoplasm via the

conventional NXF1 nuclear export pathway. The generation of Tat early on in this process allows for more efficient transcriptional elongation. It is able to bind to a stem loop structure within the viral RNA termed the transactivating response (TAR) region and recruits components of the positive activating transcription elongation factor complex (P-TEFb) (Mancebo et al., 1997). Tat binds with high affinity to Cyclin T, a component of this complex, and this interaction also increases the binding affinity of Tat with TAR. Cyclin T recruits and stimulates the kinase activity of cell cycle dependent kinase 9 (Cdk9), which leads to hyperphosphorylation of the C-terminal domain of RNA Pol II. This increases its processivity along the DNA and therefore enables more efficient transcription (Wei et al., 1998). The essential role of Cyclin T in this process is demonstrated by the observation that a single amino acid substitution in the mouse orthologue of this protein disrupts binding of the Cyclin T-Tat complex to TAR and contributes to one of the many blocks to HIV-1 replication in murine cells (Bieniasz and Cullen, 2000).

1.4.8 Nuclear export

Cellular mRNAs are fully spliced to remove introns before they can be transported out of the nucleus by the NXF1 nuclear export pathway. This checkpoint prevents the production of aberrant proteins that could potentially be toxic and deleterious to the cell, but it presents a problem for HIV-1. For the generation of infectious virions it requires export of the unspliced full-length 9.2 kb mRNA that will serve as the genomic RNA (gRNA) as well as the template for the Gag and Gag-Pol polyprotein precursors. It must also export the singly spliced mRNAs encoding Env, Vif, Vpr and Vpu. To overcome this obstacle, HIV-1 bypasses the traditional mRNA nuclear export pathway and instead utilises an alternative pathway normally reserved for the export of certain proteins and small non-coding RNAs. This is mediated by the viral protein Rev (Malim et al., 1989), an early product of an initial fully spliced mRNA, which is trafficked back to the nucleus via its nuclear localisation signal (NLS). It also encodes a leucine rich nuclear export sequence (NES). Rev binds to a 350 nt stem loop structure termed the Rev response element (RRE), situated within the *env* gene, and present in all unspliced or partially spliced transcripts. Rev is capable of multimerisation and thus several proteins are believed to bind to the RRE at any one time, which appears to be important for its activity (Malim and Cullen, 1991). Rev binds to the Chromosome regional maintenance 1 (Crm1) protein, also known as Exportin 1, which is a member of the Importin-β

family of nuclear transport proteins. Crm1 interacts with a small guanine nucleotide binding protein termed Ran and this interaction facilitates binding between Crm1 and Rev. In the nucleus, Ran is bound to GTP but in the cytoplasm it is associated with GDP. Thus a gradient is established between these two forms of Ran that provides the energy and directionality of transport into and out of the nucleus. RanGTP in the nucleus allows the Rev-RRE cargo to be loaded onto Crm1 and this complex is then transported out of the nucleus. When it reaches the cytoplasm, RanGTP is converted to RanGDP, which favours disassociation of the complex and release of the cargo. Rev continually shuttles between the nucleus and cytoplasm, ensuring the constant export of intron containing viral RNAs. The importance of Crm1 in this process is demonstrated by the use of leptomycin B, an antibiotic which blocks nuclear export of Rev dependent RNAs by targeting Crm1 (Fornerod et al., 1997). More recently, another cellular protein, the DEAD box helicase DDX3, has also been reported to contribute to Crm1 mediated export of the Rev-RRE complex (Yedavalli et al., 2004). Its depletion leads to a reduction in the export of HIV-1 RNA, though its exact mechanism of action remains unclear. In other retroviruses, such as Mason-Pfizer monkey virus (MPMV), a stem loop structure termed the constitutive transport element (CTE) directly binds NXF1 and thus functionally replaces Rev in the orchestration of nuclear export.

1.4.9 Assembly

Once the necessary viral proteins and polyproteins have been produced they must assemble at the plasma membrane (PM) and initiate first the assembly and then the release of fully infectious progeny virions. The main instigator of the assembly process is Gag, which is sufficient in itself to form virus like particles (VLPs). Approximately 1,500 - 2,000 Gag polyproteins are required for efficient virion assembly (Briggs et al., 2004), that associate into oligomers and form spheres predominantly through protein-protein interactions involving the C-terminal domain of CA (Dorfman et al., 1994; Krausslich et al., 1995). Within the PM, it is likely that virion assembly and budding takes place in specific lipid and cholesterol rich microdomains such as lipid rafts and tetraspanin enriched membranes (TEM) (Campbell et al., 2001; Deneka et al., 2007; Nguyen and Hildreth, 2000). Myristylation of the MA domain of Gag is necessary to target Gag proteins to these lipid microdomains and tether them there during the assembly process. This is mediated by the cellular PM associated protein $PI(4,5)P_2$, which binds to MA leading to exposure of its myristyl group (Ono et al., 2004; Saad et

al., 2006). However, for infectious particle production other components are also required. The MA domain is also involved in the incorporation of Env glycoproteins, a process which may additionally involve the cellular protein Tip47 (Bauby et al., 2010). Vpr is packaged through interactions with the p6 region of Gag, whereas Nef and Vif are believed to be packaged non-specifically. The NC region of Gag binds the Ψ packaging signal found only in the full length viral RNA, which ensures that only unspliced transcripts are incorporated as the genomic RNA. This RNA is also required for the synthesis of the Gag and Gag-Pol polyprotein precursors. How translation and packaging of this RNA are segregated and differentiated within the cell remains an issue of much debate. For some simple retroviruses, such as MLV, two distinct populations of RNA are produced that are either translated or packaged. However for other retroviruses, including HIV-1, a single RNA species is produced that serves as both the mRNA and genomic RNA interchangeably (Butsch and Boris-Lawrie, 2002). It has been postulated that sub-cellular compartmentalisation, such as in mRNA Processing Bodies (P-bodies), may facilitate sequestration of the genomic RNA away from the cellular translational machinery and thus allow it to be packaged into virions (Swanson and Malim, 2006) (discussed in more detail in section 1.9).

A multitude of cellular factors are also incorporated into viral particles. A comprehensive list of those identified in virions derived from purified monocyte derived macrophages (MDMs) has been reported [(Chertova et al., 2006) and reviewed in (Ott, 2008)]. Predominantly these proteins are packaged through interactions with Gag and they can positively or negatively influence viral replication. The NC domain of Gag enables the incorporation of the cellular protein $tRNA_{lys3}$, used as the primer to initiate reverse transcription, while Cyclophilin binds to the C-terminal of CA. In human cells, this protein is required for maximal HIV-1 infectivity, though its mechanism of action is unknown. Other positive factors include ICAM-1 (CD54), which increases infectivity, Actin, involved in assembly, and Staufen, which mediates HIV-1 genome packaging and Gag multimerisation. Conversely, under certain circumstances, virions can also incorporate inhibitory factors such as APOBEC3G and its family members which interact with the NC region of Gag and restrict viral replication in the target cell [reviewed in (Ott, 2008)], and Mov10 (Chertova et al., 2006), which can similarly decrease viral infectivity (Burdick et al., 2010).

1.4.10 Budding and release

Once the various viral and cellular factors required for virion formation have assembled at the plasma membrane, the virion must bud from the cell and be released into the extracellular compartment. This budding event is largely dependent upon the ESCRT (endosomal sorting complex required for transport) machinery comprising the protein complexes I, II and III [reviewed in (Martin-Serrano and Neil, 2011)]. The ESCRT proteins play fundamental roles in cellular membrane deformation and scission events. They were originally found to be involved in the formation of budding vesicles at multivesicular bodies in both yeast and humans, a process which is important for the sorting and concentration of endosomal cargo. However, the expansion of the ESCRT machinery to a possible 16 different complexes in humans is associated with additional functions that are topologically similar. The ESCRT components, Tsg101 (tumor susceptibility gene 101) and ALIX [apoptosis linked gene 2 (ALG-2) interacting protein] are involved in mediating the scission of the daughter cell from the mother cell during cytokinesis (Carlton and Martin-Serrano, 2007). These proteins have also been usurped by HIV-1 in order to release immature virions from infected cells through scission of a membrane stalk, which tethers them together during the budding process. Deletion of the proline-threonine-alanine-proline (PTAP) motif within the p6 region of Gag abrogated the release of HIV-1 particles with virions remaining attached to the cell (Gottlinger et al., 1991). This was termed a late (L) domain phenotype and other enveloped viruses were found to contain L domains that could be functionally interchangeable (Parent et al., 1995). It was subsequently demonstrated by two independent groups, through knock down and dominant negative mutants, that Tsg101 was the cellular factor which interacted with the PTAP domain and recruited the ESCRT machinery in order to facilitate budding and release (Garrus et al., 2001; Martin-Serrano et al., 2001). However, HIV-1 along with other viruses also contains binding sites for ALIX, which mediates budding through recruitment of the CHIMP3 ESCRT proteins and recruits the NEDD4 family of ubiquitin ligases (Strack et al., 2003). The existence of auxillary late domains for budding may aid the virus in its competition for host cellular machinery. Release of mature HIV-1 particles is also facilitated by Vpu in certain cell types, which antagonises the action of the host restriction factor, tetherin (Neil et al., 2008) (see section 1.6.2).

1.4.11 Maturation

The released virion is of an immature form and must undergo a process of maturation in order to generate an infectious viral particle. This is initiated by cleavage of the Gag and Gag-Pol polyproteins by the viral protease, which yields the structural proteins CA, NC, MA and p6 and the enzymes PR, RT and IN. This cleavage event is highly ordered and begins in a sequential manner between the p1 and NC sites. The RNA genome is surrounded by an NC protein coat, which is then encased in a condensed cone shaped core created by the CA proteins. The mature virion is composed of the following viral components: MA, CA, NC, p6, p2, p1, PR, IN, RT, Env, Vpr, Vpu, Vif and Nef (Frankel and Young, 1998) (Figure 1.4).

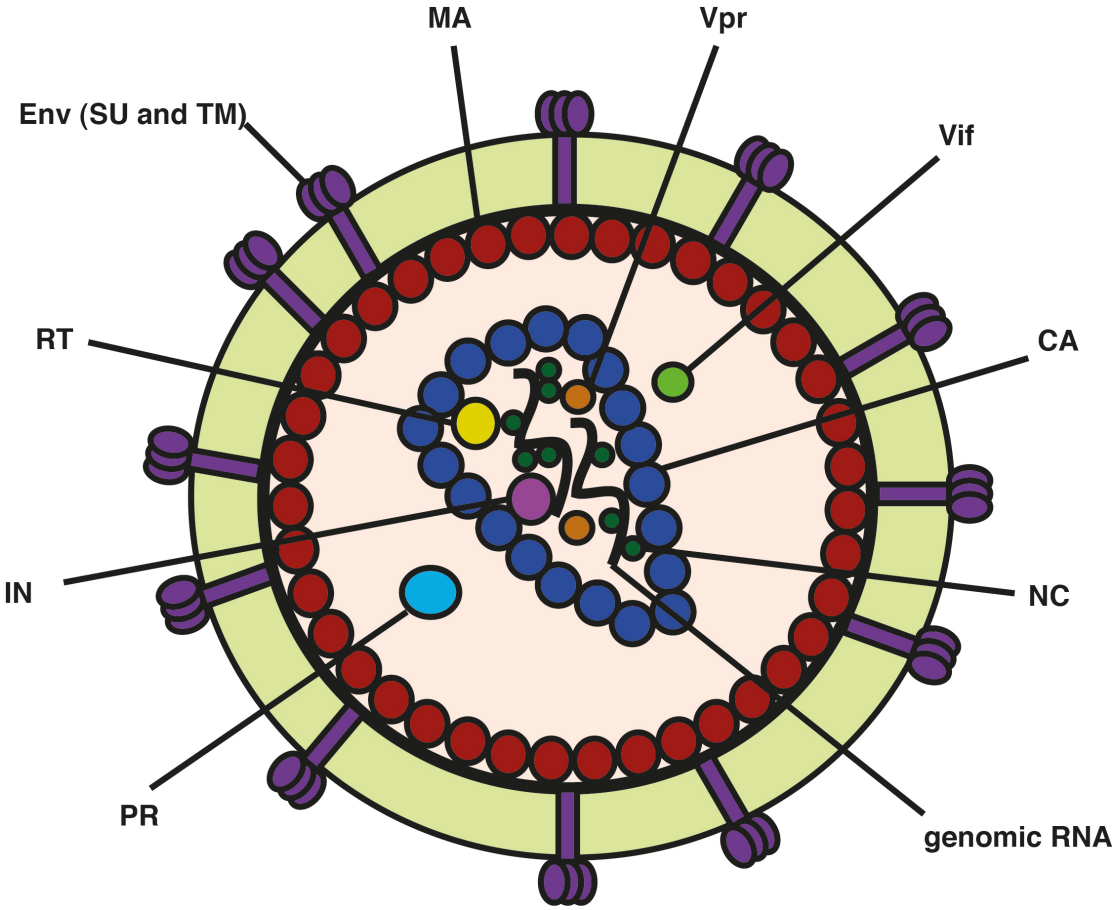

Figure 1.4: Composition of a mature HIV-1 virion.

The mature HIV-1 virion is composed of the genomic RNA coated with Nucleocapsid (NC) and enclosed within a Capsid (CA) core. The other viral proteins present are Envelope (Env), Matrix (MA), Integrase (IN), Reverse transcriptase (RT), Protease (PR), Vpr and Vif. Adapted from (Freed and Martin, 2001).

1.5 HIV-1 accessory proteins

HIV-1 must not only exploit numerous cellular factors in order to complete its life cycle, but must also modify the cellular environment to support its replication and evade host immune reponses. This is mainly achieved through the actions of its accessory proteins Nef, Vpr, Vpu and Vif. A common mechanism of action of these proteins is proteasomal degradation of their targets through recruitment of cullen-RING finger ubiquitin ligases [reviewed in (Malim and Emerman, 2008)]. Vpu and Vif specifically downregulate cellular proteins which act to restrict replication of the virus and so these will be discussed in greater detail in relation to the proteins that they target.

1.5.1 Nef

The 27 kDa membrane associated protein, originally named negative factor (Nef) is, contrary to its name, essential for virus infection *in vivo*. Nef deleted strains of both HIV-1 and SIV-1 show a much slower progression to AIDS and a reduced viral load (Deacon et al., 1995). Nef appears to participate in several processes. Firstly, it is believed to interfere with cellular signaling pathways that would activate the host immune response. It activates expression of FasL, which induces apoptosis of bystander cells that express Fas including cytotoxic T lymphocytes (CTLs) that would potentially destroy infected cells (Xu et al., 1999). It also downregulates MHC Class I from the surface of infected cells to similarly avoid detection by CTLs (Collins et al., 1998). Along with Vpr, it may also be involved in inhibiting apoptosis through inhibition of the apoptosis signal regulating kinase 1 (ASK-1). Several of the accessory proteins including Nef, Vpr and Vpu also mediate the downregulation of CD4 from the cell surface (Lama et al., 1999), which partially protects infected cells from further infection. While Nef mediates the endocytic degradation of cell surface CD4 (Chaudhuri et al., 2007), Vpu binds to CD4 in the ER and recruits the βTrcp-Skp1 complex involved in proteasomal degradation (Margottin et al., 1998). This prevents the Env polyprotein precursor, gp160, from prematurely interacting with CD4 before it has reached the cell surface.

1.5.2 Vpr

The 14 kDa Vpr protein is packaged at high levels into viral particles through interactions with the p6 domain of Gag. It has been implicated in mediating the transport of the PIC into the nucleus and more convincingly, it is involved in causing the arrest of infected cells while in the G2 phase of the cell cycle, which occurs within hours of infection (Goh et al., 1998; Zimmerman et al., 2006). This is when the HIV-1 LTR is most active and thus this action increases the rate of viral transcription and consequently gene expression. This appears to be dependent on the interaction between Vpr and the cellular receptor DCAF1 and subsequent recruitment of the Cullin4A-DDB1-Rbx E3 ubiquitin ligase complex (Hrecka et al., 2007; Schrofelbauer et al., 2007).

HIV-2 and the SIVs of both sooty mangabeys (SIVsm) and rhesus macaques (SIVmac) also encode a Vpx gene, which is thought to have arisen from a gene duplication of Vpr or else through recombination with the Vpr gene from the African green monkey SIV (SIVagm). In these viruses, the role of Vpr has been functionally divided between these two proteins, with Vpx being responsible for the infection of non-dividing cells and Vpr inducing cell cycle arrest (Freed and Martin, 2001). Vpx is also necessary for HIV-2 and SIVsm infection of macrophages and monocyte derived dendritic cells (Goujon et al., 2007), through counteraction of SAMHD1, a cellular restriction factor (see section 1.6.3).

1.6 Cellular restriction factors

As well as cellular proteins that have been co-opted by HIV-1 to facilitate its replication, several proteins have now been identified that are able to restrict replication of the virus at various different stages of its lifecycle. These factors form part of the innate immune system and as such, are often induced by Type 1 interferons. Importantly HIV-1, in most cases, has evolved countermeasures to circumvent these restrictive proteins [reviewed in (Malim and Emerman, 2008),], which has important consequences for the species tropism of this virus. The first such human restriction factor to be identified was the cytidine deaminase APOBEC3G and its family members. The following paragraphs summarise what is known about these cellular mediators of intrinsic resistance against HIV-1.

1.6.1 Trim5α

Trim5α was identified as the restriction factor that mediated the block to HIV-1 infection in Old World Monkeys (OWM) (Stremlau et al., 2004). Similar inhibition to N-tropic strains of MLV in human cells and HIV-1 and/or SIVmac infection in non-human primate cell lines, originally termed Ref1 and Lv1 respectively (Besnier et al., 2002; Cowan et al., 2002) were eventually recognised as species specific variants of Trim5α (Hatziioannou et al., 2004). The exact mechanism by which this protein mediates its restrictive phenotype is unclear. It has been shown to act early on in infection by binding to Capsid through its PRY-SPRY domain and interfering with the poorly defined process of viral uncoating. Since it possesses a RING domain, with E3 ubiquitin ligase activity, it was believed that it recruited retroviral cores to the proteasome where they are subsequently degraded. However, proteosomal inhibitors fail to rescue viral infectivity implying that a second block is also present, where reverse transcription products accumulate but fail to integrate [reviewed in (Towers, 2007)]. This latter mechanism is analogous to the effects of the murine restriction factor, Fv1, the first retroviral restriction protein to be identified. Human Trim5α only weakly inhibits HIV-1 most likely due to inefficient recognition and binding of Capsid (Towers et al., 2000).

The cellular protein Cyclophilin A (CypA), a peptidyl propyl isomerase, also plays a part in Trim5α mediated restriction, most probably by facilitating its binding to the viral Capsid protein [reviewed in (Sokolskaja and Luban, 2006)]. This is highlighted by the discovery of the TrimCyp fusion protein (Sayah et al., 2004), which also inhibits HIV-1,

and remarkably arose through a retrotransposition event independently in both New World Monkeys and Asian Macaques. TrimCyp restriction is dependent upon binding of CypA to Capsid. Intriguingly, in humans, CypA is necessary for the facilitation of viral infectivity but the reasons for this remain unclear. It has been proposed to protect the virus from an unidentified restriction factor, distinct from Trim5α (Sokolskaja et al., 2006) or it may act as a viral co-factor.

1.6.2 Tetherin

A second restriction factor, which acts against HIV-1 and a range of other enveloped viruses is tetherin (also called BST-2/CD317). This membrane bound, highly interferon inducible protein inhibits the release of fully formed mature HIV-1 particles from the cell surface, thereby preventing the spread of infection in a cell free system (Neil et al., 2008). These viruses can also be re-internalised and targeted to late endosomes for degradation although the precise molecular mechanisms of tetherin action are not yet fully understood. As tetherin is able to restrict the replication of a diverse array of enveloped viruses it is not thought to target any specific viral protein and instead may be packaged into virions and crosslink viral and cellular membranes (Hammonds et al., 2010). It had been known for some time that in certain cell lines, Vpu deficient HIV-1 viruses failed to detach from infected cells (Klimkait et al., 1990). It was subsequently shown that protease treatment could reverse this phenotype implying it was the result of a cellular protein (Neil et al., 2006), eventually identified as tetherin by microarray analyses comparing permissive and non-permissive cell types in the absence of Vpu (Neil et al., 2008). The mode of Vpu antagonism of tetherin is still incompletely defined. Similar to its effects on the CD4 receptor, it can downregulate tetherin from the cell surface and mediate its lysosomal degradation [reviewed in (Martin-Serrano and Neil, 2011)], which may also be dependent on the ESCRT protein HRS (Janvier et al., 2011). However, degradation of tetherin by Vpu is not necessary for its antagonistic effects and instead it may predominantely alter the sub-cellular trafficking of tetherin and sequester it away from sites of viral assembly (Dube et al., 2010; Dube et al., 2009; Mitchell et al., 2009; Van Damme et al., 2008).

Other retroviruses such as HIV-2 and the SIVs do not encode a Vpu protein and thus have utilised their Env (Gupta et al., 2009; Le Tortorec and Neil, 2009) and Nef (Jia et al., 2009; Zhang et al., 2009) proteins respectively to combat tetherin. However, the action of tetherin is not just restricted to retroviruses but also extends to the filovirus,

ebolavirus (Neil et al., 2007) and the DNA virus Kaposi's sarcoma associated herpesvirus (KSHV) among others. These viruses have also evolved their own antagonists of tetherin (Douglas et al., 2010; Kaletsky et al., 2009).

1.6.3 SAMHD1

It is well known that macrophages and more prominently dendritic cells are largely refractory to HIV-1 infection owing to a block imposed during reverse transcription. It has also been shown that the Vpx gene of SIVsm/HIV-2 can overcome this block to productive infection, although the identity of the restriction factor remained unknown (Goujon et al., 2007). Very recently, two groups have attributed this restriction to the action of the cellular protein SAMHD1 (Hrecka et al., 2011; Laguette et al., 2011). Vpx causes the ubiquitin mediated proteosomal degradation of this protein and knockdown of SAMHD1 increases the susceptibility of non-permissive cells to HIV-1. Unlike other restriction factors, HIV-1 has not evolved a means to counteract it.

Intriguingly SAMHD1 has also been implicated as a negative regulator of the interferon response (Rice et al., 2009) as has the cellular DNase TREX1 (Yan et al., 2010). This enzyme is involved in clearing excess cytoplasmic HIV-1 DNA from infected cells thereby avoiding activation of the Type 1 interferon response (Yan et al., 2010). Mutations in both of these proteins can lead to Aicardi Goutieres syndrome (AGS) (Crow et al., 2006; Rice et al., 2009), a genetic encephalopathy that mimics congenital viral infections. The exact mechanism of action of these proteins, particularly in terms of control of the innate immune response, requires further investigation but presents exciting challenges ahead in the area of intrinsic immunity.

1.6.4 APOBEC3G

It had long been established that the HIV-1 accessory protein, viral infectivity factor (Vif), was absolutely necessary for viral replication in CD4+ T cells, the natural targets of HIV-1 *in vivo*, as well as certain T cell lines such as Hut78 and CEM (termed non-permissive) but not in others such as CEM-SS and SupT1 (termed permissive) (Fisher et al., 1987; Gabuzda et al., 1992; Strebel et al., 1987; von Schwedler et al., 1993). It was also apparent that although the quantity of the virions produced was not altered in the absence of Vif, the quality of these virions, in terms of replication competence, was severely attenuated (Simon et al., 1998; Sova and Volsky, 1993). Heterokaryon analysis between a non-permissive and permissive cell line revealed that the non-permissive

phenotype was dominant demonstrating that it was attributable to the presence of a cellular inhibitory factor that Vif was able to circumvent (Madani and Kabat, 1998; Simon et al., 1998). Through a subtractive hybridisation screen comparing CEM, and its clonal derivative, CEM-SS cell lines, APOBEC3G (A3G) (originally named CEM15) was identified as the elusive inhibitory factor (Sheehy et al., 2002). It was expressed in all the non-permissive lines tested and ectopic expression in permissive cells rendered them unable to support HIV-1 delta *vif* (Δ*vif*) replication. In the presence of Vif, however, the restriction imposed by APOBEC3G was relieved (Sheehy et al., 2002). It was known that Vif and APOBEC3G activity was manifest in virus producing cells and subsequently it was shown that Vif is able to downregulate APOBEC3G protein levels and prevent its packaging into virions (Conticello et al., 2003; Marin et al., 2003; Mehle et al., 2004; Sheehy et al., 2003; Stopak et al., 2003; Yu et al., 2003), which is essential for its restrictive phenotype. It was later revealed that upon directly binding to A3G, Vif recruits an E3 ubiquitin ligase complex consisting of ElonginB, ElonginC, Cullin5 and Ring-box-2 (Yu et al., 2003). This induces the polyubiquitination and subsequent proteosomal degradation of A3G (Figure 1.5).

The interaction between A3G and Vif is a major determinant of the species tropism of HIV-1 and the related SIVs. Human APOBEC3G is sensitive to the actions of HIV-1 Vif but the mouse APOBEC3 protein as well as A3G from African green monkeys are resistant and therefore can be packaged into HIV-1 virions and mediate their restrictive effects (Mariani et al., 2003). Conversely, human A3G is not degraded by the Vif protein of SIVagm and therefore humans cannot be infected by this virus. Interestingly this species specificity appears to be dependent upon a single amino acid residue at position 128 of human A3G. Mutation of this residue (D128K) conferred resistance to degradation by HIV-1 Vif but rendered the protein susceptible to the effects of Vif from SIVagm (Schrofelbauer et al., 2004). Therefore it appears that viral Vif proteins have evolved to target the APOBEC3G proteins of their hosts, which thus governs zoonotic transmissions of these viruses.

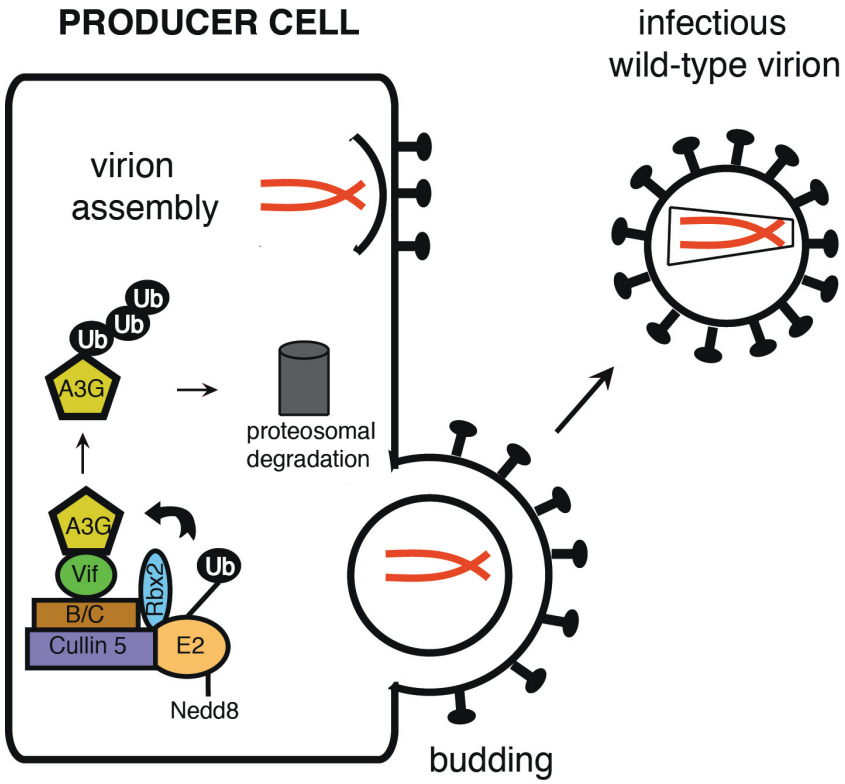

Figure 1.5: Vif mediated degradation of A3G.

In the presence of Vif, A3G is prevented from being incorporated into virions and is recruited instead to an E3 ubiquitin ligase complex consisting of ElonginB, ElonginC, Cullin 5 and Ring-box-2 (Rbx2), which mediates its polyubiquitination and hence proteosomal degradation.

1.7 APOBEC3 family of cytidine deaminases

1.7.1 Overview

APOBEC3G is a member of a family of cytidine deaminases, clustered on chromosome 22, that are named in relation to their founder member, Apolipoprotein B mRNA editing catalytic like polypeptide 1 (APOBEC1). Seven members of the APOBEC3 subfamily have been identified in higher primates, APOBEC3A (A3A), APOBEC3B (A3B), APOBEC3C (A3C), APOBEC3D/E (A3D/E), APOBEC3F (A3F), APOBEC3G (A3G) and APOBEC3H (A3H), which arose through several gene duplication events (Jarmuz et al., 2002). APOBEC3E was originally believed to be a pseudogene before it was realised that it is the C-terminal half of the APOBEC3D protein and is thus now named APOBEC3D/E. Therefore, A3B, A3D/E, A3F and A3G all contain two deaminase domains, although only the C-terminal half is usually catalytically active, with the N-terminal involved in nucleic acid binding (Navarro et al., 2005). The remaining APOBEC3 proteins (A3A, A3C and A3H) harbour only one deaminase domain (Figure 1.6A). These proteins are expressed in a variety of tissues and immune related cell types (Jarmuz et al., 2002; Koning et al., 2009; Refsland et al., 2010). This locus has undergone massive expansion in primates as only one APOBEC3 gene exists in mice (Harris and Liddament, 2004). The reason for this expansion is most probably due to ancient and now extinct exogenous retroviruses, whose remnants can still be detected in the human genome (Kazazian, 2004). This is supported by findings that the APOBEC3 proteins are under very strong levels of positive selection and have been throughout the history of primate evolution, long before the emergence of modern lentiviruses in the human population (Sawyer et al., 2004).

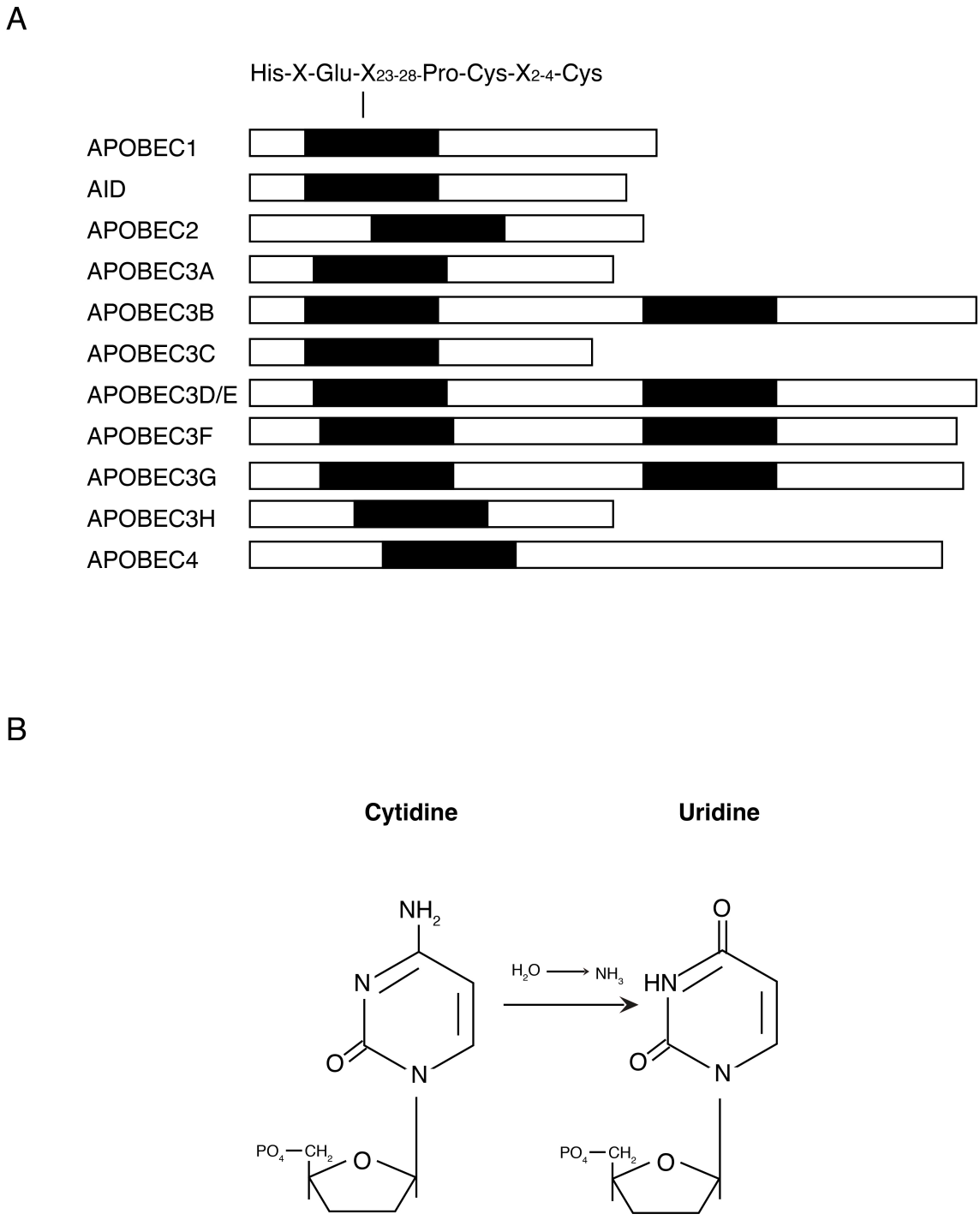

Figure 1.6: The human family of APOBEC cytidine deaminases.

A. There are eleven members of the APOBEC family including APOBEC1, AID, APOBEC2, APOBEC3A – H and APOBEC4. All proteins contain either one or two cytidine deaminase domains. **B**. The conversion of cytidine to uridine is a result of hydrolytic deamination of the C-4 position of the cytosine base. The process is catalysed by the APOBEC proteins and is referred to as editing. Adapted from (Holmes et al., 2007b).

1.7.2 Editing dependent means of viral inhibition

The discovery of A3G as an innate antiviral factor was concurrent with characterisation of the APOBEC3 family in terms of their enzymatic activity (Jarmuz et al., 2002). This independent finding hinted at a possible mechanism of A3G viral inhibition, through cytidine deamination, which was subsequently demonstrated in a bacterial editing assay (Harris et al., 2002a). The cytidine deaminase domain comprising a His-X-Glu-X-Pro-Cys-X-Cys motif provides catalytic potential for nucleophilic attack of the C4 position of the pyrimidine ring, causing a base change from cytidine to uridine in a process termed editing (Figure 1.6B). It is now well established that A3G is incorporated into nascent HIV-1 virions, in the absence of Vif, through interactions with the nucleocapsid region of Gag. This interaction is also dependent on cellular and/or viral RNA, postulated to be 7SL and genomic RNA, though this issue remains controversial at present (Bogerd and Cullen, 2008; Khan et al., 2005; Luo et al., 2004; Schafer et al., 2004; Svarovskaia et al., 2004; Wang et al., 2007; Zennou et al., 2004). The ability of A3G to oligomerise is also important for its encapsidation into virions (Burnett and Spearman, 2007; Huthoff et al., 2009) but this has also been disputed (Khan et al., 2009). In the viral core, A3G is able to associate with the reverse transcription complex (RTC) and upon entry into target cells mediates deamination of cysteine residues to uridines in nascent minus strand reverse transcripts. These register as guanosine to adenosine changes on the plus strand, which when occurring at a high rate [A3G induces approximately 1.5 - 1.7 changes per 100 bases, (Zhang et al., 2003)] is referred to as hypermutation (Harris et al., 2003a; Mangeat et al., 2003; Mariani et al., 2003; Zhang et al., 2003). This fits with data demonstrating that A3G preferentially acts on single stranded DNA substrates (Yu et al., 2004b). The extensive mutational burden leads to loss of sequence integrity and proviruses that no longer encode infectious progeny virions. The recovery of highly mutated reverse transcription products in the presence of A3G and in the absence of Vif, lends strong support to this mode of viral inhibition, as does the discovery of hypermutated sequences from HIV-1 infected individuals (Janini et al., 2001; Kieffer et al., 2005; Vartanian et al., 1991), which clearly illustrates the physiological relevance of A3G activity. In addition, it was originally hypothesised that the U bases may be recognised and excised by cellular DNA repair enzymes such as UNG2 and SMUG1, which would lead to degradation of the single stranded DNA as there is no complementary strand to act as a template (Harris et al., 2003b). This would explain the reduced accumulation of reverse

transcription products associated with Vif minus HIV-1 infection, in the presence of A3G (Bishop et al., 2006; Mangeat et al., 2003; Mariani et al., 2003). However, inhibition of UNG2 and/or SMUG1 did not affect A3G mediated HIV-1 Δ*vif* restriction, indicating that this particular cellular repair machinery is not important for this phenotype (Kaiser and Emerman, 2006; Langlois and Neuberger, 2008; Mbisa et al., 2007).

It has been proposed that low levels of A3G (and other APOBEC3) induced mutations may actually be advantageous to the virus as this contributes to sequence divergence, which may facilitate immune evasion and drug resistance (Jern et al., 2009; Mulder et al., 2008; Mulder et al., 2010; Sadler et al., 2010). Therefore, *in vivo,* the interplay between A3G and HIV-1 is clearly complex and often precariously balanced.

1.7.3 Editing independent means of viral inhibition

Although editing dependent mechanisms of A3G retroviral restriction are clearly important both *in vitro* and *in vivo*, other means of inhibition are also evident. This is based on findings that A3G mutants that are no longer catalytically active, as demonstrated in bacterial editing assays, can still inhibit HIV-1 (Holmes et al., 2007b; Newman et al., 2005). Recovered viral cDNAs were not hypermutated, although these mutants were still packaged into virions. This conclusion is further supported by studies demonstrating that APOBEC3 inhibition of other viruses and retroelements may not be fully or even partially dependent on editing as once again, highly mutated sequences are not always readily detectable (Bogerd et al., 2006; Nguyen et al., 2007; Sasada et al., 2005; Stenglein and Harris, 2006). Alternative means of inhibition have thus been sought and it has now been hypothesised that A3G may directly interfere with the movement of reverse transcriptase along its RNA template (Bishop et al., 2008). Reverse transcription was shown to initiate but elongation was impeded in an A3G dose dependent manner. This model of steric hindrance would also account for the lack of accumulation of reverse transcription products (Bishop et al., 2008). Thus the mechanism of A3G mediated viral restriction may be more multi-faceted than originally perceived and whether other mechanisms also exist remains to be determined (Figure 1.7).

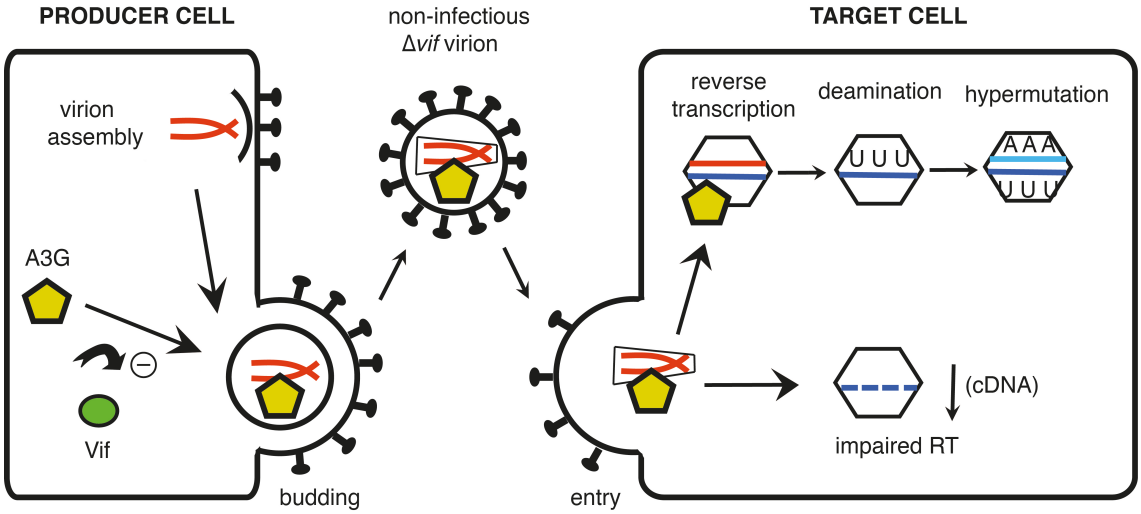

Figure 1.7: APOBEC3G mediated inhibition of HIV-1.

In the producer cell, in the absence of Vif, APOBEC3G (A3G) is packaged into budding virions. Upon entry into the target cell, it can mediate its anti-viral effect by one of two mechanisms. Firstly, it can deaminate cytidines to uridines in minus reverse strand transcripts, thus causing hypermutation of the viral DNA. Secondly, it may directly interfere with the elongation of reverse transcripts thus causing a decrease in viral cDNA levels.

1.7.4 Inhibition of HIV-1 by the APOBEC3 proteins

Whether any of the other APOBEC3 proteins possess anti-viral activity against HIV-1 has been an issue of intense investigation. APOBEC3F was quickly shown to inhibit HIV-1 replication, though not nearly as potently as A3G (Bishop et al., 2004; Wiegand et al., 2004). Although these proteins share almost 50% sequence identity, they differ in several respects. Firstly, the preferred nucleotide sequence context for cytidine deamination is different between these proteins. A3G preferentially deaminates in a C<u>C</u> dinucleotide context (Bishop et al., 2004; Harris et al., 2003a; Suspene et al., 2004; Yu et al., 2004b), while A3F, along with the other APOBEC3 proteins, targets T<u>C</u> dinucleotide sequences (edited base is underlined) (Liddament et al., 2004). Secondly, although A3F is able to associate in large ribonucleoprotein (RNP) complexes, which have a similar composition to those within which A3G is contained (see section 1.9), there is the noticeable absence of small RNAs, with the exception of Alu RNAs (Gallois-Montbrun et al., 2008). This is of interest as it has been reported that 7SL RNA is necessary for A3G virion incorporation, which would suggest that A3G and A3F are packaged by alternate means. However the role of 7SL RNA in A3G packaging is highly controversial and others have reported that A3F does in fact interact with this RNA (Wang et al., 2008). Also, A3F associated RNP complexes appear to be more resistant to RNase treatment implying that either the RNA components are shielded or that the majority of interactions occur by direct protein-protein binding (Gallois-Montbrun et al., 2008). Finally, it has been argued that non-editing mechanisms of viral inhibition may be more important for A3F restriction than for A3G (Holmes et al., 2007a). The basis for these differences remains to be resolved. Nevertheless, similar to A3G, A3F is also Vif sensitive (Wiegand et al., 2004), is expressed in CD4+T cells and hypermutated sequences displaying A3F preferred sequence contexts have been recovered from infected individuals (Liddament et al., 2004), indicating that these proteins may act in concert to co-ordinate anti-viral defence during a natural infection. However, its *in vivo* relevance to HIV-1 resistance has recently been questioned (Miyagi et al., 2010; Mulder et al., 2010).

The anti-HIV-1 activities of the remaining APOBEC3 proteins are not so definitive. On the whole A3A and A3C are not thought to possess any HIV-1 restrictive capabilities (Bishop et al., 2004) but there is some contradictory data on this issue. A3C is considered by some to have very weak activity, is reported to be packaged into virions and degraded by Vif (Langlois et al., 2005; Rose et al., 2005), whereas A3A may mediate restriction of viruses in myeloid cells (Berger et al., 2011; Peng et al., 2007). A3B and A3D/E have also been shown to have some anti-HIV-1 activity though the magnitude and relevance of their effects is somewhat controversial (Dang et al., 2006; Doehle et al., 2005; Duggal et al., 2011; Rose et al., 2005). Four different haplotypes of A3H exist in the human population with only one of these, haplotype 2, producing a stable protein, which is anti-viral (OhAinle et al., 2008). This may explain the earlier discrepancies regarding the anti-viral nature of this protein (Dang et al., 2008; OhAinle et al., 2006). Like A3F and A3G, A3D/E is sensitive to Vif, whereas A3H is only partially sensitive (OhAinle et al., 2008) and A3B appears to be resistant (Doehle et al., 2005). The Vif insensitive nature of A3B can be explained by the fact that it is primarily expressed in B cells (Koning et al., 2009) and is therefore unlikely to encounter HIV-1 during the course of a natural infection. All APOBEC3 proteins are reportedly incorporated into assembling virions (Dang et al., 2008; Dang et al., 2006; Goila-Gaur et al., 2007; Wiegand et al., 2004; Yu et al., 2004a). Recently, a comprehensive analysis of the anti-viral activities of all seven APOBEC3 family members was reported and found that only A3G, A3F, A3D/E and A3H were inhibitory to HIV-1. Further these proteins were all expressed in CD4+T cells, packaged into virions and sensitive to degradation by Vif (Hultquist et al., 2011).

1.7.5 Inhibition of other viruses

Nevertheless, the APOBEC3 proteins are not solely inhibitors of HIV-1 as A3G and A3F inhibit equine infectious anemia virus (EIAV) and MLV (Bishop et al., 2004; Bogerd et al., 2008; Zheng et al., 2004; Zielonka et al., 2009) and all APOBEC3s, apart from A3A, restrict the SIVs of rhesus macaque and African green monkeys (Dang et al., 2006; Yu et al., 2004a). Another retroviral substrate is primate foamy virus (PFV), which is targeted by A3F and A3G (Russell et al., 2005). Aside from retroviruses, they can also inhibit the replication of the DNA virus, hepatitis B virus (HBV), which undergoes an obligate intracellular reverse transcription step in its life cycle, converting its RNA genome into a partially double stranded form inside core particles in producer

cells. All APOBEC3s, apart from A3A and A3H restrict HBV, which may or may not be the result of editing (Nguyen et al., 2007; Suspene et al., 2005; Turelli et al., 2004). A3A has also been shown to inhibit adeno associated virus (AAV) (Chen et al., 2006) and human papilloma virus (HPV), the latter of which is also targeted by A3C and A3H (Vartanian et al., 2008). Interestingly these proteins have all been found to be predominantly nuclear (Muckenfuss et al., 2006). Nuclear localisation may also influence the restriction of the LINE-1 retroelement, which is most potently inhibited by A3A and A3B (Bogerd et al., 2006; Chen et al., 2006). These proteins may be able to directly interfere with the process of target primed reverse transcription which for this retrotransposon occurs at the site of integration and hence in the nucleus. However, other APOBEC3 proteins (A3C, A3F and A3H) also limit the activity of this retrotransposon (Stenglein and Harris, 2006), which subsequently impacts upon Alu retrotransposition as they depend on LINE-1 encoded proteins for their replication. A3G, on the other hand, only weakly inhibits LINE-1 but is able to restrict Alu retrotransposition by potentially sequestering these elements in high molecular weight complexes, away from the LINE-1 machinery (Chiu et al., 2006). APOBEC3 proteins have also been demonstrated to restrict the retrotransposition events of retrotransposons from both mice and yeast (Esnault et al., 2005). The anti-viral effects of the different human APOBEC3 proteins for a range of known substrates are summarised in Table 1.1 [and see (Chiu and Greene, 2008)].

Table 1.1: Anti-viral activities of the human APOBEC3 proteins.

APOBEC3 Protein	No.of Domains	Inhibition of retroviruses	Inhibition of other viruses	Inhibition of retrotransposons
A3A	1	HIV-1 (myeloid cells)	AAV, HPV	LINE-1, Alu, IAP, MusD
A3B	2	HIV-1, SIV,	HBV	LINE-1, Alu, IAP, MusD
A3C	1	SIV, PFV	HBV, HSV-1, HPV	LINE-1, Alu, IAP, MusD, Ty1
A3D/E	2	HIV-1, SIV		
A3F	2	HIV-1, SIV, MLV PFV	HBV	LINE-1, IAP, MusD, Ty1
A3G	2	HIV-1, SIV, MLV, EIAV, PFV	HBV	Alu, IAP, MusD, Ty1
A3H	1	HIV-1	HPV	LINE-1, Alu

The fact that they form part of a broad antiviral immune response is highlighted by their upregulation upon interferon alpha stimulation. Although A3DE, A3F, A3G and A3H show modest increases at the RNA level in CD4+T cells, macrophages and dendritic cells, A3A shows a much more substantial increase at both the RNA and protein levels (Koning et al., 2009). This would indicate its prominent involvement in first line anti-viral defence though its exact contribution requires further exploration. It has recently been proposed that several of the APOBEC3 proteins, particularly A3A, are able to mediate the clearance of foreign DNA from cells in response to interferon stimulation through editing dependent means (Stenglein et al., 2010). This helps protect the cell from aberrant DNA, viral or otherwise. The authors found that cellular genomic DNA was not targeted, implying a degree of specificity to the actions of the APOBEC3 proteins. However, it has recently been reported that A3A is able to deaminate nuclear DNA (Suspene et al., 2011a).

1.8 Other APOBEC proteins

1.8.1 APOBEC1

APOBEC1 is an RNA editing enzyme that preferentially edits the mRNA encoding the ApoB protein. It binds to its target RNA through recognition of an 11 nucleotide 'mooring sequence' which is essential for editing (Shah et al., 1991). It introduces a stop codon into the transcript, generating two protein products, both of which are involved in lipid transport in the blood [reviewed in (Keegan et al., 2001)]. APOBEC1 works in conjunction with a co-factor termed APOBEC1 complementation factor (ACF) (Mehta et al., 2000), which acts to suppress nonsense mediated decay (NMD) of the edited RNA and may recruit APOBEC1 to its target RNA (Chester et al., 2003). Additional targets of APOBEC1 have also now been identified with editing target sites primarily located in AU rich regions of the 3'UTR (Rosenberg et al., 2011). APOBEC1 has a very limited tissue distribution and appears to be restricted to the small intestine, whereas ACF displays wider expression (Mehta et al., 2000). Unlike its closely related APOBEC3 family members it does not appear to be involved in the restriction of exogenous viruses.

Murine and rat APOBEC1 are also involved in the stabilisation of mRNAs containing AU rich elements (ARE) within their 3'UTRs. These AU rich sequences serve to post-

transcriptionally modify protein expression through binding of cellular proteins that can either induce the stabilisation or degradation of these mRNAs (see section 1.11.6). Targets of murine APOBEC1 include c-myc RNA and cyclooxygenase 2 (Cox-2) (Anant and Davidson, 2000; Anant et al., 2004). Analagous activity has not yet been reported for the human protein.

1.8.2 AID

AID (Activation Induced Deaminase) is expressed in B cells and stem cells and is involved in fundamental processes relating to antibody diversification, namely somatic hypermutation, class switch recombination and gene conversion (Arakawa et al., 2002; Harris et al., 2002b; Martin et al., 2002; Muramatsu et al., 2000). Mutations in AID lead to immunodeficiencies characterised by the presence of solely IgM antibodies (hyper IgM) (Muramatsu et al., 2000). Initially it was assumed that AID, like APOBEC1 would target RNA substrates, as these proteins share several similar features. However, it is now known that AID, like the APOBEC3 proteins, edits single stranded DNA (Bransteitter et al., 2003). Similar to APOBEC1, AID achieves its function with the help of a co-factor, this time replication protein A (RPA), a single stranded DNA binding protein with roles in RNA metabolism (Chaudhuri et al., 2004).

1.8.3 APOBEC2 and APOBEC4

In comparison, relatively little is known about the remaining family members, APOBEC2 and APOBEC4. APOBEC2 is expressed exclusively in heart and skeletal muscle cells but mice lacking this protein show no defects in development, survival or fertility (Mikl et al., 2005). It may possess some cytidine deaminase activity, albeit weak, though the relevance of this in terms of function and target substrates has not yet been addressed (Liao et al., 1999). However, the fact that it is subject to negative or purifying selection (Sawyer et al., 2004) suggests that it does have an important functional role. APOBEC4 was discovered via computational prediction methods (Rogozin et al., 2005) and interestingly it is primarily expressed in the testes, postulating a potential role in defence of the germline. However, its editing capabilities are currently unknown.

1.9 APOBEC3 proteins and ribonucleoprotein (RNP) complexes

The fact that all of the APOBEC3 proteins are catalytically functional raises the important question of how their enzymatic activities are regulated such that they do not erroneously mutate cellular nucleic acid. Although A3A has very recently been reported to edit such DNA, other APOBEC3 proteins that also localise to the nucleus were not found to have the same effect (Suspene et al., 2011a). As has been mentioned the APOBEC3 proteins may be involved in targeting and editing foreign DNA, which would have to be differentiated from that of host DNA as no mutations in genomic DNA were found (Stenglein et al., 2010). It has also been reported that in certain cell lines which express high levels of A3G, for instance, only very moderate amounts are found incorporated into Δ*vif* virions, implicating the existence of cellular and/or viral regulatory mechanisms (Rose et al., 2005). A3F and A3G associate in high molecular mass (HMM) ribonucleoprotein (RNP) complexes under normal cellular conditions. Chiu *et al* have reported that A3G contained within these complexes is enzymatically inactive and its function is only restored upon dissolution of the complex through RNase treatment (Chiu et al., 2005). Similarly, A3G's interaction with viral RNA in virions has been suggested to repress its deaminase activity. Only during reverse transcription, when the RNA is degraded by the RNase H activity of RT is A3G liberated to edit the nascent cDNA transcript (Soros et al., 2007). Relevantly, the activities of both APOBEC1 and AID are regulated by cellular RNA (Bransteitter et al., 2003; Sowden et al., 1996). For example, in order for AID to target single stranded DNA substrates it must first be pre-treated with RNase in order to remove inhibitory bound RNA (Bransteitter et al., 2003). A similar finding has recently been published for A3G (McDougall and Smith, 2011). These examples highlight the importance of interactions with cellular and viral components for functional regulation and highlight the many levels at which this regulation can occur.

Several groups have therefore sought to identify the specific protein and RNA compositions of these complexes to gain better insight into APOBEC3 function. The identification of these interacting factors may help uncover the determinants of the substrate specificities of the different APOBEC3 proteins, their involvement in cellular processes and potential cellular co-factors, all of which remain largely uncharacterised. Through a combination of affinity purifications, mass spectrometry and co-immunoprecipitations, a large number of A3F and A3G associated proteins have now

been identified (Chiu, 2011; Chiu et al., 2006; Gallois-Montbrun et al., 2008; Gallois-Montbrun et al., 2007; Kozak et al., 2006; Wichroski et al., 2006). Predominantly these are RNA binding proteins, involved in the metabolism and turnover of RNA, implying that the APOBEC3 proteins may contribute to the regulation of RNA. Although the majority of these interactions were bridged by RNA, the Argonaute proteins appeared to interact with A3F and A3G in a partially RNase insensitive manner (Gallois-Montbrun et al., 2008; Gallois-Montbrun et al., 2007), suggestive of a close and potentially direct interaction, although this was not reproduced by another group (Wichroski et al., 2006). The APOBEC3 proteins also co-localised with the Argonautes and a subset of other identified associated cellular factors to cytoplasmic foci termed mRNA Processing Bodies (P-bodies, discussed in more detail in section 1.10.1) in both primary cells and cell lines (Gallois-Montbrun et al., 2007; Wichroski et al., 2006). The Argonaute proteins are fundamental components of the RNA induced silencing complex (RISC), which is involved in the post-transcriptional control of gene expression through small non-coding RNAs, both microRNAs (miRNAs) and small interfering RNAs (siRNAs) (see section 1.11.1). The functional relevance of this interaction has yet to be determined but it has been reported that the APOBEC3 proteins can inhibit miRNA and siRNA mediated regulation of protein expression (Huang et al., 2007a), thus attributing an antagonistic role to the APOBEC3 proteins in this cellular pathway. However, these findings have yet to be independently verified.

Therefore the full functional roles of the APOBEC3 proteins, both cellular and anti-viral, have yet to be determined, as well as the basis for the underlying differences in anti-viral activities and target substrate specificities. The identification of associated proteins involved in a diverse array of functions relating to RNA regulation may provide some insight into helping address these outstanding issues but requires further exploration.

1.10 Cytoplasmic foci

1.10.1 mRNA Processing bodies (P-bodies)

The dynamic equilibrium between translation and decay is an important mechanism in the control of gene expression. mRNAs exiting the nucleus may be translated immediately, degraded or be diverted into a state of repression, followed by either translation or decay. These differential fates of an mRNA transcript will be governed by changing cellular requirements in response to both internal and external stimuli.

An mRNA marked for degradation requires removal of the pre-initiation complex consisting of the small 40S ribosomal subunit, eIF4F factors (eIF4A, eIF4E, eIF4G) and the poly A binding protein (PABPC1), among others, and formation instead of a translationally repressed messenger ribonucleoprotein (mRNP) complex. The first step in this process is removal of the 3'-polyadenosine [poly(A)] tail in a process called deadenylation. In mammalian cells this is initiated by the PARN2-PARN3 poly(A) nucleases and continued by the CCR4/Pop2/Not complex of deadenylases. This is then followed by degradation which can occur by one of two pathways in eukaryotic cells. The first is mediated by a series of 3' - 5' exonucleases, termed the exosome, which executes decay of the RNA from the 3' end. Alternatively, the mRNA may first be decapped by the Dcp1a/Dcp2 decapping enzymes and several co-activators such as DDX6, Lsm1, Ge1, Pat1 and EDC3, and is then subject to 5' - 3' exonucleolytic degradation by Xrn1 [reviewed in (Parker and Song, 2004)]. These two pathways appear to be spatially segregated as components of the latter, as well as several deadenylases (Zheng et al., 2008), have been found to concentrate in non-membraned cytoplasmic foci termed mRNA Processing Bodies (P-bodies) (Cougot et al., 2004; Sheth and Parker, 2003). These RNP aggregates have been implicated in the storage and/or decay of untranslated mRNA and thus components of several post-transcriptional regulatory pathways have also been identified in P-bodies. These include miRNAs, siRNAs, the Argonaute proteins, GW182 and Mov10 (miRNA/siRNA mediated silencing) (Eystathioy et al., 2003; Liu et al., 2005b; Meister et al., 2005); Upf1, Upf2, Upf3 and SMG-7 (nonsense mediated decay) (Sheth and Parker, 2006); TTP, FXR1 and Brf1 (ARE mediated decay) (Franks and Lykke-Andersen, 2007). These pathways will be discussed in more detail in the following sections. Intriguingly, several APOBEC3 proteins have also been found associated with P-bodies, including A3F and A3G (Gallois-Montbrun et al., 2008; Gallois-Montbrun et al., 2007; Niewiadomska et al.,

2007; Wichroski et al., 2006). The relevance of their localisation to these structures however, remains to be determined. P-bodies are further characterised by the relative absence of ribosomes and translation initiation factors, except for eIF4E. However, it is most likely to be in an inactive state as its binding partner and functional antagonist, eIF4E-T, co-localises with it to these foci (Andrei et al., 2005).

P-bodies are highly conserved and in yeast they consist of a similar, though not identical, protein composition. There are no GW182 or Ge1 homologues in yeast, nor is there a functional miRNA pathway. Further, although Lsm1 depletion leads to loss of P-bodies in human cells, in yeast it results in an increase in their size and number, indicating that even if the same proteins are present they may not function in the same way (Teixeira and Parker, 2007). What is absolutely fundamental, however, is the presence of RNA. The formation of P-bodies is dependent upon the pool of untranslated mRNA (Teixeira et al., 2005) and drugs which inhibit translation initiation (eg puromycin) result in larger P-body formation. Conversely, those that inhibit translation elongation, such as cyclohexamide, decrease the size and number of P-bodies (Brengues et al., 2005; Teixeira et al., 2005). Further, partially purified P-body fractions are disassembled upon treatment with RNase (Teixeira et al., 2005) indicating that RNA is necessary for structural integrity.

Nevertheless, the manner in which P-bodies assemble is not fully understood. It is most likely based on associations between RNA and proteins and several P-body proteins have been shown to interact either directly or indirectly via co-immunoprecipitation and yeast 2 hybrid analysis (Hock et al., 2007; Landthaler et al., 2008; Meister et al., 2005; Zheng et al., 2011). Intriguingly, several P-body proteins contain a glutamine/asparagine (Q/N) rich like prion domain which may allow the self aggregation of proteins such as GW182 and Ge1 both of which are essential for P-body formation (Jakymiw et al., 2005; Reijns et al., 2008; Yu et al., 2005). These proteins may then act as scaffolds with which other proteins could interact, which is analogous to the assembly of the closely related stress granule structures (discussed in section 1.10.2). Also some components appear to be more important than others as knockdown of DDX6 or Lsm1 but not EDC3, will cause the dissolution of visible P-bodies. This may be related to their effects on translation, as P-body formation may be dependent on a critical mass of untranslated mRNA. Thus, DDX6, which is a known translational

repressor may impact upon this threshold more than other proteins [reviewed in (Parker and Sheth, 2007)].

It has also been suggested that different populations of P-bodies may exist within the cell and may serve to segregate the repressive and degradative functions of these structures. This is based on the observation that although GW182 and Dcp1a co-localise and interact with a variety of P-body proteins, the foci that they mark only partially overlap, which implies they represent two separate pools of mRNP complexes (Gibbings et al., 2009). Further, different types of P-bodies may be present at different stages of the cell cycle, which has been noted in yeast as well as in human cells (Teixeira et al., 2005; Vasudevan et al., 2008; Yang et al., 2004). In yeast, P-bodies are highly sensitive to cellular stress, with the size and number of these foci increasing in response to external stimuli with a concomitant decrease in translation rates. In human cells, several P-body components, such as the Argonautes and DDX6, re-localise to stress granules during periods of cellular stress. This highlights the very dynamic and mobile nature of P-bodies with proteins continually shuttling between these foci and the diffuse cytoplasm. In fact, it has been reported that for Ago2, only 1.3% of the total amount of cellular protein is in P-bodies at any one time (Leung et al., 2006). Therefore even though the local concentration is high in P-bodies, it may represent only a small fraction of the total cellular pool.

1.10.2 Stress granules (SGs)

Related to P-bodies, though distinct foci found in human cells are stress granules (SGs), which are rapidly and reversibly formed in response to cellular stresses such as heat shock. Stress granules are conserved in *S. pombe* but are not found in *S. cerevisae*. In response to stress, mRNAs encoding housekeeping proteins are translationally repressed while those encoding proteins involved in the stress response such as molecular chaperones and damage repair enzymes are preferentially translated (Kimball et al., 2003).

Formation of SGs is triggered by phosphorylation of eIF2α by one of several stress induced kinases, such as protein kinase R (PKR). This results in ribosome run off whereby stalled initiation complexes assemble on the mRNA, leading to the disassembly of polysomes and hence inhibition of translation initiation (Kedersha et al., 1999). These complexes are then targeted to SGs, supported by the fact that several

translation initiation factors such as eIF2, eIF3, eIF4E and eIF4G, PABPC1 and the small 40s ribosomal subunit have been found to localise to them (Buchan and Parker, 2009). SG assembly is dependent upon self-aggregation of RNA binding proteins such as TIA-1 and G3BP, which are also involved in RNA metabolism. They aggregate through their glutamine rich prion like domains and thus form a scaffold on which other proteins can assemble (Gilks et al., 2004). Other components of SGs include FXR1, HuR and TTP, proteins associated with ARE mediated RNA regulation (see section 1.11.6). Upon relief of the stress, SGs disassemble and normal translation is resumed with mRNAs released back into the cytoplasm or targeted to P-bodies. Certain P-body proteins have been identified in or re-localise to SGS during their formation including the Argonaute proteins, DDX6 and Xrn1 (Buchan and Parker, 2009), though the implications of this are not known and in fact the majority of these proteins may be re-directed from the cytoplasm rather than from P-bodies. Other proteins such as GW182 and Dcp1a are exclusively associated with P-bodies (Anderson and Kedersha, 2006). In many ways, P-bodies and SGs are intimately linked. Both are dependent on untranslated mRNA for their maintenance and SGs are similarly affected by inhibition of translation initiation and elongation as observed for P-bodies (see section 1.10.1). Also these foci are often in close physical proximity (Kedersha et al., 2005). Arsenite treatment, for instance, results in the assembly of P-bodies and SGs that are physically connected, but how material is exchanged between them is not well understood. Translationally repressed mRNAs may be targeted to SGs for translation initiation complex formation before being directed to polysomes. On the other hand, mRNAs in SGs may be sent to P-bodies for degradation. Most probably, components shuttle bi-directionally between both structures dependent upon cellular requirements (Balagopal and Parker, 2009).

1.11 Post-transcriptional regulatory pathways

Once an mRNA has been transcribed it can either be translated into protein or may be subject to several post-transcriptional regulatory mechanisms that serve to regulate gene expression at the RNA level. These processes allow the cell to rapidly respond to changing environmental conditions and external stimuli, such as viral infection, by fine tuning expression of individual genes (Bartel and Chen, 2004). The preceding sections will serve to outline the cellular RNA regulatory pathways of miRNA mediated translational repression, ARE-mediated decay and nonsense mediated decay, and highlight their close interplay in the control of RNA.

1.11.1 miRNA mediated translational repression

microRNAs (miRNAs), small interfering RNAs (siRNAs) and PIWI-interacting RNAs (piRNAs) are three types of small non-coding, endogenously encoded RNAs that serve to regulate both cellular and foreign RNA transcripts. Although they are closely related and interact with similar complexes of proteins to mediate their effects, their biogenesis and mechanisms of actions, as well as their target RNAs appear to be somewhat distinct.

miRNAs are approximately 18 - 22 nucleotides long and are conserved from plants to mammals. Approximately 1000 miRNAs have been described thus far in humans and more than 60% of all cellular mRNAs are predicted to be targets of miRNAs (Sayed and Abdellatif, 2011). They have been implicated in influencing a number of cellular processes including cell proliferation, differentiation, apoptosis, development and the stress response (Bushati and Cohen, 2007). The importance of miRNA control is highlighted by their dysregulation, which is often associated with diseases such as cancer (Farazi et al., 2011).

miRNAs are found mostly within introns and are transcribed, like cellular mRNAs, by RNA polymerase II. This yields a primary miRNA transcript (pri-miRNA) containing a stem loop structure. This transcript is first processed in the nucleus by the RNase III enzyme Drosha (Lee et al., 2003; Lee et al., 2002) and its binding partner, DGCR8/Pasha, which cleave the hairpin structure to generate a pre-miRNA precursor. The 2 nt 3' overhang created by this cleavage event is recognised by Exportin 5, which directs its transport out of the nucleus and into the cytoplasm (Lund et al., 2004; Yi et al., 2003). A second processing event then occurs, this time mediated by the RNase III enzyme Dicer (Hutvagner et al., 2001) and its interacting partners TAR RNA binding

protein (TRBP) and PKR associated protein activator (PACT). This produces a double stranded duplex which is unwound to release the two strands, one of which is subsequently degraded (Schwarz et al., 2003). However, recent reports in *Drosophila* suggest that both strands may in fact be functionally active (Czech et al., 2009; Ghildiyal et al., 2010; Okamura et al., 2009)). The remaining strand, termed the guide strand, is incorporated into an RNA induced silencing complex (RISC) (Gregory et al., 2005; Hammond et al., 2001), recruited by TRBP. Minimally RISC comprises one member of the Argonaute protein family and the miRNA. The miRNA will then guide RISC to the target mRNA based on sequence complementarity of its seed region (between the 2nd and 8th base) with the 3'UTR of the mRNA (Hutvagner and Zamore, 2002). Perfect complementarity results in endonucleolytic cleavage mediated by Argonaute 2 (Martinez and Tuschl, 2004), the only catalytically active Argonaute protein in mammals (Liu et al., 2004; Meister et al., 2004). However endogenous mammalian miRNAs tend to be imperfectly base-paired with their targets and are thus translationally repressed and usually degraded by any one of the four Argonaute proteins expressed in humans (Figure 1.8). The lack of necessity for perfect homology between the miRNA and its target means that one miRNA can potentially influence the expression of hundreds of mRNAs within the cell.

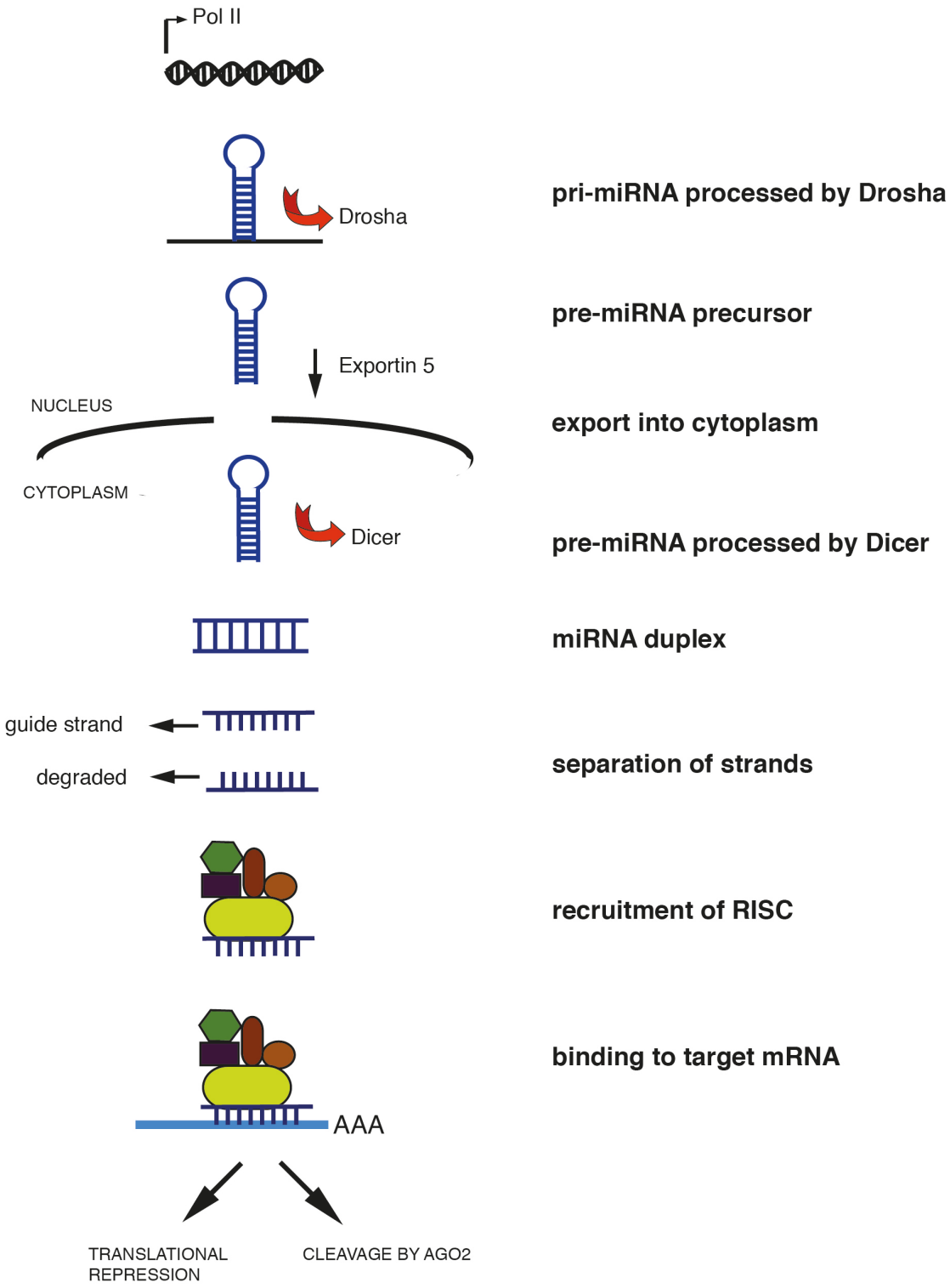

Figure 1.8: miRNA biogenesis and mechanism of action.

miRNAs are transcribed by RNA Pol II into pri-miRNA precursors and are subsequently processed by the RNase III enzyme Drosha and exported into the cytoplasm as a pre-miRNA. This is then processed by the RNase III enzyme Dicer, which cleaves the hairpin structure to yield a miRNA duplex. The two strands are unwound and the guide strand is incorporated into RISC and directs its binding to the 3'UTR of the target mRNA. The degree of complementarity between the miRNA and the mRNA determines whether the mRNA is cleaved by Argonaute 2 or translationally repressed and subsequently degraded.

The mechanism of translational repression, instigated by the Argonaute proteins, is very poorly understood and highly controversial [reviewed in (Eulalio et al., 2008a)]. It has been proposed that translation initiation is inhibited, as cap independent translation is not affected by miRNAs. The mode of inhibition has been attributed to direct competition between Ago2 and the eIF4E translation initiation factor for binding to the m7G Cap (Kiriakidou et al., 2007). However, these findings have since been challenged (Eulalio et al., 2008b). It is also possible that a step after translation initiation is affected, such as elongation, summarised by the ribosome drop off model where ribosome binding to mRNA transcripts is of low affinity and hence short lived. The controversies surrounding this issue may imply that a multitude of mechanisms may exist that are dependent on the specific miRNAs and mRNAs involved as well as the cellular conditions. However, other cellular factors have also been shown to be necessary for miRNA mediated repression, most prominently GW182 (Jakymiw et al., 2005; Liu et al., 2005a; Meister et al., 2005). This protein directly interacts with the Argonautes yet it can independently mediate effects that promote translational repression (Behm-Ansmant et al., 2006; Li et al., 2008). This is reportedly a result of its interaction with PABPC1 and subsequent recruitment of the CCR4-NOT deadenylase complex (Zekri et al., 2009)

Repressed transcripts may be temporarily stored at P-bodies. Importantly, this can be a reversible process where, if cellular conditions permit, these mRNAs can be released back into the cytoplasm for translation. For example, the Cat1 mRNA, targeted by the mir122 miRNA, is translationally repressed and stored in P-bodies. Upon cellular stress, however, the mRNA is released from P-bodies and transported to polysomes with the aid of the ARE-rich-element (ARE) binding protein HuR (Bhattacharyya et al., 2006). Aside from cleavage and repression, mRNAs may also be degraded by the 5’ - 3’ exoribonuclease Xrn1, in P-bodies. Recently, miRNAs have also been implicated in promoting mRNA translation indicating that their affects are not solely limited to downregulation of protein expression (Vasudevan et al., 2007b).

1.11.2 Other small non-coding RNAs

As mentioned, other small non-coding RNAs also exist. siRNAs (approximately 21-23 nt in length) are transcribed from long double stranded RNA and subsequently processed by Dicer (Kim et al., 2009). siRNAs are nearly always identical to their RNA targets and are thus dependent on Argonaute 2 and endonucleolytic cleavage for silencing, in a process commonly referred to as RNA Interference (RNAi). It was widely believed that animals, unlike plants and fungi, did not encode siRNAs. Recently, however, endo-siRNAs have been identified in the germline of mice (Tam et al., 2008; Watanabe et al., 2008) and the germline and somatic cells of flies (Czech et al., 2008; Ghildiyal et al., 2008; Kawamura et al., 2008; Okamura et al., 2008) that are products of Dicer processing. It is believed that these endo-siRNAs depend upon Ago2 for silencing and primarily function to target transposable elements, thereby protecting cells from their deleterious effects. This is analogous to the actions of piRNAs present in the germline of both flies and mammals (Aravin et al., 2006; Girard et al., 2006; Grivna et al., 2006; Lau et al., 2006). These RNAs are typically longer than miRNAs and siRNAs, at 26 – 31 nucleotides in length. They are encoded in areas of the genome that also contain fragments of transposable elements thus generating antisense transcripts directed at these mobile genetic elements (Aravin et al., 2007; Klattenhoff and Theurkauf, 2008). In contrast to endo-siRNAs, however, piRNAs are generated by a Dicer independent mechanism (Vagin et al., 2006) and associate with a separate sub-family of Argonaute proteins, termed PIWI proteins, to mediate silencing. Nevertheless this highlights the close interplay and overlapping functions of small non-coding RNAs.

1.11.3 Argonaute proteins

The Argonaute proteins are fundamental components of the RISC complex which mediates miRNA mediated translational repression and RNAi. Because of this they are highly conserved from plants to mammals, though they differ in number. Fission yeast have only one Argonaute protein, for example, whereas *C. elegans* has twenty-four. In humans, eight members of the Argonaute protein family have been identified (Sasaki et al., 2003) and are equally divided into two sub-families; the Argonaute proteins which are ubiquitously expressed and the PIWI proteins whose expression is restricted to the germline but are still involved in RNA silencing (see section 1.11.2).

The four Argonaute proteins expressed in human somatic cells, Argonautes 1 - 4, share approximately 80% amino acid sequence identity (Sasaki et al., 2003). The structure of

these proteins can be divided into four main domains; the N-terminal, PAZ, PIWI and MID domains. Crystal structures of the full length Argonaute protein from *P.furiosis* (Song et al., 2004) and the PAZ domains of the *Drosophila* Argonaute proteins (Lingel et al., 2003; Song et al., 2003; Yan et al., 2003) have shed light on the contributions of these domains to Argonaute function. The MID domain forms a highly basic pocket and binds the 5' phosphate of RNAs, thus helping maintain association with the Argonaute protein. The PAZ domain is found in all Argonaute and Dicer proteins and contains an OB fold, which is critical for nucleic acid binding. This domain forms a binding module for 2 nt 3' overhang RNAs generated by RNase III type enzymes. The PIWI domain is unique to the Argonautes and consists of an RNase H fold with conservation of two aspartate residues forming a critical active site, common to all RNase H proteins. However, unlike these other proteins, in the Argonautes, this is followed by a histidine rather than another aspartate, garnering a unique Asp-Asp-His motif [reviewed in (Tolia and Joshua-Tor, 2007)]. Although all of the Argonaute proteins are able to facilitate miRNA mediated repression, as demonstrated by direct tethering experiments (Pillai et al., 2004), only Argonaute 2 has retained its enzymatic capacity and is therefore capable of endonucleolytic cleavage (Liu et al., 2004). However the Asp-Asp-His motif is necessary but not sufficient to confer enzymatic activity as it is also present in the catalytically inactive Argonaute 3 protein. This points towards a contribution of either cellular co-factors or post-translational modifications for endonuclease activity. In *Drosophila* the two Argonaute proteins retain very distinct functions with Argonaute 1 involved in repression and Argonaute 2 mediating cleavage (Forstemann et al., 2007). The Argonaute proteins may also be involved in miRNA biogenesis as it has been reported that they cleave the pre-miRNA hairpin structure and thus aid removal of the passenger strand of the RNA duplex (Cheloufi et al., 2010; Cifuentes et al., 2010). Further Argonaute 2 has been implicated in miRNA mediated translational upregulation of mRNAs in stress induced serum starved conditions (Vasudevan and Steitz, 2007a). The Argonaute proteins are predominantly cytoplasmic and components of P-bodies but can re-locate to stress granules during periods of cellular stress (Liu et al., 2005b; Pillai et al., 2005; Sen and Blau, 2005). This allows control of cellular translation in response to changing environmental conditions as various translational initiation factors are also found in these structures. These findings highlight the varied roles played by the Argonaute protein in RNA regulation.

1.11.4 miRNAs and viruses

RNAi has long been established as a means of antiviral defence in both plants and invertebrates. Conversely viruses that infect these organisms encode inhibitors of the RNAi pathway as a means of overcoming this innate immunity. For example, the P19 protein, encoded by the tomato bushy stunt virus is able to bind to siRNAs and prevent their loading onto RISC (Voinnet et al., 1999). Whether a similar system exists in mammals remains to be determined. The components of this pathway, e.g. Argonaute 2, are present and functional in mammals but only very recently have endogenous siRNAs been shown to exist and the subject of virally encoded siRNAs remains controversial. Further, unlike plants and nematodes, mammals do not appear to encode an RNA dependent RNA polymerase (RDRP), which in these organisms greatly increases the number of siRNAs for an mRNA target, thereby amplifying the RNAi response (Aoki et al., 2007; Diaz-Pendon et al., 2007). More importantly, mammals have developed a more sophisticated form of immunity that is based on protein recognition and induction of the interferon response, which may make more ancient nucleic acid based immunity somewhat redundant.

However there is increasing interest in the interplay between cellular and/or viral miRNAs in both the control and promotion of virus replication. Potentially, this can work in one of four ways: virally encoded miRNAs targeting viral mRNAs, virally encoded miRNAs targeting cellular mRNAs, cell encoded miRNAs targeting cellular mRNAs and cell encoded miRNAs targeting viral mRNAs [reviewed in (Umbach and Cullen, 2009)]. The fact that miRNAs are small and non-antigenic means that host and/or viral gene expression can be modulated without eliciting cellular immune responses.

Virally encoded miRNAs have now been identified, mostly from DNA viruses with a nuclear phase of their life cycle, thus granting them access to the miRNA processing machinery (Cullen, 2011; Grundhoff and Sullivan, 2011). Whether RNA viruses, including retroviruses, also harbor miRNAs is the subject of much debate as endonucleolytic processing of RNA genomes to generate encoded miRNAs may prove detrimental to the virus. Thus the identification of putative miRNAs, for this subset of viruses, remains controversial. The first virally derived miRNAs were identified from the gamma herpes virus, Epstein Barr virus (EBV), by Pfeffer and colleagues (Pfeffer et al., 2004). To date more than 200 miRNAs from members of the herpesvirus family

have since been discovered which suggests that they may make important contributions to the life cycle of these viruses. It has been proposed that herpesvirus encoded miRNAs may facilitate latent infection of the virus by downregulating viral protein synthesis. This self-regulation allows the virus to avoid cellular immune responses as well as anti-viral therapies. Latent infection of herpes simplex virus 1 and 2 (HSV1 and HSV2) is accompanied by miRNA expression but not viral protein expression. On the other hand, infection with a miRNA deleted EBV mutant strain did not result in increased replication of the virus, indicating that these miRNAs may not be involved in establishing latency for this particular virus (Seto et al., 2010).

In several instances, virally encoded miRNAs are able to perturb cellular function. In most cases, this relates to inhibition of either an apoptotic response or a cellular immune response. One example of the latter is the downregulation of MICB by the human cytomegalovirus (HCMV) encoded miRNA, mir UL112-1 (Stern-Ginossar et al., 2007). MICB is expressed on the surface of cells in response to cellular stress, such as viral infection, and is recognised by the NKG2D receptor found on natural killer (NK) cells. This subsequently results in NK mediated destruction of the infected cell, which HCMV avoids by miRNA mediated targeting of MICB expression. Through a mechanism of convergent evolution, EBV and Kaposi's sarcoma associated herpes virus (KSHV) also encode miRNAs that target MICB (Nachmani et al., 2009), highlighting this as an important means of immune avoidance by herpesviruses.

More rarely, viruses can also utilise cellular miRNAs for their own propagation. mir122 which is abundantly expressed in the liver, facilitates replication of hepatitis C virus (HCV) and unusually binds to sites contained within the 5'UTR of the virus rather than the conventional 3'UTR observed for all animal miRNAs (Jopling et al., 2005). The underlying mechanism behind this is not completely understood but it explains the inability of HCV to replicate in cells that do not express mir122. Relatedly, knockdown of Dicer and/or the Argonaute proteins decreases HCV replication (Randall et al., 2007).

On the other hand, it has also been demonstrated that cellular miRNAs are able to target RNA sequences within viruses, such as primate foamy virus (PFV) (Lecellier et al., 2005) and influenza A (Song et al., 2010), and inhibit their replication. However, the impact of these miRNAs during the course of a natural infection remains to be determined. Therefore the complex dynamics of host and viral miRNAs in the life cycle of a range of different viruses is becoming increasingly evident.

1.11.5 miRNAs and HIV-1

Since the miRNA pathway appears to be important for both the control and promotion of several DNA and RNA viruses, including a retrovirus (PFV), increasing attention has turned to the role it may play in the replication of HIV-1. However, despite continued investigation into this area, it remains a highly controversial issue.

HIV-1 encoded miRNAs have been identified, including those generated from the structured TAR element of the viral RNA, located within all HIV-1 transcripts (Klase et al., 2007; Ouellet et al., 2008). This RNA is potentially recognised and cleaved by Dicer and protects cells from stress induced cell death, by targeting cellular mRNAs (Klase et al., 2009). However, the expression of these miRNAs appears to be very low and work by Lin and Cullen (2007) failed to find significant levels of miRNAs or siRNAs in HIV (and human T-cell lymphotropic virus, HTLV-1) infected T cells (Lin and Cullen, 2007). This questions the contribution of these putative miRNAs to HIV-1 replication.

Alternatively, HIV-1 may perturb host encoded miRNAs and the miRNA pathway for its own benefit. HIV-1 infection is reported to cause global changes in cellular miRNA expression as determined by miRNA profiling of uninfected versus infected individuals (Houzet et al., 2008). Several cellular miRNAs were found to be downregulated and similar results have been obtained from *in vitro* infection studies in cell lines (Hayes et al., 2011; Yeung et al., 2005). This also implies that humans may be able to utilise the miRNA pathway for viral restriction despite the presence of more sophisticated forms of innate immunity. Plant viruses encode suppressors of RNA silencing (SRS) that act to antagonise the RNAi pathway, which is the primary mechanism of anti-viral defence in these organisms. Similarly, SRS activity has been attributed to the viral accessory proteins Tat and Vpr, a subject that remains heavily debated. Both proteins have been proposed to interact with Dicer and affect its function in miRNA biogenesis (Bennasser and Jeang, 2006; Bennasser et al., 2005; Coley et al., 2010; Hayes et al., 2011). The viral TAR RNA may also compete with Dicer for binding to its essential co-factor TRBP. However, other groups have found that expression of Tat in infected cells does not inhibit miRNA production or expression (Lin and Cullen, 2007; Sanghvi and Steel, 2011). The reason for these discrepancies remains unclear at present but the role of Tat and its effects on the miRNA pathway requires further experimental validation.

Other studies have also alluded to the fact that the miRNA pathway may be inhibitory to viral replication. Knockdown of Drosha and/or Dicer has been shown to increase both HIV-1 virus production and infectivity (Nathans et al., 2009; Triboulet et al., 2007). However, it must be noted that knockdown of these enzymes will also affect cellular miRNA expression which may subsequently impact upon cell growth and metabolism. Thus these results have to be interpreted with some caution and disentangling direct and indirect effects of the miRNA pathway on HIV-1 replication may not be a straightforward task.

Nevertheless, specific host encoded miRNAs have also been identified which are thought to regulate the life cycle of this virus. The mir17/92 polycistronic cluster is downregulated by HIV-1 and has been proposed to target PCAF, a cellular co-factor of Tat, which results in reduced viral protein expression (Triboulet et al., 2007). Also, the mir29a miRNA acts to repress HIV-1 mRNA expression by facilitating the association of Gag mRNA with Ago2 and P-bodies. Conversely, this may be beneficial to the virus in terms of establishing a latent infection and avoidance of host immune responses. Other studies show that mir29a instead targets the Nef protein to interfere with viral replication (Ahluwalia et al., 2008) and is actually downregulated upon HIV-1 infection (Houzet et al., 2008). On a similar note, expression of five cellular miRNAs, also targeting Nef, in resting CD4+ T cells, have been reported to contribute to viral latency by minimising viral protein expression and maintaining a pool of HIV-1 infected cells that are not accessible by HAART (Huang et al., 2007b). Inhibition of these miRNAs resulted in increased HIV-1 protein translation. However, this has been difficult to verify due to the low absolute expression of these miRNAs and debates over whether they still constitute resting cells after experimental manipulation.

These examples highlight the complexities and controversies surrounding the involvement of the miRNA pathway in HIV-1 replication. Therefore, whether viral or host encoded miRNAs can influence the life cycle of HIV-1 is unresolved at present and is an issue of continued research.

1.11.6 ARE mediated decay (AMD)

A second form of post-transcriptional gene regulation is that mediated by adenosine (A) and uridine (U) rich elements (ARE). These are repetitive and often overlapping AUUUA pentamers contained within U rich regions of the 3'UTR, although no formal consensus sequence exists. These elements have been classified into three groups (class I, II and III) based on loose sequence homology rather than any biological function [reviewed in (Chen and Shyu, 1995)]. ARE sequences are often found within mRNAs coding for proteins that regulate cell growth or determine the cells ability to respond to external stimuli, such as transcription factors, cytokines and cell cycle regulatory proteins (Bakheet et al., 2006). ARE sites are recognised and bound by ARE binding proteins (ARE-BPs), which will typically promote the degradation or stabilisation of the mRNA.

Several ARE-BPs, along with their mRNA targets have now been identified [reviewed in (Barreau et al., 2005)], and one such example, mouse APOBEC1, has already been described (see section 1.8.1). Others include AUF1 (Zhang et al., 1993), which can affect c-myc, c-fos and granulocyte-macrophage colony-stimulating factor (GM-CSF) mRNAs both positively and negatively, with the effects most likely to be cell type specific. The Elav related protein, HuR, increases the stability of mRNAs that it associates with (Fan and Steitz, 1998), which includes c-fos, tumor necrosis factor alpha (TNFα), Cox-2 and interleukin 3 (IL3). Tristetraprolin (TTP) on the other hand is mostly destabilising for its targeted mRNAs, such as TNFα (Carballo et al., 1998), Cox-2 and interleukin 2 (IL2). These data demonstrate that ARE containing mRNAs can be bound by more than one ARE-BP and these proteins can thus have overlapping and often antagonistic functions. This highlights the versatility of this system and the ability of the cell to influence protein expression in response to changing conditions.

The precise mechanism by which ARE-BPs modulate these effects is not completely understood. It is believed that they recruit other cellular components that can either degrade or translationally repress the bound mRNA. Indeed it has been shown that ARE mediated decay (AMD) is initiated by deadenylation followed by 3' to 5' exosomal mediated degradation (Mukherjee et al., 2002). However it is now well established that degradation can also occur in the opposite direction, where this time loss of the poly A tail is followed by decapping and then exonucleolytic decay by the 5' to 3' exonuclease Xrn1, associated with P-bodies (Stoecklin et al., 2006). Importantly these ARE

associated proteins are often found in the closely related, stress induced foci termed stress granules (Kedersha and Anderson, 2002). It is believed that a function of ARE-BPs may be to shuttle mRNAs between P-bodies and stress granules, thereby arresting translation without causing degradation in response to the changing requirements of the cell.

Not only do miRNA and ARE effectors localise to the same cytoplasmic structures they may also work in unison to regulate translation. As has already been discussed, the ARE-BP HuR is able to mitigate the effects of the miR122 miRNA and release the translationally repressed Cat1 mRNA from P-bodies into polysomes for translation during periods of cellular stress (Bhattacharyya et al., 2006). Jing *et al* (2005) have also reported that Dicer and the Argonaute proteins are involved in the decay of TNFα mRNA. Specifically the mir16 miRNA was identified as binding to ARE sequences and recruiting the ARE-BP TTP, which indirectly leads to the destabilisation of the mRNA (Jing et al., 2005). However the sequence targeted by the miRNA is thought to reside outside the ARE region (Vasudevan et al., 2007b). It has also been shown that the translational upregulation induced by fragile X mental retardation protein 1 (FXR1) and Ago2 on TNFα transcripts during serum starvation is directed by the mir369-3 miRNA (Vasudevan et al., 2007b). This miRNA orchestrates the binding of these proteins to the ARE sequence and thus allows them to activate translation but only during cell cycle arrest. Other miRNAs, such as let-7, were shown to have similar effects. These examples highlight the complex interplay between different RNA regulatory mechanisms in the control of RNA translation.

1.11.7 Nonsense mediated decay (NMD)

A third RNA regulatory pathway is termed nonsense mediated decay (NMD). This is where mRNAs harbouring premature termination codons (PTC) are rapidly degraded. Premature in frame termination codons can be generated by a number of means including insertions, deletions and mutations, which links NMD to a number of genetic disease phenotypes. Like the pathways described above, NMD is conserved from plants to mammals although the exact mechanism of degradation and the key components involved are the not the same in all cases [reviewed in (Shyu et al., 2008)]. A core component of the NMD machinery is the RNA helicase Upf1 which can catalyse the unwinding of double stranded RNA (Bhattacharya et al., 2000). The precise mechanism of NMD mediated degradation has not been well defined but in mammals it appears to

be triggered by accelerated decapping, deadenylation and then decay via the 5' - 3' pathway, with Upf1 interacting with several components of these processes (Lejeune et al., 2003). NMD factors have also been linked to P-bodies, implying that degradation may be facilitated by targeting mRNAs to these structures (Sheth and Parker, 2006). However, NMD can still occur in the absence of visible foci (Stalder and Muhlemann, 2009).

The manner is which these PTCs are recognised and degradation is mediated is not well understood but several features appear to be important, though not necessary, such as the presence of an exon junction protein complex (EJC) (Le Hir et al., 2000), competition between the Poly A Binding Protein (PABPC1) and Upf1 for binding to translation release factors (Hilleren and Parker, 1999) and the distance between the PTC and the 3'UTR. Recently it has been reported that Upf1 is able to sense the length of 3'UTRS and preferentially binds to those mRNAs that are sensitive to NMD and thus prepares them for decay (Hogg and Goff, 2010) (Figure 1.9).

1.11.8 Pumilo and FBF (PUF) proteins

Additionally, PUF proteins, expressed in a wide variety of organisms ranging from yeast to humans, also act to modulate mRNA translation and stability with roles in differentiation, development, the cell cycle and mitochondrial biogenesis [reviewed in (Wharton and Aggarwal, 2006; Wickens et al., 2002)]. These proteins are traditionally considered post-transcriptional repressors, as they are able to recruit the CCR4-Pop2-Not deadenylase complex to mRNAs by directly binding to Pop2 and the 3'UTR of the target mRNA (Goldstrohm et al., 2006). This may also lead to recruitment of DDX6 and Dcp1a, who also interact with the deadenylase complex, leading to decapping and subsequent mRNA degradation (Goldstrohm et al., 2006). However, other mechanisms of translational repression also exist, such as inhibition of eIF4E binding to the mRNA cap thus preventing translation initiation (Cao et al., 2010; Cho et al., 2005). Recently, PUF proteins have been attributed with addtitional roles including translation activation and mRNA localisation [reviewed in (Quenault et al., 2011)].

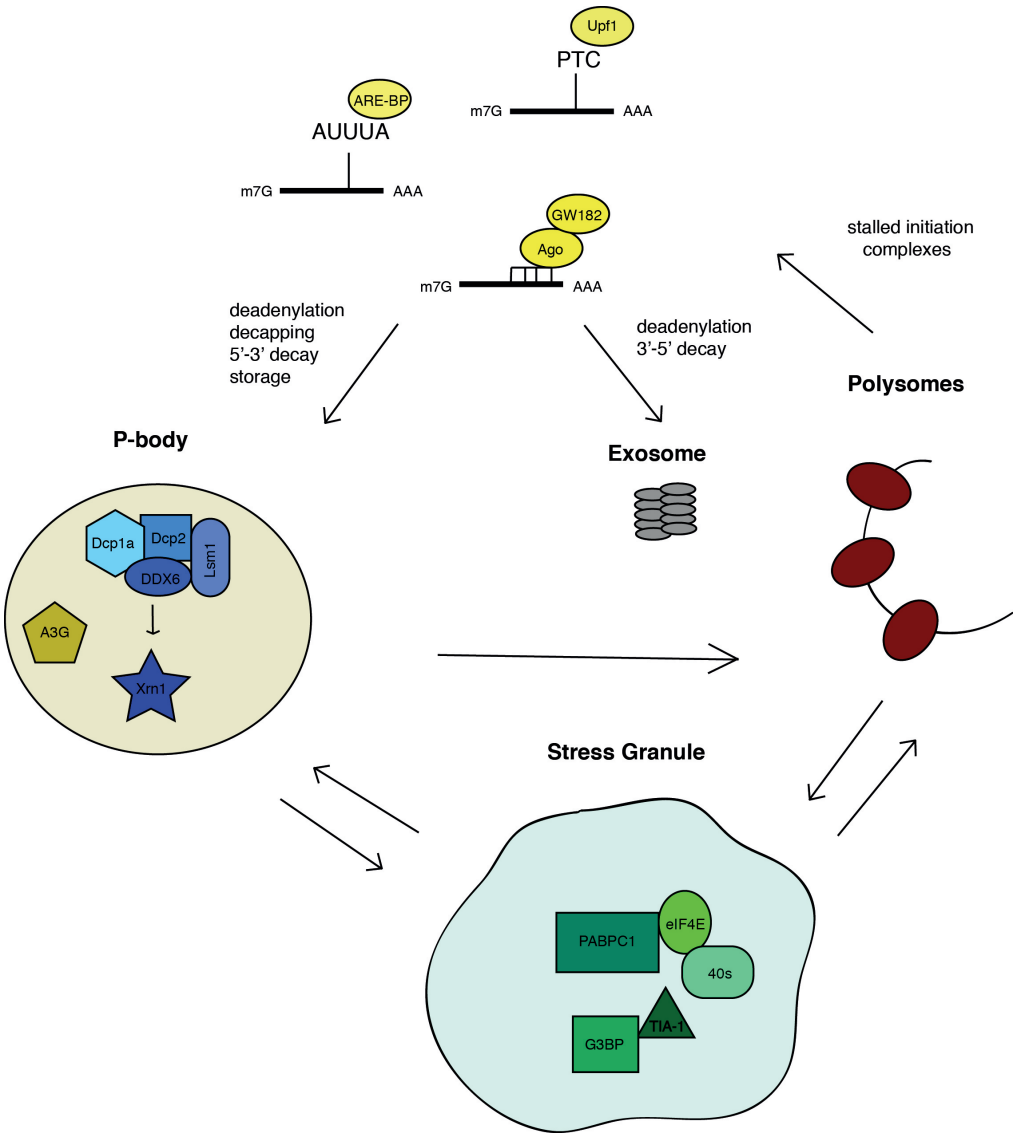

Figure 1.9: mRNA regulatory pathways.

mRNAs exiting translation due to post transcriptional regulatory mechanisms including miRNA mediated repression, ARE mediated decay or nonsense mediated decay, undergo removal of the polyA tail (deadenylation) and then either decay via the exosome (3'-5') or subsequent decapping and then decay by Xrn1 (5'-3') in P-bodies. mRNAs may be temporarily stored in P-bodies and released back to polysomes to be translated or may be trafficked to stress granules. mRNAs in stress granules may then be re-directed to polysomes after formation of a pre-initiation complex. During periods of stress mRNAs temporarily repressed in stress granules may be directed to P-bodies for decapping and decay.

1.12 Functional role of P-bodies

As has been discussed, components of various different RNA regulatory pathways have been found to localise to P-bodies, and decapping, degradation and repression actively occur in these foci demonstrating that they are not just storage facilities for these proteins (Sheth and Parker, 2003). However, whether P-bodies are necessary for post-transcriptional processes to occur has been the subject of much debate. Knockdown of the essential P-body proteins, GW182 (Eulalio et al., 2008b) and DDX6 (Chu and Rana, 2006), leads to impairment of miRNA mediated translational repression but the effects of individual proteins must be separated from the effects of P-bodies in general. In light of this it has been demonstrated that P-body integrity is not necessary for either siRNA mediated silencing or DDX6 dependent miRNA repression as concluded from depletion of DDX6 and Lsm1 respectively (Chu and Rana, 2006). Similarly in *Drosophila*, loss of P-bodies did not impact upon miRNA, siRNA nor NMD mediated RNA regulation suggesting that these processes can occur independently of these foci (Eulalio et al., 2007b). In fact, it appears that P-bodies are dependent upon the translationally repressed mRNAs that these pathways generate (Eulalio et al., 2007b; Stalder and Muhlemann, 2009). This can be explained, in part at least, by the fact that mRNA degradation/decay can occur outside of P-bodies and in the yeast *S.cerevisiae* it may even occur co-translationally, while the mRNA is still engaged with ribosomes (Hu et al., 2010; Hu et al., 2009). Others have proposed the existence of smaller P-bodies which are undetectable by light microscopy but which can serve the same functions as their more visible counterparts.

Since P-bodies are not functionally necessary for RNA regulatory pathways to occur, and since most P-body proteins are actually diffuse in the cytoplasm, the conservation of these microscopically visible RNA-protein aggregates is intriguing. One advantage may be that spatially segregating the decay machinery away from the translating pool of mRNA helps avoid unwanted degradation of cellular transcripts. It may also make the decay process more efficient, if the necessary machinery is concentrated in one place. As has already been discussed, P-bodies also allow mRNAs to be temporarily repressed and later released for translation, providing a useful facet in the control of gene expression.

1.13 P-bodies and viral life cycles

1.13.1 P-bodies as positive regulators of viral replication

Recently, attention has also focused on the role that P-bodies may play in viral life cycles (Beckham and Parker, 2008). Viruses often utilise host machinery in order to promote translation of their own mRNAs and certain cellular components will work to interfere with this, but the interplay between host factors and viral translation is not well understood. Since P-bodies are devoid of translation initiation factors and ribosomes, they represent attractive cellular compartments within which viruses may segregate translation and assembly or replication of their genetic material. This is especially pertinent for retroviruses where the RNA serves as both the template for translation of viral gene products and the genomic RNA which needs to be packaged into virions (Swanson and Malim, 2006). Therefore P-bodies may positively impact upon the replication of viruses.

In support of this hypothesis, several examples have now been uncovered whereby P-bodies/P-body components appear to promote replication of both exogenous viruses and endogenous retroelements. Firstly, replication and/or translation of the plant brome mosaic virus (BMV), which can fully complete its replication cycle in yeast, has been shown to require normally repressive P-body components including Dhh1p/DDX6 and Lsm1 (Mas et al., 2006; Noueiry et al., 2003). Further, viral proteins were also found to localise to P-bodies, which could associate with the plasma membrane, providing a link between P-bodies and viral assembly (Beckham et al., 2007). Similarly, hepatitis C virus (HCV) replication is also facilitated by P-body components, with the Lsm1 - 7 hepatmeric complex specifically binding to regulatory elements controlling translation and replication in the untranslated regions of the viral RNA (Galao et al., 2010; Scheller et al., 2009). This may stabilise the mRNA by protecting it from decapping and subsequent decay. Also, the DEAD box helicase protein DDX3 has been shown to interact with the HCV core protein, with loss of DDX3 resulting in reduced HCV replication (Ariumi et al., 2007; Owsianka and Patel, 1999). The yeast homologue of DDX3, Ded1p has been identified as a component of P-bodies (Beckham et al., 2008). Although the protein appears to be highly conserved across organisms, whether the human protein behaves reciprocally remains to be formally verified. Finally, the replication of the yeast Ty1 and Ty3 retroelements is also dependent upon these cytoplasmic foci and components contained therein. Ty3 mRNA, proteins and virus like

particles (VLPs) have been demonstrated to localise to P-bodies and knockdown of P-body associated proteins leads to a decrease in retrotransposition events (Beliakova-Bethell et al., 2006; Checkley et al., 2010). The authors indicate that assembly of VLPs appears to be dependent upon P-body integrity. The situation for replication of the Ty1 retroelement appears to be slightly more complex as although P-body proteins appear to enhance formation of retrotransposition competent VLPs, viral mRNA and Gag proteins accumulated in foci that were distinct from P-bodies (Checkley et al., 2010). However, another group found significantly greater overlap between P-bodies and Ty1 components (Dutko et al., 2010). Both groups did report that knockdown of P-body components decreased formation of VLP clusters and levels of viral proteins as well as the association of these viral factors with these particular foci. This suggests that P-body proteins may be involved in the trafficking of viral mRNA and Gag to these foci, which appear to be sites of virus assembly.

1.13.2 P-bodies as negative regulators of viral replication

Conversely, P-bodies could play an inhibitory role in virus replication as viral mRNA once targeted to P-bodies may be maintained in a state of translational repression and more fatally, be subject to degradation. Several lines of evidence are now emerging to lend credence to this theory. Firstly, poliovirus infection causes the disruption of P-bodies and the degradation of key components such as Dcp1a and Xrn1 (Dougherty et al., 2011). Similar observations were also made for stress granules. This data implies that to some extent these cytoplasmic foci can somehow antagonise viral replication. Secondly, contrary to what has been observed for the Ty retrotransposons in yeast, depletion of P-bodies in human cells results in an increase in retrotransposition events for the murine intracisternal A particle (IAP) retroelement (Lu et al., 2011). IAP mRNA was found to localise to P-bodies thus preventing its association with Gag, which accumulated at the ER. These effects were not due to perturbation of the miRNA pathway upon knockdown of P-body components. Finally, with regards to HIV-1, two groups have recently reported that depletion of P-body and miRNA associated components, including Ago2, DDX6 and Lsm1, leads to increases in both virus production and infectivity (Chable-Bessia et al., 2009; Nathans et al., 2009). This suggests that P-bodies can limit HIV-1, most likely via the miRNA pathway. Both studies demonstrated the localisation of HIV-1 viral components, either gRNA and/or

Gag at P-body foci. This suggests that HIV-1 may traffic to P-bodies, which in turn may serve to limit its replication.

The fact that several APOBEC3 proteins are known to localise to P-bodies (Gallois-Montbrun et al., 2008; Gallois-Montbrun et al., 2007; Niewiadomska et al., 2007; Wichroski et al., 2006), postulates a possible mechanism of viral inhibition. It has recently been claimed that visible 'A3G complexes' that partially overlap with P-bodies, inhibit HIV-1 particle production, mediated by a reduction in the half-life of Gag (Martin et al., 2011). APOBEC3 localisation to these structures may also enable their incorporation into nascent virions if indeed Gag does transit through these foci. This is further supported by the fact that A3G localisation to P-bodies in yeast is important for its inhibition of the Ty1 retroelement, most likely through facilitating its interaction with viral components which mediates its incorporation into VLPs (Dutko et al., 2010; Dutko et al., 2005). The putative DEAD box helicase, Mov10, which is strongly inhibitory to HIV-1 infectivity when overexpressed (Burdick et al., 2010; Furtak et al., 2010; Wang et al., 2010), is packaged into HIV-1 virions (Chertova et al., 2006) and is also a component of P-bodies (Meister et al., 2005). Therefore, the influence that P-bodies may have in regulating viral life cycles, either positively or negatively, appears to be highly complex and multi-faceted. Whether cellular proteins that are able to modulate virus replication, such as the APOBEC3 proteins, require P-bodies for their anti-viral function requires further investigation.

1.14 Aims

It has been demonstrated that the anti-viral proteins A3F and A3G assemble in large RNP complexes and associate with a multitude of proteins involved in RNA metabolism and turnover. They also localise with a subset of these proteins to P-bodies, sites of RNA storage and degradation, which have recently been implicated in influencing diverse viral life cycles, both positively and negatively. Of particular interest are the Argonaute proteins which interact with A3F and A3G in a partially RNase independent manner suggestive of a close and potentially direct association. Further, although no known cellular function has been defined for the APOBEC3 proteins, their interaction with the Argonuate proteins and localisation to P-bodies suggests an involvement in the regulation of RNA through post-transcriptional processes. How specific proteins or sub-cellular localisation may influence the anti-viral and potential unidentified cellular activities of the APOBEC3 proteins remains to be determined, either as co-factors or functional regulators.

Therefore, this thesis aims to address several outstanding issues. Firstly, the interaction between the APOBEC3 and Argonaute families will be examined in more detail to determine whether interaction with the Argonaute proteins is correlated to the anti-viral phenotypes of the APOBEC3 proteins. Further, the functional implications of this interaction will also be addressed, in terms of both Argonaute involvement in APOBEC3 anti-viral activity and a potential cellular role for the APOBEC3 proteins in the regulation of RNA. Finally, the significance of APOBEC3 localisation to P-bodies in relation to their anti-viral phenotypes will also be investigated and consequently the influence that these foci may have on the replication of HIV-1 in general.

CHAPTER 2

MATERIALS AND METHODS

2. MATERIALS AND METHODS

2.1 Plasmids

All expression plasmids used in this study were confirmed to be correct by restriction enzyme mapping and/or sequencing where necessary. A list of the primers used for cloning is provided in the Appendix.

2.1.1 Plasmids for transfection

pCMV4 expression plasmids containing cDNA sequences of APOBEC3A, APOBEC3B, APOBEC3C, APOBEC3F, APOBEC3G and APOBEC3G point mutants (described in section 5.1) with a 3 x C-terminal HA epitope tag have been previously described (Bishop et al., 2004; Huthoff et al., 2009; Huthoff and Malim, 2007). APOBEC3D/E, APOBEC3H (haplotype 2) and green fluorescent protein (GFP) cDNAs were cloned into the same vector using the HindIII and Xba1 restriction endonucleases. The Argonaute 2 cDNA was similarly cloned into the same vector. This Argonaute 2 clone contains a HindIII restriction site requiring a 3-way ligation of the insert in order to obtain the full cDNA sequence. Wild type DDX6 cDNA was also cloned into this vector, again using the HindIII and Xba1 restriction endonucleases. The DDX6 double point mutant R89A+K91A (DDX6-A), and the single mutants G346A (DDX6-B) and R423Q/HRIGQ (DDX6-C) were generated by site directed mutagenesis using overlapping PCR. cDNAs containing the desired mutations were then subcloned into the pCMV4 expression vector as described above.

Untagged APOBEC3A, APOBEC3F and APOBEC3G cDNAs in the pCDNA3.1 vector, as well as human and rat APOBEC1 in the same vector are as previously described (Bishop et al., 2004)

An untagged Luciferase expression plasmid was generated for use in infectivity assays by cloning Luciferase cDNA, using the Asp718 and HindIII restriction endonucleases, with two stop codons encoded in the 3' primer. This was then inserted into the pCMV4 vector described above but due to the presence of the stop codons, the HA tag is not expressed.

The NL43 Δ*vif* proviral plasmid was created by insertion of two stop codons at the end of the Pol/Vif reading frame by overlapping PCR in pCMS309 (Vif transfer vector) using the Age1 and EcoR1 restriction endonucleases. The mutated insert was then sub-cloned into the full length NL43 proviral sequence using the Sph1 and EcoR1 restriction endonucleases. The wild-type NL43 proviral plasmid was a kind gift from Dr Malcolm Martin. The IIIB Δ*vif* proviral clone and the pVSV-G expression plasmid are as previously described (Bishop et al., 2004; Fouchier et al., 1997).

cDNAs of DDX6 and Luciferase were cloned into the p3xFLAG CMV expression vector as controls for mlin41 assays using the HindIII and BamH1 restriction endonucleases.

Expression plasmids for yeast 2 hybrid assays were generated by insertion of Argonaute 1 and Argonaute 2 cDNAs into the myc epitope tagged KT7 and HA epitope tagged HB18 vectors (kindly provided by Dr Juan Martin-Serrano) using the EcoR1 and Xho1 (for Argonaute 1) and the EcoR1 and Sal1 (for Argonaute 2) restriction endonucleases. The KT7 and HB18 expression plasmids containing the APOBEC3G cDNA had been previously generated by Dr Hendrik Huthoff. The Tsg101 cDNA expressed in the KT7 vector and the Vps28 cDNA expressed in the HB18 vector were kindly provided by Dr Juan Martin-Serrano.

For HIV-1 gRNA and Gag localisation studies, NL43 constructs containing 24xMS2 binding loops and Gag-Cherry fusions were generated by Dr Nathan Sherer. Briefly, the SacII and BsmB1 restriction sites were introduced at the end of the Gag reading frame in the wild-type pNL43 expression plasmid by overlapping PCR. The 24xMS2 binding loops were then directly sub-cloned into the proviral plasmid using the SacII and BsmB1 sites to give pNL43-24xMS2. For generation of the proviral plasmid additionally containing mCherry, Gag was fused to mCherry by overlapping PCR and sub-cloned into pNL43-24xMS2 using the SacI and SacII restriction sites to give pNL43-mCherry-24xMS2. The MS2-YFP fusion plasmid was a kind gift from Dr Robert Singer.

For FRET/FLIM analyses, Argonaute 2 was cloned in frame with the mCherry cDNA in the pCMV2B vector (Stratagene) with the EcoR1 and Sal1 restriction endonucleases to generate an Argonaute 2 expression plasmid with an N-terminal mCherry fusion.

pCMV2B expressing mCherry, YFP and an A3G-YFP fusion had been previously generated by Dr Sarah Gallois-Montbrun.

For pulse labelling experiments, the codon-optimised Gag construct is as previously described (Swanson et al., 2010).

The Argonaute 1, Argonaute 2, Argonaute 3, Argonaute 2-PAZ9 and Argonaute 2-PAZ10 mutants in the myc epitope tagged pCDNA3.1 vector were kind gifts from Dr Gregory Hannon. The Argonaute 2-F2V2 mutant was a kind gift from Dr Zissimos Mourelatos.

The luciferase reporter constructs for the let-7/miRNA assays (wild type/FF4LCS and mutant/FFrm4LCS) and for the ARE assays (ARE, AREmt, CTRL and UTR) as well as the FXR1 expression plasmid containing both an N-terminal λN and C-terminal FLAG epitope tags and HuR expressed in pCDNA3.1 were kind gifts from Dr Joan Steitz. The luciferase reporter construct used for the siRNA assay (Lucmir30p) as well as the mir30p miRNA and the VA1 expression plasmid were kind gifts from Dr Brian Cullen. The DND1 expression plasmid and the pCS2+ empty vector were kind gifts from Dr Reuven Agami. The mlin41 expression plasmid containing a 3xFLAG N-terminal epitope tag was a kind gift from Dr F. Gregory Wulczyn. The Tat expression plasmid in the pCDNA3.1 vector had been previously generated by Dr Chad Swanson.

The Renilla expression plasmid under the control of the TK promoter was purchased from Promega.

2.1.2 Plasmids for transduction

For production of stable cell lines wild type and mutant DDX6 cDNAs were also cloned into the pCMS28 retroviral vector already containing the yellow fluorescent protein (YFP) cDNA (kindly provided by Dr Juan Martin-Serrano) to enable production of N-terminal YFP fusion proteins. The pCMS28 retroviral vector is a bi-cistronic construct derived from MigR1, which contains a polylinker and puromycin resistance gene in place of GFP. The resistance gene is linked via an internal ribosomal entry site (IRES) to the multi-cloning site, thereby coupling antibiotic selection to mRNA production of the gene of interest. This vector was engineered to contain an EcoR1, Not1, Xho1 multiple-cloning site after the YFP cDNA with a GST linker sequence placed between the EcoR1 and Not1 endonuclease restriction sites. The cDNAs of wild type and mutant

DDX6 sequences were inserted into this vector using the Not1 and Xho1 restriction endonucleases. APOBEC3G was cloned into the pNG72 retroviral vector (as described for pCMS28) using the EcoR1 and Xho1 restriction endonucleases. The YFP cDNA expressed in pNG72 was kindly provided by Dr Juan Martin-Serrano. The p8.91 packaging plasmid was a kind gift from Dr Didier Trono. The pCgp packaging plasmid was a kind gift from Dr Paula Cannon.

2.1.3 Reagents for RNAi

The shRNA encoded lentiviral GIPZ vectors targeting Ago2, DDX6 and Lsm1 as well as the non-silencing control were obtained from Open Biosystems. siRNA oligonucleotides targeting the ALIX and DDX6 proteins were purchased from Dharmacon and Ambion Life Technologies respectively. The control scrambled siRNA oligonucleotide was also purchased from Ambion Life Technologies. Sequences of the shRNAs and siRNAs used in this study are presented in Table 2.1.

Table 2.1: Sequences of siRNAs and shRNAs. Only sequences of the sense strand are presented. For DDX6 the shRNA used for knockdown studies in HeLa cells is underlined.

Target	Type	Sequence
Ago2	shRNA	GGCAAGAAGAGATTAGCAA
DDX6	shRNA	GGGTTATTCTTGCTTCTAT (1)
		CACAAAGCCTTGAGTATAA (2)
		CTGAGTTTATAAGGTTCCA (3)
		CGGAGTCTGCTGAGTTTAT (4)
		<u>CAGATAATGGAGGATATTA</u> (5)
Lsm1	shRNA	GGCATAGACTCCTTCACAC
ALIX	siRNA	GCAGUGAGGUUGUAAAUGU
DDX6	siRNA	GAUGAUCGCUUCAACCUGATT
Luciferase	siRNA	CUGCCUGCGUGAGAUUCUC

2.2 Bacteria

2.2.1 Bacterial Strains and Maintenance

Transformations were conducted using Top10 competent cells (Invitrogen) with the exception of proviral DNA, in which case Stable 2 cells (Stbl2, Invitrogen) were used instead. Bacterial cells were grown in Luria-Bertani Broth [LB, 1% tryptone (w/v), 0.5% yeast extract (w/v), and 1% NaCl (w/v) dissolved in ddH_2O) or on LB-Agar (37 g/1L ddH_2O) set in 10 cm sterile dishes for solid phase growth cultures. Where appropriate media was supplemented with the following antibiotics: 100 µg/ml Ampicillin (Calbiochem), 50 µg/ml kanamycin monosulfate (Fisher) or 100 µg/ml zeocin.

2.2.2 Production of competent bacterial cells

Top10 competent cells were inoculated in 5 ml of LB overnight at 30°C with shaking at ~200 rotations per minute (rpm). The following day 0.5 ml of this culture was then used to inoculate 50 ml of LB which was again grown at 30°C with shaking until an OD_{550} of between 0.5 - 0.6 had been reached, typically after 5 - 6 hours. The cells were then chilled on ice for 10 minutes before being pelleted by centrifugation for 10 minutes at 3,500 rpm at 4°C. The pellet was re-suspended in 20 ml of pre-chilled, filter sterilised buffer TfB1 (30 mM KAc, 100 mM RbCl, 10 mM $CaCl_2$, 50 mM $MnCl_2$ and 15% glycerol, made up to 100 ml with ddH_2O) and chilled on ice for 5 minutes. The cells were then centrifuged as before and re-suspended in 2 ml of pre-chilled, filter sterilised buffer TfB2 (10 mM PIPES, 75 mM $CaCl_2$, 10 mM RbCl and 15% glycerol, made up to 100 ml with ddH_2O) before being incubated for 10 minutes on ice. Cells were then aliquoted into sterile eppendorf tubes on dry ice and stored at -80°C.

2.2.3 Transformation of competent bacterial cells

30 µl of competent bacterial cells were incubated with 3 µl of ligated DNA or 2 µl of plasmid stocks for 30 minutes on ice. Cells were heat shocked at 42°C for 45 seconds and then allowed to recover on ice for 2 minutes. 1 ml of sterile LB was then added to the cells and incubated at 37°C for 1 hour or at 30°C for 2 hours (in the case of proviral DNA and lentiviral and retroviral vectors), in a shaking incubator. For ligated DNA, reaction mixtures were pelleted by brief centrifugation and the pellet re-suspended in 100 µl LB before plating onto LB-Agar plates containing the appropriate antibiotic and

incubated at 37°C or 30°C. For transformation of plasmid stocks, the reaction mixture was diluted 1:10, without centrifugation, before plating.

2.3 DNA extraction

2.3.1 Plasmid DNA purification from bacteria by miniprep

From a transformed bacteria plate, a single colony was used to inoculate 5 ml of sterile LB broth containing appropriate antibiotics. This was then incubated at 37°C or 30°C overnight in a shaking incubator. The following day, 1 ml of the culture was transferred to an eppendorf tube and cells pelleted at 14,000 rpm for 30 seconds. The supernatant was removed and another 1 ml of culture transferred to the same tube and the process repeated. The pellet was re-suspended in 250 µl Buffer P1 (50 mM Tris-HCL pH 8.0, 10 mM EDTA) and vortexed. Cells were then lysed in 250 µl Buffer P2 [200 mM NaOH and 1% SDS (w/v)], mixed by inverting the tubes and incubated at room temperature for 5 minutes. This was followed by the addition of 250 µl of Buffer P3 and incubation for 10 minutes on ice, to neutralise the mixture. Samples were then centrifuged at 14,000 rpm for 10 mins to pellet bacterial debris and chromosomal DNA. The supernatant was transferred to new eppendorf tubes and incubated with 800 µl of 96% ethanol at room temperature for 2 minutes to precipitate the DNA. Mixtures were then centrifuged at 14,000 rpm for 1 minute, the supernatant removed and the pellet air dried at room temperature for 5 minutes. The pellet was then washed in 70% ethanol and centrifuged at 14,000 rpm for 5 minutes. The ethanol was removed and the pellet dried using a vacuum centrifuge (Speedvac, eppendorf concentrator 5301) for 5 minutes. DNA was then re-suspended in 50 µl ddH_2O containing 0.5% RNaseA.

2.3.2 Plasmid DNA purification from bacteria by midi/maxi prep

From a transformed bacteria plate, a single colony was used to inoculate 50 ml/200 ml of sterile LB broth containing appropriate antibiotics. Cultures were grown overnight at 37°C or 30°C in a shaking incubator. Cells were pelleted by centrifugation at 6,000 x *g* for 15 minutes. Plasmid DNA was then purified by alkaline lysis using the Machery-Nagel Nucleobond Xtra midi/maxi prep kit as per the manufacturer's instructions. Briefly, cell pellets were re-suspended in 8 ml/12 ml of Buffer RES and then mixed with 8 ml/12 ml of Buffer LYS by gentle inverting, followed by incubation at room temperature for 5 minutes. This was followed by addition of 8 ml/12 ml of Buffer NEU

which was again mixed by gentle inverting. The lysate was then immediately added to Nucleobond Xtra Columns that had been pre-equilibrated with 12 ml/25 ml of Buffer EQU. The column and filter were then washed by adding 5 ml/15 ml of Buffer EQU to the rim of the filter and allowed to empty by gravity flow. The filter was then removed and the column was washed again with 8 ml/25 ml of Buffer WASH and allowed to empty by gravity flow. To elute the DNA from the column, 5 ml/15 ml of Buffer ELU was added and collected in 50 ml costar falcon tubes. The eluted DNA was then precipitated with 3.5 ml/10.5 ml of room temperature isopropanol, vortexed and incubated at room temperature for 2 minutes. The DNA was pelleted by centrifugation at 15,000 x *g* for 30 minutes at 4°C, the supernatant was then removed and the pellet washed by re-suspension in 1 ml of 70% ethanol. The DNA was transferred to sterile eppendorf tubes and centrifuged at 14,000 rpm for 10 minutes. The ethanol was removed by aspiration and the pellet was washed again as before. After removal of the ethanol, the pellet was air dried at room temperature for 15 minutes before being re-suspended in 100 µl/250 µl of ddH_2O. To aid homogenous re-suspension of the DNA, samples were heated at 50°C for 10 - 20 minutes. To ensure all the ethanol had been removed from the DNA, the solution was dried in a vacuum centrifuge for 12 minutes.

2.3.3 DNA Concentration Determination

DNA concentrations were determined using a Nanodrop ND-1000 Spectrophotometer (Labtech International), with optical density measurements at 260 nm [with the assumption that 1 OD_{260} unit corresponds to 50 µg/ml of double stranded (ds) DNA]. All DNA stocks were diluted to 1 mg/ml where possible.

2.4 Polymerase chain reaction (PCR)

2.4.1 Standard PCR conditions

PCR reactions were carried out in a total volume of 50 µl. Reaction mixtures contained 2 µl of plasmid DNA (10 ng/µl), 2.5 µl of sense and anti-sense oligonucleotide primers (10 pmol/µl), 10 µl of F-518 5X Phusion HF or 10µl 5X Phusion GC buffer (both of which contain 1.5 mM $MgCl_2$), 1 µl dNTP mix (10 mM each of dATP, dCTP, dGTP and dTTP) and 0.5 µl of F-530L Phusion DNA polymerase (2 U/µl). Buffers and enzymes were supplied by Finnzymes, New England Biolabs (NEB). Oligonucleotide primers were synthesised by MWG Eurofins (formerly MWG Biotech) and stock solutions of 100 pmol/µl were made using ddH_2O. PCR reactions were performed using an Eppendorf Mastercycler epgradient S thermocycler. Standard PCR conditions are presented in Table 2.2. 5 µl of the PCR reaction was run on an agarose gel.

Table 2.2: Standard PCR thermal cycling conditions

	Temperature	Time	Step
1	98°C	30 seconds	Initial denaturation
2	98°C	10 seconds	Denaturation
3	55°C	30 seconds	Annealing
4	72°C	30 seconds	Elongation
5	(go to step 2, repeat 27 times)		
6	72°C	10 minutes	Final extension
7	4°C	Hold	

2.4.2 Site directed mutagenesis by overlapping PCR

For site directed mutagenesis, the first round of PCR was performed as described in section 2.4.1, generating fragments of the insert containing the desired mutation(s). For the second round of PCR, equal amounts of the purified DNA fragments were used as templates for the DNA reaction. 5 cycles of PCR were first performed without primers, to allow annealing of the DNA templates. PCR was then performed as outlined in Table 2.2.

2.4.3 Agarose gel electrophoresis

1% (or 1.5% for smaller DNA fragments) agarose gels were made by adding 0.5 g of powdered agarose to 50 ml of TBE (supplied by Fisher, 0.09 M Tris, 0.09 M borate, 2 mM EDTA, pH 8.4) and heating to dissolve. Once the solution had cooled, 0.5 µg/ml of ethidium bromide was added and the mixture was poured into an electrophoresis tank and allowed to set. DNA samples were mixed with 6X loading dye (30% glycerol, 25 mg bromophenol blue, ddH_2O) and run on the gel in 1x TBE buffer. Band sizes were assessed by also running the DNA ladders λ DNA-HindIII digest and ΦX174 DNA-HaeIII (NEB) giving band sizes of 23130, 9146, 6557, 4361, 2322 and 2027 and 1353, 1078, 872, 603, 310, 281, 271, 234, 194, 118 and 72 base pairs respectively. Gels were run at 80V for approximately 1 hour, depending on the expected size of the bands. DNA was visualised on an ultra violet trans-illuminator using a CCD camera and gel quantification software (all supplied by BioRad).

2.5 DNA manipulation

2.5.1 PCR Purification

After verification of the size and quantity of the PCR product by gel electrophoresis, the PCR reaction mixture was purified using the QIAquick PCR purification kit supplied by QIAgen. 50 µl of ddH_2O was added to ~50 µl of the PCR reaction mix, followed by the addition of 500 µl of buffer PB. This was then thoroughly mixed and transferred to a QIAquick spin column. The column was centrifuged at 14,000 rpm for 1 minute and the flow through was discarded. 750 µl of buffer PE was then added and centrifuged as before. After removal of the flow through, the column was spun again for an additional 2 minutes to remove any residual ethanol. The column was then transferred to a sterile eppendorf tube and DNA eluted with the addition of 30 µl ddH_2O. The column was left to stand for 2 minutes at room temperature before centrifugation at 14,000 rpm for 1 minute to collect the DNA.

2.5.2 DNA digestion by restriction endonucleases

For cloning digests, reactions were performed in 50 µl total volume. 30 µl of PCR purified DNA (or 3 µl of purified expression plasmid DNA plus 27 µl of ddH_2O) was digested with 1 µl of each restriction enzyme (supplied by NEB in all cases), 5 µl of the appropriate 10X buffer and 0.5 µl of 100 µg/ml bovine serum albumin (BSA), where recommended (NEB). For analytical digests, reactions were performed in 15 µl total volume. 3 µl of DNA was digested with 0.5 µl of each restriction enzyme, 1.5 µl of the appropriate 10X buffer and 0.15 µl of BSA, where recommended. All reactions were carried out at 37°C for 2 - 3 hours, unless recommended otherwise by manufacturers instructions.

2.5.3 De-phosphorylation of digested DNA

In order to prevent re-ligation of the compatible ends of the digested vector DNA, it was de-phosphorylated using calf intestinal alkaline phosphotase (CIP, supplied by NEB). 1 µl of CIP was added to 50 µl of the digested DNA and incubated at 37°C for 1 hour.

2.5.4 Gel extraction and purification

In order to purify the DNA from the digest reaction mixture, digested DNA was run on agarose gels as described in section 2.4.3 and visualised using ultra violet radiation. DNA fragments of the correct size were isolated from the gel using a clean razor blade. Gel fragments were transferred into eppendorf tubes and purified using the QIAgen QIAquick gel extraction kit. 3 volumes of Buffer QG were added to 1 volume of gel slice and incubated at 50°C for 10 minutes or until the gel had completely dissolved. 700 µl was first transferred to a QIAquick column and centrifuged at 14,000 rpm for 1 minute. The flow-through was discarded and the rest of the solution was applied to the column as before. 500 µl of Buffer QG was then added to the column and centrifuged at 14,000 rpm for 1 minute. The flow through was discarded and the column was washed with 750 µl Buffer PE before being centrifuged at 14,000 rpm first for 1 minute (with removal of the flow through) and then for an additional 2 minutes to ensure the complete removal of ethanol. The columns were then placed into sterile eppendorf tubes and 50 µl of ddH_2O was added to the columns to elute the DNA. Columns were left to stand at room temperature for 2 minutes before centrifugation at 14,000 rpm for 1 minute to collect the DNA.

2.5.5 DNA Ligation

Prior to ligation, 4 µl of the purified digested DNA was run on an agarose gel (as described in section 2.4.3) in order to check the yield of DNA following purification.

Ligation reactions were carried out in a total volume of 20 µl. Typically 9 µl of the digested insert and 1 µl of the digested vector was ligated with 2 µl of T4 DNA ligase buffer and 1 µl of T4 DNA ligase (both supplied by NEB). The reaction mixture was incubated at room temperature from 4 hours to overnight and used to transform competent bacterial cells.

2.6 Cell lines and cell culture

2.6.1 Cell lines, media and maintenance

293T cells derived from human embryonic kidney fibroblasts, HeLa cells derived from a human epithelial cervical adenocarcinoma and TZM cells, a modified HeLa cell line engineered to express CD4+, CXCR4+ CCR5+ as well as the *luciferase* and *lacZ* genes under the control of the HIV-1 LTR promoter, were grown in Dulbecco's modified Eagle medium (DMEM, Invitrogen), supplemented with 10% heat inactivated foetal calf serum (GIBCO, 30 minutes at 56°C) and 1% penicillin/streptomycin (Invitrogen). The Hut78 T-cell line was maintained in Roosevelt Park Memorial Institute medium (RPMI, Invitrogen), supplemented with 10% heat inactivated foetal calf serum and 1% penicillin/streptomycin, as described above. All cell lines were kept at 37°C and 5% CO_2 in a humidified chamber and passaged every 2 days. Adherent cells were first washed in 1x phosphate buffered saline (PBS, Sigma) and then detached from tissue culture plates by the addition of 1 ml of the Trypsin substitute TrpLE Express + Phenol Red (Invitrogen). Cells were incubated at 37°C for approximately 5 minutes before being re suspended in fresh pre-warmed DMEM. Non-adherent cells were split into new culture dishes with fresh RPMI.

All tissue culture plastic consumables were obtained from Corning Incorporated.

2.6.2 Freezing and thawing

Long-term frozen stocks of all cell lines were kept in liquid nitrogen. Cells from a semi-confluent plate, were pelleted by centrifugation at 1,200 rpm for 5 minutes. Cell pellets were then re-suspended in medium containing 30% foetal calf serum and incubated on

ice for 15 minutes. Freezing medium was then added consisting of 30% foetal calf serum plus 20% DMSO (in either DMEM or RPMI). Cells were immediately slow cooled at -80°C before being transferred to liquid nitrogen the following day.

Frozen vials of cells were thawed at 37°C for approximately 1 minute before being rapidly transferred to 10ml of pre-warmed media. Cells were centrifuged at 1,200 rpm for 5 minutes before re-suspension of the pellet in 5 ml media and transfer to a 6 cm tissue culture dish.

2.7 Transfection

2.7.1 Transient transfection with cDNA

All transfections were performed on sub-confluent monolayers of cells plated 24 hours beforehand, unless otherwise stated.

HEK-293T cells were transfected with polyethylenimine (PEI, Polysciences). For cells seeded in a 24 well cell culture plate, 1 µg of DNA was mixed with 1 µl of PEI and 96 µl of serum free DMEM by gentle vortexing and incubated at room temperature for 10 minutes. The transfection mixture was then added dropwise to cells and culture media was replaced 6 - 8 hours post-transfection.

HeLa cells were transfected with Fugene 6 (Roche) or specifically for luciferase reporter assays with Lipofectamine 2000 (Invitrogen). For the former, 3 µl of Fugene 6 transfection reagent was mixed with 100 µl of Optimem (GIBCO, Invitrogen) by gentle vortexing. The transfection mixture was then added dropwise to 1 µg of DNA in separate eppendorf tubes and incubated at room temperature for 10 minutes. The transfection mixture was then added dropwise to the cells. For Lipofectamine transfections in a 24 well cell culture plate, 1 µl of Lipofectamine 2000 transfection reagent was mixed with 49 µl of Optimem. Separately, 1 µg of DNA was mixed with 49 µl of Optimem, before the two mixtures were combined and incubated at room temperature for 20 minutes. The transfection mixture was the added dropwise to cells and the cell culture media was replaced 6 hours post transfection.

In all cases, quantities were increased as appropriate for larger scale transfections.

2.7.2 Transient transfection with siRNAs

Stock solutions of 50 μM or 75 μM siRNA oligonucleotides (obtained from either Dharmacon or Ambion Technologies) were made in RNase free ddH_2O (supplied by the manufacturer).

HEK-293T and HeLa cells were seeded 24 hours and 2 hours, respectively, prior to transfection in 24 well cell culture plates. Cells were transfected with Dharmafect1 transfection reagent (Dharmacon) as described for Lipofectamine 2000 transfections (section 2.7.1) and typically with 50 pmol of siRNA. 24 hours later, HEK-293T cells were re-seeded into new cell culture plates and transfected as before, the following day. For HeLa cells, 24 hours after the initial transfection, cell media was replaced and the following day, cells were re-seeded and transfected again 2 hours later. 24 hours later, cell media was replaced and 48 hours post the second transfection cells were harvested. Alternatively, 12 hours post the second transfection cells were infected with virus or transfected with DNA as required.

2.7.3 Generation of stable cell lines

Sub-confluent monolayers od 293T cells, seeded in 10 cm dishes, were transfected with 8 μg of the lentiviral or retroviral expression plasmid, 8 μg of the p8.91 or pCgp Gag-Pol expression plasmid (for production of lentiviral and retroviral vectors respectively) and 4 μg of a Vesicular Stomatitis Virus-G envelope protein (VSV-G) expression plasmid, using PEI (as described in section 2.7.1). 48 hours later, viral supernatants were harvested and filtered through a 0.45 μm PVDF Millex®-HA filter (Millipore) and used to transduce either HEK-293T or HeLa cells, seeded in 24 well plates 24 hours beforehand, in the presence of polybrene (5 μg/ml). 48 hours post transduction, cells were placed under selection, either puromycin dihydrochloride (1 μg/ml) for lentiviral vectors or G418 disulphide (neomycin, 1mg/ml) for retroviral vectors. Cells were maintained under selection and analysed for protein expression when all untransduced control cells had died, at least 3 (puromycin) or 10 (neomycin) days after the start of selection.

2.8 Protein manipulation

2.8.1 Sodium dodecyl sulphate polyacrylamide gel electrophoresis (SDS-PAGE)

SDS-PAGE was used to separate proteins according to size. Denaturing separating gels [7-12% (30% acrylamide bis/solution 37.5:1, Biorad), 375 mM Tris-HCL (pH 8.8), 0.1% SDS, 0.1% ammonium persulphate, 0.0004% N, N, N', N'-tetramethylethyenediamine (TEMED)] of either 7% (proteins > 80kDa), 10% (20kDa < proteins > 80kDa) or 12% (proteins < 20kDa), were cast using the Mini-PROTEAN® 3 electrophoresis system (Biorad). Gels were levelled with the addition of 70% ethanol, which was removed before addition of the stacking gel [4% acrylamide mix, 125 mM Tris-HCL (pH 6.8), 0.1% SDS, 0.1% ammonium persulphate and 0.001% TEMED), using 0.75mm spacers. Samples were diluted in 3x gel loading dye [30% glycerol, 9% SDS, 180 mM Tris-HCL (pH6.8), 0.00125% bromophenol blue), made to 1x with 10 mM DL-Dithiothreitol (DDT) and ddH_2O. Lysates were homogenised either by sonication (Branson Sonifier 250) for 2 x 10 seconds or by passing through a 25G x 5/8" needle (Terumo Neolus) with a 1 ml sterile syringe (BD Plastipak™) approximately 10 times. Before loading, samples were boiled for 5 - 10 minutes. Gels were run at 100V for approximately 2 hours in running buffer [0.1% SDS, 27.6 mM Tris base, 0.2 M glycine, pH >8.8]. Protein sizes were determined by comparison to the Benchmark Pre-stained protein ladder (NEB).

2.8.2 Immunoblot analysis

Proteins were transferred onto 0.45 μm nitrocellulose (Anachem) or PVDF (BDH-VWR) membranes. PVDF membranes must be pre-activated by soaking in methanol prior to transfer. Transfers were carried out at 16V overnight in transfer buffer (0.1% SDS, 27.6 mM Tris Base, 0.2 M glycine, 20% methanol, pH > 8.8).

Following transfer, membranes were first blocked in 1% milk solution (milk powder, 0.1% tween, dissolved in PBS) for 1 hour at room temperature. Membranes were then incubated with the primary antibody, diluted in milk solution, for approximately 2 hours at room temperature, followed by 4 washes for 5 minutes in wash buffer (0.1% tween in PBS). Membranes were then incubated for 1 hour with either horseradish peroxidase (HRP) conjugated secondary antibodies (for detection by enhanced chemiluminescence, ECL) or with 680λ or 800λ Infrared IRDye® conjugated secondary antibodies (for detection by Li-cor Odyssey infrared imaging systems). In the latter case, upon addition

of the antibody, membranes were protected from light. Subsequently blots were washed 4 times for 10 minutes in wash buffer, as before.

For ECL development, HRP-conjugated antibodies were detected by incubation of the membrane for 5 minutes with either SuperSignal® West Pico Chemiluminescent substrate (Pierce) or ECL Plus Western Blotting Detection System (Amersham), for more difficult to detect proteins, as per manufacturer's instructions. Proteins were visualized using an ImageQuant LAS 4000 mini system consisting of a Luminescent Image Analyser and F0.85 43mm LAS high sensitivity lens (Fujifilm), all provided by GE Healthcare. For Li-cor analysis, membranes were rinsed in 1x PBS and imaged using the Li-cor Odyssey infrared imaging systems (Li-cor Biosciences).

Details of the antibodies used for immunoblot, as well as immunofluorescence and immunoprecipitation, analyses are provided in Tables 2.3 and 2.4.

Table 2.3: Primary antibodies.

Antibody	Species	Source	Dilution
α A3G	Rabbit	(Newman et al, 2005)	1/1000 (WB) 1/500 (IF)
α Ago2 (11A9)	Rat	Sigma	1/1000 (WB)
α ALIX	Rabbit	kind gift from Dr Wesley Sundquist	1/10,000 (WB)
α β-actin	Mouse	Abcam	1/1000 (WB)
α DDX6	Rabbit	Cambridge Biosciences	1/2000 (WB) 1/500 (IF)
α FLAG (MS2)	Mouse	Stratagene	1/1000 (WB)
α Ge1/s6 kinase	Mouse	Santa Cruz	1/500 (IF)
α GFP	Mouse	Roche	1/2000 (WB) 1/500 (IF)
α HA (12CA5)	Mouse	(Chen et al., 1993)	1/1000 (WB/IP) 1/500 (IF)
α HA	Rabbit	Rocklands	1/3000 (WB) 1/500 (IF)
α HSP90	Rabbit	Santa Cruz	1/3000 (WB)
α Lsm1	Chicken	Sigma	1/500 (WB)
α myc (9E10)	Mouse	(Evan et al., 1985)	1/1000 (WB/IP)
α $p24^{Gag}$ (24.2)	Mouse	(Fouchier et al., 1997)	1/1000 (WB)
α $p24^{Gag}$ (UP598)	Rabbit	(Simon et al., 1997)	1/500 (IP)

IF = immunofluorescence, IP = immunoprecipitation, WB = western blot

Table 2.4: Secondary Antibodies.

Antibody	Conjugation	Source	Dilution
Goat α-chicken	HRP	Sigma	1/1000
Goat α-mouse	HRP	Chemicon	1/2000
Goat α-rabbit	HRP	Cell Signalling	1/2000
Goat α-rat	HRP	Cell Signalling	1/2000
800nmλ Goat α-mouse	IRDye	Li-cor Biosciences	1/5000
800nmλ Goat α-rabbit	IRDye	Li-cor Biosciences	1/5000
680nmλ Goat α-mouse	IRDye	Li-cor Biosciences	1/5000
680nmλ Goat α-rabbit	IRDye	Li-cor Biosciences	1/5000
488nmλ Goat α-mouse	Alexa Fluor 488	Molecular Probes	1/500
488nmλ Goat α-rabbit	Alexa Fluor 488	Molecular Probes	1/500
594nmλ Goat α-mouse	Alexa Fluor 594	Molecular Probes	1/500
594nmλ Goat α-rabbit	Alexa Fluor 594	Molecular Probes	1/500

2.9 Single cycle infectivity assay

2.9.1 Production of virus stocks

Virus stocks were produced from HEK-293T or HeLa cells seeded in 6 well culture plates and transfected accordingly as described in section 2.7. Typically 48 hours post-transfection, viral supernatants were harvested and filtered through a 0.45 µm PVDF Millex®-HA filter (Millipore). 100 µl of supernatant was removed for quantification by $p24^{Gag}$ ELISA (see section 2.9.2) and stored at either 4°C for no longer than 6 hours (for virion incorporation assays, see section 2.9.4) or at -80°C for long-term storage. Infected HEK-293T cells were removed from the plate in 1 ml 1x PBS and centrifuged at 500 x *g* for 5 minutes. Pellets were then re-suspended in 3x loading dye and subjected to immunblot analysis (see section 2.8.2). HeLa cells were directly harvested in 3x loading dye.

2.9.2 $p24^{Gag}$ quantification by ELISA

This assay was performed using a $p24^{Gag}$ enzyme-linked immunosorbent assay (ELISA) kit (Perkin Elmer™) with all described reagents supplied with the kit. 100 µl of virus stock was diluted in 400 µl of 0.1% Triton X-100® in PBS (protected from light). From this initial 1:5 dilution, further dilutions were made as necessary, typically of between 1:50 - 1:250. 200 µl of the diluted virus stock was then loaded onto a pre-washed [6 times with plate wash (0.05% Tween-20 in PBS with 0.1% 2-chloroacetamide as a preservative)] antibody covered microplate (96-well microplate coated with monoclonal antibody to HIV-1 $p24^{Gag}$ with 0.01% Proclin-300 as a preservative). The plate was also loaded with 6 standard solutions of the following concentrations: 1000, 2000, 500, 150, 60 and 25 pg/ml. The standards were prepared using the $p24^{Gag}$ positive control (containing 200 ng/ml HIV-1 $p24^{Gag}$ in PBS plus PBS and Triton X-100® with 0.1% sodium azide as a preservative) diluted in lysis buffer (0.5% Triton X-100® in PBS plus an inert blue dye and 0.002% sodium azide as a preservative). The first well (A1) was left empty and the second was loaded with 200 µl of lysis buffer only, as negative controls, before addition of 200 µl of the standards and then the samples, in that order. The plate was then incubated at 37°C for 30 minutes to allow binding of the $p24^{Gag}$ protein to the monoclonal antibody coating the plate. The plate was then washed 6 times as before and 100 µl of detector antibody (biotinylated rabbit polyclonal anti-$p24^{Gag}$ antibody in PBS containing animal sera, casein and human serum non-reactive for hepatitis B surface antigen and antibodies to HIV-1, HIV-2 and HCV with 0.2%

Proclin-300 and <0.1% sodium azide as a preservative) was added to each well (except A1), and incubated at 37°C for 1 hour, before the plate was washed 6 times. Streptavidin-HRP [streptavidin-HRP (horseradish peroxidase) concentrate in citrate buffer with BSA, detergent and 0.5% 2-chloroacetamide] was diluted 1:100 in streptavidin-HRP diluent (PBS with BSA, 0.05% Tween-20 and 0.5% 2-chloroacetamide as preservative), and 100 µl of this was added to each well (except A1) and incubated at 37°C for 30 minutes. This allows the streptavidin-HRP to form a complex with the biotinylated secondary antibody. An orthophenylenediamine-HCL (OPD) tablet was then dissolved in 11 ml of substrate diluent (citrate buffer containing 0.03% hydrogen peroxide and 0.002% sodium stannate as a stabilizer) by vortexing and 100 µl of this OPD substrate solution was added to all wells (including A1) after the plate had been washed 6 times. The OPD substrate reacts with the streptavidin-HRP/biotinylated secondary antibody complex that is bound to the $p24^{Gag}$ protein, producing a yellow colour that is directly proportional to the amount of HIV-1 $p24^{Gag}$ protein present in each well. The plate was then incubated for 15 - 20 minutes at room temperature in the dark before addition of 100 µl of STOP solution to all wells, to quench the reaction. The plate was then read using a Benchmark Plus™ microplate spectrophotometer (Bio-Rad) at dual (subtractive) wavelengths of 405 and 630 mm. Values were analysed using the Microplate Manager 5.2.1 software (Bio-Rad) to give a quantified concentration of $p24^{Gag}$ protein in pg/ml.

2.9.3 β-galactosidase reporter assay

TZM-βL cells harbouring the *lacZ* gene under the control of the HIV-1 LTR promoter were seeded in 24 well plates at 1 x 10^5 cells per well, 24 hours before infection. Cells were challenged with virus equivalent to 5 ng of $p24^{Gag}$ for 24 - 30 hours, before media was removed, cells washed in 1x PBS and subsequently lysed in 100 µl of Galacto-*Star*™ Lysis Solution (100 mM potassium phosphate pH7.8, 0.2% Triton X-100®, Applied Biosystems) for 5 minutes at room temperature before the plate was frozen at -80°C, typically overnight. Tropix Galacton-*Star*™ substrate for β-galactosidase, diluted 1:50 in Reaction Buffer Diluent [100 mM sodium phosphate (pH 7.5), 1mM $MgCl_2$, 5% Sapphire-II™ enhancer], both from Applied Biosystems, was prepared and 100 µl was added to 20 µl of thawed cell lysate in white polystyrene 96 well plates (Costar). The substrate and Sapphire-II™ enhancer produce light emissions upon contact with β-

galactosidase that was measured using a luminescence counter (Perkin Elmer) and Wallac 1420 Workstation software.

2.9.4 Virion incorporation analysis

20 ng of virus stocks, quantified by $p24^{Gag}$ ELISA (see section 2.9.2), were loaded onto a 20% sucrose cushion (20% sucrose in PBS) and purified by centrifugation at 14,000 rpm for 2 hours at 4°C. The supernatant was then removed by aspiration and the pellet re-suspended in 3x loading dye and subjected to immunoblot analysis (see section 2.8.2).

2.10 Replication curve

Virus stocks were produced in 293T cells seeded in 10 cm cell culture plates and transfected at 70% confluency as described in section 2.9.1. 48 hours later, viral supernatants were harvested, filtered through a 0.45 µM PVDF Millex®-HA filter (Millipore) and 100 µl removed for quantification by $p24^{Gag}$ ELISA (see section 2.9.2). The remainder was aliquoted and stored at -80°C.

5 ng, 25 ng or 125 ng of $p24^{Gag}$ quantified virus (wild-type or Δ*vif*) was used to infect approximately 3 x 10^6 Hut78 cells in 1 ml of RPMI media total, at 37°C for 2 hours. Cells were then pelleted by centrifugation at 300 x *g* for 5 minutes. The pellet was re-suspended in 5 ml of 1x PBS and centrifuged as before. This was repeated a further 2 times, to ensure that all input virus had been removed. Cells were then re-suspended in 10 ml RPMI media and centrifuged as before. 100 µl of supernatant was removed as time point zero and diluted in 400 µl of 0.1% Triton X-100® for $p24^{Gag}$ analysis by ELISA (see section 2.9.2). The cells were then re-suspended in RPMI media, transferred to 25 cm^2 flasks and incubated at 37°C with 5% CO_2. Every 2 days post infection, 5 ml of cells was centrifuged as before, with 100 µl of supernatant removed for $p24^{Gag}$ quantification as described for time point zero. Cell pellets were washed in 1x PBS and lysed in 3x loading dye for immunoblot analysis. 5 ml of fresh RPMI media was added back to the flasks to maintain cell cultures, which were continued for approximately 8-10 days post infection. Viral supernatants were quantified by $p24^{Gag}$ ELISA (see section 2.9.2) and cell lysates analysed by immunoblotting (see section 2.8.2).

2.11 Infections

Virus stocks were produced in 293T cells seeded in 10 cm cell culture plates and transfected at 70% confluency as described in section 2.7. For wild type and Δ*vif* but not Δ*env* viral stocks, viruses were produced in the presence of VSV-G to generate pseudotyped virions for infection of HeLa cells, which do not express the necessary receptors to allow HIV-1 infection. Transfections were carried out at a ratio of 3:1 (proviral plasmid DNA to VSV-G plasmid DNA). 48 hours later, viral supernatants were harvested, filtered through a 0.45 μM PVDF Millex®-HA filter (Millipore) and 100 μl removed for quantification by $p24^{Gag}$ ELISA (see section 2.9.2). The remainder was aliquoted and stored at -80°C.

Virus equivalent to 50 ng or 100 ng of $p24^{Gag}$ was used to infect HeLa cells seeded at 2 x 10^5 cells per well in 6 well cell culture plates in 800 μl of DMEM total, at 37°C for 4 hours. Cells were then washed 4 times in 1x PBS to remove all input virus and 2 ml of fresh DMEM was added back. 48 hours later, viral supernatants were harvested, quantified by $p24^{Gag}$ ELISA and a β-galactosidase reporter assay performed and virion incorporation assessed (see section 2.9).

2.12 Protein interaction assays

2.12.1 Co-immunoprecipitation

293T cells seeded at 5 x 10^5 cells per well in 6 well cell culture plates were transfected as described in section 2.7. 24 - 48 hours later, media was removed and cells were harvested in 1 ml of chilled 1x PBS and centrifuged at 500 x *g* for 5 minutes at 4°C. The supernatant was removed and cells were lysed in 600 μl of immunoprecipitation (IP) buffer [150 mM NaCl, 50 mM Tris (pH 7.5), 1% Nonidet P-40 (NP-40) and complete protease inhibitor cocktail (Roche)] for 30 minutes at 4°C on a rotational tumbler. Lysates were then cleared by centrifugation at 18,000 x *g* for 15 minutes. 10 μl of supernatant was removed and resuspended in 3x loading dye for immunoblot analysis to check for cellular protein expression. 580 μl was transferred to new eppendorf tubes containing 30 μl of Protein G agarose (Invitrogen) per sample that had been pre-washed (3 times in IP buffer) and pre-incubated with the appropriate antibody for immunoprecipitation on a rotational tumbler for 90 minutes at 4°C. The agarose beads

and cell lysate mix was then incubated on a rotational tumbler at 4°C for 2 - 4 hours. Agarose beads were then washed 3 times in IP buffer and bound complexes eluted in 3x loading dye for immunoblot analysis (see section 2.8.2).

2.12.2 Co-immunoprecipitation with formaldehyde cross-linking

293T cells seeded at 5 x 10^5 cell per well in 6 well cell culture plates were transfected as described in section 2.7. 48 hours later, cells were harvested in 1 ml of chilled 1x PBS and centrifuged at 500 x *g* for 5 minutes to pellet the cells. The pellet was re-suspended in 0.05% formaldehyde (36.5%), diluted in PBS and incubated at 37° for 10 minutes. Cells were then pelleted by centrifugation at 18,000 x *g* for 1 minute and washed in 1x PBS, before re-suspension in 0.25 M Glycine (pH 7.0) and incubation at room temperature for 5 minutes. Cells were washed again as before and then lysed in 1x BB Lysis Buffer [150 mM NaCl, 10 mM Hepes (pH 7.0), 6 mM $MgCl_2$, 2 mM DDT, 10% Glycerol, 0.5% NP-40 and complete protease inhibitor cocktail] for 10 minutes on ice. Lysates were then sonicated (Branson Sonifer 250) 3 times for 10 seconds and then clarified by centrifugation at 1000 x *g* for 10 minutes. 10 µl of supernatant was removed and re-suspended in 3x loading dye for immunoblot analysis to check cellular protein expression levels. The remaining supernatant was transferred to new eppendorf tubes containing Protein G agarose and antibody prepared as described in section 2.12.1. The agarose beads and cell lysate mix was then incubated on a rotational tumbler at 4°C for 2 hours before being washed 5 times in filter sterilised RIPA Buffer [NaCl, 100 mM Tris-HCl (pH 7.5), 1% Triton X-100®, 0.1% SDS, 1% sodium deoxycholate, 1 mM EDTA]. After the final wash, agarose beads were re-suspended in reverse cross-linking buffer (10 mM EDTA, 5 mM DDT, 0.5% SDS) and heated at 65°C for 45 minutes. Samples were then re-suspended in 3x loading dye for immunoblot analysis (section 2.8.2).

2.12.3 Yeast 2 hybrid

Y190 cells (a kind gift from Dr. Juan Martin-Serrano), encoding the β-galactosidase enzyme under the control of the GAL4 transcriptional activator and with mutations in the LEU2 and TRP1 genes, were used. Cells were grown in liquid cultures of YPD broth (50 g/L) and YPD agar (67 g/L, Q-BIO gene) plates for yeast stocks, both supplemented with Adenine sulphate (100 mg/L, Q-BIO gene). Experimentally transformed yeast were grown on synthetic drop-out (SD) agar (46.7 g/L) supplemented with synthetic drop-out medium without Leucine and Tryptophan (1.54 g/L).

Y190 cells from stock culture plates were used to inoculate SD media at a dilution of 1:8. Overnight cultures were grown at 30°C in a shaking incubator until they reached an OD_{600} of 0.5 - 0.7. Cells were pelleted by centrifugation at 1,800 rpm for 5 minutes. The pellet was then washed in 200 ml ddH_2O and centrifuged as before. Cells were then re-suspended in 500 µl of filter sterilised Lithium Acetate (LiAc) solution [0.1 M LiAc (pH 7.5), 10 mM Tris-HCL (pH7.5), 1 mM EDTA) per 100 OD's. Cells were then either incubated at room temperature for 90 minutes before transformation or aliquoted in sterile eppendorf tubes with 25% glycerol for long-term storage at -80°C.

For transformation of competent yeast cells, salmon sperm carrier ssDNA (10 mg/ml) at 10% the volume of re-suspended yeast cells was boiled for 8 minutes, chilled on ice for 5 minutes and then added to the competent yeast cells and mixed by gentle tapping. 30 µl of this mixture was then added to eppendorf tubes already containing 1 µg each of plasmid DNA in the pGBKT7 (DNA binding domain) and HB18 (transcriptional activation domain) vectors. This was followed by addition of 230 µl of 40% Polyethylene glycol (PEG) solution [50% PEG 3350, 0.1 M Liac (pH 7.5), 10 mM Tris (pH 7.5), 1 mM EDTA]. The mixture was gently vortexed and incubated at 30°C for 45 minutes before heat shocking at 42°C for 15 minutes. Cells were then plated onto -Leucine, -Tryptophan SD agar plates and incubated at 30°C for 3 - 4 days.

Colonies of transformed yeast cells were scraped off culture plates using a clean pipette tip and re-suspended in 0.5 ml lysis buffer [1 ml filter sterilised 5X Z buffer [1 M $Na_2HPO_{4.7}H_2O$, 1 M KcL, 1M $MgSO_{4.7}H_2O$ (pH7.0), 14 µl 2-Mercaptoethanol, 4 µl 10% SDS, 4 ml ddH_2O]. This was followed with the addition of 25 µl of chloroform and the sample was vortexed to mix. The reporter gene substrate, chlorophenol red β-D-galactopyranoside (CPRG) (Roche) was used to measure β-galactosidase production as a read-out of *lacZ* activation. 50 µl of CPRG was added to the samples, vortexed and incubated at room temperature for 30 minutes. Samples were then centrifuged at 14,000 rpm for 30 seconds and 100 µl of supernatant was assayed for optical density measurements at OD_{540} using a Benchmark microplate spectrophotometer (BIORAD).

2.12.4 FRET/FLIM

HeLa cells were seeded onto coverslips in 12 well plates and transfected as described in section 2.7. 24 hours later, cells were washed in 1x PBS and fixed in 4% formaldehyde.

Cells were washed again and then permeabilised with 0.25% Triton X-100® to enable staining of HA-tagged Ago2 included as a negative control. Cells were then quenched with the addition of 1 mg/ml sodium borohydride for 5 minutes which was subsequently removed and cells washed as before. Primary anti-mouse Cy-5 conjugated antibody (Jacksons Immunoresearch Laboratories) was diluted 1/1000 in 1% BSA and incubated with the cells for 2 hours at room temperature in the dark. Cells were then washed 3 times for 5 minutes in 1x PBS before addition of the anti-mouse secondary antibody (kindly provided by Dr Simon Ameer-Beg), for 1 hour. Cells were washed as before and coverslips were mounted onto slides using Mowiol mounting medium (ICN) containing 2.5% (w/v) 1,4-diazabicyclo (2.2.2) octane as an antifade reagent. Slides were dried overnight. All FLIM measurements were undertaken with a 40x (1.3 NA) Nikon Plan-Fluor oil objective lens on a modified multiphoton microscopy system and were conducted and analysed by Dr Simon Ameer-Beg.

2.13 Immunofluorescence analysis

HeLa, HEK-293T and Hut78 cells were seeded onto coverslips in 12 well cell culture plates. In order for Hut78 cells to adhere, coverslips were pre-treated with poly-L-lysine according to manufacturer's instructions. Cells were then either transfected (see section 2.7) or fixed 24 hours later, if they had been previously transduced with lentiviral and/or retroviral vectors. For fixation, cells were carefully washed 3 times in 1x PBS and then fixed with 4% paraformaldehyde (Electron Microscopy Sciences), diluted in PBS, for 10 minutes at room temperature. Once fixed, cells were protected from light as much as possible. Cells were then washed again, as before and permeabilised (where necessary) with 0.2% Triton X-100® for 12 minutes at room temperature. Cells were then blocked and simultaneously quenched in NGB buffer (50 mM NH_4Cl, 2% goat serum, 2% BSA and 0.05% sodium azide in PBS) for 30 minutes. Primary antibody diluted in NGB buffer was then added for 2 hours at room temperature. Coverslips were then washed 3 times for 5 minutes in 1x PBS before addition of the appropriate Alexa Fluor conjugated secondary antibody (see Table 2.4), again diluted in NGB buffer, for 1 hour. The secondary antibody was removed and cells were additionally stained for 1 minute with 4',6-diamidino-2-phenyllindole (DAPI) dilactate (Molecular Probes) diluted 1:25,000 in PBS, for visualisation of the nucleus. Coverslips were then washed again as

before and mounted onto glass slides (Fisher) using 12 µl of Mowiol mounting media (Calbiochem). Slides were dried overnight in the dark.

Images were collected using a TCS SP2 AOBS confocal laser scanning microscope (DM IRE2: Leica), with a 63.0x oil objective lens and processed with the LSC software (version 2.02, Leica), Openlab (Improvision, Openlab, version 5.02) and Adobe Photoshop (version 8.0).

2.14 Luciferase reporter assays

Assays were performed using the Dual Luciferase® Reporter Kit, supplied by Promega. HeLa cells seeded at 1 x 10^5 cells per well in 24 well plates were transfected as described in section 2.7. 24 - 48 hours later, supernatants were removed and cells washed in 1x PBS before addition of 100 µl of Passive Lysis Buffer (supplied as a 5X stock, diluted in ddH_2O) for 15 minutes at room temperature with gentle agitation. 20 µl of cell lysate was transferred to a white polystyrene 96 well plate (Costar). Luciferase Assay Reagent II (LAR II) was prepared by dissolving Luciferase Assay Substrate in Luciferase Assay Buffer II and 100 µl of this reagent was added to each well in order to measure firefly luciferase activity. Samples were mixed by pipetting, and light emissions were immediately read using a luminescence counter (Perkin Elmer) and Wallac 1420 Workstation software. 100 µl of Stop & Glo® reagent was then added to simultaneously quench firefy luciferase activity and activate *Renilla* luciferase. This solution was prepared by mixing Stop & Glo® substrate with Stop & Glo® Buffer at a 1:50 ratio. Samples were then mixed by pipetting and measurements taken as before.

Typically results are presented as firefly luciferase values divided by *Renilla* luciferase values (after subtraction of background values which were measurements taken from untransfected cell lystates), when *Renilla* values were equivalent across all samples, giving a ratio of firefly to *Renilla* luciferase values.

2.15 Pulse labelling

2.15.1 Radiolabelling

HeLa cells seeded in 6 well cell culture plates were transfected with siRNAs and DNA as described in section 2.7. 48 hours post transfection, viral supernatant was removed and filtered through a 0.45 µM PVDF Millex®-HA filter (Millipore) with 100 µl removed for quantification by $p24^{Gag}$ ELISA (see section 2.9.2). Cells were then washed twice in warm 1x PBS. 1 ml of pre-warmed and equilibrated depletion media (-Cys, -Met DMEM, 10% dialysed serum, 1% glutamine) was added and cells incubated at 37°C for 20 minutes. ^{35}S[cysteine/methionine] (Perkin-Elmer) was then added directly to each well, equivalent to 0.25 mCi, and cells incubated at 37°C for 5 minutes, this time contained within a Perspex charcoal trap. Media was then removed and cells washed in 1x PBS. 1 ml of RIPA buffer (see section 2.12.2) was then added to each well and using cell scrapers, lysates were transferred to screw-capped tubes and stored at -80°C. All radioactive waste was disposed of appropriately and as directed by King's College London Health and Safety guidelines.

2.15.2 Immunoprecipitation

Lysates were thawed, vortexed and briefly centrifuged before homogenisation using a 25G x 5/8" needle (Terumo Neolus) and 1 ml sterile syringe (BD Plastipak™). Lysates were then clarified by centrifugation at 14,000 rpm for 30 minutes. 20 µl of lysate, post clarification, was removed for immunoblot analysis. 750 µl of lysate was added to new screw capped tubes and incubated with the Gag specific UP598 antibody (see Table 2.3) overnight at 4°C on a rotational tumbler. Samples were then centrifuged and 30 µl of pre-washed Protein G Agarose beads (see section 2.12) was added to each tube and incubated at 4°C for 1 hour on a rotational tumbler. Samples were then centrifuged for 1 minute at 4,500 rpm and supernatant removed by aspiration before the agarose beads were washed 3 times in 500 µl RIPA buffer (see section 2.12). Agarose beads were then re-suspended in 30 µl of 3x loading dye and subjected to freezing and thawing to aid lysis.

2.15.3 Imaging

Before loading onto denaturing polyacrylamide gels, samples were boiled for 10 minutes. 10 µl was loaded onto 10% polyacrylamide gels, made using New Brunswick apparatus, which were run at 50V overnight. The following day, gels were transferred

onto PVDF membranes as per immunoblot analysis (see section 2.8.2) for 4 hours at 325 mA. Membranes were then dried by successive placement between clean sheets of Whatman paper for 10 minutes at a time. Once dried, membranes were placed in a phosphoimager screen (Molecular Dynamics) in a Kodak BioMAX cassette overnight and visualised by autoradiography using a Typhoon TRIO Variable Mode Imager (GE Healthcare). Membranes were also transferred onto Kodak BioMAX T-MAT MS film with a Transcreen Intensifying Screen (Kodak) for 5 days at -80°C and subsequently developed with a Kodak X-OMAT 2000 Processor.

All chemicals were supplied by Sigma-Aldrich unless otherwise stated.

CHAPTER 3

Interactions between the APOBEC3 and Argonaute protein families

3. RESULTS

Interactions between the APOBEC3 and Argonaute protein families

3. 1 Introduction

Several APOBEC3 proteins are known to associate in large ribonucleoprotein (RNP) complexes comprised of a variety of cellular proteins involved in RNA regulation (Chiu et al., 2006; Gallois-Montbrun et al., 2008; Gallois-Montbrun et al., 2007; Kozak et al., 2006; Wichroski et al., 2006). Whether any of these proteins act as co-factors for APOBEC3 activity and how these interactions may impact upon both the anti-viral and cellular functions of the APOBEC3 proteins remains poorly understood. In this regard, the interaction with the miRNA associated Argonaute proteins is particularly intriguing as this association is partially resistant to RNase treatment (Gallois-Montbrun et al., 2008; Gallois-Montbrun et al., 2007), suggestive of a close and possibly direct interaction. Therefore it was important to first establish the extent of the interactions between these protein families and subsequently to unearth any correlations which may exist with the anti-viral phenotypes of the APOBEC3 proteins

3.2 Antiviral activities of the APOBEC3 proteins

The discovery that human APOBEC3G is a potent inhibitor of Vif-deficient HIV-1 (Sheehy et al., 2002) led to intense interest in the anti-viral properties of the other APOBEC3 proteins. However, only one very recent study has compared them all at the same time and in the same experimental context (Hultquist et al., 2011), which has therefore led to uncertainties over which APOBEC3 proteins are indeed anti-viral and to what extent (Bishop et al., 2004; Bogerd et al., 2006; Dang et al., 2008; Dang et al., 2006; OhAinle et al., 2008; OhAinle et al., 2006; Wiegand et al., 2004; Yu et al., 2004a). Therefore, it was necessary to first verify the antiviral activities of all the APOBEC3 proteins in a comparable experimental setting. To this end, a single cycle infectivity assay was employed. 293T cells were co-transfected with APOBEC3 protein encoding plasmids and a HIV-1 delta *vif* (Δ*vif*) proviral construct. 24 - 48 hours later, viral

supernatants were harvested and the amount of $p24^{Gag}$ quantified using an enzyme linked immunosorbent assay (ELISA). Virus equivalent to 5 ng of $p24^{Gag}$ was then used to infect the TZM-bl reporter cell line (Wei et al., 2002). These modified HeLa cells stably express the CD4 and CCR5 receptors and more importantly, express both the *lacZ* and *luciferase* genes under the control of the HIV-1 LTR promoter. Upon infection, expression of the viral protein Tat drives expression of the reporter genes and thus productive infection can be measured by determining the activity of the reporter gene of choice (Figure 3.1). TZM-bl cells were harvested approximately 30 hours post infection and β-galactosidase activity was measured using a chemiluminscent-based reaction.

Figure 3.2 shows the anti-viral activities of the different APOBEC3 proteins, with increasing amounts of input DNA (ranging from 0.03 μg to 1 μg), against HIV-1 Δ*vif*. As can be seen, and in agreement with previous reports, A3G is strongly anti-viral, even when titrated down to less than 0.05 μg of DNA, compared to the other APOBEC3 proteins. A3F and A3H also show strong anti-viral activity at the highest concentration of DNA but their affects appear to be lost when expressed at lower levels. A3B and A3D/E show a similar level of HIV-1 inhibition but once again these effects are quickly titrated out especially for A3D/E. As has been published, A3A and A3C did not appear to possess any anti-viral activity against Δ*vif* HIV-1 (Bishop et al., 2004). These findings are in good general agreement with the work of Hultquist *et al* in the context of transient transfection in 293T cells. Similar results were obtained with a NL43 Δ*vif* proviral construct and when using HeLa cells as the virus producer cells (data not shown).

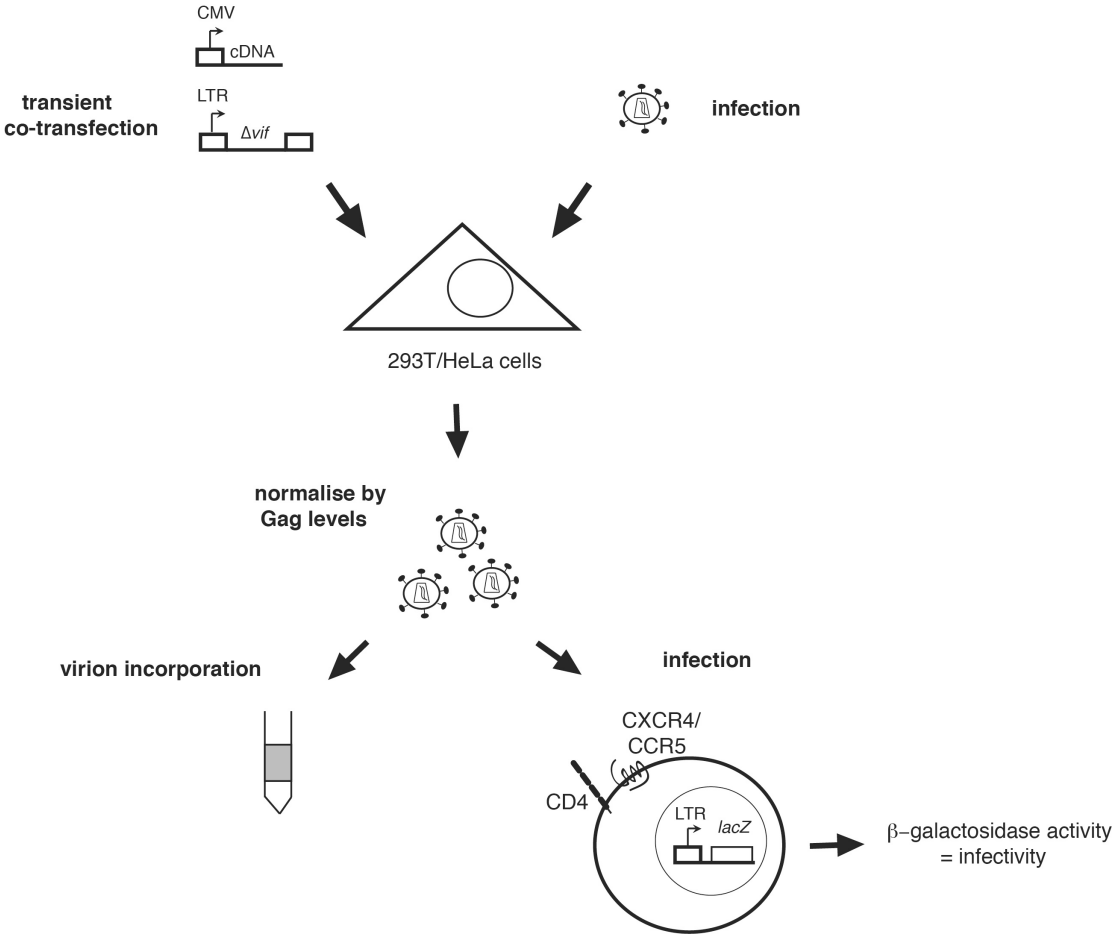

Figure 3.1: Single cycle infectivity assay.

Schematic diagram of the single cycle infectivity assay used in this study, utilising the TZM-bl reporter cell line. 293T or HeLa cells are either co-transfected with plasmids encoding the protein of interest and a provirus or else infected with virus. Typically 48 hours later, viral supernatants are harvested and quantified by $p24^{Gag}$ ELISA. Virus equivalent to 5 ng of $p24^{Gag}$ is then used to infect the TZM-bl reporter cells which express the CD4, CXCR4 and CCR5 receptors. These cells also harbour the *lacZ* gene under the control of the HIV-1 LTR promoter. Infectivity is determined as a measure of β-galactosidase levels approximately 30 hours post infection. Virus equivalent to 20 ng of $p24^{Gag}$ is also concentrated through a 20% sucrose cushion to assess virion incorporation of the protein(s) of interest.

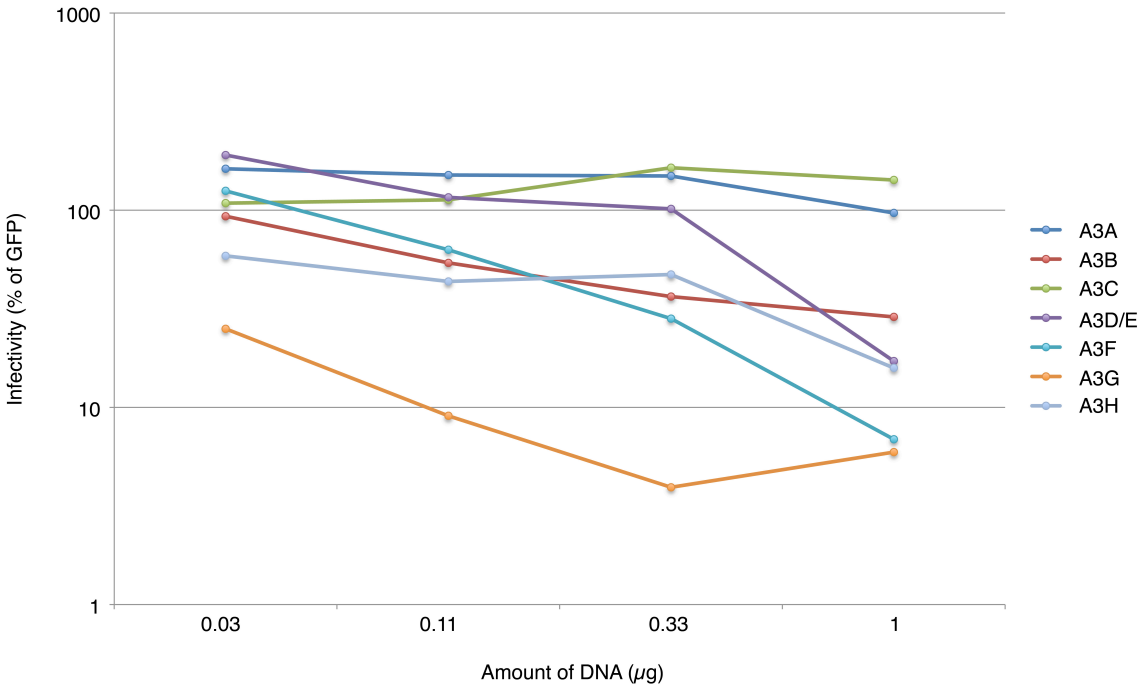

Figure 3.2: Anti-HIV-1 activities of the APOBEC3 proteins.

293T cells were co-transfected with increasing amounts of HA-tagged APOBEC3 expression vectors (0.03 µg, 0.1 µg, 0.3 µg and 1 µg) and 1 µg of the IIIB Δ*vif* proviral plasmid. DNA concentrations were kept constant at 2 µg by the addition of an untagged Luciferase expression vector. 48 hours later, viral supernatants were harvested, quantified by $p24^{Gag}$ ELISA and 5 ng was used to challenge TZM-bl reporter cells. 30 hours later TZM-bl cells were harvested, lysed and assayed for β-galactosidase activity. Data is presented as the average of three independent experiments and all values are normalised to the infectivity of GFP, at a concentration of 1 ug, which is set at 100%.

3.3 Virion incorporation of the APOBEC3 proteins

The inhibition of HIV-1 by the APOBEC3 proteins requires that they are packaged into assembling viruses in producer cells so that they are able to exert their anti-viral effects during reverse transcription in the target cell. As with the anti-viral nature of the APOBEC3 proteins, their incorporation into assembling virions is also an issue of contention as they have all been reported to be packaged (Dang et al., 2008; Dang et al., 2006; Goila-Gaur et al., 2007; Wiegand et al., 2004; Yu et al., 2004a), but as shown in Figure 3.2, not all are anti-viral. Therefore it was of interest to determine which APOBEC3 proteins were incorporated into budding virions and whether this corresponds with their anti-viral activity. Viral supernatants were prepared in 293T cells as described in section 3.2 and 20 ng of $p24^{Gag}$, normalised by ELISA, was concentrated through a 20% sucrose cushion. Viral pellets were then lysed and prepared for immunoblotting and corresponding cell lysates were collected in parallel. Figure 3.3 reveals that A3G, the most potent APOBEC3 family member in terms of HIV-1 inhibition, is also packaged most efficiently, closely followed by A3F. A3H and A3D/E are also present in virions but to a much lower extent. However the cellular expression level of A3D/E is greatly reduced when compared to the other APOBEC3 proteins which may also explain its reduced anti-viral activity. When stably expressed in human T cells, it has been shown to be more anti-viral than what is observed in transient overexpression systems (Hultquist et al., 2011). Therefore the full anti-viral nature of this protein may not be apparent in the infectivity assay described above due to its inherently poor expression, which makes it difficult to draw any conclusions for this protein. Overall, these data demonstrate that the most anti-viral APOBEC3 proteins, A3G, A3F and A3H, are also the ones that are most effectively incorporated into HIV-1 virions thus establishing a positive correlation between packaging and anti-viral activity.

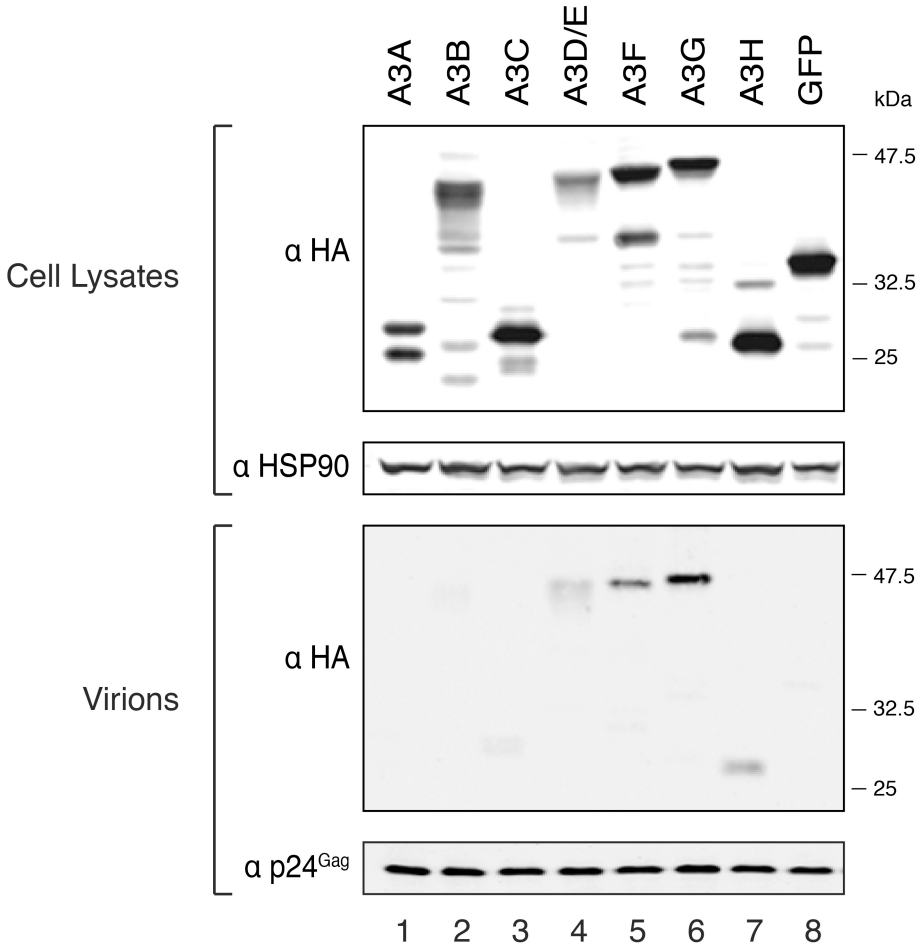

Figure 3.3: Incorporation of APOBEC3 proteins into HIV-1 particles.

Virions produced from 293T cells co-transfected with HA-tagged APOBEC3 plasmids and an NL43 Δ*vif* proviral plasmid at a ratio of 1:3, were concentrated through a 20% sucrose cushion and lysed. Corresponding lysates from the virus producing cells were prepared in parallel. Immunoblots were analysed with an anti-HA and then either an anti-HSP90 or anti-$p24^{Gag}$ antibody as loading controls for cellular and viral lysates respectively. Data is representative of three independent experiments.

3. 4 Sub-cellular localisation of the APOBEC3 proteins

3.4.1 Co-localisation of APOBEC3 proteins with Argonaute 2

It is clear from the data presented thus far that not all of the APOBEC3 proteins are anti-viral nor are they equally anti-viral, but what accounts for these differences remains to be elucidated. As previously discussed, a potential contributory factor may be their cellular interactions and in this respect the Argonaute proteins are of particular interest. It has been shown that A3F and A3G are able to co-localise with these proteins at mRNA Processing bodies (P-bodies) (Gallois-Montbrun et al., 2008; Gallois-Montbrun et al., 2007; Wichroski et al., 2006), which are sites of mRNA storage and/or degradation. To determine whether other APOBEC3 proteins behaved similarly and whether this related to their anti-viral phenotypes, immunofluorescence studies were performed to establish their subcellular localisation and possible co-localisation with Argonaute 2 (Ago2). HeLa cells were co-transfected with equivalent amounts of HA-tagged APOBEC3 plasmids and a myc-tagged Ago2 construct. 24 hours later cells were fixed, permeabilised and stained with primary antibodies directed against the epitope tags and appropriate secondary antibodies, before images were taken using a Leica confocal microscope. From Figure 3.4 it can be seen that A3A, A3B and A3C possess both a nuclear and cytoplasmic distribution within the cell (panels 1 - 3). In some cells A3H displayed a weak nuclear localisation (panel 7), but in others it appeared to be entirely cytoplasmic (see Figure 3.5, panel 7). The remaining APOBEC3 proteins are exclusively cytoplasmic (panels 4-6). These results are summarised in Table 3.1. In agreement with previous reports (Gallois-Montbrun et al., 2008; Gallois-Montbrun et al., 2007; Wichroski et al., 2006), A3F and A3G localise to Ago2 marked foci and this is also true for A3DE and A3H. However, the remaining APOBEC3 proteins only weakly co-localise with Ago2 (A3B and A3C) or not at all (A3A).

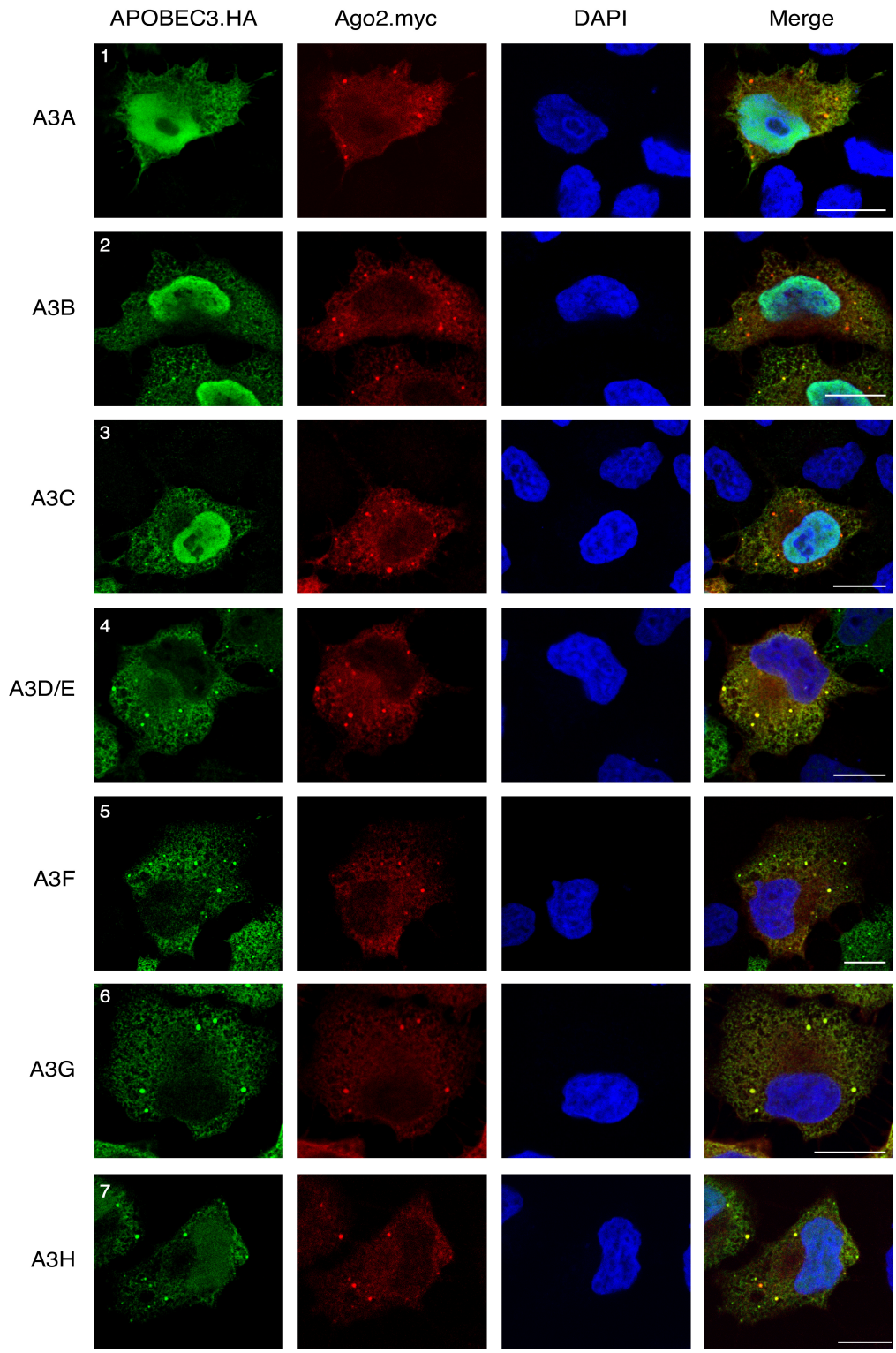

Figure 3.4: Several APOBEC3 proteins co-localise with Argonaute 2.

HeLa cells were co-transfected with equivalent amounts of HA-tagged APOBEC3 plasmids and a myc-tagged Ago2 plasmid and 24 hours later fixed in 4% formaldehyde and then permeabilised. Cells were first stained with rabbit anti-HA and mouse anti-myc primary antibodies and then with Alexa Fluor conjugated rabbit 488 and mouse 594 secondary antibodies, as well as DAPI for visualisation of the nucleus. Coverslips were mounted onto slides and dried overnight before imaging on a Leica confocal microscope. Images are Z-series compilations of 4 - 6 images in a stack with merged views displayed on the right. Images are representative of four independent experiments. Scale bar = 10 μm.

Table 3.1: Subcellular localisation of the APOBEC3 proteins

Protein	Sub-Cellular Localisation	Co-localisation with Ago2 and DDX6?
A3A	Nuclear/Cytoplasmic	No
A3B	Nuclear/Cytoplasmic	Weak
A3C	Nuclear/Cytoplasmic	Weak
A3D/E	Cytoplasmic	Yes
A3F	Cytoplasmic	Yes
A3G	Cytoplasmic	Yes
A3H	Nuclear/Cytoplasmic	Yes

3.4.2 Co-localisation of APOBEC3 proteins with DDX6

Since different populations of P-bodies have been postulated to exist within the cell (Gibbings et al., 2009; Vasudevan and Steitz, 2007a), it was necessary to ascertain whether the APOBEC3 proteins were associating solely with Ago2 marked bodies or P-bodies in general, as has already been reported for a subset of them (Niewiadomska et al., 2007). Consequently, APOBEC3 co-localisation with the known P-body marker, DDX6, was also investigated (Figure 3.5) and a similar pattern of co-localisation was observed, as described for Ago2. To obtain a more quantitative analysis, 100 cells were counted for each APOBEC3 protein and their presence at both Ago2 and DDX6 marked foci was scored. These data are presented in Figure 3.6, where in more than 90% of cases, co-localisation was observed between Ago2 and A3DE, A3F, A3G and A3H. Near equivalent results were also obtained when DDX6 was used as the marker. A3B and A3C only localised to Ago2 bodies in approximately 50% of the cells counted and this was substantially reduced when looking at DDX6 bodies. This difference may be explained by the fact that overexpression of DDX6 induces more P-bodies [(Chu and Rana, 2006) and compare the number of P-bodies per cell with ectopic expression of Ago2, Figure 3.4 with that of DDX6, Figure 3.5] and thus weak co-localisation phenotypes may be exaggerated. A3A co-localisation with either Ago2 or DDX6 was virtually non-existent. Therefore the most anti-viral APOBEC3 proteins appear to localise most strongly to Ago2 and DDX6 marked foci.

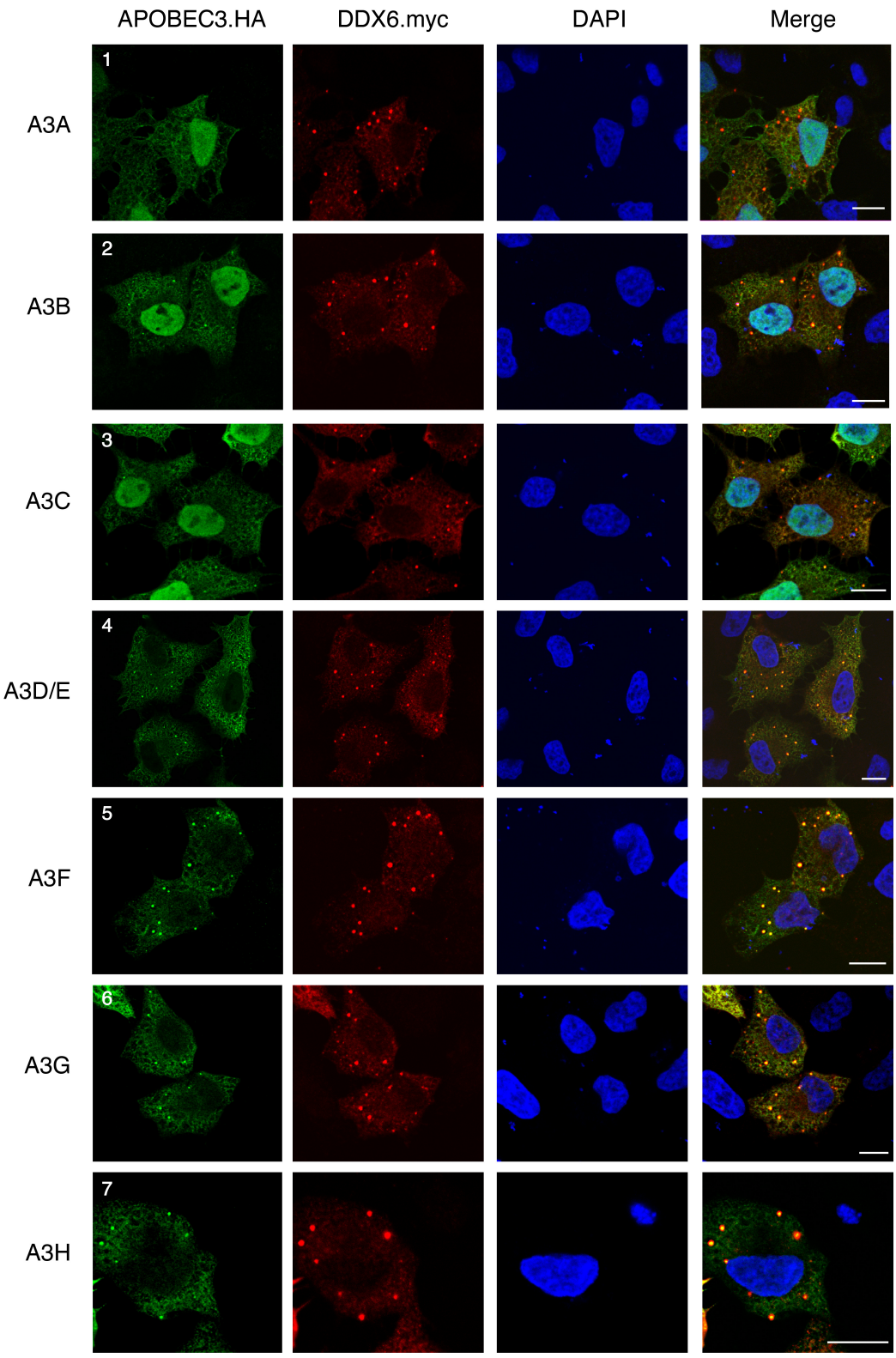

Figure 3.5: Several APOBEC3 proteins co-localise with DDX6.

HeLa cells were co-transfected with equivalent amounts of HA-tagged APOBEC3 plasmids and a myc-tagged DDX6 plasmid and 24 hours later fixed in 4% formaldehyde and then permeabilised. Cells were first stained with rabbit anti-HA and mouse anti-myc primary antibodies and then with Alexa Fluor conjugated rabbit 488 and mouse 594 secondary antibodies, as well as DAPI for visualisation of the nucleus. Coverslips were mounted onto slides and dried overnight before imaging on a Leica confocal microscope. Merged views are displayed on the right. Images are representative of three independent experiments. Scale bar = 10μm.

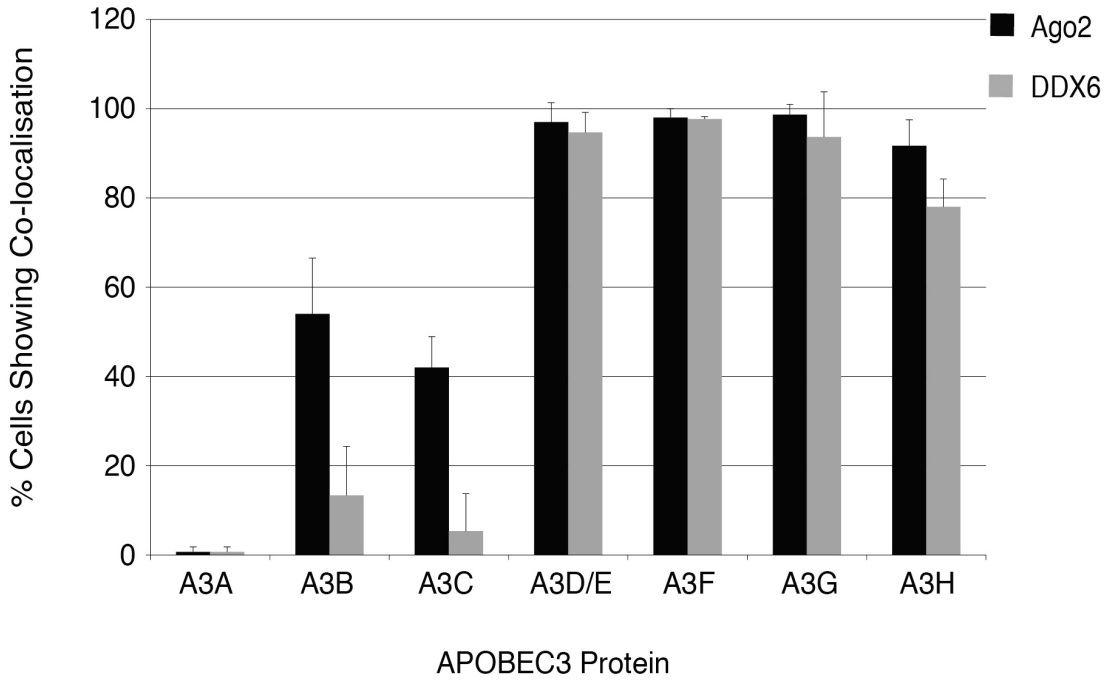

Figure 3.6: Quantification of APOBEC3 localisation to Argonaute 2 and DDX6 foci.

HeLa cells were prepared as described in Figures 3.3 and 3.4 and 100 cells were counted per APOBEC3 protein for co-localisation at Ago2 and DDX6 marked cytoplasmic foci. Only those cells in which the majority of the APOBEC3 protein co-localised at these foci were scored as positive. Any cells displaying stress granules were excluded from the analysis. Data is presented as the average of three independent experiments with error bars representing the standard deviation.

3.5 Co-immunoprecipitatation of APOBEC3 and Argonaute proteins

3.5.1 Optimisation of co-immunoprecipitation coupled to formaldehyde cross linking

As several APOBEC3 proteins demonstrated co-localisation with Ago2, it was then important to determine whether there were any detectable interactions between these proteins as previously described for A3F and A3G (Gallois-Montbrun et al., 2008; Gallois-Montbrun et al., 2007; Wichroski et al., 2006). In order to evaluate this, a modified co-immunoprecipitation (Co-Ip) protocol was adopted which incorporates formaldehyde (HCHO) cross-linking (Niranjanakumari et al., 2002; Vasudevan and Steitz, 2007a). 293T cells were transfected with HA-tagged APOBEC3 and myc-tagged Ago2 expression vectors, as used in the immunofluorescence studies described in section 3.4. 48 hours post transfection, cells were harvested and incubated with 0.05% HCHO, which was then quenched with the addition of Glycine. The cells were lysed, subjected to sonication and then immunoprecipitated as standard using an anti-myc antibody. Prior to immunoblotting, cross-links were reversed by heating samples at 65°C for 45 minutes. Conventional Co-Ip protocols that do not involve the cross-linking of protein – protein or protein – nucleic acid interactions may be vulnerable to artificial interactions that are generated from the re-association of molecules after cell lysis (Mili and Steitz, 2004). Therefore, these protocols may not always reflect true *in vivo* interactions. Other advantages of this cross-linking assay include more stringent washing to remove any non-specific binding and the break-up of large insoluble complexes, such as P-bodies, by sonication, thereby making more protein available in the soluble fraction. When cross-linking is not used, and a conventional Co-Ip protocol is followed (Figure 3.7A), approximately 50% of the protein is found in the insoluble (pelletable) fraction, especially evident for A3G (compare lanes 1 - 4 with 5 - 8), and therefore lost from subsequent analysis. However, when samples are cross-linked, the majority of the protein is now retained in the supernatant (Figure 3.7B, compare amount of protein present in the supernatant, S, versus pellet, P, lanes). This is also the case, but to a lesser extent, for those samples treated with 0% formaldehyde indicating that the slower clarification spin used in this protocol also helps maintain proteins in the soluble fraction. The concentration of formaldehyde used also needs to be optimised for the different proteins studied, as Ago2 may be more readily degraded in the presence of higher amounts of formaldehyde (Figure 3.7B, compare Ago2 protein levels at 0.05%

with 0.2%, for example). Therefore, for this work, a concentration of 0.05% formaldehyde was determined to be optimal.

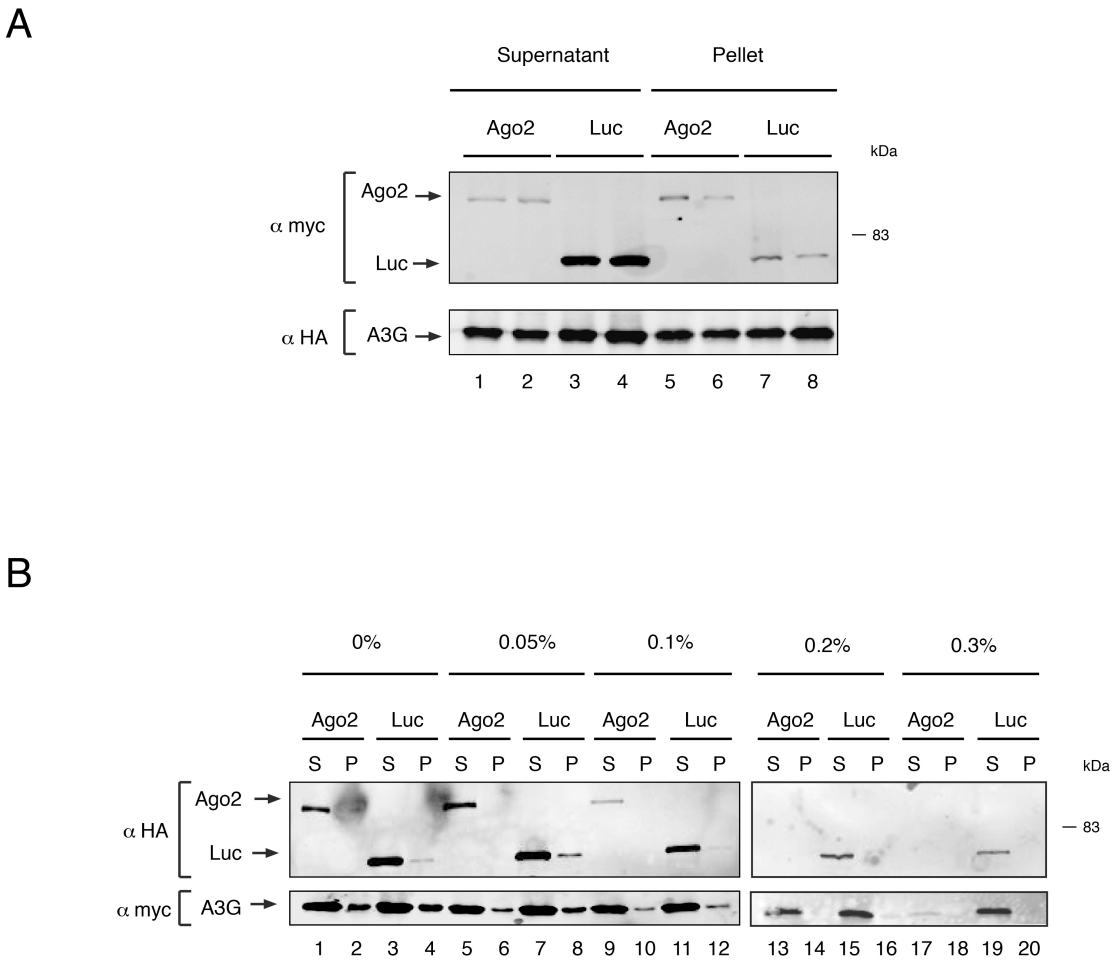

Figure 3.7: Optimisation of formaldehyde cross-linking protocol for co-immunoprecipitations.

A. 293T cells were transfected with equivalent amounts of a HA-tagged A3G plasmid and either myc-tagged Ago2 or Luciferase (Luc) as a negative control. 48 hours later, cells were harvested and lysates clarified by centrifugation at 14,000 rpm for 30 minutes. The pellet and a sample of the supernatant was collected and re-suspended in gel loading buffer and samples were loaded onto the gel in duplicate. Immunoblots were analysed by probing with anti-myc and anti-HA antibodies. **B**. Cells were transfected as in A. 48 hours post transfection cells were lysed and incubated in either PBS (0%), 0.05%, 0.1%, 0.2% or 0.3% formaldehyde for 10 minutes at 37°C. The formaldehyde was then quenched by the addition of 0.25 M Glycine for 5 minutes at room temperature. Cells were then re-suspended in 1x BB lysis buffer for 10 minutes on ice prior to sonication for 3 x 10 seconds. Lysates were then clarified for 30 minutes at 1000 x *g*. The pellet and a sample of the supernatant was collected and re-suspended in gel loading buffer. Immunoblots were analysed by probing with anti-myc and anti-HA antibodies.

3.5.2 Co-immunoprecipitation of APOBEC3 proteins with Ago2

The APOBEC3 proteins were then co-expressed with Ago2 in 293T cells and a co-immunoprecipitation assay coupled with formaldehyde cross-linking was performed as described for Figure 3.7B. From Figure 3.8, and in agreement with previously published reports (Gallois-Montbrun et al., 2008; Gallois-Montbrun et al., 2007; Wichroski et al., 2006), it is clear that A3G and to a lesser extent A3F, co-immunoprecipitate with Ago2. The weaker interaction between A3F and Ago2, seen here, may be due to the harsher washing conditions employed in this protocol (and discussed further in section 3.5.3). It is also apparent that some of the other APOBEC3 proteins are also able to interact with Ago2, namely A3H, A3C and very weakly A3A. There were no interactions observed for the negative control GFP, nor A3B or A3DE, although once gain the cellular expression of the latter is not comparable with its family members. Therefore several APOBEC3 proteins are able to interact with Ago2 to some extent, though none as strongly as A3G. Unlike localisation to Ago2 foci/P-bodies, the ability to interact with Ago2 does not appear to closely correlate with the anti-viral phenotypes of the APOBEC3 proteins, although the most anti-viral proteins (A3F, A3G and A3H) do interact most strongly with Ago2. However, an important point to note with this experiment is that due to the lack of particular negative controls, such as using no antibody or an irrelevant antibody for the immunoprecipitation, means that it cannot be conclusively ruled out that the APOBEC3 proteins are not simply binding to the beads rather than interacting with Ago2.

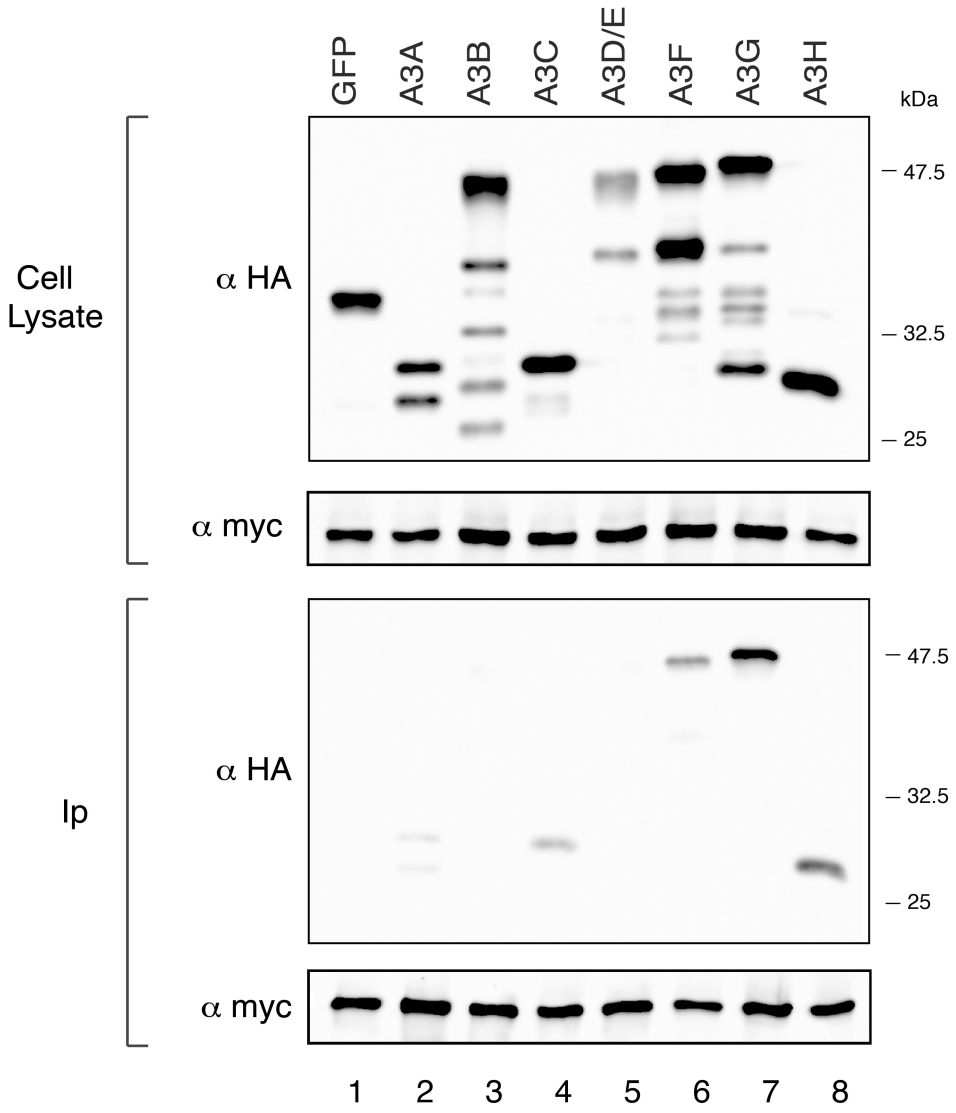

Figure 3.8: Several APOBEC3 proteins interact with Argonaute 2 by co-immunoprecipitation.

293T cells transfected with equivalent amounts of HA-tagged APOBEC3 plasmids (or GFP as a negative control) and a myc-tagged Ago2 plasmid were cross-linked with 0.05% formaldehyde 48 hours later. The formaldehyde was quenched by the addition of 0.25 M Glycine before cells were lysed in 1x BB lysis buffer. Samples were then sonicated for 3 x 10 seconds before immunoprecipitation for 2 hours with an anti-myc antibody and protein G coupled Agarose. Before immunoblotting cross-links were reversed by the addition of reverse cross-linking buffer and heating at 65°C for 45 minutes. Immunoblots were analysed using anti-myc (Ip) or anti-HA (Co-Ip) antibodies. Data is representative of four independent experiments.

3.5.3 APOBEC3 interaction with other Argonaute proteins

The four human Argonaute proteins share approximately 80% amino acid identity (Sasaki et al., 2003) yet functionally distinct differences exist. They are all involved in miRNA mediated repression (Pillai et al., 2004) but only Ago2 has retained its catalytic activity and is therefore able to cleave target mRNAs, characteristic of siRNA mediated silencing (Liu et al., 2004; Meister et al., 2004). Because of this there is much more experimental focus on Ago2 than the other Argonaute proteins, yet they may not behave in the same way. It has recently been reported that Ago2 unlike the other Argonaute proteins may not act co-operatively with its family members to mediate its repressive effects (Broderick et al., 2011). Therefore Ago1 and Ago3 were also assessed for their ability to interact with the APOBEC3 proteins, specifically A3F, A3G and A3H as they showed the strongest association with Ago2. Unfortunately Ago4 could not be included in this analysis as this protein was very poorly expressed (data not shown).

Co-immunopreciptation was carried out as described in section 3.5.1 (with formaldehyde cross-linking) and results are presented in Figure 3.9. The APOBEC3 proteins tested were all able to interact with Agos 1 and 3, and to the same extent as described for Ago2. Even though Ago3 is not as well expressed or immunoprecipitated as the other Argonaute proteins (lanes 9 - 12), detectable interactions were still observed. An interesting point to note is that the Argonaute proteins do not appear to be as well immunoprecipitated in the presence of A3F when compared to the other APOBEC3 proteins (bottom panel, lanes 1, 5 and 9). The reasons for this are unclear but either overexpression of A3F is detrimental to the cells in general or more specifically it affects Argonaute expression levels. There may be some evidence for the latter in the cell lysate blots (bottom left hand panel) but this is not conclusive. This would also explain the weaker interaction observed between Ago2 and A3F as if less Argonaute protein is imunoprecipitated, then less A3F will also be pulled down. Overall, these results confirm that the APOBEC3 interactions presented in Figure 3.8 are not specific to Ago2 but extend to other members of the Argonaute protein family as well. However, as before, the interpretation of a conclusive interaction between the APOBEC3 and Argonaute proteins is hindered by the lack of appropriate negative controls.

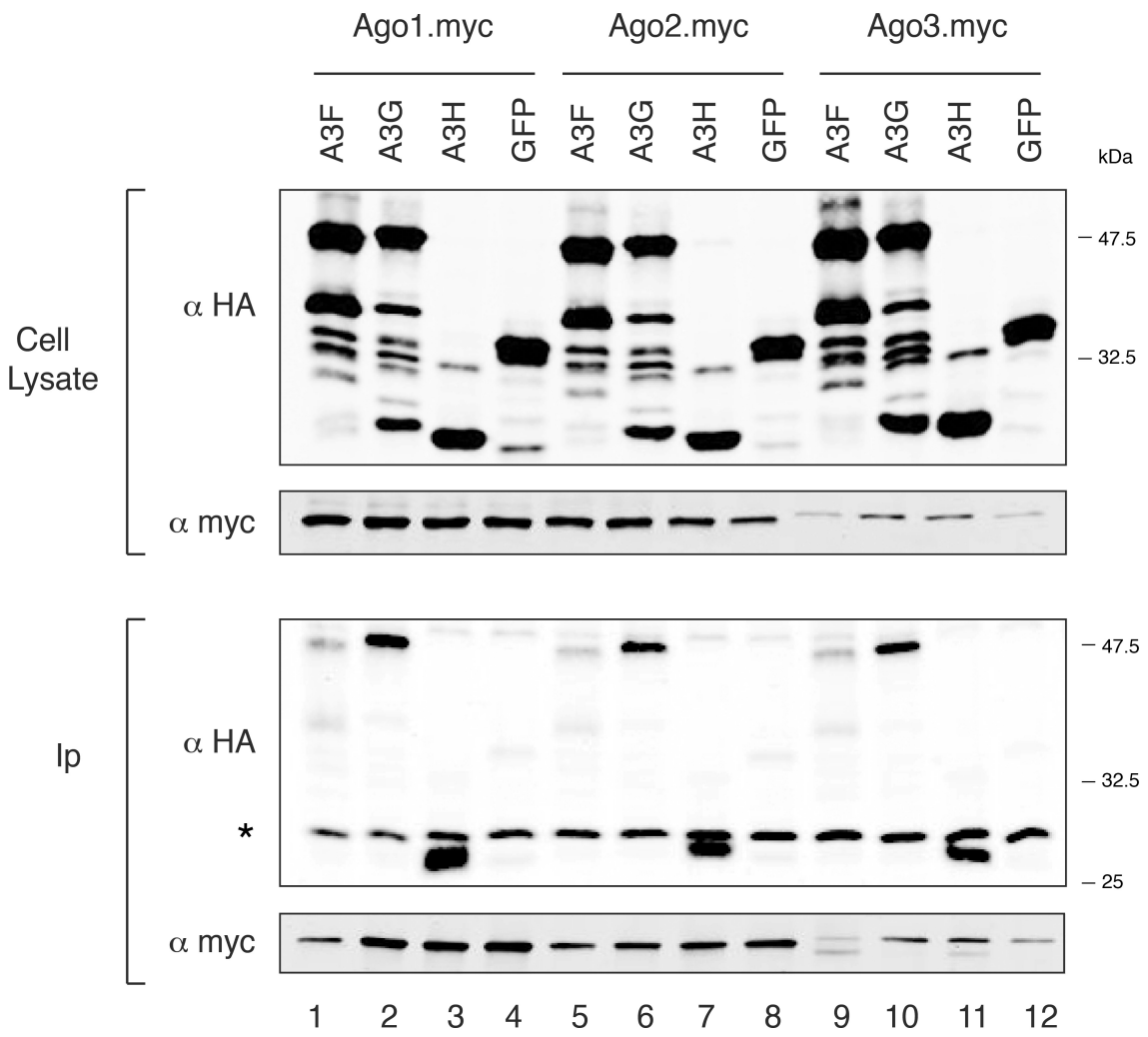

Figure 3.9: APOBEC3 proteins interact with other Argonaute family members.

293T cells co-transfected with equivalent amounts of either HA-tagged A3F, A3G or A3H and myc tagged Ago1, Ago2 or Ago3 expression vectors (and GFP as a negative control) were harvested 48 hours later and an anti-myc immunoprecipitation was performed as described for Figure 3.7. Immunoblots were analysed using anti-myc (Ip) or anti-HA (Co-Ip) antibodies. * denotes the position of the light chain of the antibody. Data is representative of four independent experiments.

3.6 Interaction by yeast 2 hybrid

In order to further validate the interaction between A3G, in particular, and the Argonaute proteins, a yeast 2 hybrid (Y2H) assay was performed (Fields and Song, 1989). This genetic assay is based on the principle that eukaryotic transcription factors are modular and therefore the activating and binding domains can be separated. The two proteins of interest are fused to separate halves of the transcription factor and if the proteins interact, the two domains will be in close enough proximity to activate transcription of a reporter gene.

Competent yeast cells were transformed with A3G and Ago1 or Ago2 fusion plasmids (expressed in both the KT7 DNA binding domain and the HB18 activation domain vectors) and plated on –Leu (leucine), -Trp (tryptophan) LB media. 3 days later, colonies were harvested and protein binding determined by reaction with the reporter gene (*lacZ*) substrate, chlorophenol red β-D-galacopranoside. A red colour indicates a positive result and this can be quantified by optical density measurements at 540 nm.

Tsg101 and Vps28 were included in this experiment as they are known to strongly interact in a yeast 2 hybrid system. A value at or above 1 is taken to indicate the occurrence of an interaction and this positive control pairing was in fact off the scale indicating that the assay itself is functional (Figure 3.10A and B). As A3G is known to dimerise (Huthoff et al., 2009), an A3G - A3G pairing was also included as a second positive control. This interaction was very close to the cut-off value for a positive association. However, no detectable interaction was observed between A3G and the two Argonaute proteins, irrespective of which vector pairings were used (Figure 3.10A and B). Values were at or below background values in both cases, as represented by the empty vector control. However, a large part of this may be attributable to the fact that the Argonaute proteins do not appear to be well expressed in either vector but particularly the KT7 vector as indicated in Figure 3.10C, which could help explain the lack of a positive interaction. On the other hand Tsg101 was also not particularly well expressed yet a positive interaction could still be observed when it was co-expressed with Vps28. Thus the yeast 2 hybrid assay used here fails to support the conclusion that A3G and Ago2 interact, as determined by Co-Ip.

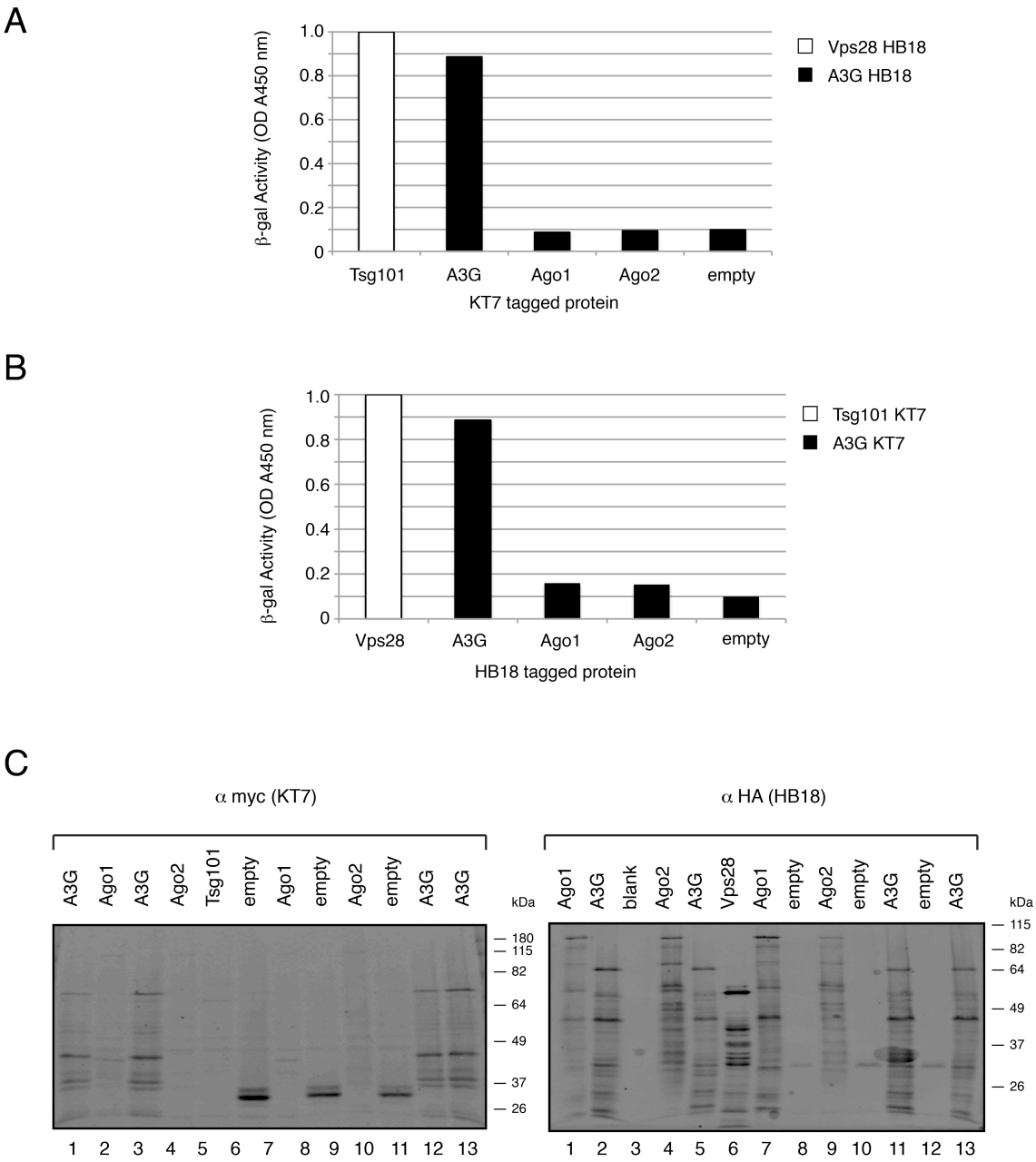

Figure 3.10: Yeast 2 hybrid analysis of the interaction between A3G and Argonaute proteins.

A. Competent yeast cells were transformed with equivalent amounts of KT7 DNA binding domain (myc-tagged) and HB18 activation domain (HA-tagged) fused expression vectors as indicated. Tsg101 KT7 and Vps28 HB18 were included as a positive control and empty vectors included as negative controls. Transformed yeast were then plated onto -Leu, -Trp LB plates and incubated at 30°C for approximately 72 hours. Pellets were then scraped from the plates and incubated with the reporter gene substrate chlorophenol red β-D-galacopranoside to measure β-galactosidase activity. A red colour indicates a positive result and this can be quantified by optical density measurements at 540 nm. **B**. As in A, except proteins of interest were expressed in the opposing vectors. **C**. Expression levels of proteins of interest in yeast were determined by immunoblotting using anti-HA and anti-myc antibodies. Data is representative of 2 independent experiments.

3.6 A3G interaction with Ago2 mutants

The interaction between A3F/A3G and the Argonautes is of particular interest since it is at least partially resistant to RNase treatment, unlike many of the other interactions described between the APOBEC3s and cellular RNA binding proteins (Gallois-Montbrun et al., 2008; Gallois-Montbrun et al., 2007). However, whether this is indeed a direct interaction or bridged by RNA, and potentially miRNAs, is unknown. To investigate these possibilities, a panel of Ago2 RNA binding mutants was employed. The structure of the Argonaute proteins can be divided into 4 domains: the N-terminal, PAZ, MID and PIWI domains (see Chapter 1, section 1.11.3). The PAZ9 and PAZ10 mutants contain either 9 or 10 point mutations respectively, within the PAZ region of Ago2. This abrogates the ability of these proteins to bind single stranded nucleic acids such as miRNAs. It was also reported that these mutants were unable to cleave target mRNAs or accumulate in P-bodies (Liu et al., 2005b). The F2V2 mutant (Kiriakidou et al., 2007) harbours two phenylalanine to valine substitutions within the Mid domain of the protein, which abolishes its silencing activity. Originally it was claimed that these mutations prevented the protein from competing with eIF4E for binding to the cap structure of mRNAs and thus inhibiting translation initiation (Kiriakidou et al., 2007). However, subsequent studies in *Drosophila* have shown that this protein no longer binds GW182 or miRNAs (Eulalio et al., 2008b), which would also explain its inability to silence mRNAs. Therefore these mutants could help determine whether the interaction between Ago2 and A3G is dependent on miRNAs. A schematic diagram of the mutant proteins is presented in Figure 3.11A.

These mutant Ago2 proteins were assessed for their ability to interact with A3G. In this case, 293Ts were transfected with HA-tagged A3G and myc-tagged Ago2 expression vectors. 24 hours later, cells were lysed and the Ago2 proteins immunoprecipitated, without formaldehyde cross-linking, using an anti-myc antibody before cells were subjected to immunoblotting with anti-myc and anti-HA antibodies. From the two upper panels in Figure 3.11B it can be seen that the mutant Ago2 proteins are expressed and immunoprecipitated just as well as the wild type protein. Although A3G is able to interact with all of the mutant proteins (4^{th} panel down), the efficiency of this interaction is five fold lower than with wild type Ago2 (compare lanes 2 - 4 with lane 1). This implies that the inability of Ago2 to bind miRNAs impacts upon its ability to interact with A3G. This may be because miRNAs are required to bridge the interaction

between these two proteins. An alternative explanation, however, is that these mutations have induced conformational changes in Ago2 which partially hinder its interaction with A3G. Therefore, further characterisation of these mutant Ago2 proteins may be required to determine the nature of the interaction between Ago2 and A3G.

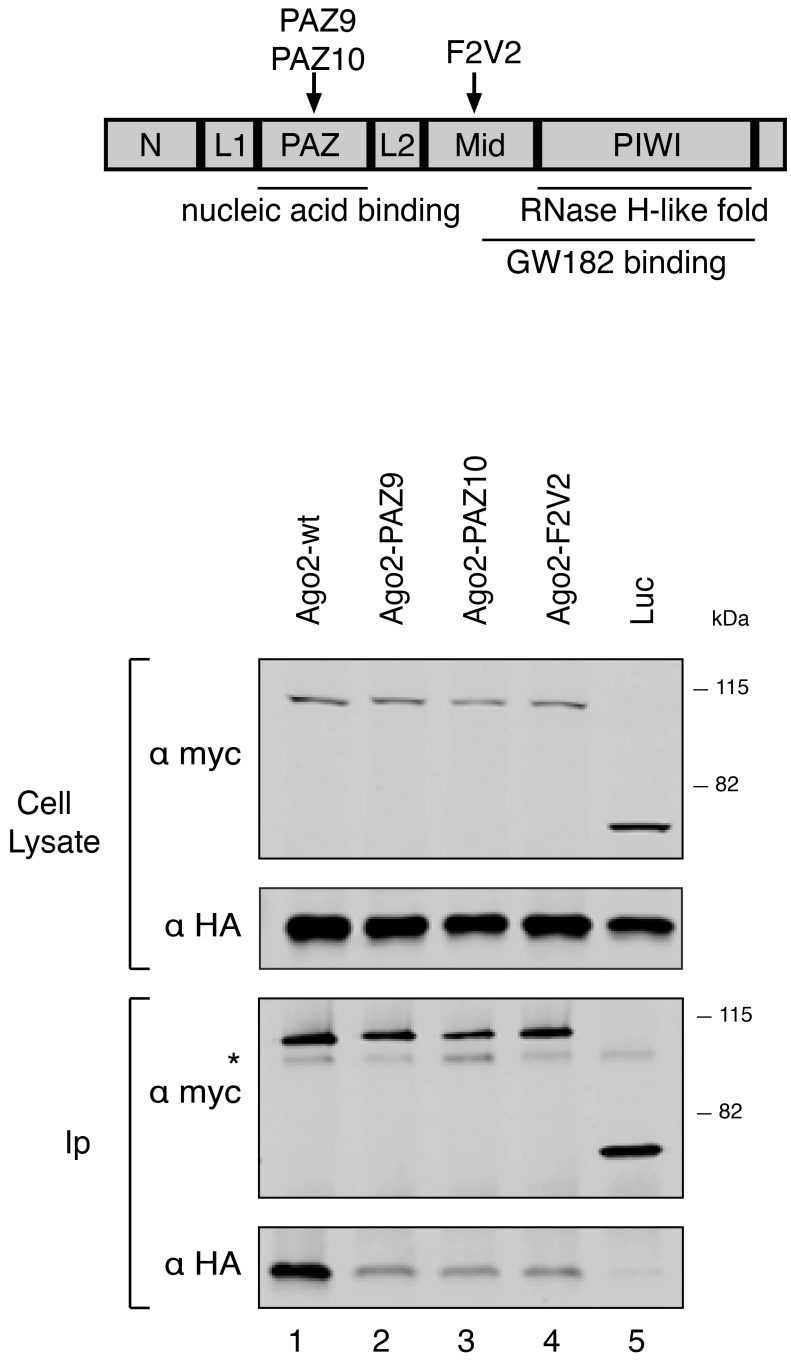

Figure 3.11: Ago2 miRNA binding mutants show reduced association with A3G.

A. Schematic diagram of the Ago2 protein outlining the various domains with the positions of the PAZ9, PAZ10 and F2V2 mutants indicated. **B**. 293T cells were transfected with equivalent amounts of expression vectors encoding HA-tagged A3G and either myc-tagged wild-type Ago2 or the PAZ9, PAZ10 and F2V2 mutants as well as Luciferase (Luc) as a negative control. 24 hours later cells were harvested and immunoprecipitated with an anti-myc antibody and G protein coupled Agarose. Samples were then washed and lysed before immunoblot analysis using anti-myc (Ip) and anti-HA (CoIp) antibodies. Protein bands were quantified using Licor Odyssey software. * denotes the position of a background band. Data is representative of 3 independent experiments.

3.8 Interaction by FRET/FLIM

The interaction between A3F/A3G and Ago2 may also be a direct protein-protein interaction as Ago2 directly interacts with several other P-body proteins such as GW182 and DDX6 (Behm-Ansmant et al., 2006). This is often difficult to prove, however, without purified protein and attempts to purify A3G have so far proved unsuccessful due to its insoluble nature. Another way in which to measure direct interactions between two proteins is by fluorescence resonance energy transfer (FRET). This is based on the principle that two fluorophores that are in close enough proximity and with partially overlapping emission and absorption spectra, will enable the transfer of energy from one molecule (the donor) to another (the acceptor). The fluorescence of the donor is quenched as energy is transferred to the acceptor molecule, which can then be measured (sensitised emission). Alternatively, the acceptor molecule can be photobleached and the increase of fluorescence in the donor can be measured (photobleaching). Fusing proteins of interest to fluorescent molecules allows determination of protein interactions as the rate of energy transfer occurs at distances of 10 nm or less. However, there are some inherent drawbacks to FRET, as often the concentration of the donor and acceptor molecules is both difficult to control and calculate and the fact that it requires spectral overlap between the two fluorophores can often lead to increased background signals via bleed-through. Therefore, a more quantitative and robust approach is to combine FRET with fluorescence lifetime imaging microscopy (FLIM) (Lleres et al., 2007). This measures the decay in signal from the donor fluorophore (its lifetime) only, which will decrease if and when energy is transferred to the acceptor molecule. The closer the molecules are, the faster the energy will be transferred and the shorter the lifetime will be of the donor fluorophore. This combined approach allows both the spatial and temporal resolution of protein interactions [reviewed in (Chen et al., 2003)]. In fact, FRET based techniques have proved very useful in verifying interactions between P-body components and determining where in the cell these interactions are occurring (Andrei et al., 2005; David Gerecht et al., 2010; Ingelfinger et al., 2002).

Therefore, in collaboration with Professor Tony Ng and Dr Simon Ameer-Beg, of the Cell Imaging Facility in the Randall Division of Cell and Molecular Biophysics, Kings College London, a FRET/FLIM approach was attempted in order to confirm the interaction between the APOBEC3 and Argonaute proteins as well as establish its cellular location. However, this technique is particularly sensitive to

background/autofluorescence signals and therefore the expression of the proteins of interest must be considerably higher than background in order to obtain an accurate measurement of the lifetime of the fluorophores. HeLa cells were transiently transfected with A3G-YFP and Ago2-Cherry fused expression vectors before fixation and fluorescence imaging for FRET/FLIM analysis and calculation of FRET efficiency. FRET efficiency is strongly dependent on the distance between the donor and acceptor fluorophores and is inversely proportional to the lifetime of the donor, with a higher efficiency indicating a lower lifetime and thus reflecting a positive interaction. When A3G and Ago2, were significantly overexpressed, a positive interaction was observed by FRET/FLIM, as determined by the increase in FRET efficiency when these proteins were co-expressed as compared to the control (A3G expressed in the absence of Ago2) (Figure 3.12). However gross overexpression of proteins can cause mis-localisation and protein aggregation and in the specific case of A3G and Ago2, may have possibly induced their localisation to stress granules (Figure 3.13, panels a and c). This is therefore not biologically representative nor physiologically relevant. Thus attempts to utilise FRET/FLIM in this study proved unsuccessful due to these technical difficulties but may still be possible, with more stringent optimisation, as has been demonstrated for other P-body proteins.

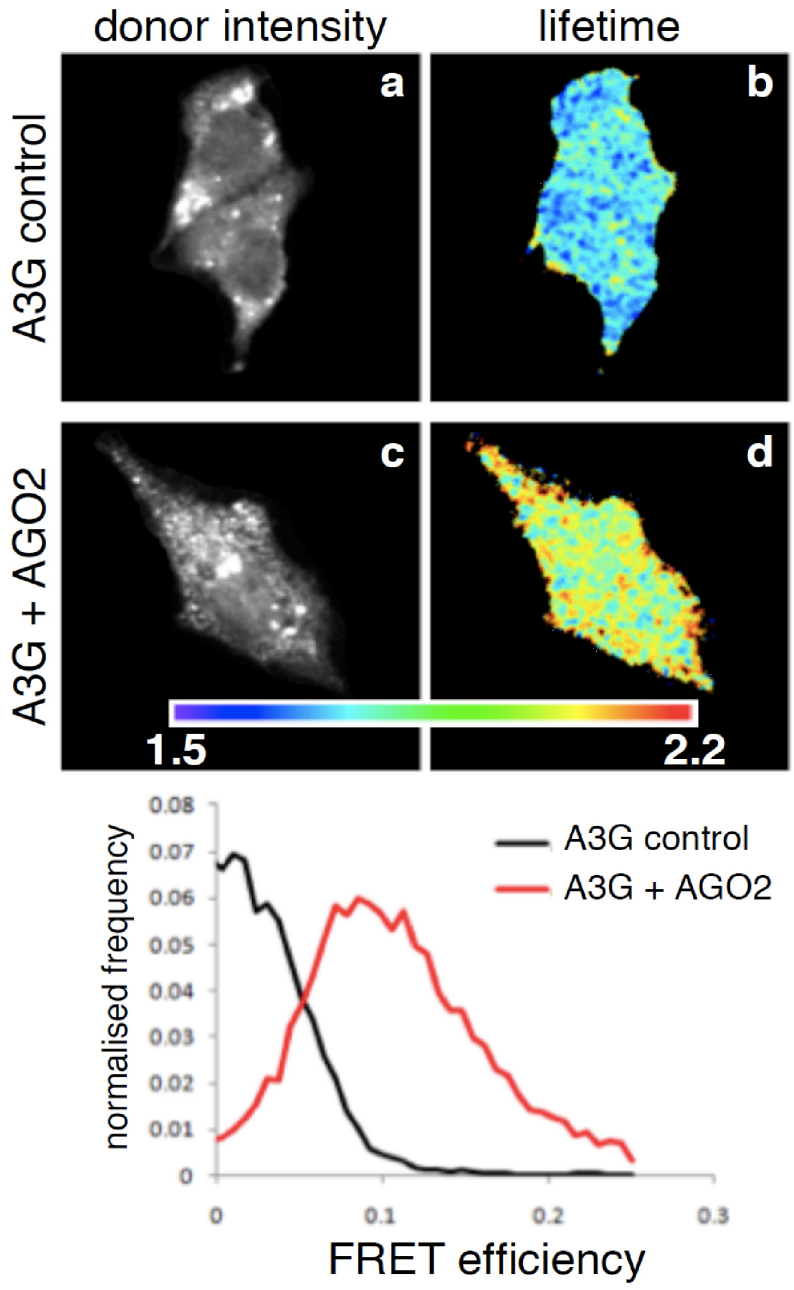

Figure 3.12: FRET/FLIM analysis of the interaction between A3G and Ago2

HeLa cells were transiently transfected with expression plasmids encoding A3G-YFP and Ago2-Cherry fusion proteins, or HA tagged Ago2 as a control. 24 hours later, cells were fixed in 4% formaldehyde, permeabilised and then treated with 1 mg/ml sodium borohydride to quench background fluorescence. Cells were then stained with an anti-HA conjugated Cy5 primary antibody and the appropriate secondary antibody, mounted and dried overnight prior to fluorescence measurements. Mean FRET efficiency was calculated using the following equation in each pixel and averaged per cell. FRET efficiency = 1 – τda/ τcontrol where τda is the lifetime displayed by cells co-expressing A3G-YFP and Ago2-Cherry and τcontrol is the mean A3G-YFP lifetime measured in the absence of acceptor. Figure produced in collaboration with Dr Simon Ameer-Beg.

3.9 Discussion

This work set out to investigate in more detail the interaction between the APOBEC3 and Argonaute protein families and subsequently identify any correlations that may exist between APOBEC3 anti-viral activity and Argonaute association. It has been shown that several APOBEC3 proteins, besides A3F and A3G, are able to co-localise and interact with Ago2 and other Argonaute protein family members. More importantly, the most anti-viral APOBEC3 proteins appear to associate most strongly with Ago2 foci/P-bodies, the relevance of which requires further investigation.

Although the anti-viral nature of A3G has been well established and extensively studied (Bishop et al., 2004; Liddament et al., 2004; Wiegand et al., 2004; Zennou and Bieniasz, 2006), the anti-viral phenotypes of the remaining APOBEC3 proteins has been controversial, especially in relation to one another. The activity of A3H, for example, is highly sensitive to epitope tag positions as C-terminally tagged constructs are not as anti-viral as their N-terminal counterparts (data not shown). Epitope tags at the C-terminal end may also affect the ability of Vif to bind to and thus degrade this protein (Hultquist et al., 2011). Variables such as this, along with differences in cell lines, expression levels and so forth will also explain much of the discrepancies. In order to directly compare them, it therefore becomes important to study these proteins in the same experimental context, as shown in Figure 3.2. This demonstrates that A3G is much more potent than any of the other APOBEC3 proteins as its effects are still evident at very low concentrations of input DNA, which is not the case for A3F and A3H, for instance. A3A and A3C displayed virtually no antiviral activity against HIV-1, which is in agreement with previous reports (Hultquist et al., 2011; Wiegand et al., 2004). The poor expression of A3D/E, even when overexpressed, has made it difficult to establish the true anti-viral nature of this protein. Recent work by Hultquist *et al*, found similarly weak expression of A3D/E in 293T cells, which resulted in only a moderate level of anti-HIV-1 inhibition as has been observed here. However, the fact that it is sensitive to degradation by Vif, is packaged into virions even when very poorly expressed (Figure 3.3) and is under very high levels of positive selection (Sawyer et al., 2004) imply that it may be more relevant to *in vivo* viral defence than what is suggested from the results presented in Figure 3.2. Conversely, A3B displayed some anti-viral activity when overexpressed (Figure 3.2) but it is not thought to encounter HIV-1 during the course of a natural infection.

In order to exert their anti-viral effects the APOBEC3 proteins must be packaged into virions and therefore it may be expected that the most anti-viral APOBEC3 proteins are also the ones that are most efficiently encapsidated. Editing independent means of viral inhibition, such as steric hinderance (discussed in Chapter 1, section 1.7.3), also rely upon packaging of A3G in order to mediate its effects in the target cell. However, A3A and A3C possess virtually no anti-HIV-1 activity yet both are reported to be packaged into viral particles (Goila-Gaur et al., 2007; Yu et al., 2004a). Thus it became important to establish how virion incorporation relates to the anti-viral activities of the different APOBEC3 proteins. The results presented in this study show that there is in fact a positive correlation between anti-viral activity and packaging (Figure 3.3). A3G is packaged to the greatest extent, followed by A3F and A3H. A3A and A3C, on the other hand, only appear to be packaged when grossly over expressed [data not shown and (Hultquist et al., 2011)] and not when expressed at the more physiologically relevant levels displayed here. A3D/E also shows some degree of virion incorporation despite its low cellular expression level (as discussed above).

The underlying basis for these differences in anti-viral activities and consequently packaging is not clear but a key consideration may be the presence (or absence) of cellular co-factors. This point is particularly noteworthy as co-factors have been shown to be necessary for the physiological functions of the closely related family members, AID (Chaudhuri et al., 2004) and APOBEC1 (Lellek et al., 2000; Mehta et al., 2000). Thus the identification and study of APOBEC3 associated cellular proteins, such as Ago2, becomes increasingly important as well as other factors which may influence their substrate specificities, such as subcellular localisation. With regards to this, the nuclear APOBEC3 proteins, for example, are more effective at inhibiting LINE-1 retrotransposition, which reverse transcribes its RNA in the nucleus rather than in the cytoplasm (Bogerd et al., 2006). Conversely, APOBEC3 proteins which are predominantly cytoplasmic, may be more likely to be incorporated into virions as this is where virus assembly takes place. From Figure 3.4, this does appear to be the case. Further and more intriguingly, the most anti-viral APOBEC3 proteins are also more effectively localised to Ago2 and DDX6 marked cytoplasmic foci (Figures 3.4 - 3.6), which has been previously implied (Wichroski et al., 2006). The importance of these structures to APOBEC3 antiviral activity will be investigated in more depth in Chapter 5.

However co-localisation is not indicative of an interaction as has been demonstrated for A3G and the P-body protein Lsm1 (Wichroski et al., 2006), and therefore the interactions between APOBEC3 proteins and Argonaute 2 was assessed via co-immunoprecipitation (Figure 3.8). Previously this has been done for A3F and A3G but it was important to look at the whole APOBEC3 family in order to draw out correlations with their anti-viral phenotypes. From this analysis, it is clear that A3G, A3F and A3H interact with Ago2 and weak interactions were also detected with A3A and A3C. Since these latter APOBEC3 proteins were poorly associated with P-bodies (Figure 3.6), this demonstrates that the majority of these interactions are most likely occurring in the diffuse cytoplasm rather than at these punctate structures. In support of this, Leung *et al* (2006) have found that only ~ 2% of total cellular Ago2 is present in P-bodies at any one time and that these foci are in fact highly dynamic structures with proteins continually shuttling between them and the cytoplasm. It is also formally possible that this interaction occurs in the nucleus, as there are some reports to suggest that Ago2 may localise to the nucleus (Rudel et al., 2008; Weinmann et al., 2009).

The fact that other Argonautes were also able to interact with the APOBEC3 proteins (Figure 3.9) indicates that the APOBEC3 interaction with Ago2 is not dependent on the catalytic activity of this protein. As has been previously mentioned, the fact that these co-imunoprecipitation experiments cannot rule out the possibility that the APOBEC3 proteins are directly binding to the beads means that these results must be interpreted with some caution. The inclusion of more stringent negative controls would help resolves this issue. On the other hand, the interactions between Ago2 and A3F and A3G have already been validated in published reports (Gallois-Montbrun et al., 2008; Gallois-Montbrun et al., 2007; Wichroski et al., 2006).

Attempts to further validate the co-immunoprecipitation results using a yeast 2 hybrid approach proved inconclusive (Figure 3.10). This is most likely due to the poor expression of the Argonaute proteins in yeast cells (Figure 3.10C). However, several known protein - protein interactions cannot be recapitulated in yeast 2 hybrid assays such as the interaction between A3G and Vif. A further means of validating this interaction was attempted through FRET/FLIM analysis, which could also be used to define the sub-cellular location of this interaction (i.e in P-bodies versus the diffuse cytoplasm). However, due to technical issues concerning this method and specifically the need to significantly overexpress the proteins of interest in order to identify positive

interactions, it was not considered a valid means of assessing the true biological nature of this interaction. Overexpression of A3G and Ago2 resulted in their association with large protein aggregates, and possibly stress granules, which are not formed under normal cellular conditions (Figure 3.12). Although confirming protein interactions in other systems is ideal, the interactions described here via co-immunoprecipitation have been consistently demonstrated even when the protocol was modified to include formaldehyde cross-linking, thus highlighting the robustness of the interaction observed.

Although it has been reported that the interaction between A3F/A3G and Ago2 is partially resistant to RNase treatment, others have claimed it is wholly dependent on RNA (Wichroski et al., 2006). Whether this interaction is in fact mediated by miRNA or mRNA remains unresolved at present. Ago2 mutants that were no longer able to bind miRNAs still retained their interaction with A3G, though not to the same extent as the wild type protein (Figure 3.11). This might suggest that a proportion of this interaction is dependent on miRNAs. However, the fact that the F2V2 mutant is no longer able to bind either GW182 or miRNAs (Eulalio et al., 2008b) implies that in fact these two point mutations have caused serious conformational changes in the protein which affects its binding interface with cellular proteins, including A3G, and nucleic acid. Mutations in the PAZ domain of Ago2 may similarly interfere with A3G binding. Although the PAZ9 and PAZ10 mutants have been claimed to still interact with Dcp1a, the efficiency of this interaction was not reported (Liu et al., 2005b). Therefore it is likely that these mutations, though not affecting expression of the protein, interfere with its ability to interact with cellular factors through conformational alterations. What can be deducted from these Ago2 mutants, however, is that the interaction with A3G appears to be dependent on more than one intact Ago2 domain as mutations in both the PAZ and Mid domains reduced the association between these two proteins.

Overall, it can be concluded that the interaction between the APOBEC3 and Argonaute proteins extends beyond A3F/A3G and Ago2 for both protein families. This interaction did not appear to closely correlate with the anti-viral phenotypes of the APOBEC3 proteins, however, their co-localisation to Ago2 foci/P-bodies did. Although the exact nature of these interactions is not yet fully understood, the Argonaute proteins may provide a means of gaining novel insight into APOBEC3 activity and thus the functional consequences of this interaction will be explored in more detail in the following chapter.

CHAPTER 4

Functional implications of the interaction between the APOBEC3 and Argonaute protein families

4. RESULTS

Functional implications of the interaction between the APOBEC3 and Argonaute protein families.

4.1 Introduction

The discovery that certain APOBEC3 proteins were able to associate with an array of cellular RNA binding proteins in RNP complexes (Chiu et al., 2006; Gallois-Montbrun et al., 2008; Gallois-Montbrun et al., 2007; Kozak et al., 2006; Wichroski et al., 2006), evoked questions regarding the relevance of these interactions for APOBEC3 activity, not just in terms of their anti-viral capabilities but also viral target specificities and potential unidentified cellular functions. It has already been proposed that high molecular weight complex formation allows A3G to sequester away Alu elements, thus inhibiting their retrotransposition, and that A3G contained within these complexes is enzymatically inactive (Chiu et al., 2006), thereby highlighting the importance of cellular interactions for functional regulation. Nevertheless, the importance of specific associated proteins to APOBEC3 activity, either as co-factors or regulators, has remained largely unexplored. Further, no cellular function has yet been defined for the APOBEC3 family, but their association with a number of proteins relevant to RNA metabolism and turnover suggest that they may be involved in similar processes. The mouse and rat APOBEC1 proteins are able to post-transcriptionally regulate the fate of AU rich element (ARE) containing mRNAs (Anant and Davidson, 2000; Anant et al., 2004) and the human APOBEC3 proteins have been reported to antagonise miRNA mediated translational repression (Huang et al., 2007a). Therefore, the functional implications of the interaction between the APOBEC3 and Argonaute proteins was investigated in more detail, firstly in terms of Argonaute involvement in APOBEC3 anti-viral activity and then in terms of the possible role of APOBEC3 proteins in RNA regulation.

4.2 Ago2 overexpression and APOBEC3 anti-viral activity

To determine whether Ago2 had any effect on APOBEC3, in particular A3G, antiviral activity, HeLa cells stably expressing either untagged A3G or YFP were generated by retroviral transduction and maintained under neomycin selection. Expression and functionality of the transduced proteins was evaluated before further experiments were performed (data not shown). These cells were then co-transfected with equivalent amounts of Ago2 or GFP (in both HA and myc epitope tagged expression vectors) and the NL43 Δ*vif* proviral plasmid. The myc tag is at the N-terminus of the protein while the HA tag is at the C-terminus. The position of epitope tags can strongly influence protein expression and/or activity, which is why two different plasmids were used in this experiment. A single cycle infectivity assay was then performed, as described in section 3.2, but briefly viral supernatants were harvested 48 hours post transfection, normalized by $p24^{Gag}$ ELISA and used to challenge the TZM-bl reporter cell line.

Expression of the transduced and transfected proteins was confirmed by immunoblotting (Figure 4.1A), with equivalent amounts of Ago2 and GFP expressed in both cell lines. Virus production from these cells, shown in Figure 4.1B, is fairly consistent between the different samples. Slightly less virus is produced from the A3G expressing cells (black bars) compared to the YFP control line (grey bars), especially evident for the GFP.HA sample, but overexpression of A3G and other APOBEC3 proteins can sometimes be mildly inhibitory to virus production. Nevertheless, when identical amounts of $p24^{Gag}$ were used to infect TZM-bl cells, HIV-1 Δ*vif* inhibition by A3G was unaffected by the presence of Ago2 as a 1.5 log decrease in viral infectivity was consistently observed from A3G containing samples. Accordingly, it can be concluded from the data presented here that overexpression of Ago2 does not appear to effect A3G mediated viral inhibition.

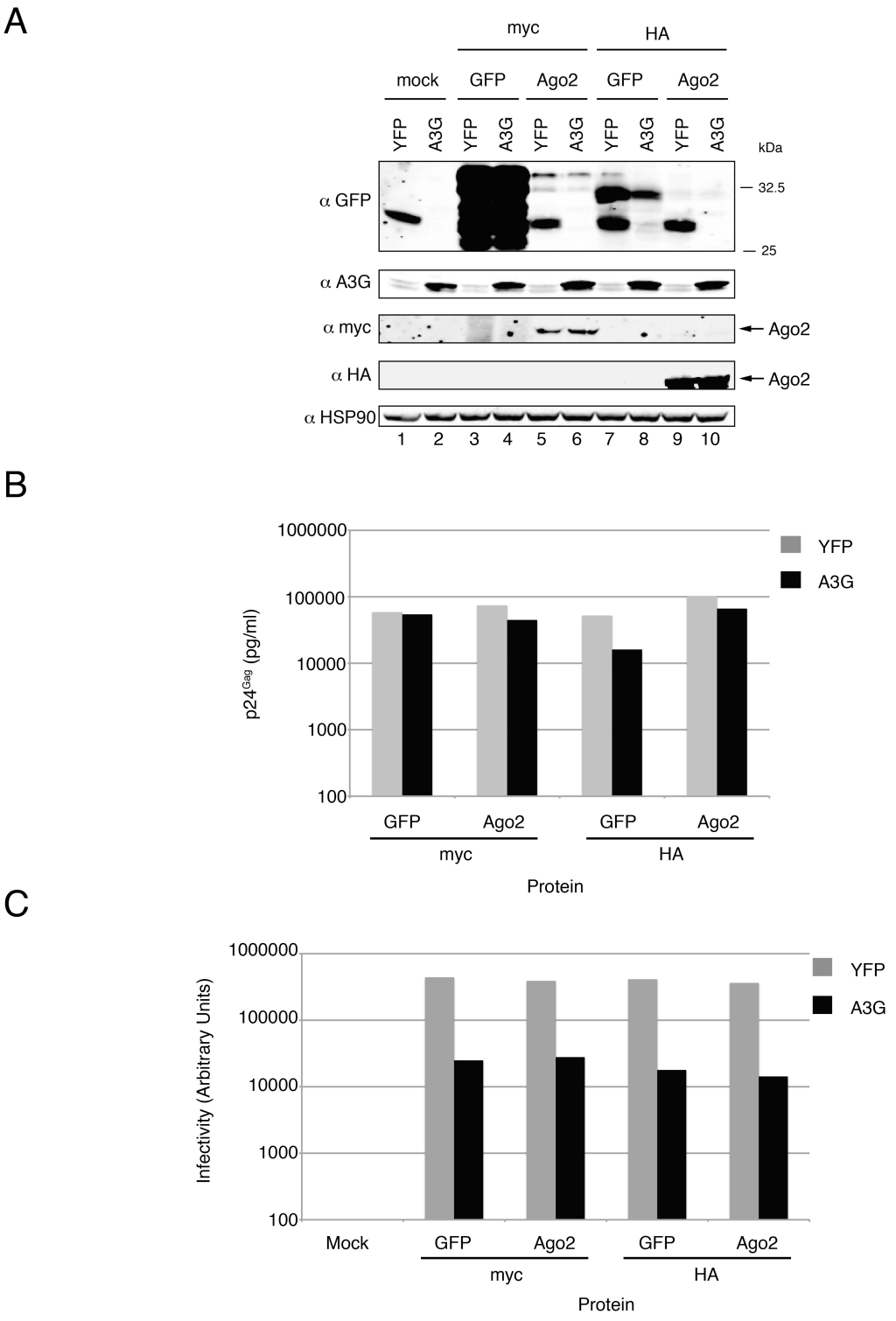

Figure 4.1: Overexpression of Ago2 does not affect A3G anti-viral activity.

HeLa cells stably expressing either untagged A3G or YFP (as a negative control) were transfected with equivalent amounts of either HA or myc epitope tagged Ago2 and GFP expression vectors and an NL43 Δ*vif* proviral plasmid. 48 hours post transfection, viral supernatants were harvested, quantified by $p24^{Gag}$ ELISA and used to infect the TZM-bl reporter cell line. **A**. immunoblot analysis of transduced and transfected proteins with anti-GFP (which also detects YFP), anti-A3G, anti-myc, anti-HA and anti-HSP90 (as a loading control) antibodies. **B**. Virion production from transfected cells. **C**. Infectivity of virions produced in B. Results are representative of 2 independent experiments.

4.3 Knockdown of Argonaute 2

4.3.1 Phenotypic analysis

Although overexpression analyses can often be informative, mostly when a protein is limiting in a particular process or pathway, they fail to demonstrate whether it is actually necessary. Thus, even though overexpression of Ago2 did not yield any instructive data, this is not to say that it is not important for A3G function. A more thorough, and nowadays obligatory, means of assessing this is through RNAi, where a protein of interest is depleted through the use of small, targeted RNAs (discussed in Chapter 1, section 1.11.2). These RNAs recruit the RISC complex to their mRNA targets by binding to complimentary sites in the 3'UTR of the mRNA. RISC components (such as the Argonaute proteins) will then induce either translational repression or cleavage of these targeted mRNAs, thereby significantly reducing protein levels.

Lentiviral vectors expressing short hairpin RNAs (shRNAs) were used to knock down Ago2. These shRNAs are perfectly complimentary to their mRNA target and therefore knockdown is achieved through Ago2 mediated cleavage. However, unlike traditional siRNAs, they are not produced from long double stranded RNA but instead from hairpin structures, as their name would suggest. This means that they are processed like miRNAs, with cleavage of the hairpin by Drosha in the nucleus and subsequent export and processing by Dicer in the cytoplasm to yield the siRNA (see Chaper 1, section 1.11.1). As these shRNAs are expressed in lentiviral vectors, stable cells knocked down for the protein of interest can be generated and maintained. They also encode GFP allowing transfection and transduction efficiencies to be easily assessed. Knockdown of Ago2 via Ago2 mediated cleavage is possible and well documented (Meister et al., 2005; Roberts et al., 2011; Schmitter et al., 2006), as this protein is highly catalytic and thus even residual amounts can have some phenotypic effect.

HeLa and 293T cells were stably transduced with either an Ago2 targeting shRNA (Ago2) or a non-silencing control shRNA (NSC). After transduction, cells were maintained under puromycin selection and subsequently harvested and lysed for immunoblot analysis. Knockdown of Ago2 was highly effective (Figure 4.2A), as there is a significant reduction of Ago2 at the protein level in the knockdown cell lines compared to those expressing the control shRNA. Equivalent amounts of protein were

loaded onto the gel as judged by the amount of β-actin. Knock down of Ago2 had no obvious effects on cell proliferation or morphology.

It was also of interest to determine whether knockdown of Ago2 led to any changes in the size and/or number of P-bodies as has been demonstrated for other P-body components. For this, stable HeLa and 293T cells were plated onto coverslips and stained with an anti-Ge1 antibody, a well-known marker of P-bodies. This antibody was primarily raised against the nuclear p70 s6 kinase protein but has subsequently been shown to cross-react with the cytoplasmic Ge1 protein (Kedersha and Anderson, 2007). Cells were imaged using a Leica confocal microscope. Contrary to published reports (Nathans et al., 2009), knockdown of Ago2 had no detectable effect on P-body formation in both HeLa and 293T cells (Figure 4.2B), which illustrates that this protein is not a key component in the assembly of these foci.

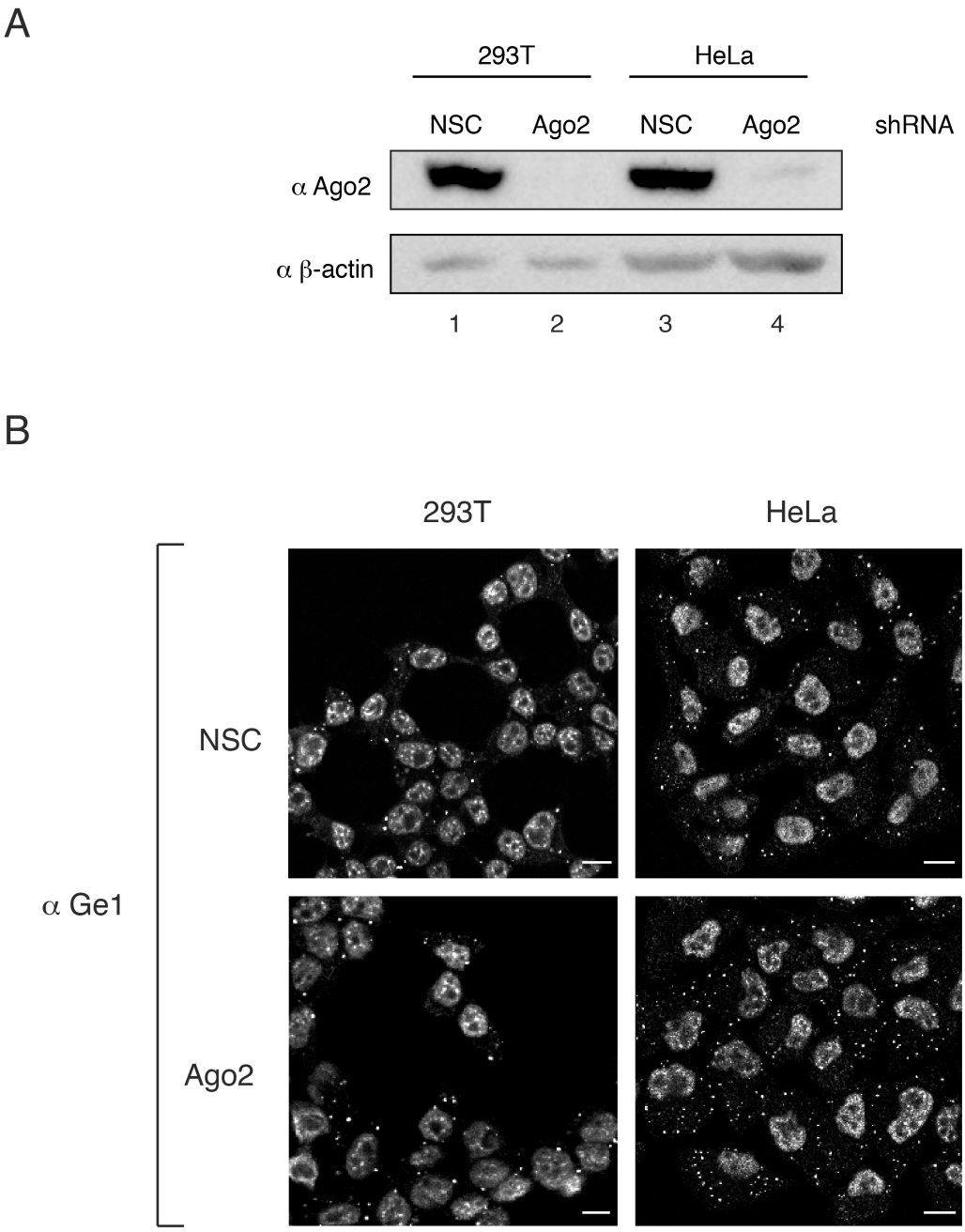

Figure 4.2: Phenotypic analysis of Ago2 knockdown by shRNA lentiviral vectors.

293T cells were transfected with an Ago2 (Ago2) or non-silencing control (NSC) shRNA encoded lentiviral vector, a Gag-Pol packaging plasmid (p8.91) and a VSVG expression plasmid (pVSVG) at a 2:2:1 ratio. 48 hours later, virus like particles (VLPs) were harvested and equivalent amounts used to transduce 293T or HeLa cells seeded in 24 well plates, with the addition of polybrene. 48 hours later, cells were checked for transduction efficiency by assessing GFP expression and placed under puromycin selection. Cells were maintained under selection for at least 5 days before immunoblot and immunofluorescence analysis. **A**. Cells were harvested, lysed and subjected to immunoblotting with anti-Ago2 and anti-β-actin (as a loading control) antibodies to check for protein expression. **B**. Cells were also plated onto coverslips and 24 hours later fixed in 4% formaldehyde. Cells were then permeablised and stained with a mouse anti-Ge1 primary antibody and an anti-mouse 594 secondary antibody. Coverslips were mounted onto slides and dried overnight before imaging using a Leica confocal microscope. Scale bar = 10 μm.

4.3.2 Functional analysis

Ago2 has been demonstrated to be the sole mediator of siRNA mediated silencing in humans as it is the only Argonaute protein that has retained its catalytic activity and is able to cleave mRNAs (Liu et al., 2004; Meister et al., 2004). Hence, it would be expected that depletion of Ago2 would lead to a reduced efficiency of silencing by siRNAs. This would thus provide a means of validating whether knockdown of Ago2, as determined by protein expression, had any functional consequences, before any further experiments with these cell lines were performed.

In order to test this, siRNAs targeting the ESCRT component, ALIX (ALIX), or a non-targeting control siRNA (control), were twice transfected into HeLa and 293T cells stably knocked down for Ago2. 48 hours after the second siRNA transfection, cells were harvested, lysed and subjected to immunoblotting (Figure 4.3). Cell lysates were probed for the expression of both ALIX and Ago2, using protein specific antibodies. Levels of HSP90 and β-actin verify that equal amounts of lysate were loaded onto the gels. Transfection of the control siRNA into both the non-silencing and Ago2 shRNA expressing cell lines (lanes 1 and 2) had no effect on ALIX expression. As would be expected, on the other hand, transfection of the ALIX siRNA into the control cell line (for both HeLa and 293T cells), led to a significant reduction in ALIX protein levels. However, using the same siRNA in the 293T Ago2 knock down cell line (Figure 4.3A), resulted in a less efficient depletion of ALIX, which would imply that in these cells, siRNA mediated silencing had been perturbed, though not completely eliminated (compare ALIX protein levels in lane 4 to lanes 1 and 2). It is unlikely that a complete inhibition of siRNA mediated silencing could be achieved with knock down of Ago2, as due to its highly catalytic nature, any residual protein remaining would still be functional. Also, without some Ago2 endonuclease activity, knockdown of this protein could not be achieved in the first place. In HeLa cells, knockdown of ALIX was equivalent in both the control and Ago2 shRNA expressing cell lines, suggesting that in this case, functional impairment of Ago2 was not as effective as in 293T cells, even when protein levels had been significantly reduced (Figure 4.3B).

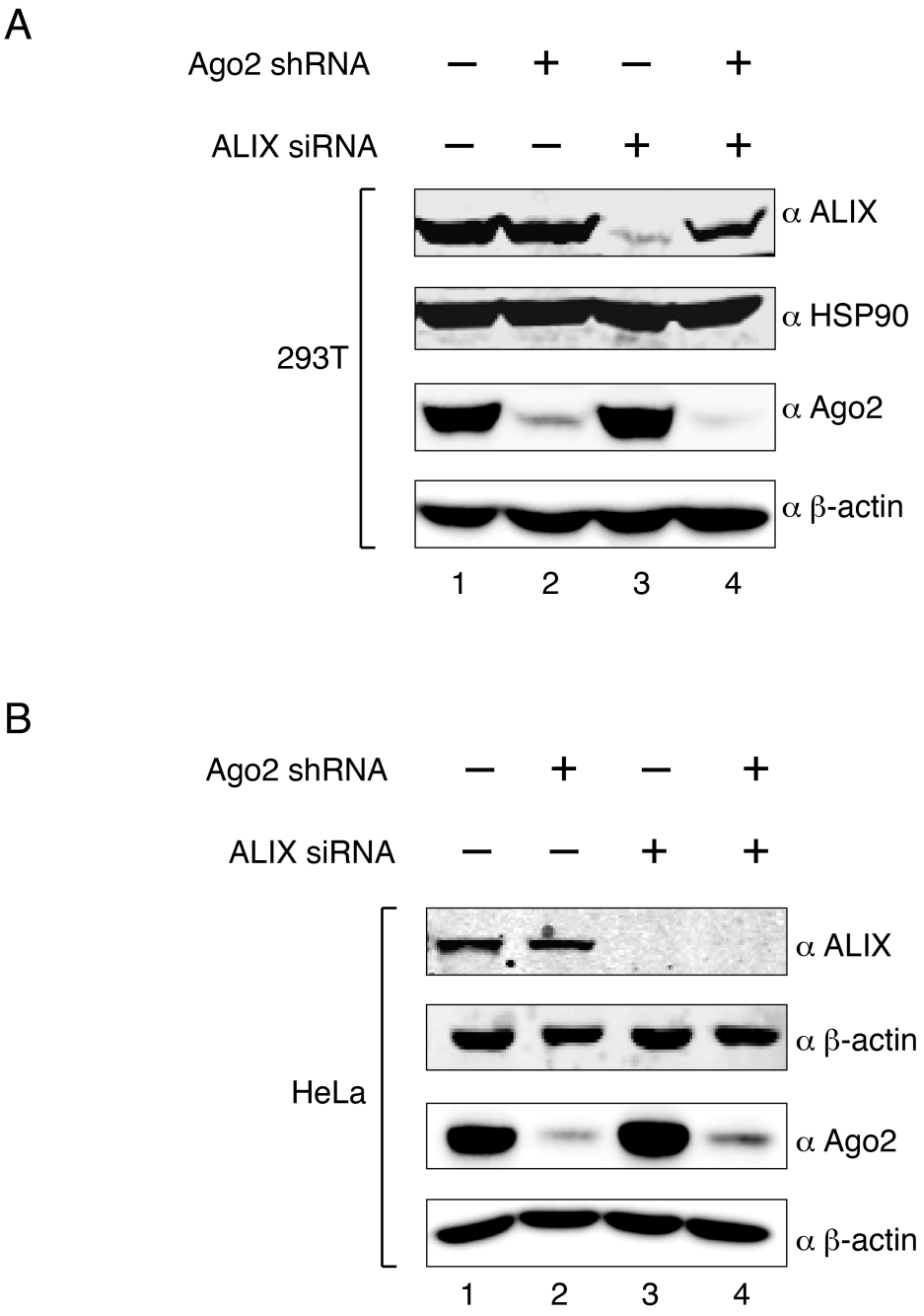

Figure 4.3: Perturbation of siRNA mediated silencing as functional confirmation of Ago2 knockdown.

Stable 293T (**A**) (seeded 24 hours before) and HeLa (**B**) (seeded 4 hours before) cells, expressing either a non-silencing control (-) or Ago2 (+) targeting shRNA, generated as in Figure 4.2, were transfected with 50 pmol of siRNAs targeting the ESCRT component ALIX (+) or a scrambled control (-), using the Dharmafect transfection reagent. 48 hours later, cells were re-seeded into 24 well plates and 4 hours later were transfected again as before. 48 hours after the second transfection cells were washed in PBS and lysed in gel loading buffer. Lysates were analysed by immunoblotting using anti-ALIX and Ago2 specific primary antibodies. Anti-HSP90 and anti-β-actin antibodies were also included as loading controls. Data is representative of four independent experiments.

4.3.3 Ago2 knockdown and APOBEC3 anti-viral activity

To help establish a functional basis for the interaction between the APOBEC3 proteins and Ago2, an infectivity assay was utilised to assess the consequences of Ago2 depletion on both HIV-1 virion infectivity and APOBEC3 anti-viral activity.

As previously described in section 4.2, stable 293T cells expressing either a control or Ago2 targeting shRNA were co-transfected with 0.5 ug each of APOBEC3.HA plasmids (with GFP as a negative control) and an NL43 Δ*vif* construct. 48 hours later, viral supernatants were harvested, and normalised amounts were used to infect TZM-bl cells. In parallel, equivalent amounts of supernatant were spun through a 20% sucrose cushion and the pellets lysed and prepared for immunoblotting in order to check for virion incorporation of the APOBEC3 proteins.

Ectopic expression of the APOBEC3 proteins led to similar levels of protein expression in both cell lines (Figure 4.4A), and near equivalent amounts of virus production from all samples tested (Figure 4.4B). This demonstrates that Ago2 neither inhibits nor facilitates HIV-1 particle production in 293T cells. From Figure 4.4C, it can also be seen that Ago2 has no significant effect on HIV-1 infectivity, as demonstrated by the equivalent levels of viral infectivity in the presence of GFP. Fundamentally, depletion of Ago2 did not alter APOBEC3 anti-viral activity (Figure 4.4C). A slight difference is observed for A3G inhibition in the control and knock down cell line but this is most likely due to these values being very close to background levels and are therefore less robust. These results are confirmed by the virion incorporation blots (Figure 4.4A), as the degree of APOBEC3 packaging is identical in both cell lines.

In order to rule out the possibility that overexpression of the APOBEC3 proteins had masked any differences in viral inhibition, a titration of A3G and GFP (as a negative control) was carried out and virus production, anti-viral activity and virion packaging were examined as before (Figure 4.5). Once again, there is near equivalent expression of the transfected proteins (except at the lowest concentration of A3G for some reason, compare lanes 11 and 12, Figure 4.5A) and of virus production from both cell lines (Figure 4.6B). HIV-1 infectivity is not affected by Ago2 depletion as judged by titration of GFP in the control and knock down cell lines. The anti-viral activity of A3G is also comparable between the two cell lines, even at lower amounts of input DNA, although as before there is slightly less inhibition in the knockdown compared to the

control cells (Figure 4.5C). However this does not appear to be a dramatic effect, though it is consistent, and the raw values in all cases were relatively low. This is supported by the fact that similar amounts of A3G are packaged into virions in both cell lines (Figure 4.5A, lower panels).

Overall it can be concluded that depletion of Ago2 does not seem to have any significant consequences, either positive or negative, for APOBEC3 anti-viral activity. Therefore, since Ago2 is the only enzymatically active Argonaute protein, siRNA mediated silencing in general, is not required for APOBEC3 mediated HIV-1 inhibition.

Figure 4.4: Knockdown of Ago2 does not affect APOBEC3 anti-viral activity.

293T cells stably transduced with either an Ago2 (Ago2) or non-silencing control (NSC) shRNA, as described in Figure 4.2, were transfected with 0.5 μg of HA-tagged APOBEC3 expression plasmids and an NL43 Δ*vif* proviral plasmid. 48 hours later, viral supernatants were harvested, normalised and used to infect the TZM-bl reporter cell line. Normalised viral supernatants were also concentrated through a 20% sucrose cushion and viral pellets analysed by immunoblotting for APOBEC3 incorporation. **A.** Immunoblot analysis of cell and viral lysates with anti-HA, anti-$p24^{Gag}$ and anti-Ago2 antibodies. Anti-HSP90 and anti-β-actin were included as loading controls. **B**. Virion production from transfected cells, described above. **C**. Infectivity of virions produced in B. Data is presented as the average of three independent experiments, with error bars denoting the standard deviation. All values are normalised to GFP expressed in the NSC cell line, which is set at 100%.

A

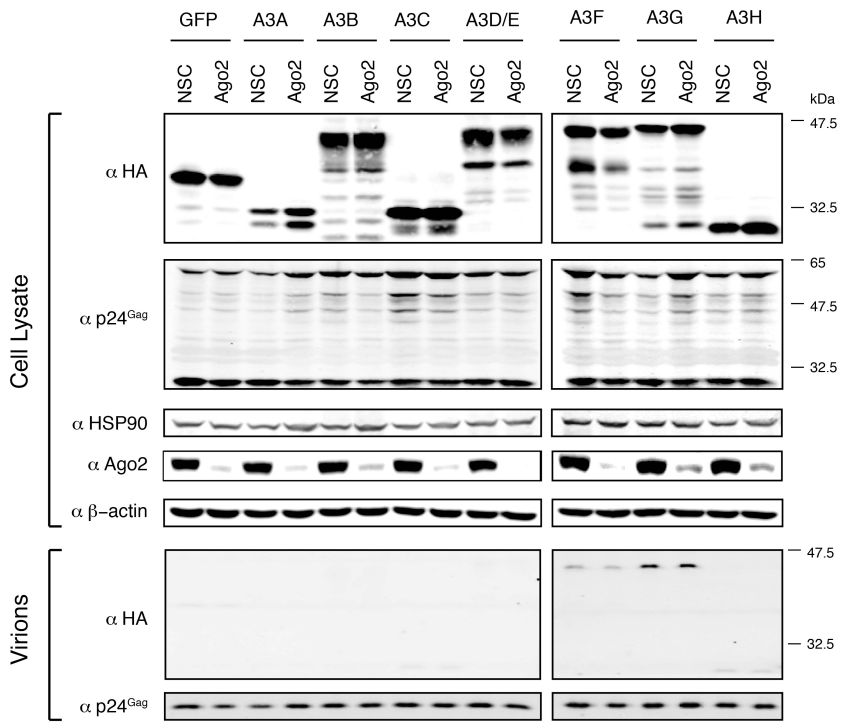
GFP
A3A
A3B
A3C
A3D/E
A3F
A3G
A3H
NSC
Ago2
kDa
47.5
32.5
65
Cell Lysate
α HA
α p24Gag
α HSP90
α Ago2
α β–actin
Virions

B

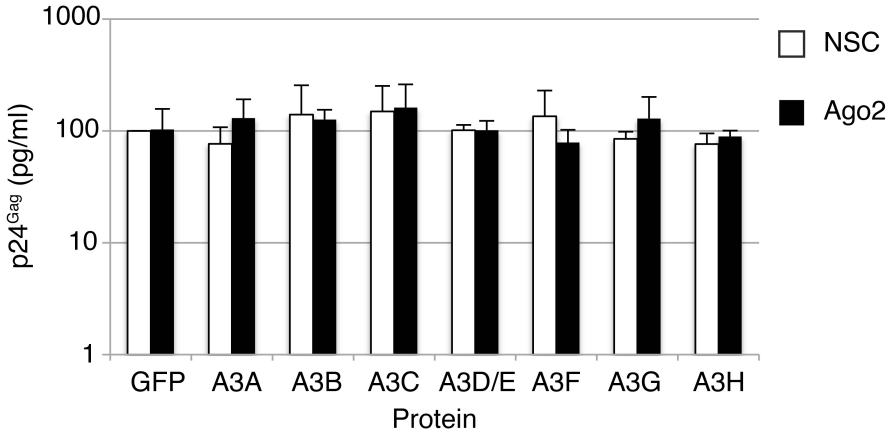
1000
100
10
1
p24Gag (pg/ml)
NSC
Ago2
GFP
A3A
A3B
A3C
A3D/E
A3F
A3G
A3H
Protein

C

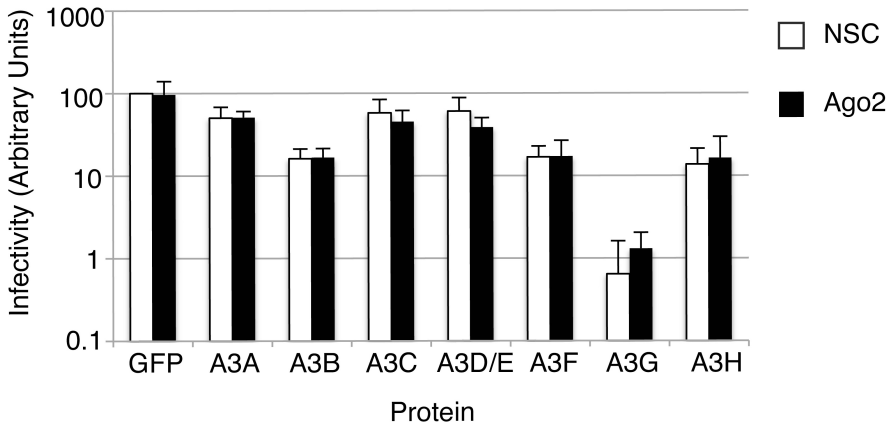
1000
100
10
1
0.1
Infectivity (Arbitrary Units)
NSC
Ago2
GFP
A3A
A3B
A3C
A3D/E
A3F
A3G
A3H
Protein

Figure 4.5: Knockdown of Ago2 does not affect A3G anti-viral activity even at lower levels of A3G expression

293T cells stably transduced with either an Ago2 (Ago2) or non-silencing control (NSC) shRNA encoded lentiviral vector, as described in Figure 4.2, were transfected with either 0.5 μg, 0.16 μg or 0.05 μg of HA-tagged A3G or GFP (as a negative control) expression plasmids and 0.5 μg of an NL43 Δ*vif* proviral plasmid. Total DNA concentrations were kept constant at 1 μg with the addition of an untagged luciferase expression plasmid. An infectivity assay was then performed as in Figure 4.4. **A**. Immunoblot analysis of cell and viral lysates with anti-HA, anti-$p24^{Gag}$ and anti-Ago2 antibodies. Anti-HSP90 and anti-β-actin were included as loading controls**. B**. Virion production from transfected cells, described above. **C**. Infectivity of virions produced in B. Data is presented as the average of three independent experiments, with error bars denoting the standard deviation. All values are normalised to GFP in the NSC cell line, which is set at 100%.

A

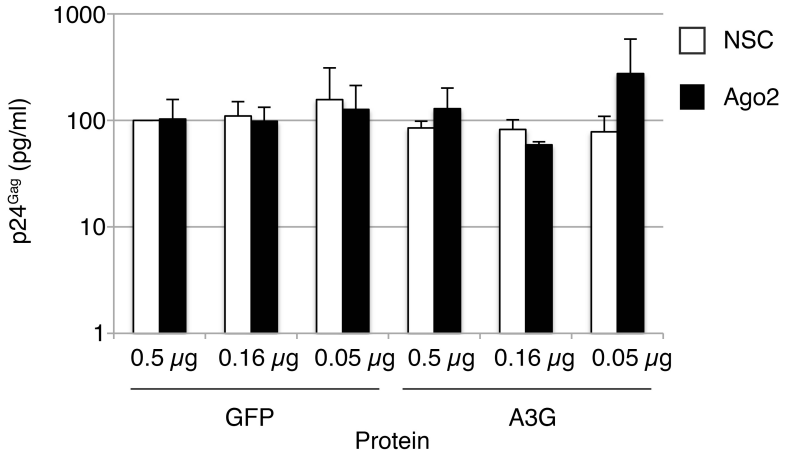
1000
100
10
1
p24Gag (pg/ml)
NSC
Ago2
0.5 μg
0.16 μg
0.05 μg
0.5 μg
0.16 μg
0.05 μg
GFP
A3G
Protein

B

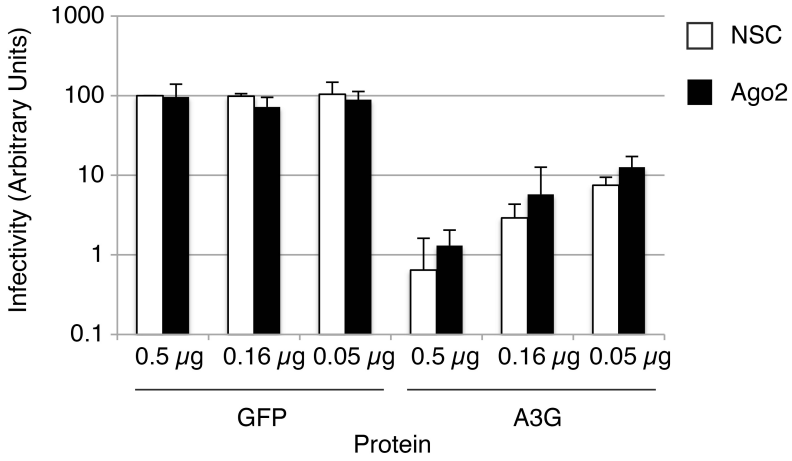
1000
100
10
1
0.1
Infectivity (Arbitrary Units)
NSC
Ago2
0.5 μg
0.16 μg
0.05 μg
0.5 μg
0.16 μg
0.05 μg
GFP
A3G
Protein

C

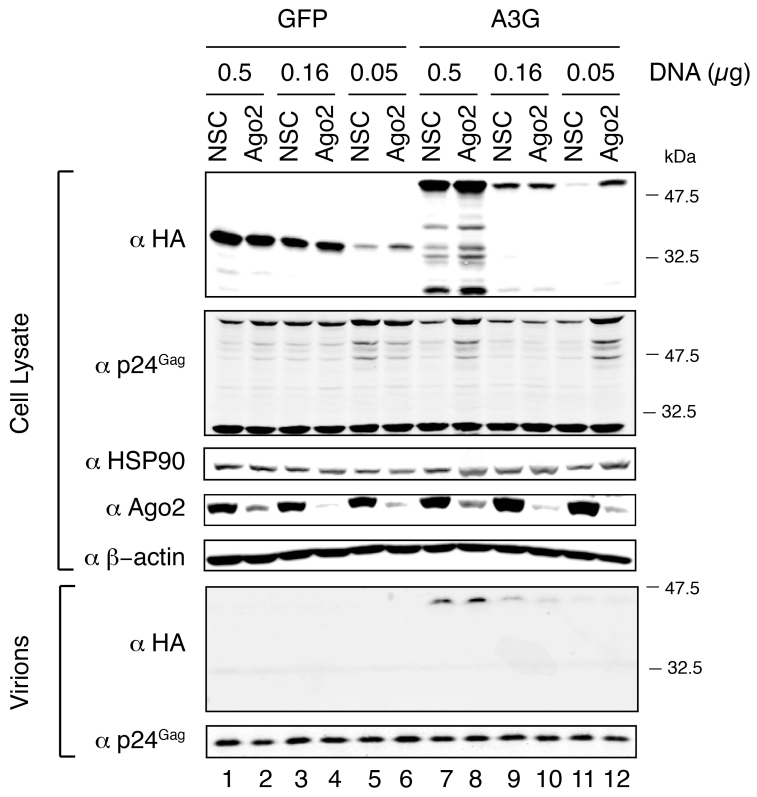
GFP
A3G
0.5
0.16
0.05
0.5
0.16
0.05
DNA (μg)
NSC
Ago2
kDa
α HA
α p24Gag
α HSP90
α Ago2
α β–actin
Cell Lysate
Virions
47.5
32.5
1 2 3 4 5 6 7 8 9 10 11 12

4.4 Ago2 knockdown and miRNA mediated repression

Although it has been demonstrated that Ago2 and siRNA mediated silencing do not appear to be important for APOBEC3 anti-viral activity, the role of the other Argonaute proteins and miRNA mediated repression, in general, has not been explored. All four Argonaute proteins are known to be involved in this process, yet the exact contributions of any one particular protein are not understood. Therefore, it was conceivable that knockdown of Ago2 may cause some reduction in miRNA mediated repression, though not abolish it completely. If true, this would help unearth any possible involvement of this pathway in APOBEC3 activity. To check this, a miRNA based assay was utilised comprising firefly luciferase reporter constructs containing four binding sites for the let-7 miRNA (wild type/FF4LCS) or a control containing mutated binding sites (mutant/FFrm4LCS) (Figure 4.6A). Expression of the wild type construct should be repressed approximately 4 - 5 fold compared to the control due to the action of endogenous let-7 miRNAs (Lytle et al., 2007). These will bind to the target sites in the wild type construct and recruit the RISC complex, which will subsequently induce translational repression or degradation of the reporter (see Chapter 1, sections 1.11.1 – 1.11.3). The mutant construct will be unaffected by the actions of these miRNAs and therefore should be expressed at normal levels. *Renilla* luciferase is also included to account for any differences in transfection efficiencies. Both the wild type and mutant constructs were transfected into HeLa Ago2 knockdown and control cell lines and luciferase expression was assessed by a Dual Luciferase Reporter Assay (Promega) as per manufacturer's instructions. This experiment could not be performed in 293T cells due to the poor repression of the wild type construct, most likely due to low amounts of endogenous let-7 miRNA expression in these cells. In the Ago2 knock down cell line, repression of the wild type construct might be expected to be reduced but this was not the case as the level of repression was equivalent in both cell lines (Figure 4.6B). This indicates that miRNA repression is not dependent upon Ago2 as it occurs just as efficiently, mediated by the other Argonaute family members, in the presence of reduced amounts of this protein.

A

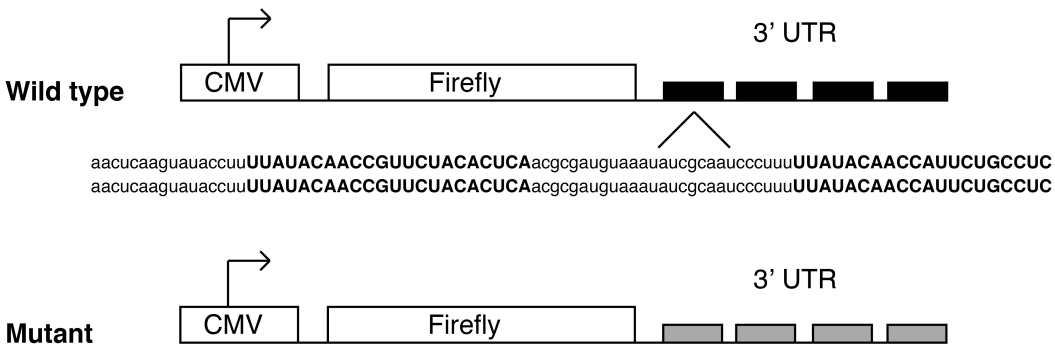

B

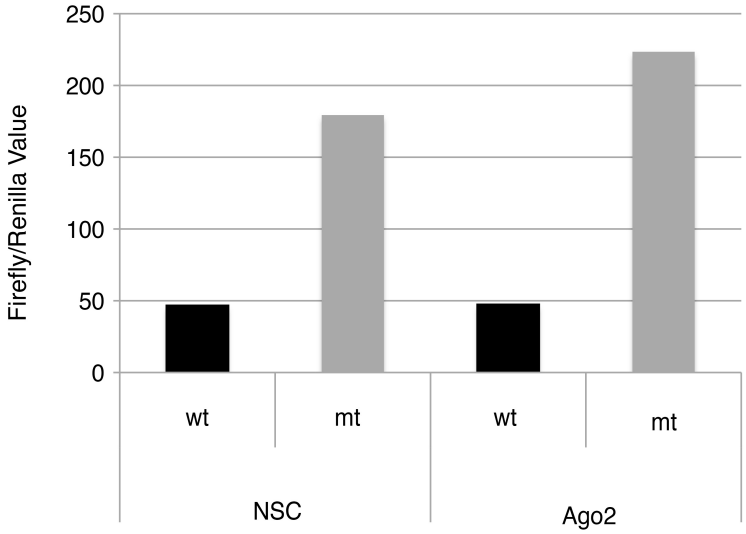

Figure 4.6: Knockdown of Ago2 does not impair miRNA mediated repression.

A. Schematic diagram of the luciferase reporter constructs used in this study. Firefly luciferase expression plasmids contain either four intact (wild type/FF4LCS) or mutated (mutant/FFrm4LCS) binding sites for the let-7 miRNA in the 3'UTR. The inserted sequences are shown with the let-7 bind§ing sites highlighted in bold. **B**. HeLa cells stably expressing either an Ago2 (Ago2) or non-silencing control (NSC) shRNA encoded lentiviral vector were transfected with 0.1 µg of the wild type or mutant reporter plasmid, 0.4 µg of HA-tagged GFP and 0.01 µg of *Renilla* luciferase as a transfection control. 30 hours later cells were harvested, lysed and a Dual Luciferase Assay performed to measure luciferase activity. Data is presented as the ratio of firefly to *Renilla* values and is representative of two independent experiments.

4.5 mlin41 overexpression and effects on Argonaute 2

The results presented above highlight the complexities of studying a family of proteins with similar functional roles, as knockdown of one particular member may have no observable effects on the pathway of interest. In a bid to address this redundancy, the mouse Trim71 protein (commonly referred to as mlin41) was employed as a means to deplete all four Argonautes simultaneously, as it has been reported to be involved in the proteosomal degradation of these proteins (Rybak et al., 2009). mlin41 is a target of the let-7 miRNA and has been shown to interact with the Argonautes and Dicer by co-immunoprecipitation and localise to P-bodies. Moreover, it acts as an E3 ubiquitin ligase, inducing the ubiquitination and hence degradation of the Argonaute proteins and as a result, interferes with mRNA translational repression. Overexpression of mlin41 in embryocarcinoma cells resulted in reduced Ago2 proteins levels to almost undetectable levels. More importantly, using reporter constructs in 293 cells, it led to inhibition of repression mediated by the let-7 and miR-124 miRNAs (Rybak et al., 2009). Thus if its effects could be replicated, it would be a useful tool in resolving the significance of miRNA repression and consequently the Argonaute proteins for APOBEC3 function.

Therefore, FLAG-tagged mlin41 was transfected into HeLa and 293T cells at increasing concentrations, along with luciferase and DDX6, as negative controls. 48 hours post transfection, cells were harvested, lysed and prepared for immunoblotting. Lysates were probed for the expression of endogenous Ago2 only, as a good commercial antibody is available for this protein.

From Figure 4.7, mlin41 appears to be well expressed in both HeLa and 293T cells, but from the Ago2 blots (bottom left and right), overexpression of mlin41 does not seem to have a dramatic effect on Ago2 protein levels when compared to the mock transfected control (compare lane 1 with lanes 4 - 6, in both cell lines). At the highest concentration of input DNA (lane 6), there is a moderate reduction in Ago2 expression, which is more evident in the 293T cells, yet a substantial amount of protein is still present. In essence, although mlin41 may cause a slight decrease in Ago2 protein levels when highly expressed, it is insufficient with which to efficiently deplete these proteins from cells and study their functional effects.

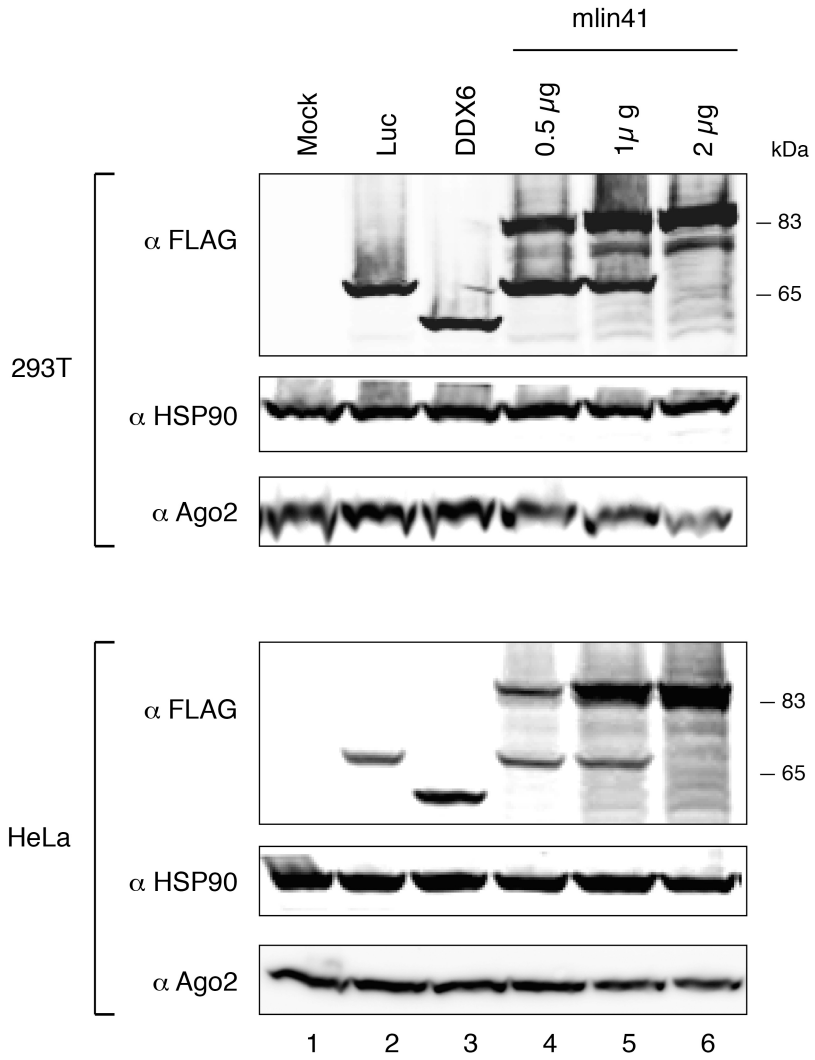

Figure 4.7: mlin41 overexpression and effects on Ago2 protein expression.

293T and HeLa cells were either untransfected (mock) or transfected with 2 µg of FLAG-tagged luciferase, FLAG-tagged DDX6 and increasing concentrations of FLAG-tagged mlin41 (0.5 µg, 1 µg and 2 µg) expression plasmids in 6 well plates using either PEI (293T) or Fugene (HeLa). Total DNA concentration was kept constant at 2 µg with the addition of an untagged luciferase expression plasmid. 48 hours later cells were lysed in gel loading buffer and analysed by immunoblotting using anti-FLAG and anti-Ago2 antibodies. Anti-HSP90 was included as a loading control. Data is representative of three independent experiments.

4.6 APOBEC3 proteins and regulation of RNA

4.6.1 miRNA mediated translational repression

Since it was evident from the data presented thus far, that there was no apparent role for Ago2 in APOBEC3 mediated HIV-1 inhibition, focus then turned to a potential role of the APOBEC3 proteins in Argonaute function. Specifically, Huang *et al* (2007) have reported that the APOBEC3 proteins are able to inhibit both siRNA and miRNA mediated translational repression through an as yet unidentified mechanism. This assigns a cellular function to the APOBEC3 proteins but also has implications for their anti-viral activity as there is increasing evidence of the importance of cellular and viral miRNAs in both viral replication and inhibition (discussed in Chapter 1, section 1.11.4). It also provides functional relevance to the APOBEC3-Argonaute interaction. To verify these findings, a miRNA based reporter assay was employed as described in section 4.4. In this case, HeLa cells were co-transfected with HA-tagged APOBEC3 expression vectors and either the wild type or mutant luciferase reporter constructs. *Renilla* luciferase was included to account for any differences in transfection efficiencies. 24 hours later, cells were harvested and lysed and luciferase activity measured.

Figure 4.8 presents the raw firefly and *Renilla* luciferase values, with all data normalised to GFP co-transfected with the mutant reporter, which is set at 100%. Firstly, with co-transfection of the negative control, GFP, there is a four fold decrease in the expression of the wild type construct relative to the mutant control (Figure 4.8A), as would be expected from previous reports (Lytle et al., 2007). Expression of A3C resulted in an increase in expression of the wild-type reporter (black bar), which would be expected if this were indeed a miRNA mediated effect. However, this change was matched by a similar increase for the mutant reporter, which implies that this is not a result of inhibition of miRNA mediated translational repression. The remaining APOBEC3 proteins either caused only modest increases in the expression of both reporters (A3A, A3G and A3H) or resulted in decreased expression, to varying degrees, with A3D/E having the strongest effect. These results were confirmed when examining expression of *Renilla* luciferase (Figure 4.8B). This plasmid contains no known miRNA binding sites and therefore its expression should be unaffected by the APOBEC3 proteins, if indeed their affects are miRNA dependent. Similar changes are observed for the expression of this protein upon co-transfection of the different APOBEC3 proteins, as seen for firefly luciferase. In both instances, A3C had the most dramatic effect,

increasing protein levels of all the constructs tested by approximately 10 fold. Expression of the different APOBEC3 proteins with both the wild type and mutant reporter was confirmed by immunoblotting (Figure 4.8C). These data indicate that the APOBEC3 proteins are not able to specifically suppress miRNA mediated translational repression and instead they act as more general modulators of protein expression. The mechanism and relevance behind this, however, requires further investigation.

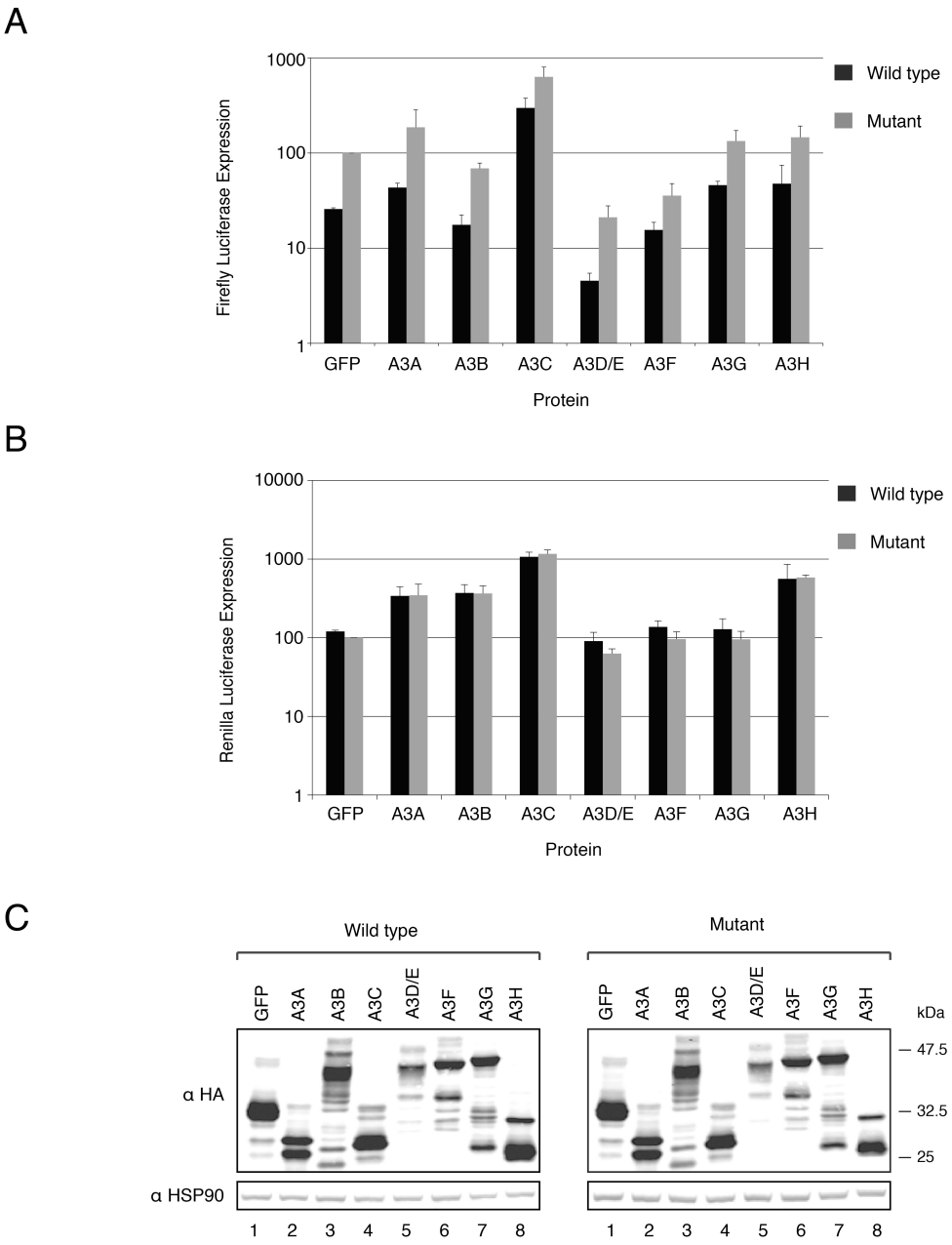

Figure 4.8: APOBEC3 proteins do not inhibit miRNA mediated translational repression by the let-7 miRNA.

HeLa cells, seeded in 24 well plates, were transfected with 0.1 µg of wild type or mutant let-7 luciferase reporter plasmids (described in Figure 4.6), 0.9 µg of HA-tagged APOBEC3 expression plasmids and 0.01 µg of a *Renilla* luciferase expression plasmid as a transfection control. 30 hours later, cells were harvested, lysed and a Dual Luciferase Assay performed to measure luciferase activity. Cells were also re-suspended in gel loading buffer for immunoblot analysis **A**. Firefly luciferase values of the wild-type and mutant reporter constructs co-expressed with the APOBEC3 plasmids or GFP as a negative control. **B**. *Renilla* luciferase values of wild type and mutant reporter constructs co-expressed with the APOBEC3 plasmids and GFP as a negative control. For both A and B, data are the raw luciferase values presented as the average of four independent experiments with error bars denoting the standard deviation. All values are normalised to GFP co-expressed with the mutant luciferase reporter plasmid which is set at 100%. **C**. Immunoblot analysis of APOBEC3 protein expression in the presence of the wild type (left panel) and mutant (right panel) luciferase reporter constructs with anti-HA and anti-HSP90 (as a loading control) antibodies.

4.6.2 Inhibitors of miRNA mediated translational repression

Few proteins have so far been described that are actually able to modulate miRNA mediated translational repression. A selection of these were tested in the miRNA system described in section 4.4 and 4.6.1 so as to identify possible positive controls for this assay.

VA1 is a non-coding structured RNA encoded by adenovirus. It has been reported to specifically inhibit miRNA function, but not siRNAs, by hindering export of miRNA precursors from the nucleus and by directly binding to Dicer (Lu and Cullen, 2004). In spite of this, overexpression of VA1 failed to relieve repression of the wild type construct in the let-7 miRNA assay (Figure 4.9A). Although cells were harvested 48 hours after transfection, it may take significantly longer for the effects of VA1 to be observed, especially when measuring let-7, which is one of the most abundant miRNAs expressed in HeLa cells. In support of this, it can take several days before phenotypic effects of Dicer depletion are manifest.

Another protein tested was the RNA binding protein Dead end 1 (DND1), which is required for germ cell survival and migration in zebrafish. Kedde *et al* (2007) state that the human orthologue is capable of directly binding to mRNAs thereby interfering with miRNAs binding at their target sites, specifically of the *LATS2* and *p27* tumour suppressor genes. Figure 4.9B demonstrates that expression of DND1 caused significant decreases in both firefly and *Renilla* expression levels. Raw values from these experiments are presented to clearly highlight this. These indiscriminate effects therefore rule out DND1 as a possible positive control in this system.

Finally, the HIV-1 accessory protein, Tat, was also investigated. It has been proposed that Tat is able to suppress global RNAi in HIV-1 infected cells by either directly binding to Dicer or through sequestration of the Dicer co-factor TRBCP (Bennasser et al., 2005; Hayes et al., 2011; Qian et al., 2009). From Figure 4.9C, although Tat does increase expression of the wild type construct, it has similar though not as strong effects on the mutant reporter as well. This fits in with the role of Tat as a general translation enhancer and is akin to the effects seen with the over expression of some of the APOBEC3 proteins. Moreover, this result supports a recent study where Tat was shown to have no role in inhibiting the actions of both exogenous and endogenously expressed miRNAs (Sanghvi and Steel, 2011).

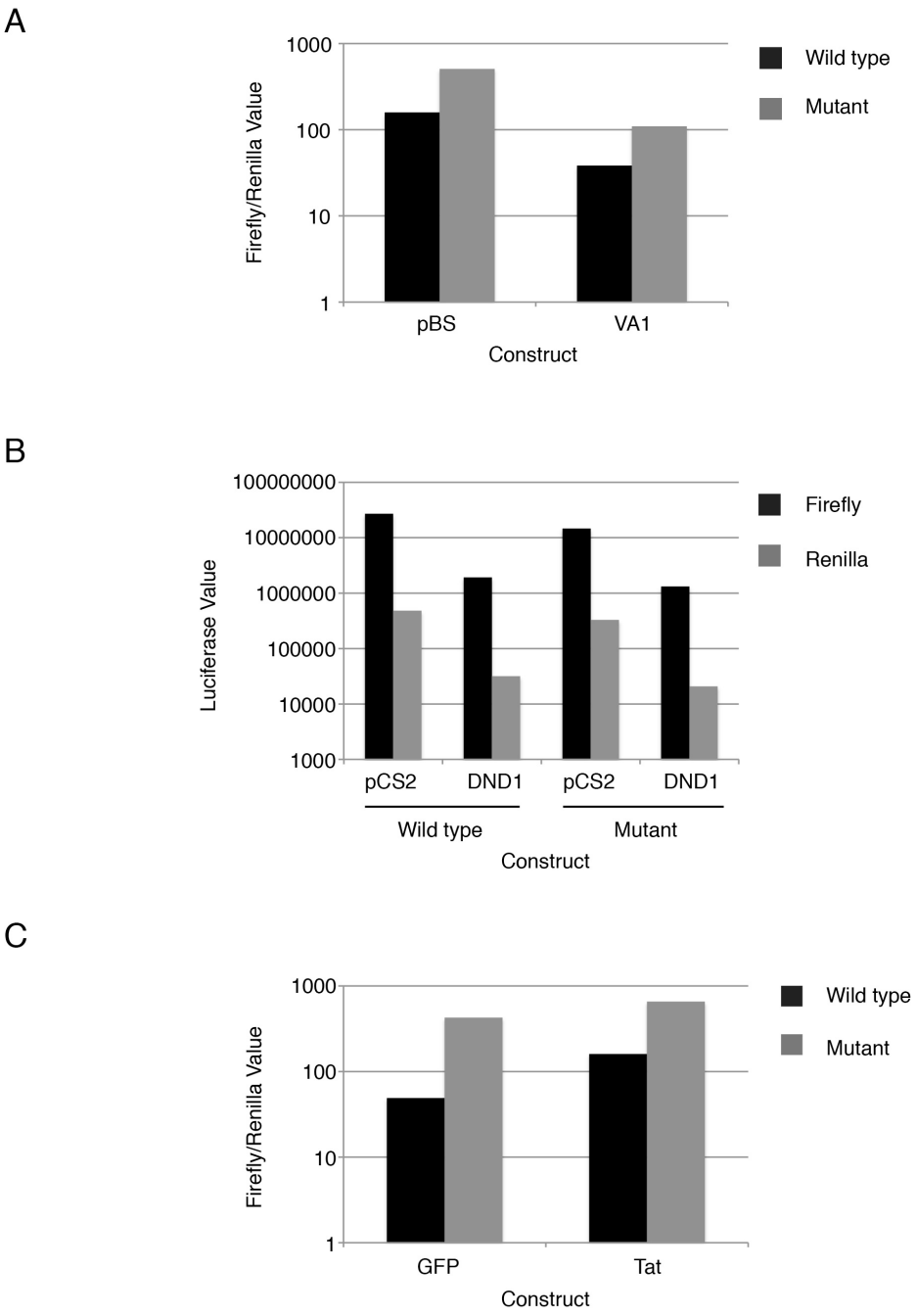

Figure 4.9: Analysis of proposed inhibitors of miRNA mediated translational repression.

A. HeLa cells seeded in 24 well plates, were transfected with 0.1 µg of wild-type or mutant let-7 luciferase reporter plasmids (as described in Figure 4.6), 0.9 µg of a VA1 expression plasmid or empty vector (pBS) as a negative control and 0.01 µg of a *Renilla* luciferase expression plasmid as a transfection control. 30 hours later, cells were harvested, lysed and a Dual Luciferase Assay performed to measure luciferase activity. Data is presented as the ratio of firefly to *Renilla* values, with *Renilla* levels equivalent across samples. **B**. As in A, except that 0.9 µg of a DND1 expression plasmid (or the pCS2 empty vector as a negative control) were co-transfected with the luciferase reporter constructs. Data is presented as the raw firefly and *Renilla* values. **C**. As in A and B except that 0.9 µg of Tat expressed in the pCDNA3.1 expression plasmid (or GFP as a negative control) was co-transfected with the luciferase reporter constructs. Data is presented as the ratio of firefly to *Renilla* values, with *Renilla* levels equivalent across all samples. In all cases, data is representative of at least two independent experiments.

4.6.3 siRNA mediated silencing

Although VA1 had no discernable effects on the miRNA constructs used within this study, its ability to interfere with miRNA biogenesis has been demonstrated and validated in a different reporter system (Lu and Cullen, 2004). This consists of firefly luciferase coupled to eight binding sites for the mir30p miRNA (Figure 4.10A). The expression of mir30p, when transfected into cells, is as a pri-miRNA precursor and it is therefore processed like a miRNA (discussed in Chapter 1, section 1.11.1). However, it is perfectly complimentary to the binding sites contained within the luciferase reporter and therefore, repression is achieved via Ago2 endonucleolytic cleavage. Because of this, the APOBEC3 proteins were analysed for their effects on this second RNAi reporter system, which would evaluate their roles in miRNA biogenesis and siRNA mediated silencing. Plasmids encoding the firefly luciferase reporter, the mir30p miRNA and either VA1 or HA-tagged APOBEC3 proteins were transfected into HeLa cells with *Renilla* luciferase also included as an internal transfection control. 48 hours later cells were harvested and a Dual Luciferase Assay was performed as previously described.

As shown and previously reported (Lu and Cullen, 2004), co-expression of the miRNA and the reporter construct leads to a substantial reduction in luciferase expression (Figure 4.10B) of approximately 6 - 10 fold (pBS and GFP samples). Addition of VA1, however, restores luciferase expression to the same level as seen in the absence of the miRNA thereby confirming that VA1 acts as a derepressor of miRNA activity. Although some of the APOBEC3 proteins, namely A3A, A3B, A3C and A3D/E did cause a modest increase in luciferase expression in the presence of the miRNA this was much smaller in comparison to the effects seen with VA1. A similar increase was seen in the absence of the miRNA (black bars) for A3A, A3B and A3C and is an effect that has also been noted and reported for VA1 (Lu and Cullen, 2004). A3F actually caused a decrease in expression, even when no miRNA was present and A3G appeared to have no effect on these reporter constructs at all. This indicates that the APOBEC3 proteins do not affect miRNA biogenesis, as has been demonstrated for VA1. It also supports the work presented earlier that the APOBEC3 proteins do not interfere with miRNA and/or siRNA mediated mRNA silencing, which is in contrast to the findings of Huang *et al* (2007).

A

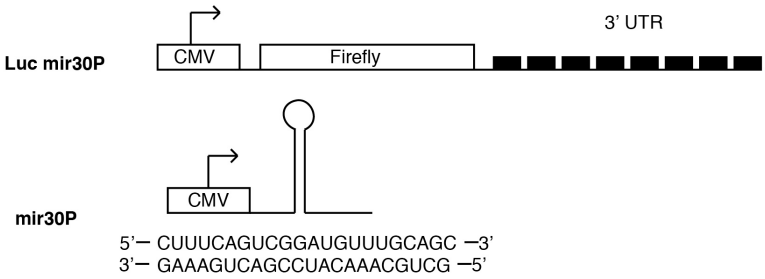

B

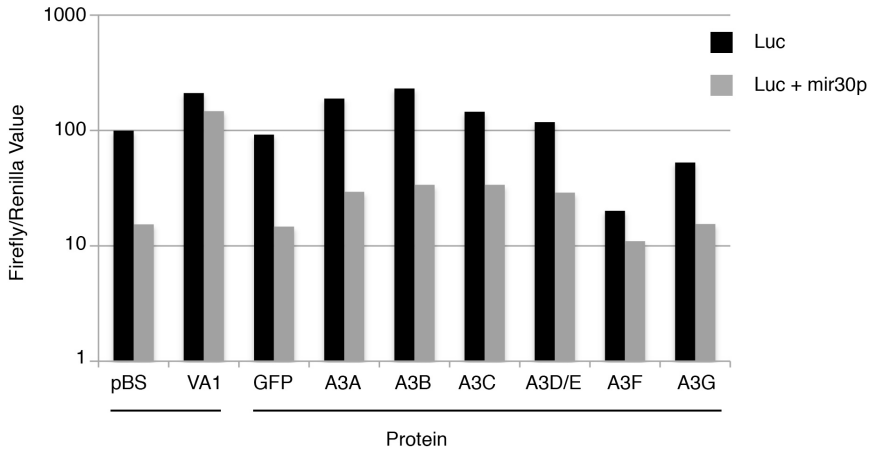

Figure 4.10: APOBEC3 proteins do not inhibit siRNA mediated silencing or affect miRNA biogenesis.

A. Schematic diagram of the siRNA luciferase reporter and miRNA construct used in this study. The firefly luciferase reporter (top) construct contains 8 perfectly complementary binding sites for the mir30p miRNA (bottom) in its 3'UTR. The sequence of the mir30p miRNA is provided. **B**. HeLa cells seeded in 24 well plates were co-transfected with the luciferase reporter and HA-tagged APOBEC3 expression plasmids in the presence (grey bars) and absence (black bars) of the mir30p miRNA. GFP is included as a negative control. VA1 expressed in the pBS expression plasmid is included as a positive control with the empty vector (pBS) included as the negative control. In all cases, a *Renilla* luciferase expression plasmid was also included as a transfection control. 48 hours later, cell lysates were harvested, lysed and a Dual Luciferase Assay performed to measure luciferase activity. Results are presented as the ratio of firefly to *Renilla* values, with *Renilla* levels equivalent across all samples, and is representative of two independent experiments.

4.6.4 ARE mediated decay (AMD)

Another means of RNA regulation is through AU-rich element (ARE) mediated decay (Chapter 1, section 1.11.6). Certain mRNAs contain AU rich sequences within their 3'UTR which are recognised and bound by particular cellular proteins. These ARE binding proteins will then contribute to either the degradation or stability of these mRNAs via mechanisms that are not completely understood. The mouse APOBEC1 protein, has been identified as one such ARE binding protein as it binds and stabilises several ARE containing mRNAs (Chapter 1, section 1.8.1). Further, the Argonauate proteins and miRNAs have also been implicated in ARE regulation (Jing et al., 2005; Vasudevan and Steitz, 2007a; Vasudevan et al., 2007b). Thus it is conceivable that the APOBEC3 proteins may also be involved in this process.

To investigate this, reporter constructs were utilised which consisted of firefly luciferase coupled to either the full length 3'UTR (UTR) or just the ARE binding sites (ARE) of TNFα, a well known AU rich RNA that is subject to ARE mediated decay. An empty vector (CTRL) and a construct harbouring mutated ARE binding sites (ARE mt) were used as the respective controls (Figure 4.11A) (Vasudevan and Steitz, 2007a). HA-tagged APOBEC3 plasmids were co-transfected with the various constructs and *Renilla* luciferase was also included to account for differences in transfection efficiencies. Results in Figure 4.11B are presented as the ratio of firefly to *Renilla* luciferase values as no difference in *Renilla* levels were observed across all samples. Co-transfection of GFP results in a four fold reduction in expression of the ARE containing constructs compared to their controls (first four bars) as would be expected based on previous reports (Vasudevan and Steitz, 2007a). Addition of A3A, A3F or A3G does not alter this (white and dark grey bars), though with A3G and more dramatically A3A, expression of all the constructs is increased. Thus it can be concluded that the APOBEC3 proteins are not involved in the regulation of ARE containing mRNAs but once again appear to have more general effects on protein expression levels.

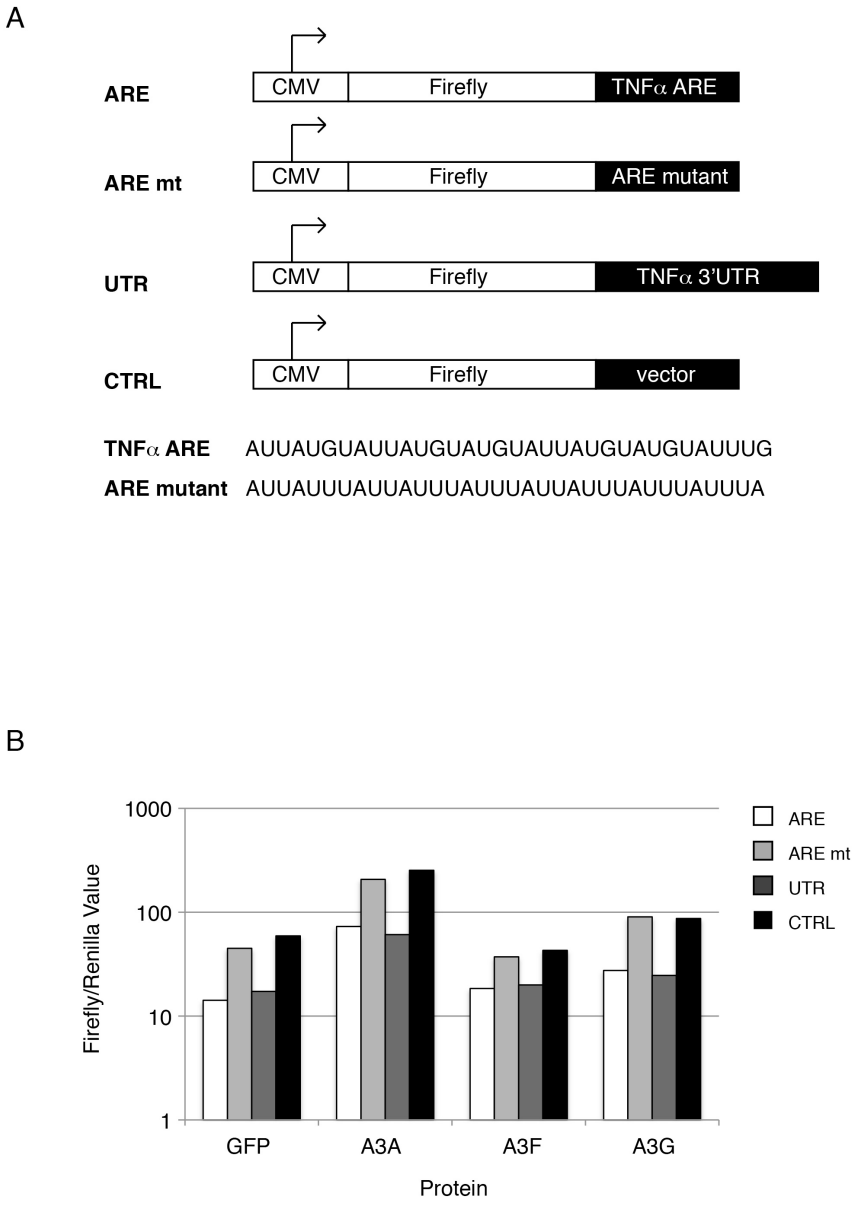

Figure 4.11: APOBEC3 proteins do not inhibit ARE mediated decay of TNFα.

A. Schematic diagram of the ARE reporter constructs used in this study. Firefly luciferase reporter plasmids contain either the full length 3'UTR of TNFα (UTR) or just the ARE binding sites (ARE). An empty vector (CTRL) and a construct containing mutated binding sites (AREmt) serve as the respective controls. The sequences of the wild type and mutated TNFα ARE are also depicted. **B**. HeLa cells plated in 24 wells plates were co-transfected with a luciferase reporter construct and untagged A3A, A3F or A3G (or GFP as a negative control). A *Renilla* luciferase expression plasmid was also included as a transfection control. 30 hours later cells were harvested, lysed and a Dual Luciferase Assay performed to measure luciferase activity. Data is presented as the ratio of firefly to *Renilla* luciferase values, with *Renilla* levels equivalent for all samples, and is representative of 2 independent experiments.

4.6.5 ARE binding proteins (ARE-BP)

Numerous ARE binding proteins have now been identified that are able to modulate the expression of ARE containing transcripts. Several of these proteins were tested against the reporter constructs described above in order to establish a positive control for this system. Firstly, and as previously mentioned, mouse and rat APOBEC1 have both been shown to stabilise expression of the c-myc mRNA among others, through binding to AU rich sequences in the 3'UTR (Anant and Davidson, 2000; Anant et al., 2004). Secondly, HuR has been reported to bind to ARE-containing mRNAs in the nucleus and protect them from degradation upon translocation to the cytoplasm (Fan and Steitz, 1998). Finally, exogenous expression of FXR1 induces translational activation of the TNFα mRNA (Vasudevan and Steitz, 2007a). However, none of these effects proved to be reproducible in this system (Figure 4.12), as all of the proteins tested were unable to counteract repression of the ARE containing reporters. The underlying basis for these discrepancies will require further investigation.

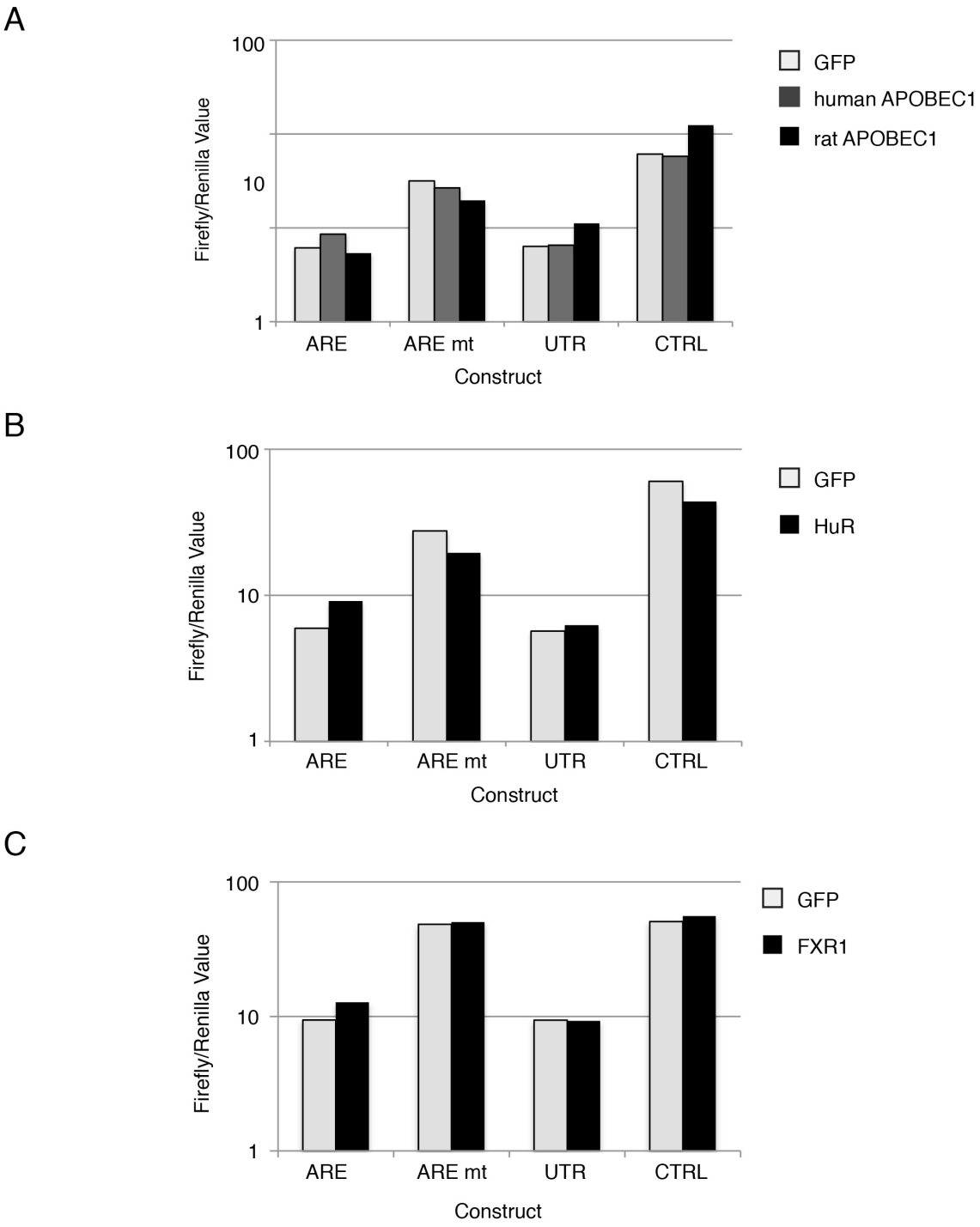

Figure 4.12: Effects of ARE binding proteins on the TNFα ARE.

A. HeLa cells plated in 24 wells plates were co-transfected with luciferase reporter constructs (as described in section 4.11) and human and rat APOBEC1 in the pCDNA3.1 expression vector, with *Renilla* luciferase included as a positive control. 30 hours later cells were harvested, lysed and a Dual Luciferase Assay performed to measure luciferase activity. **B**. As in A except in this case a HuR expression plasmid was co-transfected with the luciferase reporter constructs. **C**. As in A and B, except in this case an FXR1 expression plasmid was co-transfected with the luciferase reporter constructs. In all cases, data is presented as the ratio of firefly to *Renilla* values, with *Renilla* levels equivalent across all samples, and is representative of at least 2 independent experiments.

4.7 Discussion

The work presented in this chapter aimed to identify functional consequences for the interaction between the APOBEC3 and Argonaute proteins. It has been demonstrated that Ago2 is dispensable for APOBEC3 antiviral activity though the effects of the other Argonaute proteins and miRNA repression in general requires further exploration. Conversely the APOBEC3 proteins are not involved in the general regulation of mRNAs through miRNA, siRNA or ARE containing transcripts. Thus the implications of the APOBEC3-Argonaute interaction may be subtler than originally envisaged.

Cellular co-factors for both AID and APOBEC1 are essential for their activity (Chaudhuri et al., 2004; Mehta et al., 2000). Whether such factors exist and are necessary for the function of the APOBEC3 proteins is unknown at present. Conversely, interacting proteins may help regulate the activity of the APOBEC3 proteins, especially in light of their enzymatic capabilities. Whether or not Argonaute 2 fulfils either of these roles was investigated due to the close association of these proteins as observed through biochemical analysis (Chapter 3). Overexpression and knock down studies are now commonly used approaches to verify whether a gene of interest is necessary and/or sufficient for a particular biological process. These methods were used in an attempt to ascertain the importance of Ago2 for APOBEC3 mediated HIV-1 inhibition, and as a consequence, for HIV-1 replication in general (Figures 4.1 and 4.4). Nathans *et al* (2009) have reported that siRNA mediated knockdown of Ago2 leads to a 2 - 3 fold increase in virus production and a subsequent 2 fold increase in virus infectivity (when viruses are normalised), which coincides with a loss of P-bodies as marked by ectopic expression of an A3G-YFP fusion protein. On all accounts, the results presented here do not support these findings. Even with a highly efficient depletion of Ago2 at the protein level, DDX6 labelled P-bodies were still present in both HeLa and 293T cells. This discrepancy may be due to the different P-body markers used (an exogenous A3G fusion protein compared to endogenous Ge1), but the differences in effects in HIV-1 replication upon Ago2 knockdown are harder to resolve and will be discussed in more detail in Chapter 5.

Importantly, functional knockdown of Ago2 was confirmed in 293T cells through a reduction in siRNA mediated silencing of the ALIX protein (Figure 4.3). This approach did not work in HeLa cells, probably due to the more efficient knock down of ALIX, which made recovery more difficult. It was subsequently shown that in these cells there

was no significant impairment of APOBEC3 antiviral activity (Figures 4.4 and 4.5), ruling out the necessity of Ago2 and more specifically its endonuclease function for this process. It has been speculated that the endonuclease activity of Ago2 may be utilised for the degradation of A3G edited reverse transcripts (thus accounting for the lack of accumulation of these products associated with A3G viral inhibition), similar to the proposed and later discounted role of cellular repair enzymes such as UNG2 (Harris et al., 2003b). The data presented in this chapter fails to substantiate this hypothesis. It must be emphasised however that although the knockdown of Ago2 at the protein level was fairly substantial, the functional knockdown was only partial (Figure 4.3), which renders the possibility that a more stringent knockdown may be required to determine functional effects. A similar problem was documented with the nuclear protein LEDGF/p75 (Llano et al., 2006). Even though it appeared to be efficiently depleted at the protein level, a more rigorous knock down strategy had to be employed to conclusively identify its essential role in HIV-1 proviral integration. However, since silencing of Ago2, like all targeted mRNAs, is dependent upon the presence and endonuclease activity of Ago2, complete functional depletion cannot be achieved. This may not necessarily be a problem though as several groups have used siRNAs to target Ago2 with noticeable phenotypic effects (Lian et al., 2007; Meister et al., 2005; Randall et al., 2007; Schmitter et al., 2006; Wilson et al., 2011). This suggests that this is in fact a valid means of elucidating the functional requirements of Ago2 for a given process or pathway.

As mentioned earlier, a major detriment to these studies is the problem of functional redundancy between the Argonaute proteins. Consequently the importance of the miRNA pathway to APOBEC3 mediated HIV-1 inhibition has not been fully addressed. Cellular miRNAs have been reported to target viral RNA and they may also modulate proteins that are required for HIV-1 to complete its life cycle [reviewed in (Houzet and Jeang, 2011)]. Alternatively virally encoded miRNAs may facilitate viral replication. Thus whether the APOBEC3 proteins depend on this pathway for possible editing independent means of viral inhibition is an important point to resolve. The simultaneous knock down of all four Argonaute proteins is possible but challenging, as the efficiency of the knockdown for all the proteins, potential toxicity and cell viability would have to be optimised. Very recently, the combined depletion of all four Argonaute proteins has been published (Roberts et al., 2011), but the individual knockdown efficiencies of each

protein at the mRNA or protein level was not reported. As an alternative approach, overexpression of the mlin41 protein was trialled in an attempt to deplete the whole Argonaute family but this yielded an insufficient knockdown of Ago2 (Figure 4.7). Therefore, to comprehensively explore whether the miRNA pathway is involved in APOBEC3 antiviral activity, it may be more amenable to knock down other essential components, such as Dicer or GW182, both of which have been successfully knocked down by a number of different groups (Chable-Bessia et al., 2009; Jakymiw et al., 2005; Lian et al., 2007; Meister et al., 2005; Nathans et al., 2009; Roberts et al., 2011; Schmitter et al., 2006; Triboulet et al., 2007). Even though three orthologues of GW182 exist in mammals and all can mediate translational repression, knockdown of any one protein markedly affects miRNA mediated repression (Zipprich et al., 2009), demonstrating a lack of functional overlap. This may be due to their recruitment of and interaction with distinct complexes of Argonaute proteins (Baillat and Shiekhattar, 2009). In essence it has been established that Ago2 and siRNA mediated silencing are not required for APOBEC3 inhibition of HIV-1. Whether the miRNA pathway is important will require alternative means of investigation that may not necessarily include the Argonaute proteins.

The APOBEC3-Argonaute interaction may not have direct consequences on APOBEC3 anti-viral activity but may be more important for other functions of this protein family. Although the APOBEC3 proteins target single stranded DNA they are RNA binding proteins and associate with a variety of proteins involved in RNA metabolism and turnover. Therefore it is possible that they may also have a role to play in RNA regulation, especially as a cellular function for these proteins has not yet been identified. Whether the APOBEC3 proteins are able to regulate the miRNA pathway, for example, would also help address how important this process may be to its anti-viral phenotype. On this note, it has been reported that the APOBEC3 proteins act as inhibitors of miRNA mediated translational repression (Huang et al., 2007a) and thus are antagonists of Argonaute protein function. The data presented here fail to support these findings as the APOBEC3 proteins affected protein expression regardless of miRNA or siRNA inhibition in two separate reporter systems (Figures 4.8 and 4.10). The relevance of these general effects on protein levels, particularly for A3C, which had the most dramatic phenotype, is currently unknown. In order to decipher the mechanism behind this, it must first be established whether these changes are occurring at the protein or

RNA level. The specificity of this effect as well as its biological relevance must also be investigated. The fact that viral protein production ($p24^{Gag}$) was not upregulated upon overexpression of the APOBEC3 proteins (see Figures 4.4 and 4.5) reinforces the notion that there may be some specificity involved and also that this is not just an overexpression artefact. As the APOBEC3 proteins appear to have differing effects and because this phenotype does not correlate with their anti-viral status makes it especially intriguing and may help identify novel functions for some of the less well studied APOBEC3 proteins.

The reasons why the work of Huang *et al* could not be replicated in this study are unclear but a large part of this is most likely due to differences in experimental methods. Also, results from these types of experiments are typically presented as the ratio of firefly to *Renilla* levels but this makes it difficult to evaluate exactly where changes are taking place and thus compare results from different groups. Since the APOBEC3 proteins caused substantial changes in *Renilla* levels as well as the control construct this information may be lost if the values are normalised and may lead to inaccurate conclusions being drawn. Because of this, the raw luciferase values from all constructs were presented from the experiments in this study but are therefore not directly comparable with the data presented by Huang and colleagues. On the other hand, although the authors reported that the APOBEC3 proteins could hinder the action of the let-7 miRNA, it may not necessarily be their natural target. The identification of APOBEC3 associated RNAs, both miRNA and mRNA may help elucidate more specific and biologically relevant targets of these proteins. Identification of APOBEC3 associated RNAs has already been initiated (Kozak et al., 2006), and these RNAs may also contribute to the functional regulation of these proteins, as has already been determined for APOBEC1 and AID (Bransteitter et al., 2003; Sowden et al., 1996). Thus although the APOBEC3 proteins had no effect in the reporter systems tested here, a potential role for them in RNAi cannot yet be conclusively ruled out.

Finally, the APOBEC3 proteins were also tested for their involvement in ARE mediated repression (Figure 4.11), in light of what has been reported for both mouse and rat APOBEC1, which can stabilise the expression of several ARE containing mRNAs, including c-myc and Cox-2, that would otherwise be rapidly degraded (Anant and Davidson, 2000; Anant et al., 2004). Once again, they were not found to modulate this process with the caveat that proteins that have been shown to influence ARE mediated

repression also did not produce any positive results (Figure 4.12). As before, this could be explained, in part, by the fact that APOBEC1 and potentially the other APOBEC3 proteins do not naturally target the TNFα transcript. To address this numerous ARE containing mRNAs would have to be tested. However HuR and FXR1 have both been reported to affect the stability of TNFα mRNAs and so the lack of an effect observed in this system is somewhat unexpected. However, in the case of HuR, only effects at the level of the RNA were reported (Fan and Steitz, 1998), so it is not clear how these changes would be manifested at the protein level, as was measured here. Further the destabilisation of the luciferase reporter containing the TNFα ARE binding sites, which leads to its reduced expression, may be the result of degradation of the transcript rather than repression. In that case, its expression may not be able to be rescued, regardless as to the effects of the co-expressed protein. Therefore whether in fact this is repression or decay needs to be firmly established and perhaps a more flexible reporter system needs to be utilised, which would be able to address these effects. So, although the APOBEC3 proteins did not appear to modulate AMD of the TNFα ARE, a more thorough investigation of their role in this process is required in order to draw any firm conclusions.

In sum, APOBEC3 mediated HIV-1 inhibition is not dependent on the presence of Ago2. Whether this interaction is essential for the restriction of other viruses and viral elements is worth investigating, as is the importance of other cellular factors that could potentially affect APOBEC3 function. Although the APOBEC3 proteins did not appear to have an inhibitory role in either miRNA mediated repression or siRNA mediated silencing a detailed analysis of the RNA composition of their cellular complexes would provide a more focused approach in identifying their involvement in RNA regulatory processes. The work presented in this chapter serves to illustrate that individual proteins may not make substantial contributions to APOBEC3 activity, whereas certain cellular pathways, processes or complexes may be more relevant. Therefore, one such ribonucleoprotein complex will be investigated in more detail in the following chapter.

CHAPTER 5

Role of P-bodies in APOBEC3 anti-viral activity and HIV-1 replication

5. RESULTS

Role of P-bodies in APOBEC3 anti-viral activity and HIV-1 replication

5.1 Introduction

As discussed in Chapter 1, section 1.10.1, mRNA Processing Bodies (P-bodies) are non-membraned cytoplasmic foci that are sites for the storage and/or degradation of untranslated mRNA. They are characterised by the presence of proteins involved in mRNA turnover such as the decapping enzymes Dcp1a and Dcp2, the decapping activators, DDX6 and Lsm1 and the 5' – 3' exoribonuclease Xrn1 among others [for a comprehensive list see (Kulkarni et al., 2010) and (Eulalio et al., 2007a)]. Consequently, they are the endpoints for various mRNA regulatory pathways including NMD, AMD and RNAi. More recently, the role of P-bodies in viral life cycles, particularly RNA viruses and retroviruses, has been under intense scrutiny as they represent convenient cytoplasmic compartments within which these viruses can segregate translation and replication or packaging of their genetic material. However, the role of P-bodies in viral replication is complex, as they have also been shown to be inhibitory for virus production and infectivity, most notably for HIV-1 (Chable-Bessia et al., 2009; Nathans et al., 2009). In Chapter 3 it was demonstrated that several APOBEC3 proteins localised to P-bodies and this correlated with their anti-viral phenotypes. However, the functional significance of this has yet to be explored. If indeed P-bodies are sites of viral assembly, it is tempting to speculate that this is also where APOBEC3 proteins are packaged into HIV-1 virions. In yeast, P-bodies are necessary for efficient retrotransposition of the Ty1 and Ty3 retroelements and have been proposed to be sites of virus like particle (VLP) assembly (Beliakova-Bethell et al., 2006; Dutko et al., 2010). A3G co-localisation to P-bodies with the Gag protein and genomic RNA of the Ty1 retroelement appears to be important for its inhibition of this retrotransposon, most probably because it is within these foci that A3G is incorporated into Ty1 VLPs (Dutko et al., 2010; Dutko et al., 2005; Esnault et al., 2005). Therefore the conservation of A3G localisation to P-bodies and retroelement restriction, from yeast to humans, implies that these phenotypes may be functionally linked. In a bid to address these issues, therefore, the

importance of P-bodies for APOBEC3 anti-HIV-1 activity and HIV-1 replication in general was examined in more detail.

5.2 A3G packaging defective mutants and localisation to P-bodies

5.2.1 Expression of A3G mutants

In order to establish a more definitive link between virion incorporation and P-body localisation, A3G packaging defective mutants were assessed for their ability to localise to these foci (Figure 5.1A). These N-terminal point mutants show reduced anti-viral activity due to inefficient virion incorporation as compared to wild type A3G (Huthoff et al., 2009; Huthoff and Malim, 2007). However, whether the subcellular localisation of these proteins, specifically localisation to P-bodies, is also altered has not yet been investigated but has been speculated to contribute to their packaging defect (Huthoff and Malim, 2007). The expression levels of the mutant proteins compared to wild type A3G was first established. 2 μg of each mutant A3G plasmid and between 2 - 0.125 μg of wild-type A3G plasmid, in HA-tagged pCMV4 expression vectors, were transfected into HeLa cells. 24 hours later, cells were harvested, lysed and subjected to immunoblotting. Figure 5.1B displays the immunoblots along with quantification of band intensities by Licor-Odyssey software. As can be seen, the R24A, R30A, Y124A and W127A mutants were roughly 2 fold less well expressed than wild type A3G at the same concentration of DNA (compare lane 1 with lanes 6 - 9). The double mutants, R24+R136A and R30+R136A (lanes 10 and 11) showed slightly poorer expression than the single mutants but not dramatically so. These data are in keeping with the original reports describing these mutants (Huthoff et al., 2009; Huthoff and Malim, 2007). Thus even though the mutant proteins are not as efficiently expressed as their wild type counterpart, the level of expression is still reasonable enough with which to conduct further experiments.

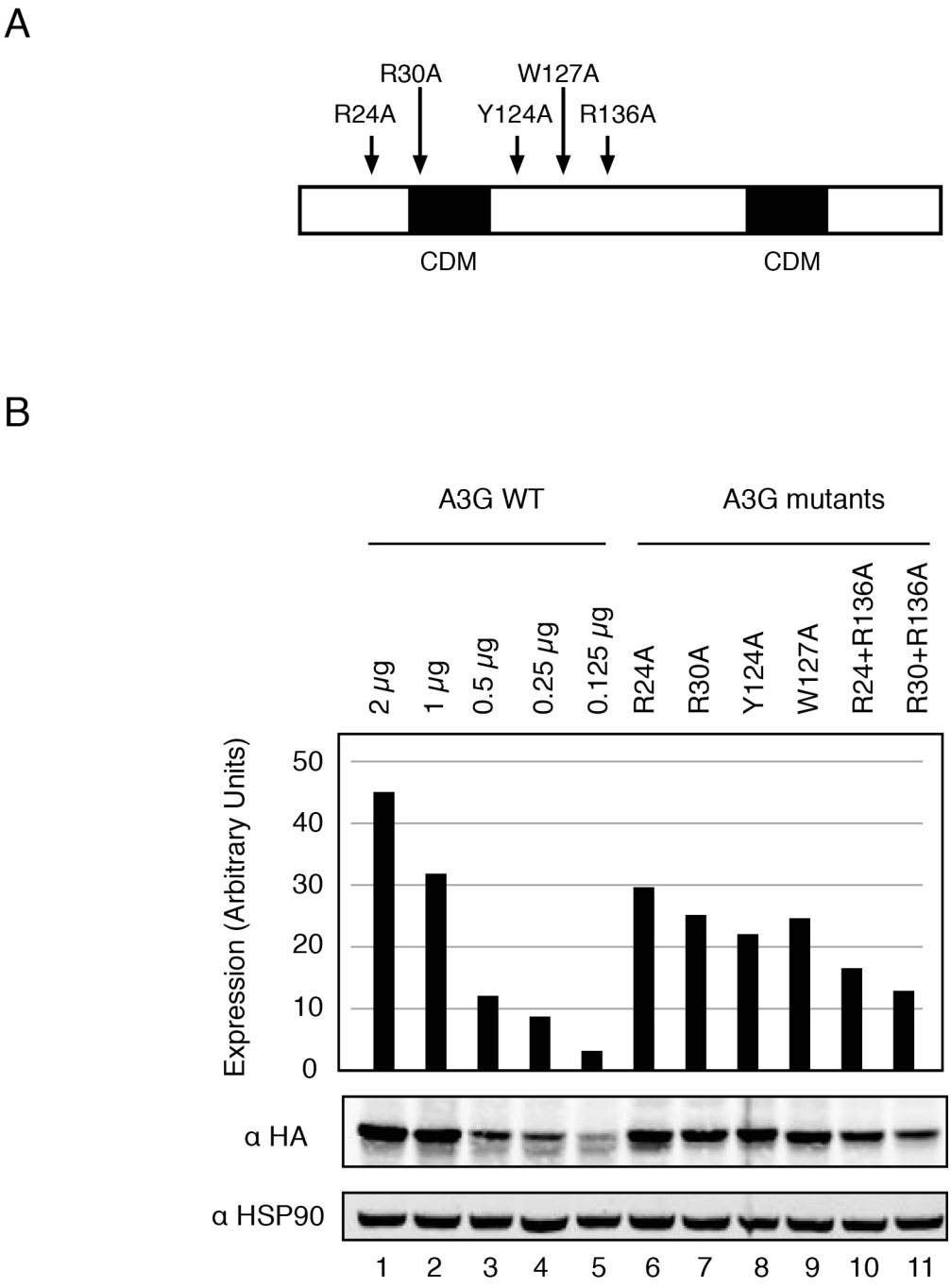

Figure 5.1: Expression of A3G packaging defective mutants.

A. Schematic diagram of the A3G protein with positions of the mutations indicated. CDM = cytidine deaminase motif. **B.** HeLa cells seeded in 12 well plates were transfected with 2 µg of plasmids encoding HA-tagged A3G single mutants, R24A, R30A, Y124A and W127A and the double mutants R24A+R136A and R30A+R136A or a titration of HA-tagged wild type A3G (A3G WT) expression plasmid at 0.125 µg, 0.25 µg, 0.5 µg, 1 µg and 2 µg. 30 hours later cells were harvested and lysed in gel loading buffer and analysed by immunoblotting with anti-HA and anti-HSP90 (as a loading control) antibodies. Protein bands were quantified using Licor-Odyssey software. Data is representative of 2 independent experiments.

5.2.2 Localisation of A3G mutants at P-bodies

In order to verify whether the mutant proteins could still co-localise with Ago2 and hence P-bodies, HeLa cells plated on coverslips were co-transfected with either 1 μg of each mutant plasmid (except for the R30A mutant, which was not included in this analysis) or wild-type A3G at the indicated amounts and 0.2 μg of myc-tagged Ago2. 24 hours later, cells were fixed, permeablised and stained with anti-HA and anti-myc primary antibodies and appropriate secondary antibodies. Coverslips were then mounted, dried and imaged using a Leica confocal microscope.

Even at the lowest amount of input DNA for wild type A3G (Figure 5.2, panel 4) localisation with Ago2 marked bodies is still clearly evident. All of the mutants displayed some degree of co-localisation with Ago2 and in all cases foci are clearly visible though not as bright as for wild type A3G, even at similar expression levels (compare panel 2 with panels 5 - 7). Thus it can be concluded that the inability of these mutant proteins to be packaged into virions does not correlate with loss of association with P-bodies. Although the mutants showed reduced efficiency of localisation to Ago2 foci compared to wild type A3G, this could potentially be a result of their impaired cellular RNA binding capabilities, which does not affect their ability to assemble into RNP complexes (Huthoff et al., 2009). These results have failed to support the correlation observed in Chapter 3, section 3.4, of a link between P-body localisation and virion incorporation of A3G.

Figure 5.2: A3G packaging defective mutants can still localise to P-bodies.

HeLa cells seeded on to coverslips in 12 well plates were co-transfected with 1 μg of the HA-tagged A3G mutants or a titration of HA-tagged wild type A3G (WT) at 0.125 μg, 0.25 μg, 0.5 μg and 1 μg with 0.2 μg of a myc-tagged Ago2 expression plasmid. 30 hours later cells were fixed in 4% formaldehyde and permeabilised. Cells were then stained with rabbit anti-HA and mouse anti-myc primary antibodies and then anti-rabbit 488 and anti-mouse 594 secondary antibodies, plus DAPI for visualisation of the nucleus. Coverslips were mounted onto slides and dried overnight before imaging on a Leica confocal microscope. Merged images are displayed on the right. Data is representative of 2 independent experiments. Scale bar = 10 μm.

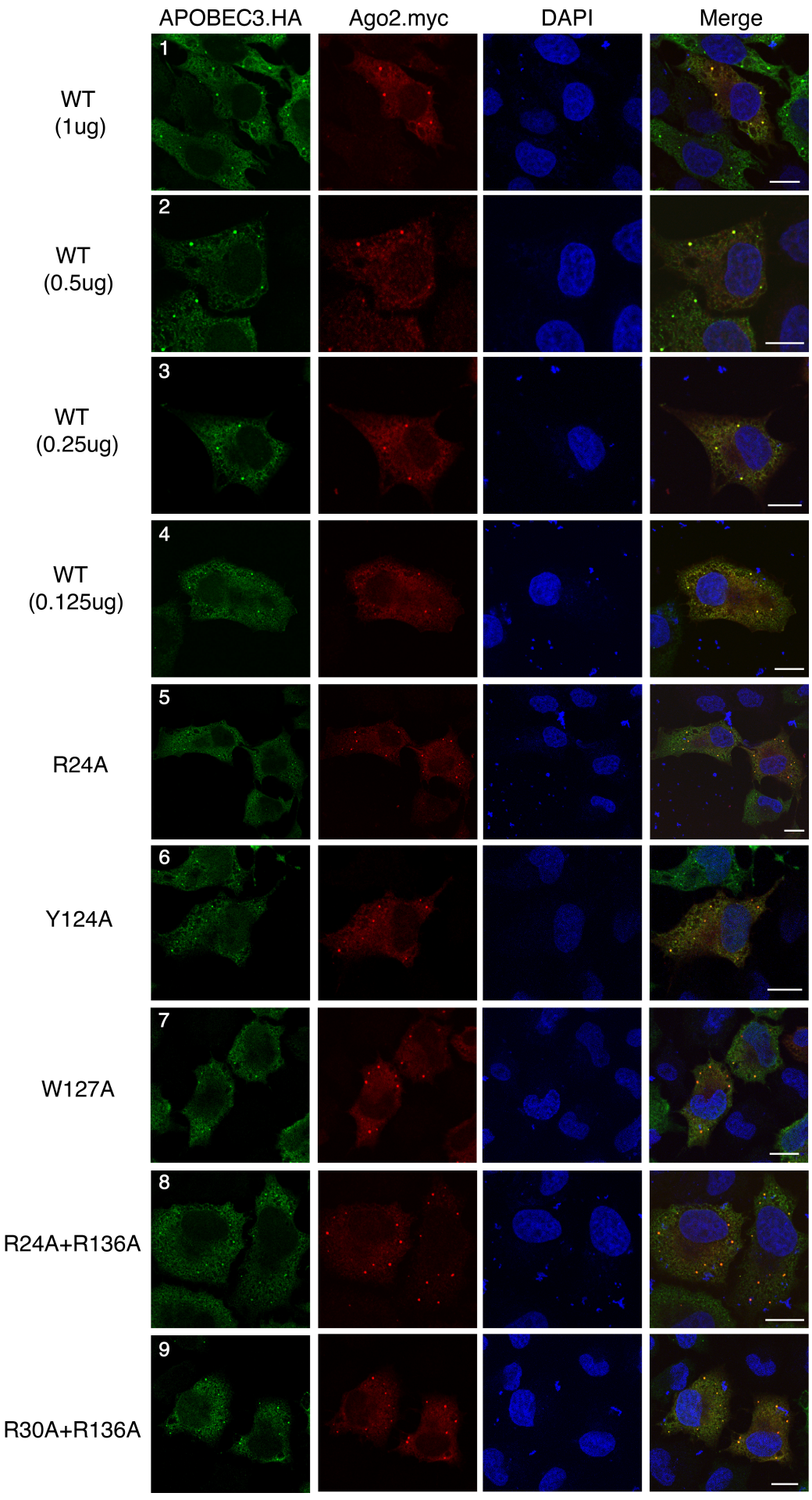
APOBEC3.HA
Ago2.myc
DAPI
Merge
1
WT
(1ug)
2
WT
(0.5ug)
3
WT
(0.25ug)
4
WT
(0.125ug)
5
R24A
6
Y124A
7
W127A
8
R24A+R136A
9
R30A+R136A

5.3 DDX6 mutant proteins and HIV-1 infectivity

5.3.1 Phenotypic analysis of DDX6 mutants

A more direct way of investigating the importance of P-bodies for HIV-1 infectivity and possibly assembly is through targeted disruption of these foci. DDX6 is a member of the DEAD box family of helicases and is known to be a general translational repressor (Coller and Parker, 2005). It regulates RNA through its roles in decapping and miRNA mediated translational repression (Chu and Rana, 2006). It is also essential for P-body formation as depletion of DDX6, unlike other proteins, prevents the re-establishment of P-bodies in arsenite treated and hence translationally inhibited cells (Serman et al., 2007). Therefore overexpression of DDX6 dominant negative proteins was employed as a first attempt at depleting P-bodies from cells as these should interfere with endogenous DDX6 function and thus inhibit P-body formation. Several such dominant negative proteins have been described in the literature and three of these were generated for use in this study. Site directed mutagenesis by overlapping PCR was used to introduce the desired mutations into the wild-type protein sequence (Figure 5.3A). Mutants A (R89A + K91A) and B (G346A) are based on studies in yeast where these mutations caused defects in RNA binding due to conformational changes between the two domains of the protein (Cheng et al., 2005). Mutant C (R423Q/HRIGQ) has been proposed to abrogate RNA binding, ATP binding and helicase activity and importantly the authors demonstrate a 98% reduction in the number of cells with P-bodies upon expression of this dominant negative protein (Minshall et al., 2009). Confirmation that these mutant proteins did in fact disrupt P-body formation was obtained by immunofluorescence analysis. HeLa cells, plated on coverslips, were transiently transfected with each DDX6 dominant negative protein, along with wild-type DDX6 for comparison, expressed in HA-tagged expression vectors. 24 hours later, cells were fixed, permeablised and stained with antibodies recognising the Ge1 P-body protein and the HA epitope tag. From Figure 5.3B, it can be seen that wild type DDX6 localises to P-bodies and co-localises with the Ge1 P-body protein. However, not only do the mutant proteins A and C no longer localise to P-bodies (panels 2 and 4), they also prevent P-body assembly as illustrated by the lack of Ge1 marked foci in transfected cells. This is most evident when comparing transfected and untransfected cells side by side as in panel 4. The mutations introduced into mutant protein B appear not to affect either P-body localisation or formation (panel 3). Therefore overexpression of certain DDX6

dominant negative mutants is one method of successfully disrupting endogenous P-body formation.

5.3.2 DDX6 dominant negative mutants and HIV-1 infectivity

Subsequently, DDX6 wild-type and dominant negative proteins were transiently transfected into 293T cells at both a 3:1 and a 1:3 ratio of plasmid DNA to an NL43 proviral plasmid. 48 hours later viral supernatants were harvested, quantified by $p24^{Gag}$ ELISA and used to challenge TZM-bl reporter cells. Cell lysates from the virus producer cells were prepared for immunoblot analysis. From Figure 5.4A, the dominant negative DDX6 proteins are expressed just as well and sometimes even better than the wild-type protein. $p24^{Gag}$ production from cells transfected with the mutant proteins was equivalent to that seen with overexpression of wild-type DDX6 (which induces P-body formation) and the negative control, GFP, at both concentrations of input DNA (Figure 5.4B). Importantly, infectivity of the virions produced in the presence of the dominant negative proteins was analogous to that produced with the controls (Figure 5.4C), implying that loss (with mutant DDX6 proteins) or overexpression (with wild-type DDX6 protein) of P-bodies does not substantially impact upon HIV-1 virus production and infectivity.

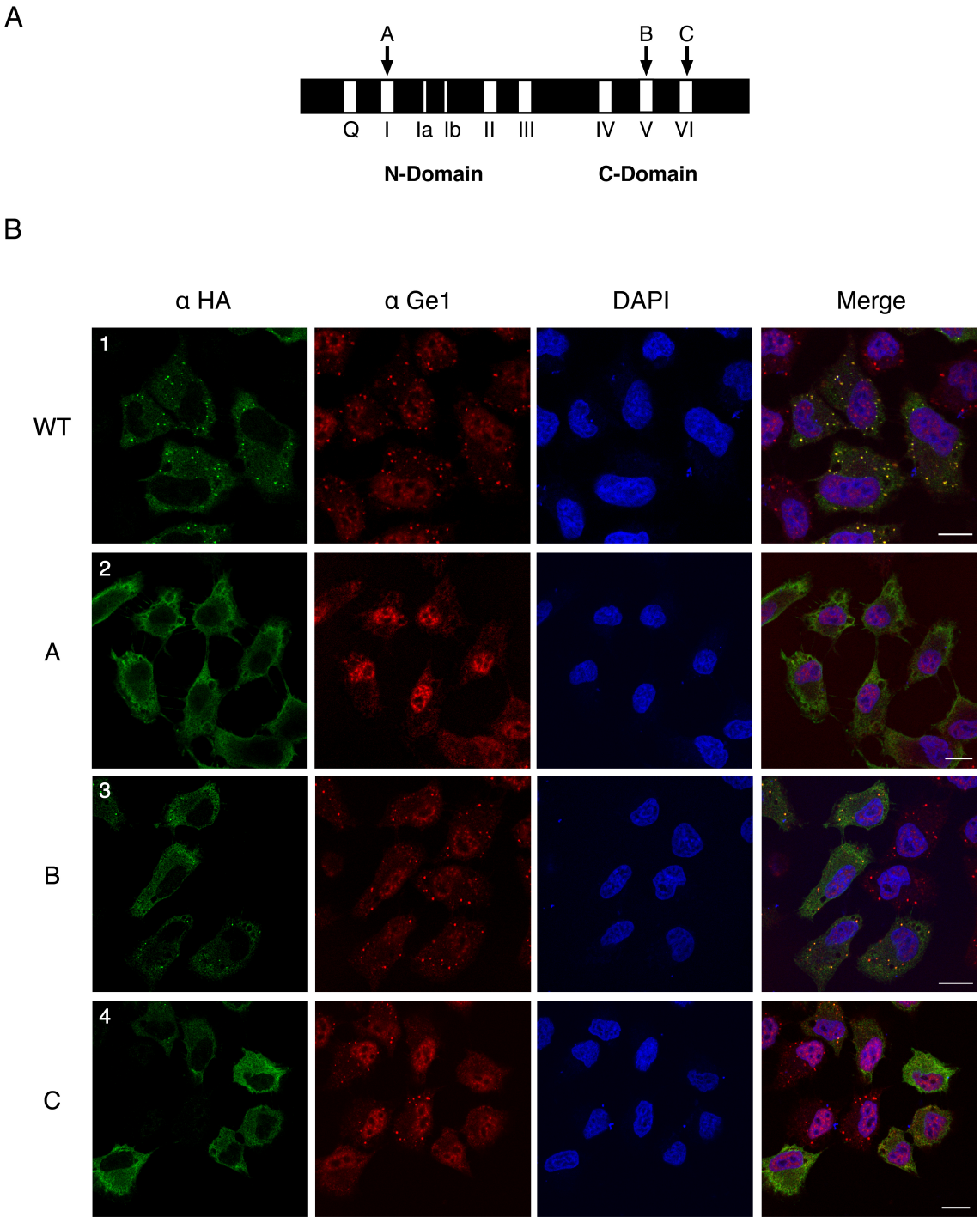

Figure 5.3: DDX6 mutant proteins disrupt P-body formation.

A. Schematic diagram of the DDX6 protein with domains and positions of mutations indicated. **B**. HeLa cells seeded onto coverslips in 12 well plates were transfected with 0.4 µg of HA-tagged DDX6 wild type or mutant (A = R89A+K91A, B = G346A, C = R423Q/HRIGQ) expression plasmids. 30 hours later cells were fixed in 4% formaldehyde and permeabilised. Cells were then stained with rabbit anti-HA and mouse anti-Ge1 primary antibodies and anti-rabbit 488 and anti-mouse 594 secondary antibodies, plus DAPI for visualisation of the nucleus. Coverslips were then mounted onto slides and dried overnight before imaging on a Lecia confocal microscope. Merged images are displayed on the right. Data is representative of 2 independent experiments. Scale bar = 10 µm.

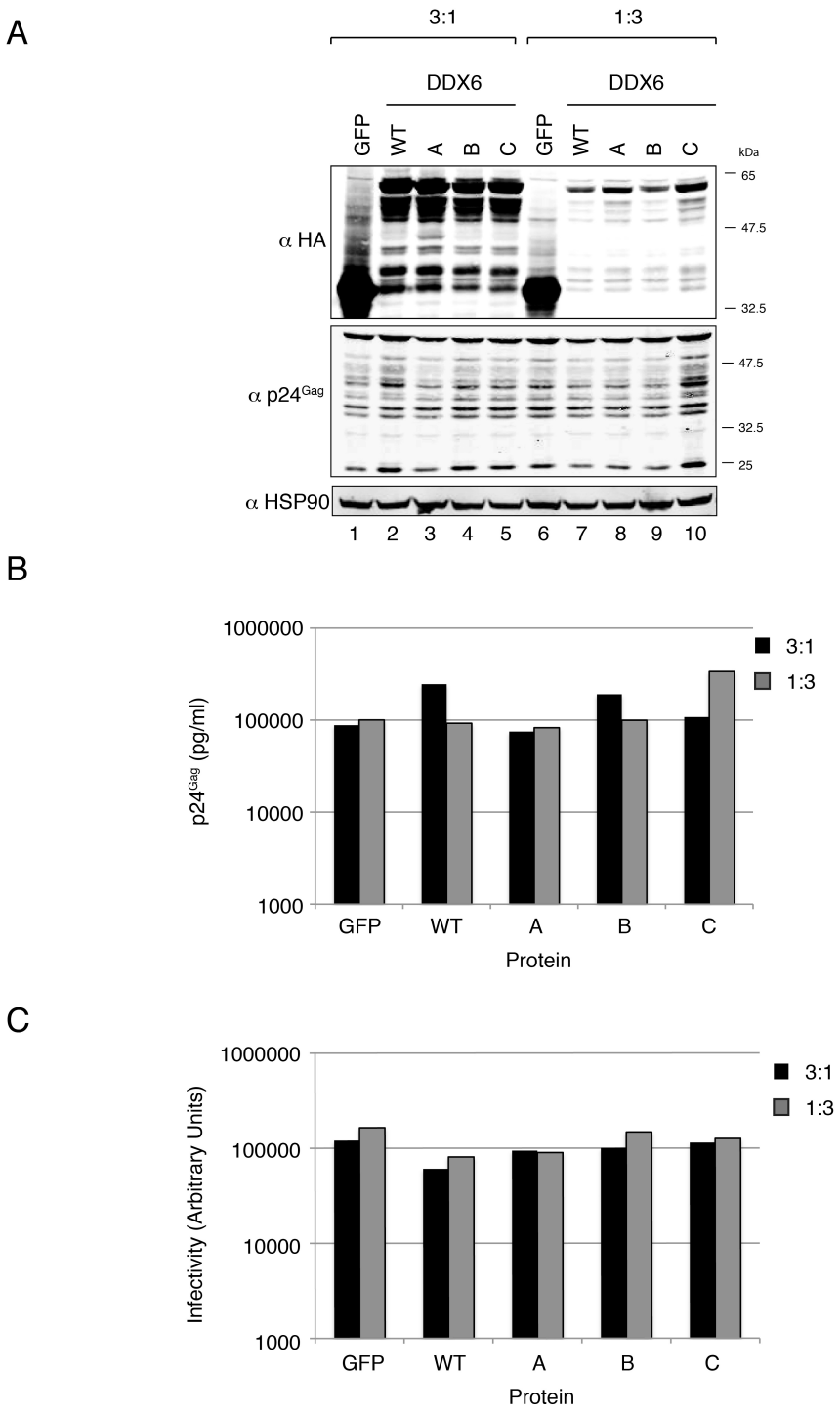

Figure 5.4: Overexpression of DDX6 mutant proteins does not affect HIV-1 infectivity

293T cells, seeded in 6 well plates were co-transfected with either 0.16 µg or 1.5 µg of HA-tagged DDX6 wild type or dominant negative expression plasmids and 0.5 µg of an NL43 Δ*vif* proviral plasmid giving a ratio of 1:3 or 3:1 of DDX6 protein to provirus. Total DNA was kept constant at 2 µg with the addition of an untagged Luciferase expression plasmid. 48 hours later, viral supernatants were harvested and quantified by $p24^{Gag}$ ELISA. Normalised amounts were then used to infect TZM-bl reporter cells which were harvested 30 hours post infection and assayed for β-galactosidase activity. **A.** Immunoblot analysis of virus producer cells with anti-HA, anti-$p24^{Gag}$ and anti-HSP90 (as a loading control) antibodies. **B.** Virus production from transfected cells as determined by $p24^{Gag}$ ELISA. **C**. Infectivity of virions produced in B as determined by TZM assay.

However a major drawback to this type of analysis, especially in HeLa cells, is that not every cell will be transfected with the dominant negative protein nor co-transfected with both the protein and the viral DNA. The use of 293T cells for the infectivity assay sought to partially address this issue but it still means that a proportion of cells will contain P-bodies. This may not be an issue if the phenotypes are dramatic but more subtle differences may be overlooked. Originally it was hoped that stable cell lines could be generated to overcome this problem. However cells stably expressing YFP tagged versions of these proteins (both wild type and dominant negative), when transfected with the NL43 Δ*vif* provirus failed to produce sufficient amounts of virus with which to conduct infectivity assays (data not shown). The reasons behind this remain unclear. Therefore, although no effects on HIV-1 infectivity and virus production were observed in the presence of the DDX6 mutant proteins, further experiments will need to be conducted in order to verify this result.

5.4 Infection of P-body depleted cells

5.4.1 Phenotypic analysis of DDX6 knockdown by shRNA

To convincingly and more thoroughly deplete P-bodies from cells, knockdown of DDX6 by RNAi was utilised. It has been demonstrated that knockdown of DDX6, by this method, leads to a significant reduction of visible P-bodies (Chu and Rana, 2006). Lentiviral vectors encoding shRNAs (as described in Chapter 4, section 4.3) targeting either DDX6 or a non-silencing control were used to transduce HeLa cells. 48 hours post transduction, cells were maintained under puromycin selection for between 5 - 7 days before they were either lysed and subjected to immunoblotting, to check for DDX6 protein levels, or plated onto coverslips for immunofluorescence analysis. In this case cells were then fixed, permeablised and stained with an anti-Ge1 antibody (as a marker for P-bodies) to evaluate P-body knockdown.

From Figure 5.5A, cells stably expressing the DDX6 shRNA show an approximate 80% reduction in DDX6 protein levels compared to control cells (quantified by Licor-Odyssey software), when equal amounts of lysate were loaded onto gels (as judged by the HSP90 loading control). Importantly, expression levels of a second P-body protein, Lsm1, are unchanged, proving that the knockdown is specific to DDX6. It was also observed that efficient knockdown of DDX6 resulted in reduced cell proliferation, with cells growing almost twice as slowly as the control cell line.

Pertinent to these studies, a reduction in DDX6 protein levels also led to a substantial depletion of P-bodies, both in terms of the number of cells containing P-bodies and the average number of P-bodies per cell, as presented in Figure 5.5B. Compared to the control cells, which on average harbour approximately 5 P-bodies per cell, the DDX6 shRNA expressing cells contained either 0 or 1 of these foci, on average. Representative images are displayed in Figure 5.5C. This dramatic loss of microscopically visible P-bodies makes these cells a useful tool for studying the effects of P-body depletion on HIV-1 infectivity and APOBEC3 anti-viral activity.

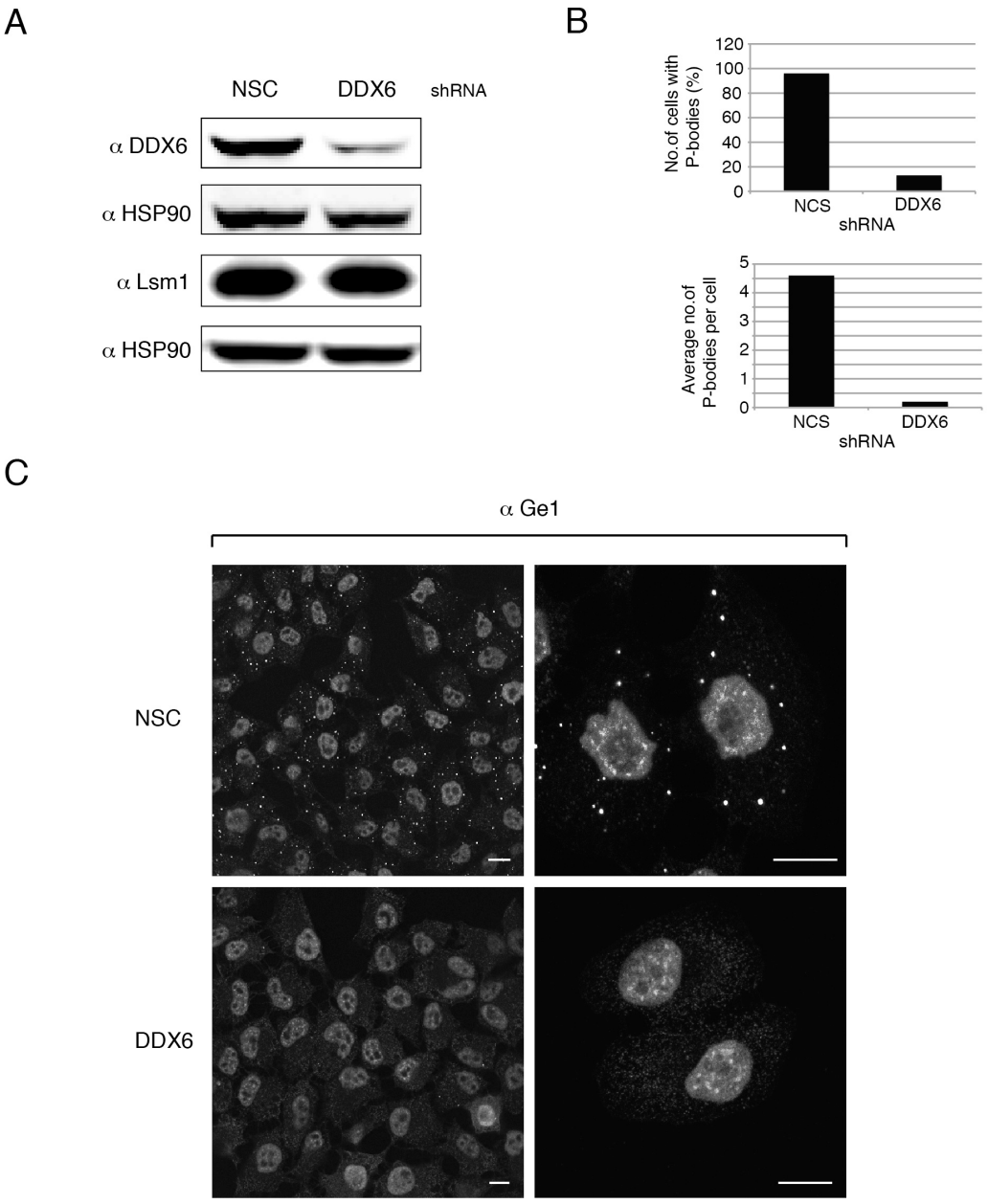

Figure 5.5: Phenotypic analysis of DDX6 knockdown by shRNA lentiviral vectors.

293T cells were co-transfected with a Gag-Pol packaging plasmid, a DDX6 (DDX6) targeting or non-silencing (NSC) shRNA encoded lentiviral vector and a VSVG expression plasmid at a 2:2:1 ratio. 48 hours later, VLPs were harvested and equivalent amounts used to transduce HeLa cells seeded in 24 well plates, with the addition of polybrene. 48 hours later transduction efficiencies were determined by analysis of GFP expression and cells were placed under puromycin selection and maintained in this way for at least 5 days before immunoblot and immunofluorescence analysis. **A**. Immunoblot analysis of protein expression in transduced HeLa cells with anti-DDX6, anti-Lsm1 and anti-HSP90 (as a loading control) antibodies. Protein bands were quantified using Licor-Odyssey software. **B**. Quantification of the number of knockdown and control cells containing Ge1 marked foci (top) and the average number of these foci per cell (bottom) (n=95). **C**. Immunofluorescence analysis of transduced cell lines to check for P-body depletion. Cells were plated onto coverslips, 24 hours later, fixed, permeabilised and stained with a mouse anti-Ge1 primary antibody and an anti-mouse 594 secondary antibody. Coverslips were mounted onto slides, dried overnight and imaged using a Leica confocal microscope. Scale bar = 10 μm.

5.4.2 Functional analysis of DDX6 knockdown

As for Ago2 (Chapter 4, section 4.4), it was also useful to determine whether knockdown of DDX6 had any functional consequences, besides the phenotypic effects observed through P-body loss. DDX6 has been reported to be necessary for miRNA mediated translational repression and specifically that mediated by the let-7 miRNA (Chu and Rana, 2006). The authors note a 1.5 fold decrease in repression of reporter constructs upon DDX6 depletion. In an attempt to reproduce this modest effect, the luciferase reporter system described in Chapter 4, section 4.4 was employed. Briefly two luciferase reporter constructs, one containing 4 binding sites for the let-7 miRNA (wild-type) and the other containing mutated binding sites (mutant) are separately transfected into HeLa cells, along with *Renilla* luciferase as a transfection control. Expression of the wild type reporter should be reduced 4 - 5 fold compared to the mutated control due to the action of endogenous let-7, which recruits the RISC complex to instigate translational repression. If there is inhibition of this repression, expression of the wild type and mutant constructs should be roughly equivalent. When these constructs were transfected into the DDX6 knockdown HeLa cells, no difference in expression of the wild type construct was observed compared to the control cell line (Figure 5.6) and the level of repression in both cases was approximately 4 fold, as would be expected. Expression of both reporters was increased in the DDX6 shRNA expressing cells indicating that general translational repression upon DDX6 knockdown may have been somewhat relieved. However these results would imply that DDX6 is not necessary for miRNA mediated translational repression or at least not to any substantial effect. They also confirm the finding that microscopically visible P-bodies are not required for this process (Chu and Rana, 2006).

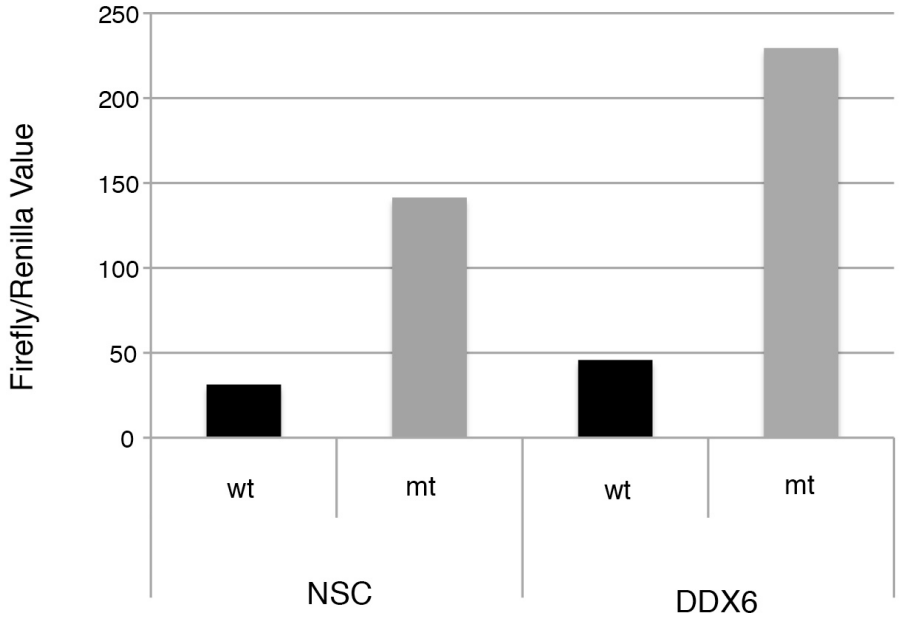

Figure 5.6: Knockdown of DDX6 does not impair miRNA mediated translational repression.

HeLa cells stably expressing either a control (NSC) or DDX6 targeting (DDX6) shRNA (generated as described in section 5.4) were co-transfected with 0.1 μg of luciferase reporter constructs containing either wild type (wt) or mutated (mt) binding sites for the let 7 miRNA (as described in Chapter 4), 0.4 μg of a HA-tagged GFP expression plasmid and 0.01 μg of a *Renilla* expression plasmid, as a transfection control. 24 hours later cells were harvested, lysed and luciferase levels measured. Data is presented as the ratio of firefly to *Renilla* values, with *Renilla* equivalent across all samples, and is representative of 2 independent experiments.

5.4.3 Generation of DDX6 knockdown and A3G expressing stable cell lines

Since knockdown of DDX6, using shRNAs, proved to be highly effective at disrupting P-bodies (section 5.4.1), this was used as a basis to evaluate HIV-1 infectivity and A3G anti-viral activity in the absence of these foci. Rather than conducting these experiments by transient transfection, as performed in Chapter 4, section 4.3.3, an infection based approach was used instead, which is considered to be more physiologically relevant. This is also the method used by two groups who found that P-bodies/P-body components were inhibitory to HIV-1 infectivity (Chable-Bessia et al., 2009; Nathans et al., 2009), thereby making results obtained here more comparable with published work.

Stable HeLa cells were generated expressing either untagged A3G or YFP as described in Chapter 4, section 4.2. These cells were then transduced again with either a DDX6 targeting or a non-silencing control shRNA encoded lentiviral vector. This led to the production of four separate stable cell lines, expressing either A3G or YFP and then either a control or DDX6 shRNA. Efficient knockdown of DDX6 and hence P-bodies and expression of A3G and YFP was first confirmed by immunoblot (Figure 5.7A) and immunofluorescence analysis (Figure 5.7B). Compellingly depletion of DDX6 bodies also led to a removal of A3G marked foci (Figure 5.7B) demonstrating that the formation of A3G bodies is dependent on DDX6.

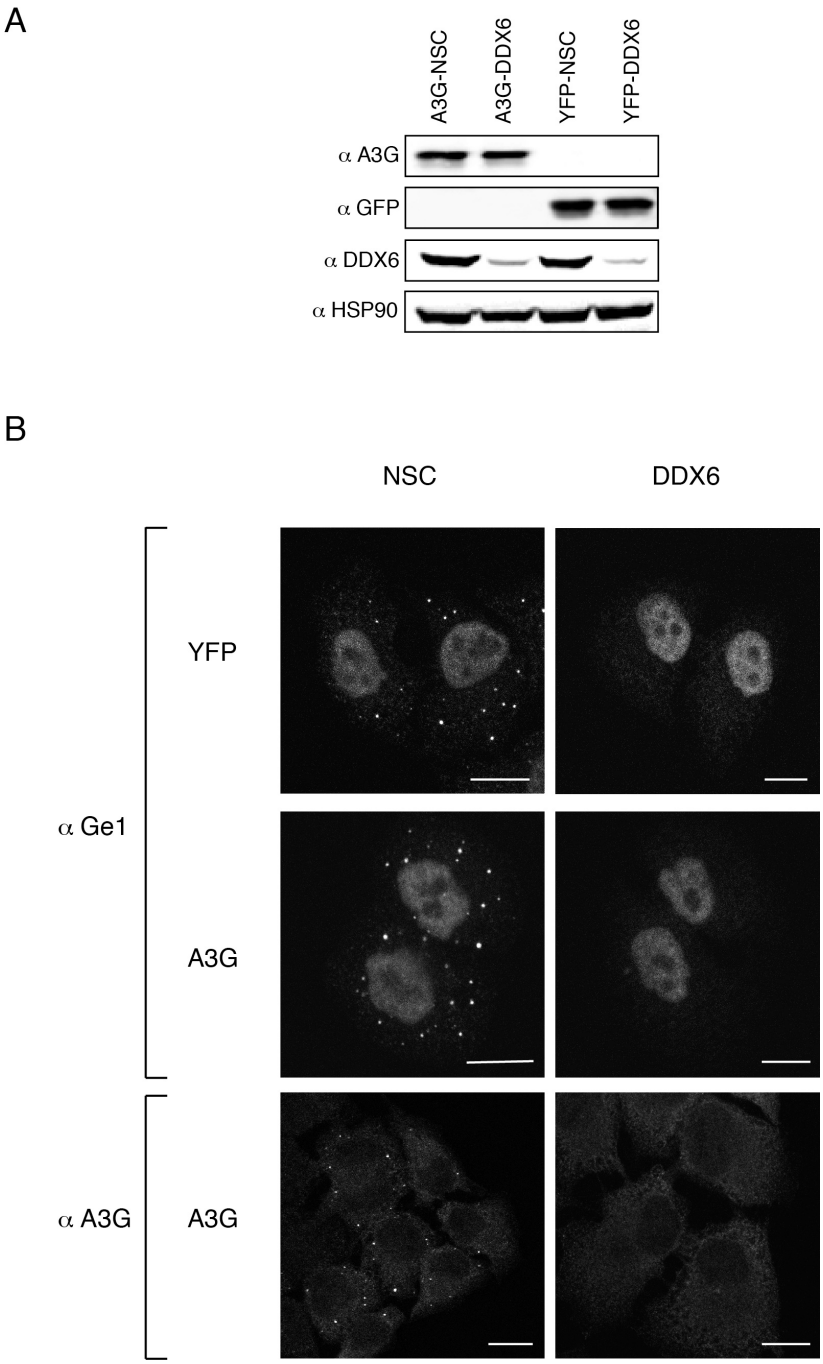

Figure 5.7: Generation of stable DDX6 knockdown and A3G expressing cell lines.

HeLa cells were first transduced with either untagged A3G or YFP by retroviral transduction and maintained under neomycin selection for approximately 10 days. They were subsequently transduced with either a DDX6 (DDX6) or non-silencing (NSC) shRNA by lentiviral transduction. Cells were then maintained under puromycin and neomycin selection for at least 5 days before immunoblot and immunofluorescence analysis. **A**. Immunoblot analysis of doubly transduced cells to check protein expression with anti-A3G, anti-GFP (which recognises YFP), anti-DDX6 and anti-HSP90 (as a loading control) antibodies. **B**. Immunofluorescence analysis of transduced cells to check for P-body depletion. Cells were plated onto coverslips and 24 hours later were fixed, permeabilised and stained with mouse anti-Ge1 or rabbit anti-A3G primary antibodies and appropriate Alexa Fluor 594 conjugated secondary antibodies. Coverslips were mounted onto slides, dried overnight and imaged using a Lecia confocal microscope. Scale bar = 10 μm.

5.4.4 HIV-1 infectivity and A3G anti-viral activity in shRNA mediated DDX6 knockdown cells

The cells described in section 5.4.3 were then infected with either 50 ng or 100 ng of VSV-G pseudotyped wild-type and Δ*vif* viruses. Virus stocks were produced by co-transfection of 293T cells with an NL43 proviral plasmid (either wild-type or Δ*vif)* and a VSV-G expression plasmid at a 3:1 ratio. Supernatants were harvested and quantified by $p24^{Gag}$ ELISA. The number of infected cells was determined by p24 intracellular staining and subsequent FACS analysis. Approximately 30% and 60% of cells were infected with 50 ng and 100 ng of input virus, respectively (data not shown). Cells were infected for 4 hours, before virus was removed by extensive washing and replaced with fresh media. 48 hours post-infection, viral supernatants were collected, normalised by $p24^{Gag}$ ELISA and used to infect TZM-bl cells. 20 ng was spun through a 20% sucrose cushion to check for virion incorporation of A3G. Corresponding cell lysates were also obtained to check for protein expression in producer cells.

From Figure 5.8A it can be seen that virus production from the wild-type and Δ*vif* viruses is roughly equivalent, though in general slightly more is produced with the latter virus. There does not appear to be any consistent nor specific effect of DDX6 depletion on HIV-1 particle production (Figure 5.8A), which is in contrast to reported work (Nathans et al., 2009). When the infectivity of the viruses produced in Figure 5.8A was measured, it appeared to decrease slightly rather than increase in the DDX6 knockdown cell lines (Figure 5.8B), implying that DDX6 does not inhibit HIV-1 infectivity, which is in disagreement with reports from two groups (Chable-Bessia et al., 2009; Nathans et al., 2009). Also, knockdown of DDX6 and hence loss of P-bodies had no effect upon A3G mediated inhibition of HIV-1 as a consistent 1.5 log decrease in Δ*vif* viral infectivity is observed in the A3G expressing cell lines. It is also clear from Figure 5.8C, that packaging of A3G, which only occurs in the absence of Vif, as would be expected, is not impaired by knockdown of DDX6. These infection-based experiments thus provide evidence that DDX6 and/or P-bodies are not relevant to A3G anti-viral activity or virion incorporation nor do they appear to negatively regulate HIV-1 infectivity.

Figure 5.8: Infection of DDX6 shRNA depleted cells does not affect A3G anti-viral activity or negatively regulate HIV-1 infectivity.

Doubly transduced HeLa cells expressing either A3G or YFP and then either a DDX6 targeting (DDX6) or non-silencing control (NSC) shRNA (generated as described for Figure 5.7) were infected with 50 ng or 100 ng of VSV-G pseudotyped wild-type or Δ*vif* NL43 virus. 4 hours later cells were extensively washed to remove any input virus and incubated in complete DMEM. 48 hours later viral supernatants were harvested and quantified by $p24^{Gag}$ ELISA. Normalised amounts were used to infect TZM-bl reporter cells which were harvested 30 hours post-infection and assayed for β-galactosidase activity. Equivalent amounts of viral supernatant was also concentrated through a 20% sucrose cushion and viral pellets along with cell lysates were subjected to immunoblot analysis. **A.** Virus production from infected cells as determined by $p24^{Gag}$ ELISA. **B**. Infectivity of virions produced in A, as determined by TZM assay. **C**. Immunoblot analysis of cell lysates from virus producer cell to check protein expression and viral pellets to check virion incorporation, with anti-A3G, anti-GFP, anti-DDX6, anti-$p24^{Gag}$ and anti-HSP90 (as a loading control) antibodies. Data is representative of 2 independent experiments.

A

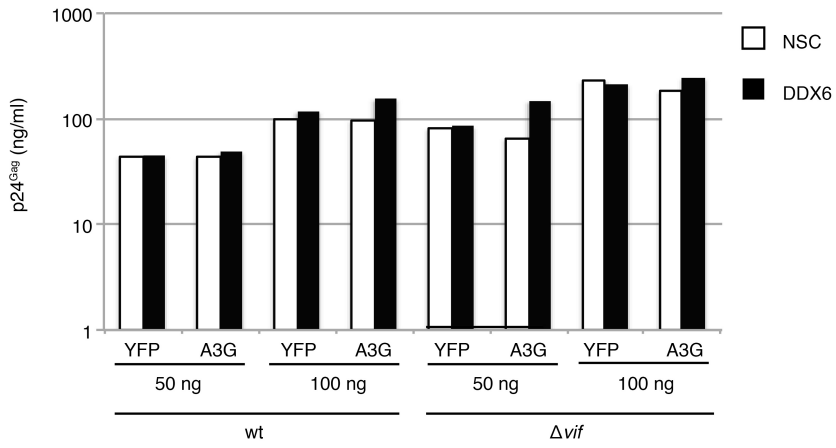
1000
100
10
1
p24Gag (ng/ml)
NSC
DDX6
YFP
A3G
YFP
A3G
YFP
A3G
YFP
A3G
50 ng
100 ng
50 ng
100 ng
wt
Δvif

B

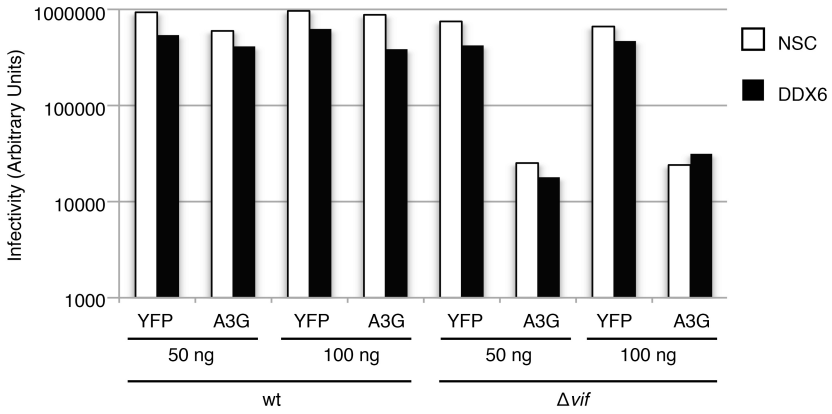
1000000
100000
10000
1000
Infectivity (Arbitrary Units)
NSC
DDX6
YFP
A3G
YFP
A3G
YFP
A3G
YFP
A3G
50 ng
100 ng
50 ng
100 ng
wt
Δvif

C

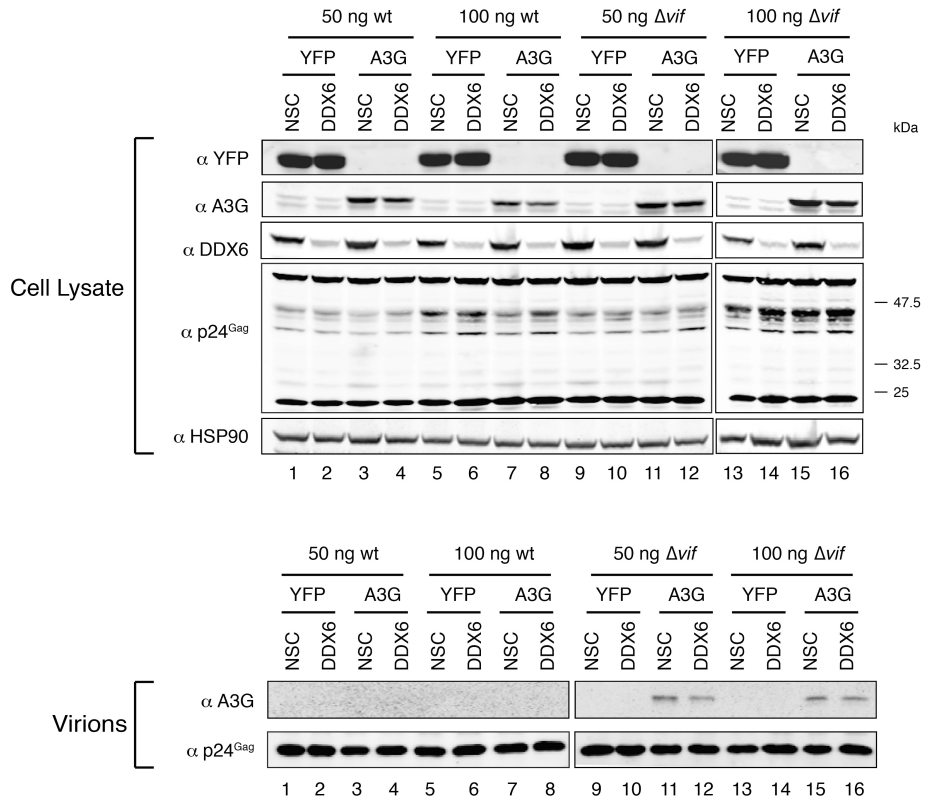
50 ng wt
100 ng wt
50 ng Δvif
100 ng Δvif
YFP
A3G
NSC
DDX6
kDa
Cell Lysate
α YFP
α A3G
α DDX6
α p24Gag
α HSP90
47.5
32.5
25
1 2 3 4 5 6 7 8 9 10 11 12 13 14 15 16
Virions
α A3G
α p24Gag

5.4.5 HIV-1 infectivity and A3G anti-viral activity in siRNA mediated DDX6 knockdown cells

Although use of the DDX6 shRNA consistently gave a knockdown of DDX6 protein levels of between 70 - 80%, a siRNA oligonucleotide was tested to determine whether an even more efficient reduction could be achieved. This would also help rule out knockdown efficiency as the basis for the discrepancy with published reports (Chable-Bessia et al., 2009; Nathans et al., 2009), as both of these groups used siRNAs to deplete P-bodies from cells. Further, any differences in cell proliferation rates, associated with depletion of DDX6 in stable cell lines, would also be eliminated.

Knockdown of DDX6 by siRNA was first verified by immunoblot and immunofluorescence analysis before further experiments were conducted. The DDX6 siRNA oligonucleotide used led to an approximate 93% reduction in protein levels (Figure 5.9A), and a significant depletion of P-bodies from these cells when compared to either a non-targeting scrambled or luciferase targeted control, respectively (Figure 5.9B). Stable A3G and YFP expressing HeLa cells were then twice transfected with either the DDX6 or non-targeting control siRNA. 12 hours after the second siRNA transfection, cells were infected with 50 ng of virus and assayed as previously described. Results are presented in Figure 5.10. Even by this method, no increase in $p24^{Gag}$ production was observed from cells knocked down for DDX6 (Figure 5.10A). Subsequent infection of TZM-bl cells led to equivalent levels of HIV-1 infectivity and A3G anti-viral activity regardless as to whether cells were transfected with the control or DDX6 targeting siRNA (Figure 5.10B). Packaging of A3G also remained unaffected by DDX6 depletion (Figure 5.10C). Expression of the stably transduced proteins and knockdown of DDX6 was comparable between the different cell lines and samples (Figure 5.10C). Therefore, from the data presented in sections 5.4.4 and 5.4.5, it would appear that knockdown of DDX6 and hence loss of P-bodies does not positively or negatively influence HIV-1 virus production and infectivity. Additional work would be required to establish the basis for the discrepancies with published reports claiming that P-bodies are in fact inhibitory to HIV-1 particle production and production of infectious virions. Further to this, A3G anti-viral activity and incorporation into virions was also unperturbed by P-body depletion which implies that these foci are not relevant to the anti-viral phenotypes of the APOBEC3 proteins and are not sites for packaging of these proteins into virions.

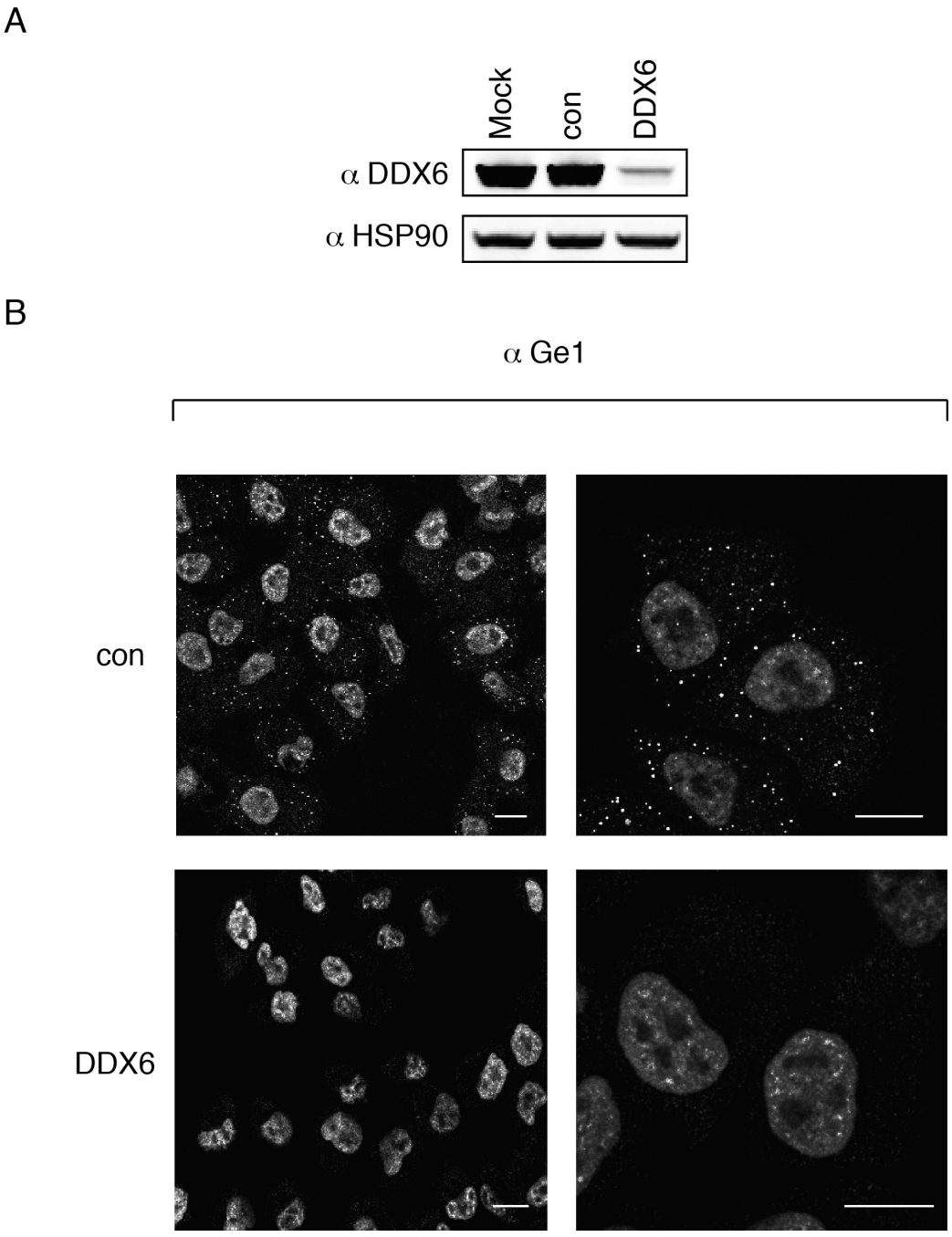

Figure 5.9: Phenotypic analysis of DDX6 knockdown by siRNA oligonucleotides.

HeLa cells, seeded in 24 well plates, were transfected with 50 pmol of either a DDX6 targeting (DDX6) or a scrambled control (con) siRNA oligonucleotide. 48 hours later, cells were split and re-seeded into 24 wells plates for immunoblot analysis or into 12 well plates plus coverslips for immunofluorescence analysis and 2 hours later transfected as before. Cells were harvested 48 hours later. **A**. Immunoblot analysis of siRNA transfected cells with anti-DDX6 and anti-HSP90 (as a loading control) antibodies. **B**. siRNA transfected cells were fixed, permeabilised and stained with a mouse anti-Ge1 primary antibody and an anti-mouse 488 secondary antibody. Coverslips were mounted onto slides, dried overnight and imaged using a Leica confocal microscope. Scale bar = 10 μm.

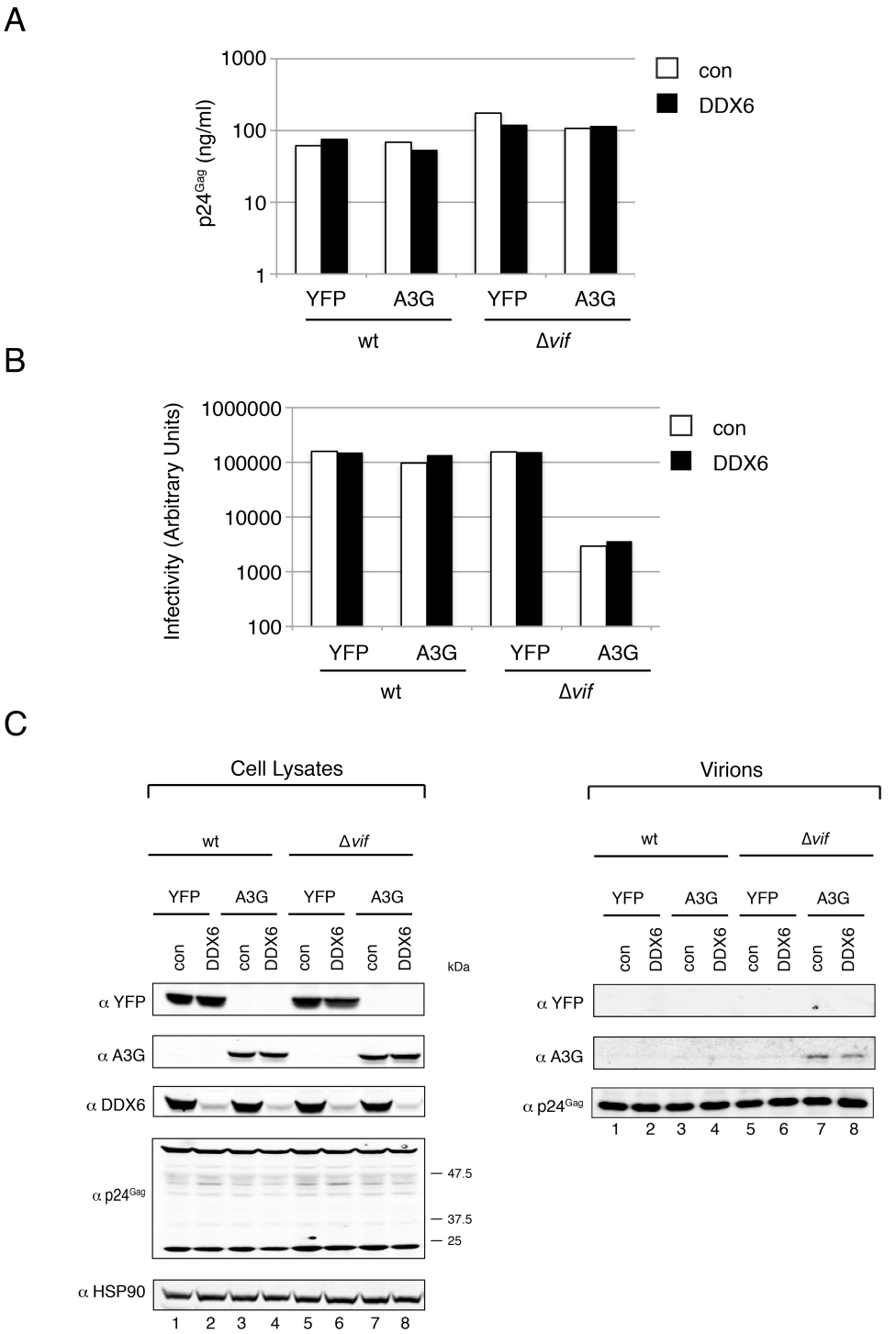

Figure 5.10: Infection of DDX6 siRNA depleted cells does not affect A3G anti-viral activity or negatively regulate HIV-1 infectivity.

HeLa cells, stably expressing either untagged A3G or YFP, seeded in 24 well plates 2 hours prior, were first transfected with 50 pmol of either a DDX6 targeting (DDX6) or a scrambled control (con) siRNA. 48 hours later, cells were re-seeded into 6 well plates and 2 hours later transfected as before. 12 hours after the 2nd transfection, cells were infected with 50 ng of either VSV-G pseudotyped wild-type (wt) or Δ*vif* virus. Cells were then assayed as described in Figure 5.8. **A**. Virus production from infected cells as determined by $p24^{Gag}$ ELISA. **B**. Infectivity of virions produced in A, determined by TZM assay. **C**. Immunoblot analysis of cell lysates from virus producer cell to check protein expression and viral pellets to check virion incorporation, with anti-A3G, anti-GFP, anti-DDX6, anti-$p24^{Gag}$ and anti-HSP90 (as a loading control) antibodies. Data is representative of 2 independent experiments.

5.5 Transient transfection of P-body depleted cells

5.5.1 HIV-1 infectivity and APOBEC3 anti-viral activity in DDX6 knockdown cells

Since the results presented in section 5.4 do not support the conclusions drawn by Chable-Bessia *et al* and Nathans *et al* of an inhibitory effect of P-bodies on HIV-1 virus production and infectivity, a transient transfection based approach was utilised to try and address this discrepancy. Both groups have shown that ectopic expression of a proviral plasmid should increase viral production in the absence of P-body proteins, such as DDX6. This method was also used to further confirm the finding that P-bodies are not required for A3G mediated viral restriction, as concluded from the infection based assays.

HeLa cells stably transduced with either a non-silecning control or DDX6 targeting shRNA, were co-transfected with 1 μg of a HA-tagged APOBEC3 plasmid and 1 μg of an NL43 Δ*vif* proviral construct. 48 hours later, viral supernatants were harvested and quantified by $p24^{Gag}$ ELISA. 5 ng was then used to infect TZM-bl reporter cells. To check for virion incorporation of the APOBEC3 proteins, 20 ng of viral supernatant was concentrated through a 20% sucrose cushion and pellets lysed and subjected to immunoblotting. Corresponding cell lysates were also prepared in parallel for immunoblot analysis. Results are presented in Figure 5.11. As shown, virus production from the DDX6 knock down cells is generally 2 - 4 fold higher than that obtained from the control cells and this is consistently observed across each sample (Figure 5.11A). This is in contrast to what was found by infection of virus producer cells but would suggest that DDX6 and/or P-bodies are mildly inhibitory for virus production as has been previously reported (Nathans et al., 2009). However, when normalised amounts of virus were used to challenge TZM-bl indicator cells, no difference in virus infectivity is observed (Figure 5.11B, compare first two bars, GFP samples). Moreover, knockdown of DDX6 had no obvious consequences for APOBEC3 anti-viral activity, as the level of viral inhibition was roughly equivalent in both cell lines, for all APOBEC3 proteins tested. There is slightly higher infectivity observed in the DDX6 depleted cells for A3F, A3G and A3H, which are the APOBEC3 proteins that most strongly associate with P-bodies, however this effect is very modest. This is further confirmed when assessing virion incorporation (Figure 5.11C). Expression of the different APOBEC3 proteins in the cell lysates is relatively similar in the two cell lines and packaging of the different

APOBEC3 proteins appears to be just as efficient in the control and knock down cell lines. These results validate the data presented earlier, that knockdown of DDX6 does not affect APOBEC3 anti-viral activity or virion incorporation. However, although HIV-1 viral infectivity was unperturbed by DDX6 depletion, a modest increase in virus production was observed from those cells expressing the DDX6 shRNA compared to the control cell line. As this effect is not seen when infecting cells, its relevance to HIV-1 replication will require further investigation.

5.5.2 DDX6 knockdown and A3G virion incorporation

As both infection and transfection based assays failed to demonstrate an influence of P-bodies on A3G anti-viral activity, a titration of A3G and GFP, as a negative control, was carried out to determine if at lower concentrations of A3G, any differences in virion incorporation could be detected. This was important to establish as overexpression of proteins can sometimes lead to artificial virion encapsidation (as noted in Chapter 3, section 3.3). Therefore to conclusively confirm that A3G packaging is not dependent on the presence of DDX6 and hence P-bodies, this protein was expressed at more physiologically relevant levels and virion incorporation was assessed (Figure 5.12), as described for Figure 5.11. Decreasing amounts of input DNA led to less protein expression in the cell lysate but even at the lowest concentration of DNA (0.1 μg, lanes 11 and 12), virion incorporation of A3G is clearly visible and is unaffected by P-body loss. This would indicate that P-bodies are not sites at which the APOBEC3 proteins, particularly A3G, are packaged into virions as this occurs just as efficiently in the absence of visible foci, even at lower levels of A3G expression.

Figure 5.11: Knockdown of DDX6 leads to an increase in HIV-1 virus production by transient transfection.

HeLa cells stably expressing either a control (NSC) or DDX6 targeting (DDX6) shRNA (generated as described in section 5.4) were co-transfected with equivalent amounts of HA-tagged APOBEC3 or GFP (as a negative control) expression plasmids and an NL43 Δ*vif* proviral plasmid. 48 hours later viral supernatants were harvested and quantified by $p24^{Gag}$ ELISA. Normalised amounts were used to infect TZM-bl reporter cells which were assayed 30 hours post infection for β-galactosidase activity. Equivalent amounts of viral supernatant was also concentrated through a 20% sucrose cushion and viral pellets as well as corresponding cell lysates were analysed by immunoblotting. **A**. Virus production from transfected cells as determined by $p24^{Gag}$ ELISA. **B**. Infectivity of virions produced in A as determined by TZM assay. Data is presented as the average of three independent experiments with error bars denoting the standard deviation. All values are normalised to GFP expressed in the NSC cell line, which is set at 100% **C**. Immunoblot analysis of virus producer cells to check for protein expression. **D**. Immunoblot analysis of viral pellets to check for virion incorporation with anti-HA, anti-$p24^{Gag}$, anti-DDX6 and anti-HSP90 (as a loading control) antibodies.

A

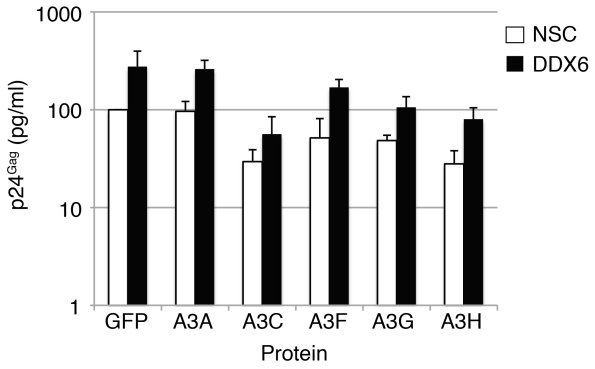
1000
100
10
1
p24Gag (pg/ml)
NSC
DDX6
GFP
A3A
A3C
A3F
A3G
A3H
Protein

B

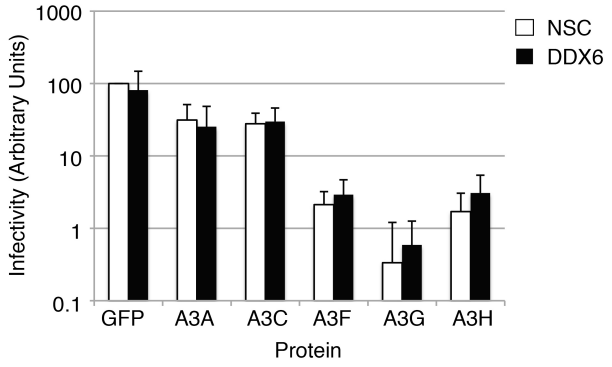
1000
100
10
1
0.1
Infectivity (Arbitrary Units)
NSC
DDX6
GFP
A3A
A3C
A3F
A3G
A3H
Protein

C

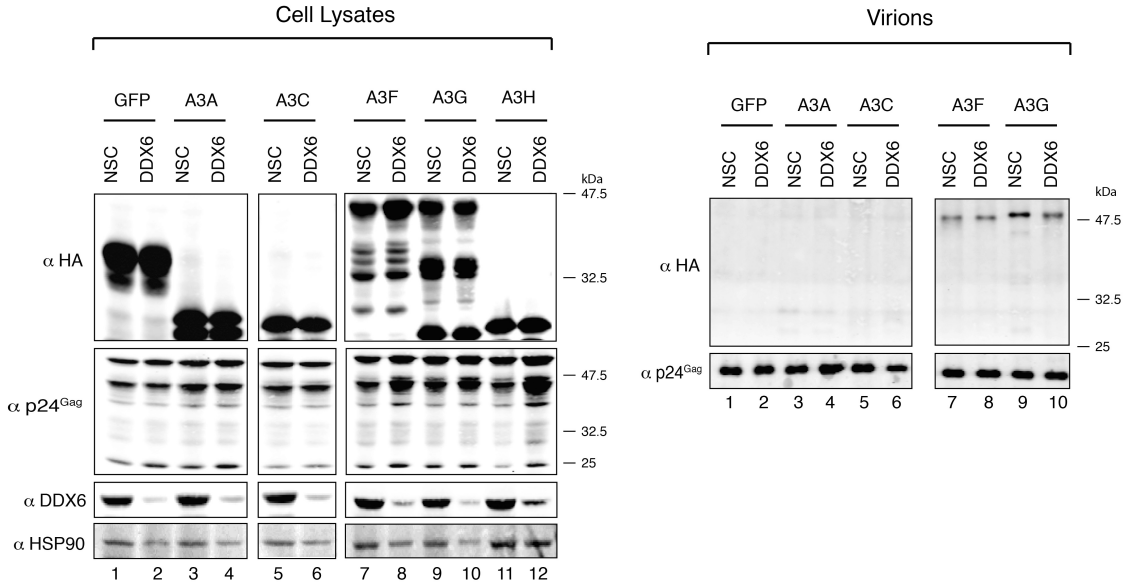
Cell Lysates
Virions
GFP
A3A
A3C
A3F
A3G
A3H
NSC
DDX6
kDa
47.5
32.5
25
α HA
α p24Gag
α DDX6
α HSP90
1 2 3 4 5 6 7 8 9 10 11 12
1 2 3 4 5 6 7 8 9 10

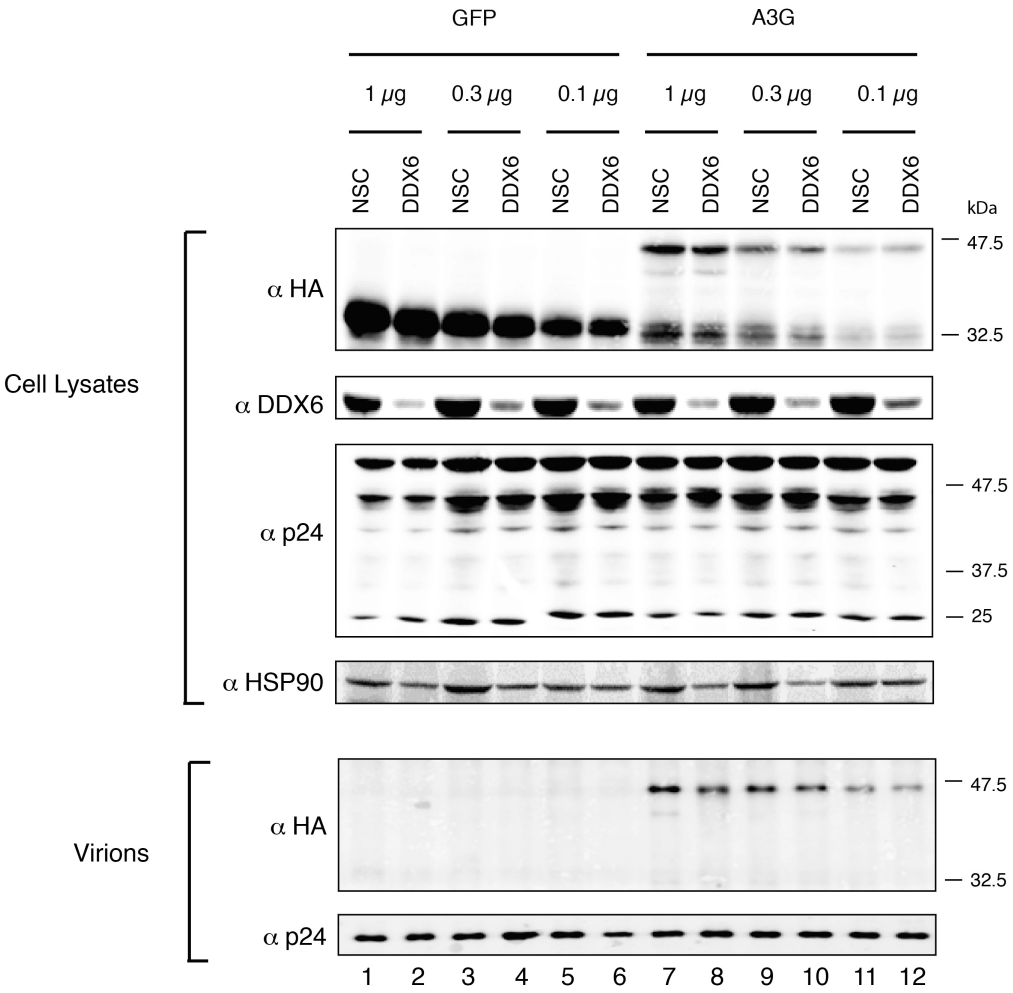

Figure 5.12: A3G is efficiently packaged, even at lower expression levels, in cells depleted of DDX6.

HeLa cells stably expressing either a control (NSC) or DDX6 targeting (DDX6) shRNA (generated as described in section 5.4) were co-transfected with decreasing amounts of HA-tagged A3G or GFP, included as a negative control (1 μg, 0.3 μg and 0.1 μg) and 1 μg of an NL43 Δ*vif* proviral plasmid. Total DNA concentration was kept constant at 2 μg with the addition of an untagged luciferase expression plasmid. Cells were then assayed for virion incorporation as described for Figure 5.11. Immunoblot analysis of virus producer cells to check for protein expression and viral pellets to check for virion incorporation with anti-HA, anti-$p24^{Gag}$, anti-DDX6 and anti-HSP90 (as a loading control) antibodies.

5.5.3 Pulse labelling analysis in DDX6 knockdown cells

As observed here by transient transfection (section 5.5.1) and noted by other groups (Chable-Bessia et al., 2009; Nathans et al., 2009), depletion of certain P-body components results in a modest increase in HIV-1 particle production. It has been suggested that this effect is specific to HIV-1 virus production and is not the result of a more general effect on protein translation due to relief of translational repression upon DDX6 knockdown (Nathans et al., 2009). Whether this is indeed the case requires further investigation and so a preliminary pulse labelling experiment was performed, comparing levels of protein synthesis for both a full-length proviral plasmid and a codon-optimised Gag construct, in control and DDX6 knock down cell lines.

HeLa cells were twice transfected with siRNAs targeting DDX6 (DDX6) or a non-targeting scrambled control siRNA (con). 12 hours after the second siRNA transfection, cells were transfected with either GFP (mock control), codon-optimised Gag or NL43 Δ*vif* proviral expression plasmids. 48 hours later, viral supernatants were harvested and quantified by $p24^{Gag}$ ELISA. Subsequently, cells were incubated in cysteine and methionine depleted (-Cys, -Met) media before the addition of [^{35}S]cysteine/methionine. All newly synthesized proteins containing cysteine and methionine thus become radiolabelled. Cells were then lysed before immunoprecipitation with a $p24^{Gag}$ specific antibody (UP598, see Table 2.3). Samples were subjected to SDS-PAGE before visualisation by autoradiography. As shown in Figure 5.13A, a highly efficient knockdown of DDX6 at the protein level is achieved through siRNA transfection of HeLa cells and this leads to an approximate 2 fold increase in virus production, compared to control cells, when transfected with a proviral plasmid (Figure 5.13B). This appears to be matched with an increase in Gag synthesis from the DDX6 siRNA transfected compared to control transfected cells (Figure 5.13C, lanes 5 and 6). However, increased expression of Gag, in the absence of DDX6, is also observed for the codon-optimised Gag construct (Figure 5.13C, lanes 3 and 4) which suggests that these effects are not specific to HIV-1 and may instead be the consequence of general effects on global cellular translation as a result of DDX6 depletion.

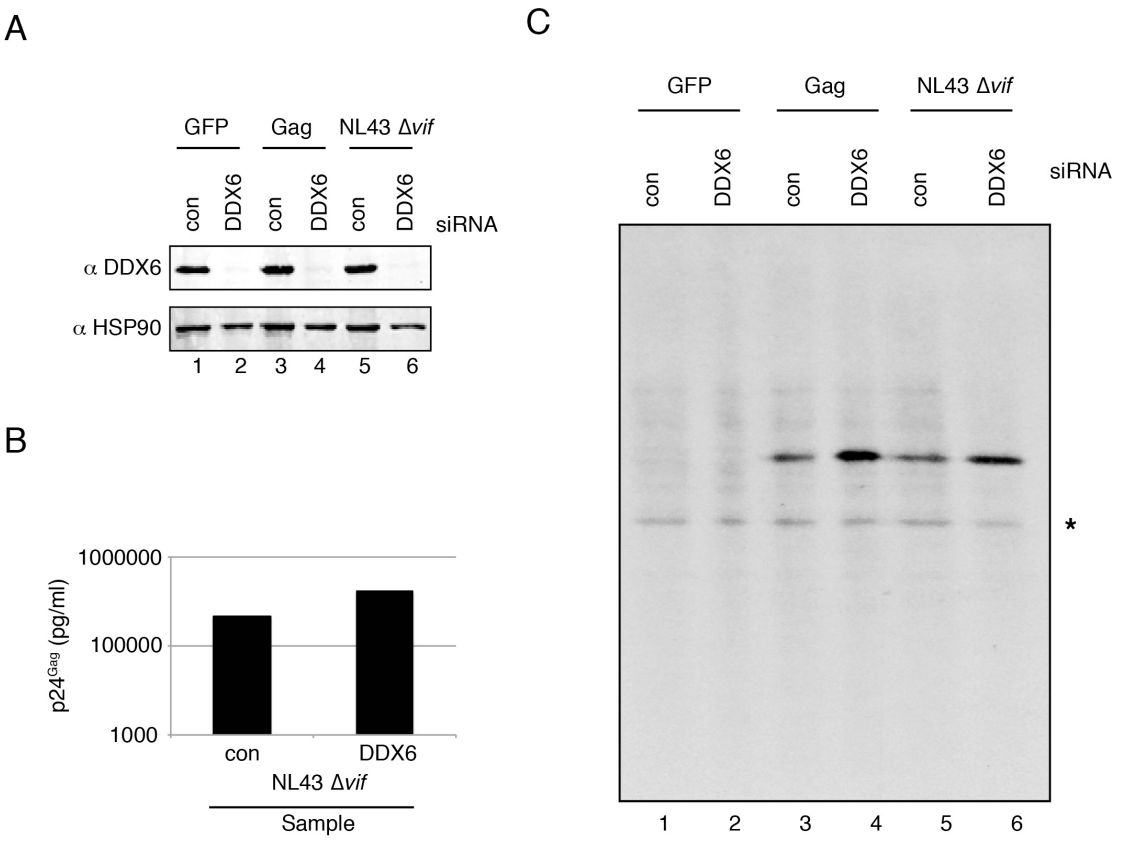

Figure 5.13: Increase in p24^{Gag} levels, upon DDX6 depletion, is not specific to HIV-1.

HeLa cells were twice transfected with siRNAs targeting either DDX6 (DDX6) or a non-targeting scrambled control (con). 12 hours after the second transfection, cells were transfected with either GFP, codon-optimised Gag or an NL43 Δ*vif* proviral plasmid and viral supernatants were harvested 48 hours later for quantification of virus production by p24^{Gag} ELISA. siRNA transfected cells were then incubated for 20 minutes in -Cys, -Met depletion media, with [^{35}S]cysteine/methionine added for an additional 5 minutes. Cells were then lysed and subjected to immunoprecipitation for 1 hour using a p24^{Gag} specific antibody and G protein coupled Agarose. Samples were loaded onto gels, transferred onto membranes and exposed to a phosphoimager screen overnight. Membranes were also transferred onto film at -80°C for 5 days and developed. **A**. Immunoblot of cell lysates (prior to immunoprecipitation) to check for DDX6 knockdown using anti-DDX6 and anti-HSP90 (as a loading control) antibodies. **B**. HIV-1 particle production in DDX6 siRNA transfected cells. **C**. Immunoprecipitation of p24^{Gag} following ^{35}S[methionine] labelling in DDX6 knockdown and control cell lines. Data is representative of 2 independent experiments. * denotes the position of a background band.

5.6 P-body depletion by knockdown of Lsm1

5.6.1 Phenotypic analysis of Lsm1 knockdown by shRNA

In order to determine whether the increase in virus production observed with knockdown of DDX6 was a specific effect of this protein or a feature of P-bodies in general and to validate the findings that P-bodies do not negatively regulate HIV-1 nor affect APOBEC3 anti-viral activity, knockdown of a second P-body protein was utilised. This time Lsm1 was targeted, which is part of a heptameric complex involved in decapping that associates with P-bodies (Ingelfinger et al., 2002). Like DDX6, this protein has also been demonstrated to be inhibitory to HIV-1 particle production and infectivity (Chable-Bessia et al., 2009; Nathans et al., 2009).

Knock down of Lsm1 was achieved as described for DDX6 (section 5.4.1) and Ago2 (Chapter 4, section 4.3) with the use of lentiviral encoded shRNAs to generate stable HeLa cell lines. Knockdown of the protein was confirmed by immunoblot analysis (Figure 5.14A) with expression of DDX6 remaining constant in both cell lines. Notably, this resulted in a significant depletion of P-bodies in the knock down cells as the number of cells containing P-bodies as well as the average number of foci per cell was substantially reduced in the absence of Lsm1 (Figure 4.14B). Representative examples of the knockdown and control cell lines are presented in Figure 5.14C. However, unlike with DDX6, no effects upon cell growth were observed. This validates the use of these cells for further functional studies.

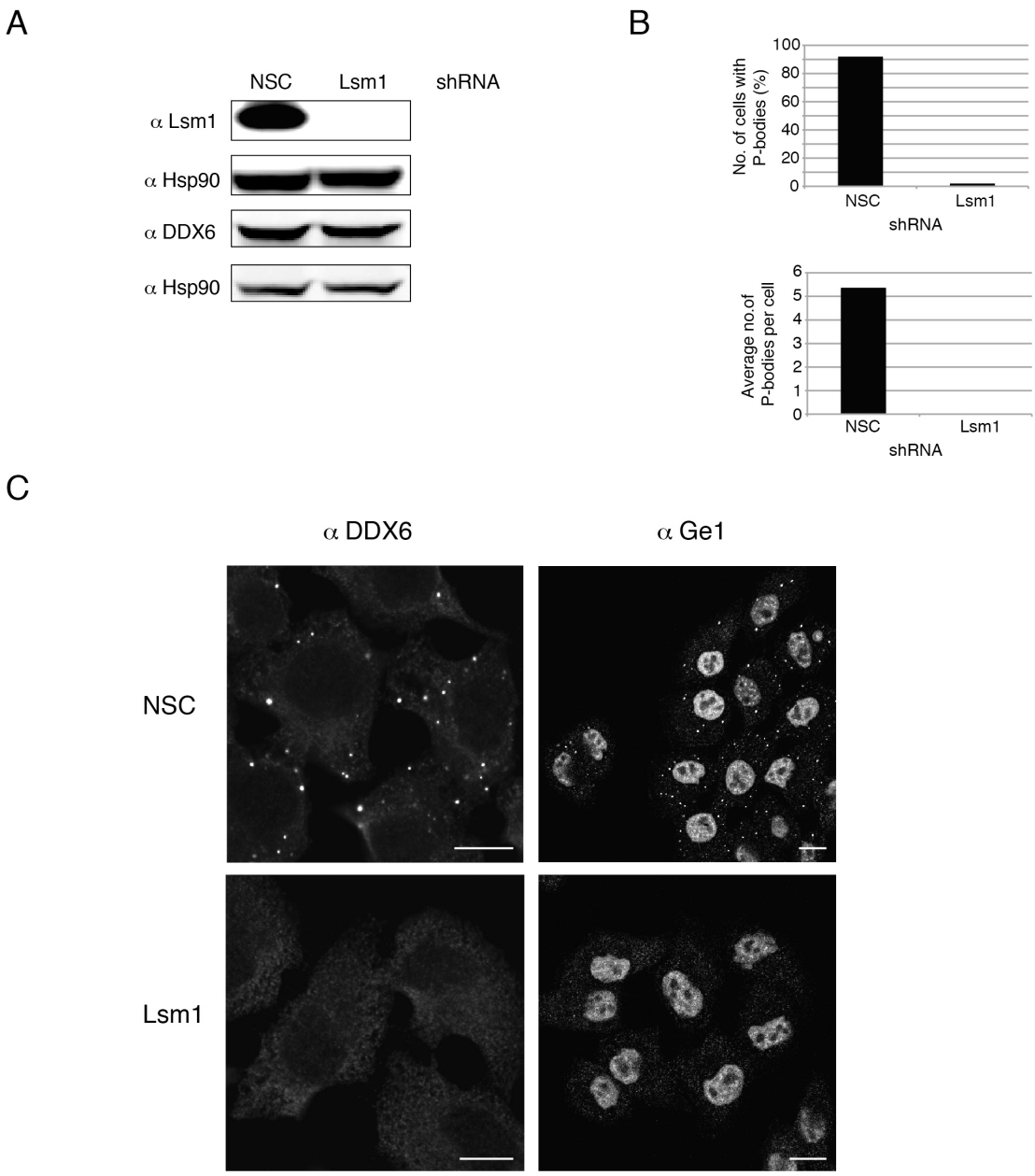

Figure 5.14: Phenotypic analysis of Lsm1 knockdown by shRNA lentiviral vectors.

293T cells were co-transfected with a Gag-Pol packaging plasmid, an Lsm1 (Lsm1) targeting or non-silencing (NSC) shRNA encoded lentiviral vector and a VSVG expression plasmid at a 2:2:1 ratio. 48 hours later, VLPs were harvested and equivalent amounts used to transduce HeLa cells seeded in 24 well plates, with the addition of polybrene. 48 hours later transduction efficiencies were determined by analysis of GFP expression and cells were placed under puromycin selection and maintained in this way for at least 5 days before immunoblot and immunofluorescence analysis. **A**. Immunoblot analysis of protein expression in transduced HeLa cells with anti-Lsm1, anti-DDX6 and anti-HSP90 (as a loading control) antibodies. **B**. Quantification of the number of knockdown and control cells containing DDX6 foci (top) as well as the average number of these foci per cell (bottom), (n=65). **C**. Immunofluorescence analysis of transduced cell lines to check for P-body depletion. Cells were plated onto coverslips, 24 hours later, fixed, permeabilised and stained with either a mouse anti-Ge1 or rabbit anti-DDX6 primary antibody and then the appropriate Alexa-Fluor 594 conjugated secondary antibody. Coverslips were mounted onto slides, dried overnight and imaged using a Leica confocal microscope. Scale bar = 10 μm.

5.6.2 HIV-1 infectivity and APOBEC3 anti-viral activity in Lsm1 knockdown cells, by transient transfection

As before (section 5.5.1) cells were transfected with equivalent amounts of HA-tagged APOBEC3 and NL43 Δ*vif* proviral plasmids. Virus production and infectivity were subsequently assessed as described in section 5.5.1. Virion incorporation was not assayed for these cell lines. The results, displayed in Figure 5.15A, demonstrate that knockdown of Lsm1 had no discernable effects on HIV-1 virus production, in contrast to what was seen with knockdown of DDX6. This would imply that enhanced virus production is specific to DDX6 depletion and not P-bodies in general. The infectivity of the virions produced in the presence of GFP did appear to be slightly higher in the knockdown compared to the control cells lines (Figure 5.15B), implying that HIV-1 infectivity may have been inhibited in the presence of Lsm1. However this was not seen with depletion of DDX6, is quite a modest effect and is not consistently observed across all samples. Once again, loss of P-bodies had no impact upon APOBEC3 anti-viral activity (Figure 5.15B). The expression of the transfected proteins was equivalent in both cell lines and the level of Lsm1 knockdown was consistent for all samples (Figure 5.15C).

These findings were further supported when A3G and GFP, as a negative control, were titrated down to more physiologically relevant expression levels. No differences in $p24^{Gag}$ production were observed between the cells lines (Figure 5.16A) and the observed increase in HIV-1 infectivity upon Lsm1 depletion was not replicated in two other samples (Figure 5.16B, titration of GFP), confirming that this is not a robust phenotype. Importantly, A3G viral inhibition was comparable even at lower amounts of DNA input demonstrating that lack of differences between the two cell lines is not due to gross overexpression of the APOBEC3 proteins. Expression of the transfected proteins was equivalent for both cell lines except at the lowest concentration of A3G (Figure 5.16C, lanes 11 and 12) where slightly more protein is expressed in the control compared to the Lsm1 knockdown cell line. The reason for this is unclear but has been consistently observed with knockdown of both Lsm1 and Ago2 (Chapter 4, Figure 4.5), but not DDX6.

Figure 5.15: Knockdown of Lsm1 does not affect HIV-1 virus production, infectivity or APOBEC3 anti-viral activity, by transient transfection.

HeLa cells stably expressing either a control (NSC) or Lsm1 targeting (Lsm1) shRNA (generated as described in section 5.4) were co-transfected with equivalent amounts of HA-tagged APOBEC3 or GFP (as a negative control) expression plasmids and an NL43 Δ*vif* proviral plasmid. 48 hours later viral supernatants were harvested and quantified by $p24^{Gag}$ ELISA. Normalised amounts were then used to infect TZM- bl reporter cells, which were assayed 30 hours post infection for β-galactosidase activity. **A**. Virus production from transfected cells as determined by $p24^{Gag}$ ELISA. **B**. Infectivity of virions produced in A as determined by TZM assay. Data is presented as the average of three independent experiments with error bars denoting the standard deviation. All values are normalised to GFP expressed in the NSC cell line, which is set at 100%. **C**. Immunoblot analysis of virus producer cells to check for protein expression with anti-HA, anti-$p24^{Gag}$, anti-Lsm1 and anti-HSP90 (as a loading control) antibodies.

A

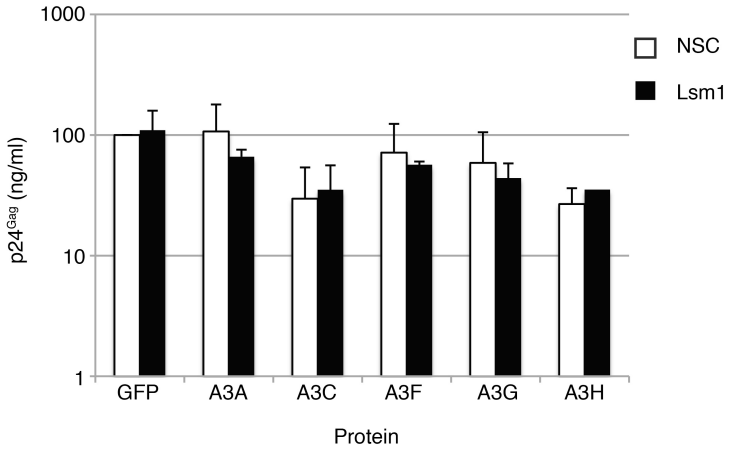
1000
100
10
1
p24Gag (ng/ml)
NSC
Lsm1
GFP
A3A
A3C
A3F
A3G
A3H
Protein

B

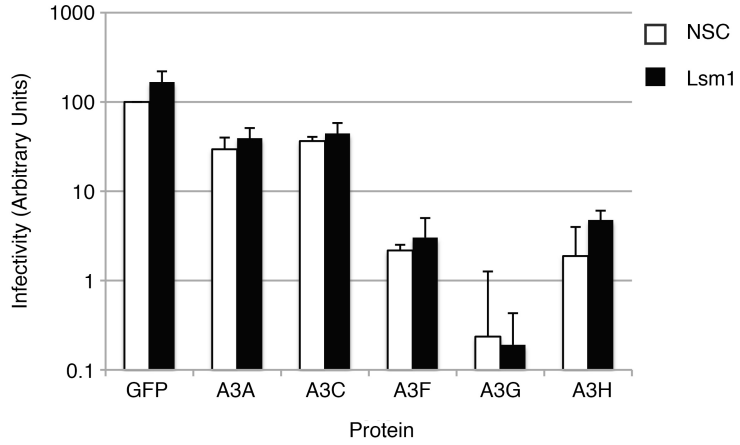
1000
100
10
1
0.1
Infectivity (Arbitrary Units)
NSC
Lsm1
GFP
A3A
A3C
A3F
A3G
A3H
Protein

C

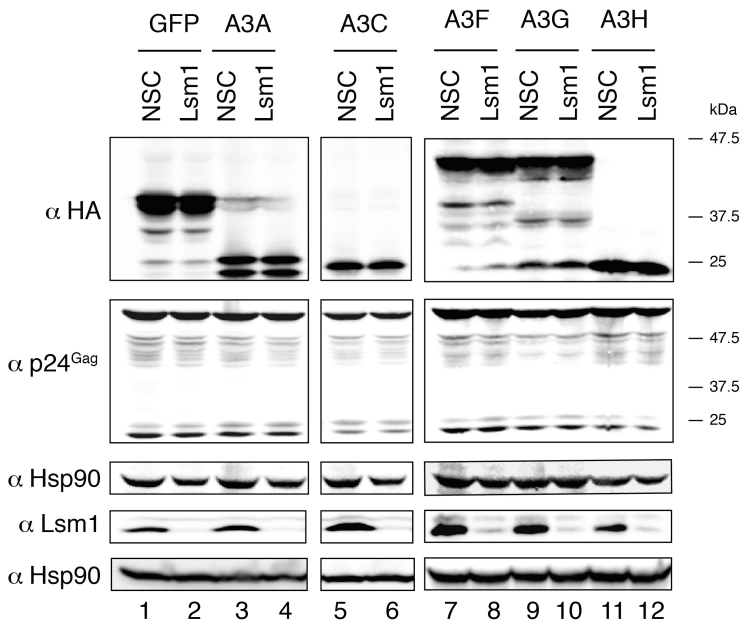
GFP
A3A
A3C
A3F
A3G
A3H
NSC
Lsm1
kDa
47.5
37.5
25
α HA
α p24Gag
α Hsp90
α Lsm1
α Hsp90
1 2 3 4 5 6 7 8 9 10 11 12

Figure 5.16: Knockdown of Lsm1 does not affect A3G anti-viral activity even at lower levels of protein expression.

HeLa cells stably expressing either a control (NSC) or Lsm1 targeting (Lsm1) shRNA (generated as described in section 5.4) were co-transfected with decreasing amounts (1 μg, 0.3 μg and 0.1 μg) of HA-tagged A3G or GFP, included as a negative control, and 1 μg of an NL43 Δ*vif* proviral plasmid. Total DNA concentration was kept constant at 2 μg with the addition of an untagged luciferase expression plasmid. Cells were then assayed as described for Figure 5.15. **A**. Virus production from transfected cells as determined by $p24^{Gag}$ ELISA. **B**. Infectivity of virions produced in A as determined by TZM assay. Data is presented as the average of three independent experiments with error bars denoting the standard deviation. All values are normalised to GFP expressed in the NSC cell line, which is set at 100%. **C**. Immunoblot analysis of virus producer cells to check for protein expression with anti-HA, anti- $p24^{Gag}$, anti-Lsm1 and anti-HSP90 (as a loading control) antibodies.

A

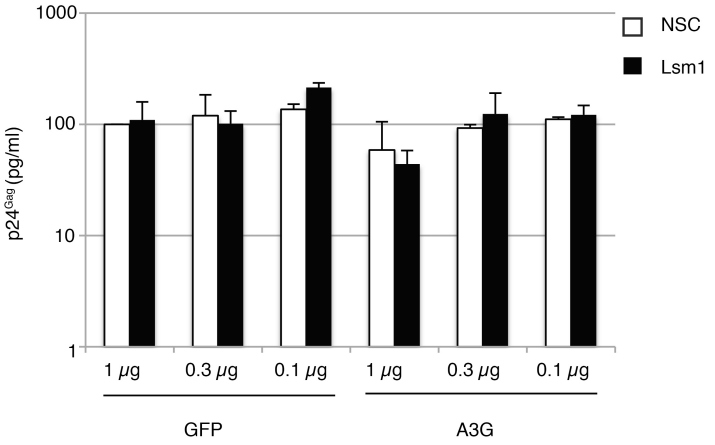
1000
100
10
1
p24Gag (pg/ml)
NSC
Lsm1
1 μg
0.3 μg
0.1 μg
1 μg
0.3 μg
0.1 μg
GFP
A3G

B

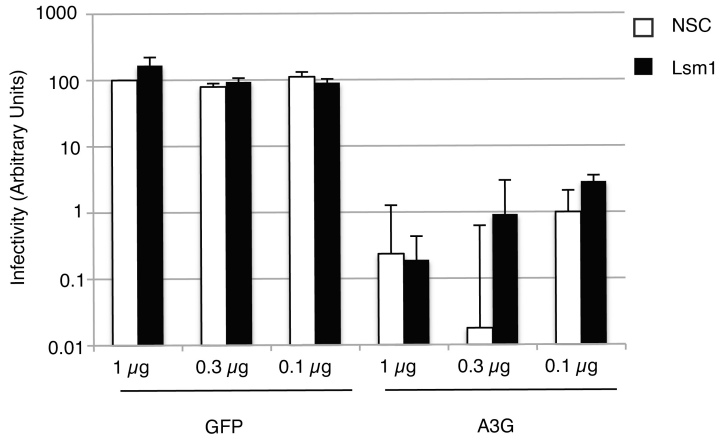
1000
100
10
1
0.1
0.01
Infectivity (Arbitrary Units)
NSC
Lsm1
1 μg
0.3 μg
0.1 μg
1 μg
0.3 μg
0.1 μg
GFP
A3G

C

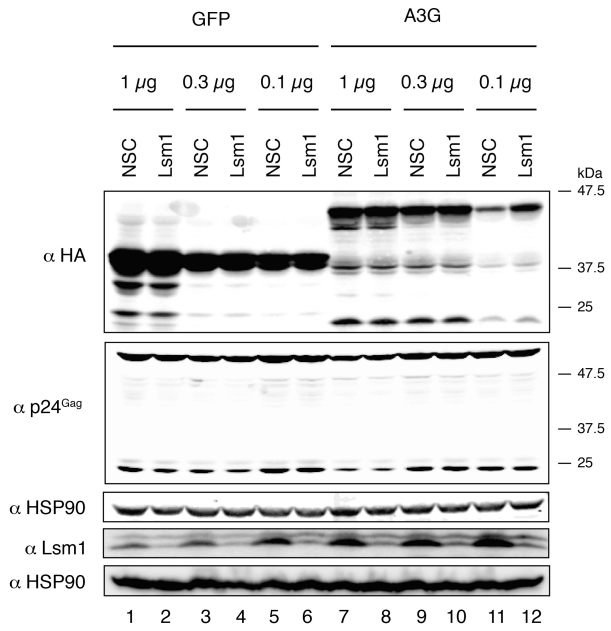
GFP
A3G
1 μg
0.3 μg
0.1 μg
1 μg
0.3 μg
0.1 μg
NSC
Lsm1
kDa
47.5
37.5
25
α HA
α p24Gag
α HSP90
α Lsm1
α HSP90
1 2 3 4 5 6 7 8 9 10 11 12

Overall, the data from transient transfection experiments, in sections 5.5 and 5.6, show that APOBEC3 anti-viral activity is unaffected by the absence of the P-body proteins DDX6 and Lsm1 in virus producer cells, similar to the findings reported for the infection based assays (section 5.4). The incorporation of these proteins into HIV-1 virions was similarly unperturbed demonstrating that P-bodies do not represent sites of APOBEC3 packaging. P-body depletion also had no effect upon HIV-1 infectivity, which is in disagreement with recently published findings (Chable-Bessia et al., 2009; Nathans et al., 2009). Knockdown of DDX6, but not Lsm1, did lead to a modest increase in virus production, which may be attributable to relief of general translational repression due to loss of DDX6 (section 5.5). However, the exact causes of this effect would require further experimental investigation, particularly as it was only observed under certain experimental conditions.

5.7 Lsm1 knockdown and HIV-1 replication

5.7.1 Phenotypic analysis of Lsm1 and DDX6 knockdown in a T cell line

All of the experiments conducted thus far, to ascertain whether P-bodies are influential in HIV-1 infectivity and APOBEC3 anti-viral activity, have centred on single cycle infectivity assays. Although these experiments are useful, they do not actually address if HIV-1 replication is affected, which would need to be monitored over several days.

In light of this, the Hut78 T cell line was employed, which naturally expresses A3G and potentially other anti-viral APOBEC3 proteins, to assess the effects of P-body loss on HIV-1 replication and endogenous A3G activity. These cells were transduced with either a DDX6 or Lsm1 targeting lentiviral encoded shRNA or a non-silencing control. Following transduction, immunoblot and immunofluorescence analyses were performed to verify the extent of the knockdown. Figure 5.17A demonstrates that a very efficient knockdown of Lsm1 is achieved at the protein level. However only a moderate reduction (approximately 30 - 50%) in the number of P-bodies (marked by the anti-DDX6 and anti-Ge1 antibodies) is observed, which is contrary to what is seen in HeLa cells, where P-bodies are more extensively depleted upon Lsm1 knockdown (section 5.6). On the other hand, use of the DDX6 targeting shRNA resulted in only a 50% knockdown of DDX6 (Figure 5.17A, shRNA 5). Several other DDX6 shRNAs were also trialled but reduction in protein expression was never greater than 2 fold (Figure 5.17A, shRNAs 1 - 4). Despite this, a more substantial P-body depletion is still observed than that obtained with knockdown of Lsm1 (Figure 5.17B). This reinforces the notion that DDX6, unlike other P-body proteins, is essential for formation of these foci. However, these cells could not be used for further replication studies, as their rate of growth was significantly slower than the control cell line, making direct comparisons difficult. Because of this the Lsm1 knockdown cells were used instead. Although the P-body phenotype was not as extensive as would be required to determine the effects of these foci on HIV-1 replication, the extent of the protein knockdown itself was considerable. Two groups have claimed that loss of Lsm1 leads to an increase in both virus production and infectivity (Chable-Bessia et al., 2009; Nathans et al., 2009), therefore the effects of Lsm1, rather than P-bodies in general, are assessed in the following experiment.

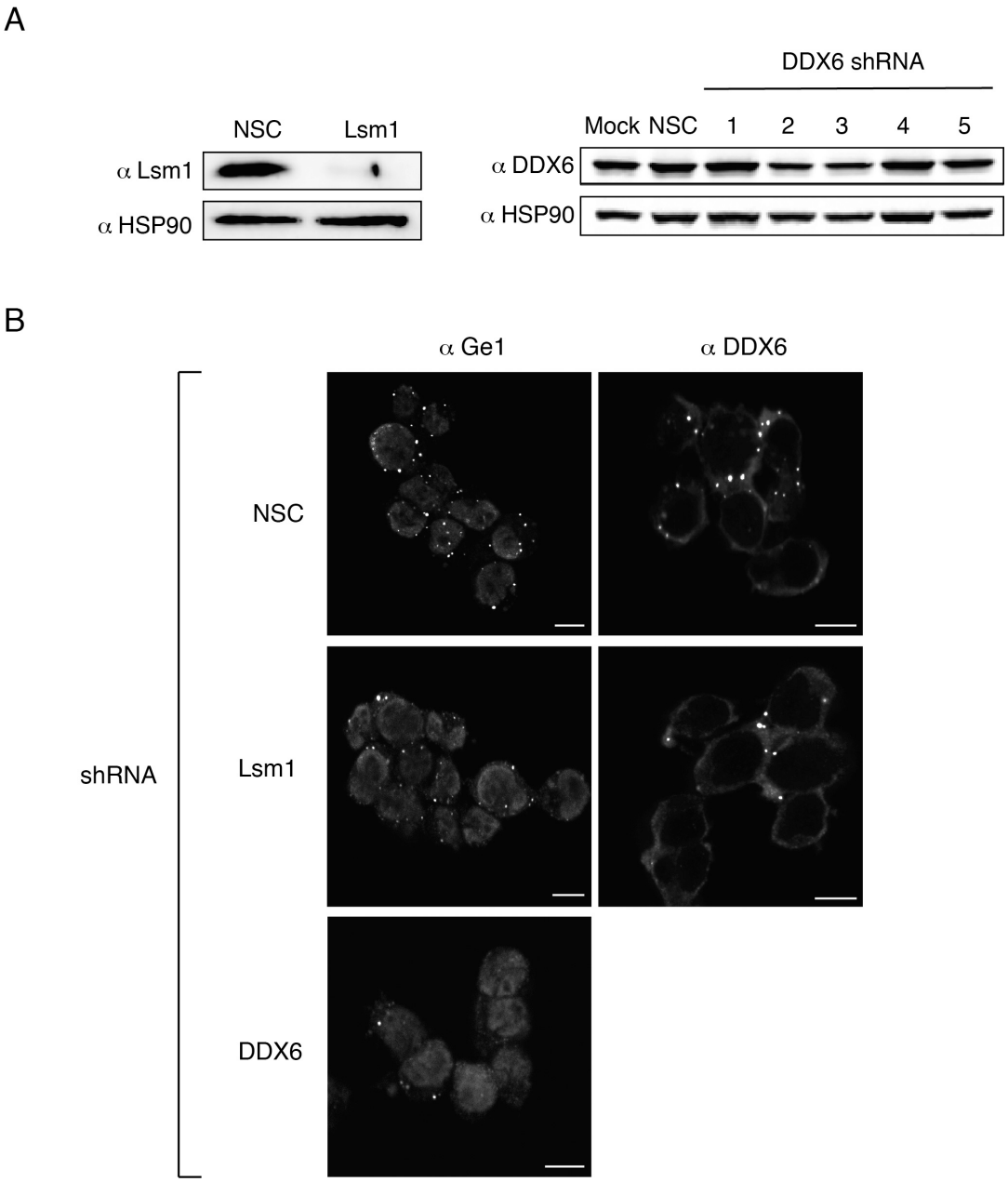

Figure 5.17: Phenotypic analysis of Lsm1 and DDX6 knockdown in Hut78 cells.

Hut78 cells were transduced with lentiviral vectors encoding shRNAs targeting either DDX6 (1 - 5), Lsm1 or a non-silencing control (NSC). Transduction efficiencies were determined by analysis of GFP expression and cells were maintained under puromycin selection for 5 - 7 days before immunoblot and immunofluorescence analysis. **A**. Immunoblot analysis of transduced cells to check levels of protein expression, with anti-Lsm1 (left panel) or anti-DDX6 (right panel) antibodies. An anti-HSP90 antibody is included in both cases as a loading control. **B**. Immunofluorescence analysis of transduced cells to check levels of P-body depletion. Coverslips were coated in Poly-L-lysine and dried overnight. Hut78 cells were then plated onto coverslips and 24 hours later were fixed, permeabilised and stained with either a mouse anti-Ge1 or a rabbit anti-DDX6 primary antibody and then appropriate Alexa-Fluor 594 conjugated secondary antibodies. Coverslips were mounted, dried overnight and imaged using a Leica confocal microscope. Scale bar = 10 μm.

5.7.2 Lsm1 knockdown and effects on HIV-1 replication and A3G anti-viral activity

The cell lines described in Figure 5.17 were infected with $p24^{Gag}$ corresponding to 25 ng of either wild-type or Δ*vif* virus, produced in 293T cells. The cells were then extensively washed to remove any input virus and re-suspended in fresh medium. Supernatant was harvested every two days post infection and quantified by $p24^{Gag}$ ELISA. Cell lysates were collected in parallel and subjected to immunoblotting to determine protein expression levels.

Virus production steadily rose, peaked at days 4 - 6 and then began to decline at day 8 (Figure 5.18A). The replication kinetics of both the Lsm1 knockdown and control cell lines was nearly identical when infected with wild-type virus. Similarly, A3G inhibition of the replication of the Δ*vif* virus appears to be unperturbed by Lsm1 depletion as a 2 log decrease in $p24^{Gag}$ production is observed for both cell lines over the course of the assay. These results were reproducible even when cells were infected with higher (125 ng) and lower (5 ng) virus titres (Figure 5.18B). Immunoblots confirm that knockdown of Lsm1 was maintained throughout the replication cycle (Figure 5.18C). This indicates that in ongoing replication, as well as single cycle infectivity assays, Lsm1 is neither necessary nor inhibitory for HIV-1 replication or A3G anti-viral activity.

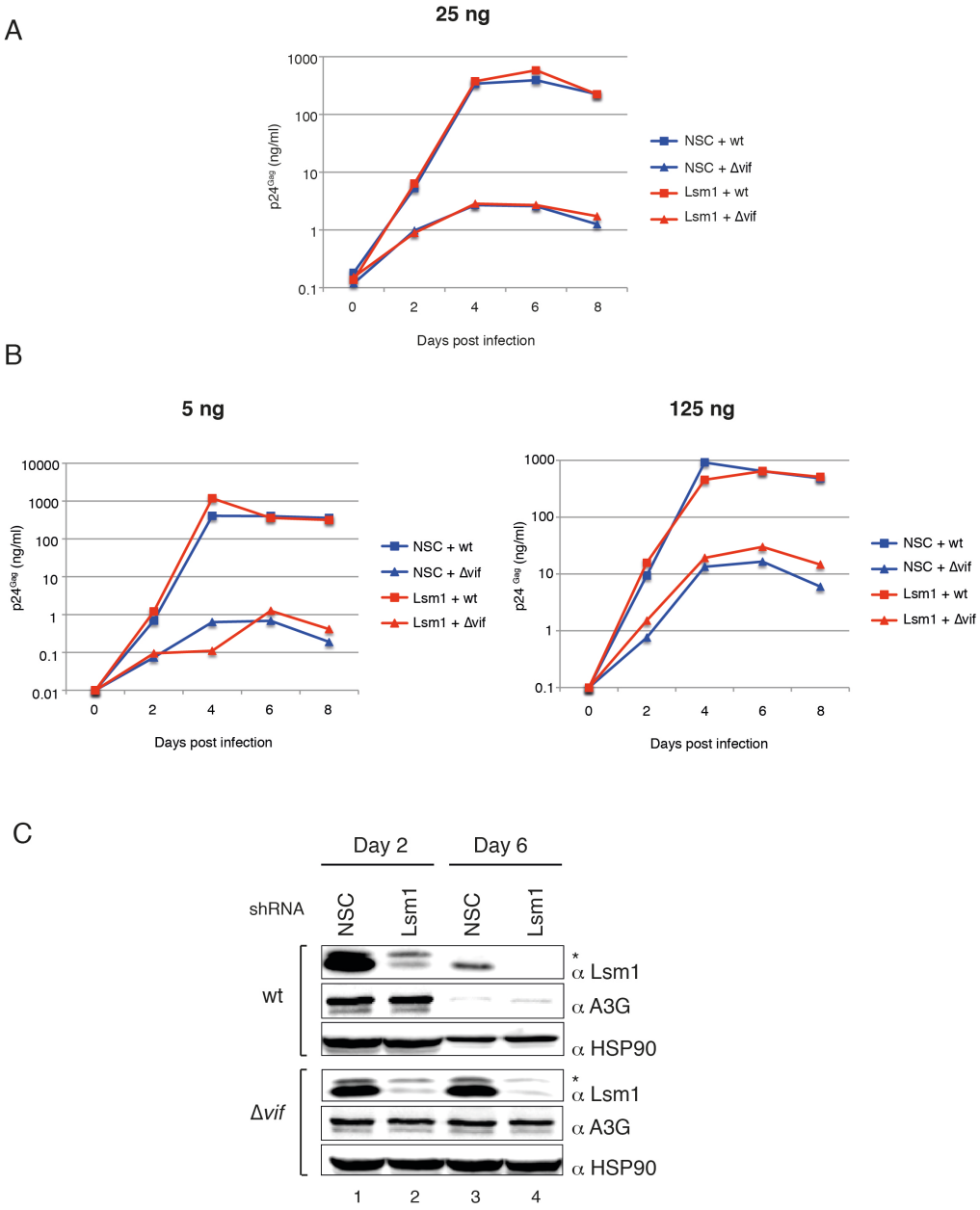

Figure 5.18: Knockdown of Lsm1 does not affect HIV-1 replication or endogenous A3G anti-viral activity.

Hut78 cells transduced with either an Lsm1 targeting (Lsm1) or non-silencing control (NSC) shRNA encoded lentiviral vector (generated as described for Figure 5.17) were infected with $p24^{Gag}$ corresponding to 5 ng, 25 ng or 125 ng of either wild-type (wt) or Δ*vif* NL43 virus produced in 293T cells. 4 hours later cells were extensively washed and re-suspended in complete RPM1. Every 2 days, cells were pelleted and a sample of supernatant collected for analysis of virus production by $p24^{Gag}$ ELISA and fresh media added. Cell lysates were also collected for immunoblot analysis. **A**. Virus production from transduced cells infected with 25 ng of input virus, monitored over 8 days, as determined by $p24^{Gag}$ ELISA. **B**. Virus production from transduced cells infected with 5 ng (left graph) or 125 ng (right graph) of input virus, monitored over 8 days, as determined by $p24^{Gag}$ ELISA. **C**. Immunoblot analysis of protein expression from transduced cells described in A at days 2 and 6 post infection. * denotes the position of a background band. Data are representative of two independent experiments.

5.8 Sub-cellular localisation of HIV-1 genomic RNA and Gag

5.8.1 Assessment of HIV-1 genomic RNA localisation to P-bodies

In support of claims as to the relevance of P-bodies to HIV-1 infectivity and virus production, both Nathans *et al* and Chable-Bessia *et al* report that HIV-1 genomic RNA (gRNA) is found to localise to P-bodies. Since the data presented thus far fails to substantiate their initial findings, it was important to determine whether viral components could be detected at these cytoplasmic foci. To investigate this, a proviral construct was created based on the MS2-bacteriophage tethering system (Bertrand et al., 1998; Jouvenet et al., 2009). A wild-type NL43 construct was engineered so as to contain 24 binding loops from the bacteriophage MS2 coat protein. These loops were introduced at the end of the Gag reading frame (Figure 5.19A). Co-expression of an MS2-YFP fusion protein then allows HIV-1 gRNA to be tracked in cells through detection of YFP fluorescence. The high affinity between the MS2 protein and the binding loops has made this system remarkably useful for visualising RNA in both living and fixed cells.

HeLa cells were thus co-transfected with equal amounts of the 24xMS2 NL43 construct and the MS2-YFP plasmid. 24 hours later cells were fixed, permeablised and stained with anti-GFP (to enhance the YFP signal) and anti-DDX6 (as a marker for P-bodies) primary antibodies and appropriate secondary antibodies. Coverslips were then mounted, dried and imaged using a Leica confocal microscope. As shown (Figure 5.19B), expression of the MS2-YFP fusion protein alone displayed a characteristic nuclear localisation due to the presence of a nuclear localisation signal (NLS). With co-expression of the NL43 proviral construct however, a more cytoplasmic distribution was evident along with significant particle formation and a more elongated morphology of the infected HeLa cell (Figure 5.19C). However, no localisation with DDX6 foci (in red) was observed in any of the cells imaged. This implies that HIV-1 gRNA does not accumulate at DDX6 marked P-body foci.

A

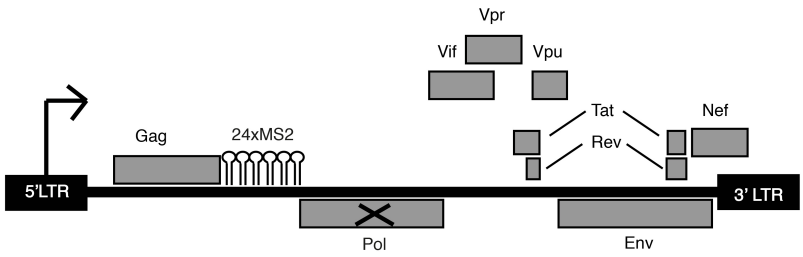

B

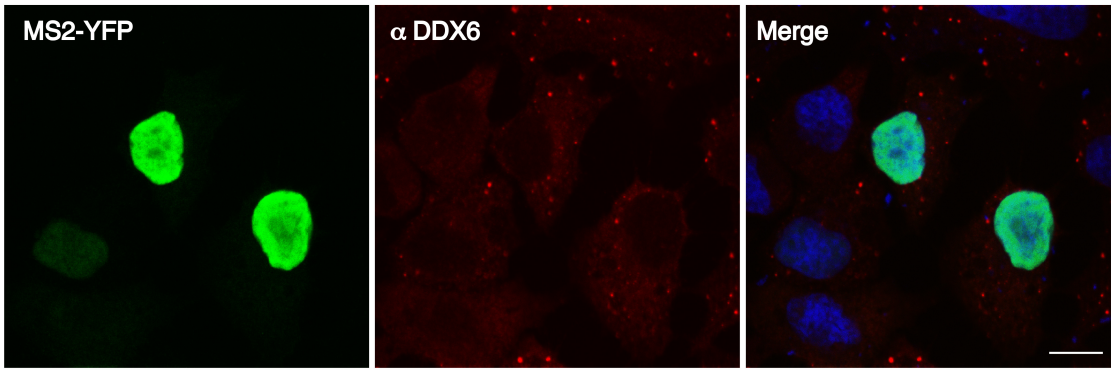

C

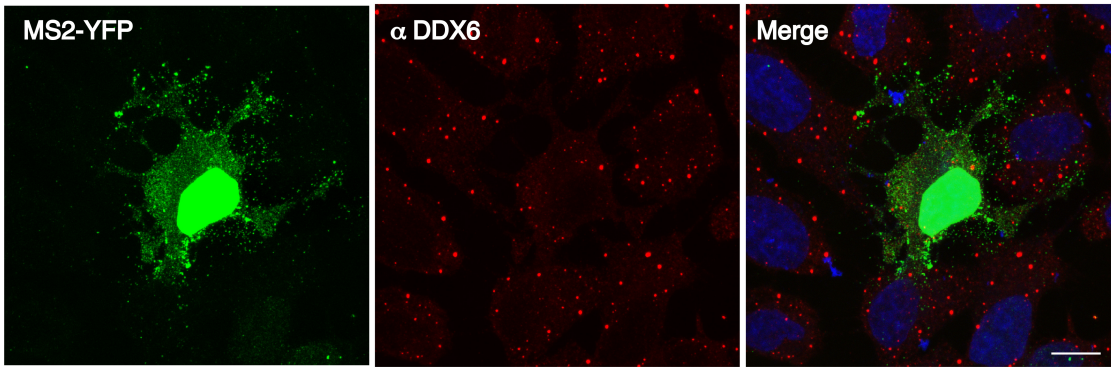

Figure 5.19: MS2 tethered HIV-1 genomic RNA does not co-localise with the P-body protein DDX6.

A. Schematic diagram of the MS2 tethered proviral construct used in this study to visualise HIV-1 genomic RNA. 24 MS2 binding loops from the coat protein of the MS2 bacteriophage were introduced at the end of the Gag reading frame in an NL43 proviral plasmid. Expression of Pol is disrupted and thus some experiments were also performed with complementation using wild-type virus. Co-expression of an MS2-YFP fusion plasmid, which binds with high affinity to the MS2 binding loops, allows visualisation of the HIV-1 viral RNA. **B**. HeLa cells were co-transfected with equivalent amounts of an MS2-YFP expression plasmid and an untagged Luciferase plasmid as a control. **C**. HeLa cells were co-transfected with equivalent amounts of an NL43 provirus containing 24xMS2 binding loops (as described in A) and an MS2-YFP fusion plasmid. For both B and C, cells were fixed 24 hours after transfection, permeabilised and stained with a mouse anti-GFP and a rabbit anti-DDX6 primary antibody and then anti-mouse 488 and anti-rabbit-594 secondary antibodies. Cells were also stained with DAPI for visualisation of the nucleus. Coverslips were then mounted, dried overnight and imaged using a Leica confocal microscope. Images are compilations of between 6-10 z-stacks, with merged images presented on the right. Scale bar = 10 μm.

5.8.2 Assessment of HIV-1 Gag localisation to P-bodies

Following this, a second construct, this time containing both the MS2 binding loops and Cherry fluorescent protein fused in frame with Gag (Figure 5.20A), was used in order to determine localisation of the viral Gag protein. In this case, co-localisation with both the DDX6 (Figure 5.20B) and Ge1 (Figure 5.20C) P-body proteins was evaluated. Gag localisation showed a characteristic cytoplasmic distribution with more intense staining at the plasma membrane. This is consistent with data detailing the plasma membrane as the main site of Gag driven viral assembly. Once again, no localisation of Gag was observed at either DDX6 or Ge1 marked foci (Figures 5.20A and B). In sum, HIV-1 viral components, neither gRNA nor Gag, are found to co-localise with two different P-body proteins indicating that they do not associate with these foci in cells.

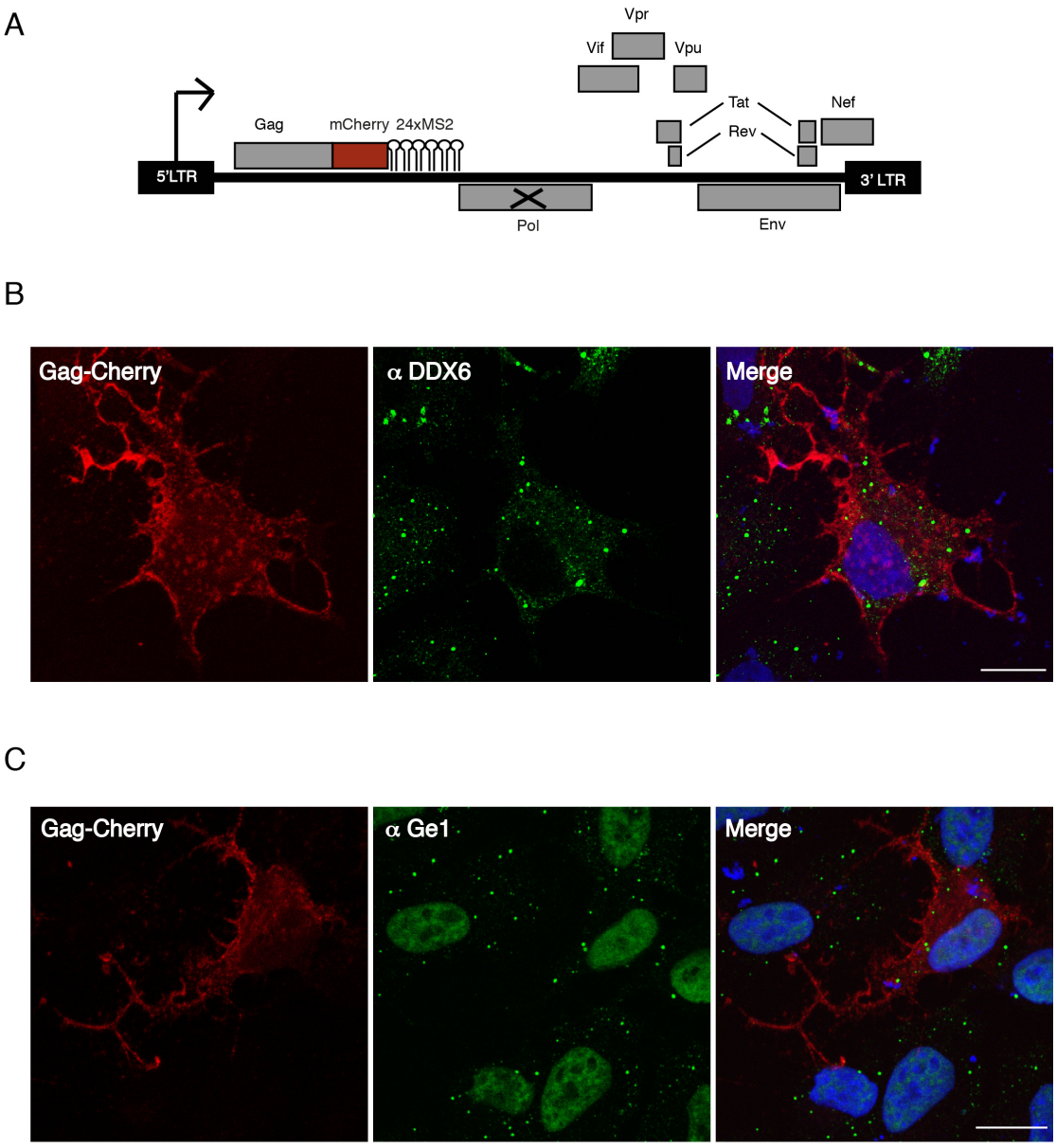

Figure 5.20: HIV-1 Gag does not co-localise with the P-body proteins DDX6 and Ge1.

A. Schematic diagram of the Gag-Cherry fusion proviral plasmid used in this study. The NL43 provirus is the same as that described in Figure 5.19 containing 24xMS2 binding loops but it also contains an additional sequence encoding Cherry fluorescent protein, fused in frame with Gag. Expression of Pol is disrupted and thus some experiments were performed with complementation using wild-type virus. **B** and **C**. HeLa cells were transfected with 0.5 µg of an NL43 24xMS2 Gag-cherry proviral plasmid, as described in A and 0.5 µg of a myc-tagged luciferase expression plasmid. 24 hours later, cells were fixed, permeabilised and stained with either a rabbit anti-DDX6 (B) or a mouse anti-Ge1 (C) primary antibody and then the appropriate Alexa-Fluor 488 conjugated secondary antibody. Cells were also stained with DAPI for visualisation of the nucleus. Coverslips were then mounted, dried overnight and imaged using a Leica confocal microscope. Images are compilations of between 6-10 z-stacks, with merged images displayed on the right. Scale bar = 10 µm.

5.9 Discussion

Results presented in Chapter 3, section 3.4 revealed that several APOBEC3 proteins localised with Ago2 to cytoplasmic P-body structures. Since this correlated with their anti-viral phenotypes, it was important to determine the functional implications of this localisation. Here it is shown that disruption of P-bodies has no observable impact upon APOBEC3 mediated viral inhibition. Further, P-bodies and P-body components do not appear to regulate HIV-1 replication and viral components could not be detected at these foci, as has been previously proposed. Therefore the relevance of APOBEC3 localisation to these structures remains unresolved and requires further investigation.

It is clear from the results presented in this study that HIV-1 replication is not influenced by P-bodies. It is important to make the distinction between the effects of individual proteins and P-bodies in general because as shown, knockdown of DDX6 but not Lsm1 led to a modest increase in virus production in certain experimental settings (section 5.5). This suggests that this effect is specific to loss of DDX6. Other groups have noted similar but weaker effects on HIV-1 particle production with knockdown of Lsm1 and Ago2 (Chable-Bessia et al., 2009; Nathans et al., 2009), which was not observed here. The reason for this discrepancy as well as the failure to reproduce this effect in a slightly different experimental context (section 5.4) is unclear but it does point to a possible weakness of the observed phenotype. An alternative explanation is that the efficiency of infection is altered in the knockdown cell lines. However, the increase in $p24^{Gag}$ production in the DDX6 knockdown cell lines in transient transfection experiments, though modest, was consistently observed (Figure 5.11). Nathans *et al* argue that this effect is specific to HIV-1 protein production as they only see a very slight change in GFP protein levels, with no change in mRNA levels for both constructs. Preliminary results from pulse labelling experiments (section 5.5.3) seem to indicate that this phenotype is most likely due to the general stimulation of global cellular translation upon reduction of the DDX6 protein, which is a known translational repressor (Coller and Parker, 2005). This is supported by the fact that certain plasmids appear to be slightly better expressed in the DDX6 depleted cell lines (Figure 5.6). Jangra *et al* also noted an increase in cellular translation rates upon DDX6 knockdown, though not in HeLa cells, as were tested here (Jangra et al., 2010). It is important to note however, that this apparent increase in protein synthesis is not accompanied by an increase in steady state levels of intracellular Gag as determined by western blot (see

Figures 5.11 and 5.12). Therefore a pulse chase analysis to track the fate of the RNA and Northern blot analysis to determine whether the RNA produced is more stable or whether translation is more efficient in the absence of DDX6 would be required to fully understand the nature of this phenotype. In essence, although an increase in $p24^{Gag}$ production was consistently observed in transient transfection experiments, the fact that it could not be observed in the more physiologically relevant context of infection based methods implies that it may not be relevant *in vivo*.

Viral infectivity was also assessed and in all methods tested, no influence of P-bodies, either positive or negative was observed. This is in disagreement with two recently published reports. However when Chable-Bessia *et al* conducted these experiments by transient transfection they also failed to see an effect of DDX6 or Lsm1 knockdown on HIV-1 infectivity. Nathans *et al* looked in target, not producer cells and the magnitude of the effects found in this case was only two fold. The work described here also specifically looked at HIV-1 replication in the context of Lsm1 depletion (section 5.7). It would be expected that any small differences in viral production and the quality of the viruses produced would be magnified when monitoring $p24^{Gag}$ production over several days. However no such effects were observed, even when a very efficient depletion of Lsm1 protein levels was obtained. This once again questions the validity of the phenotypes reported by both groups.

Finally, viral localisation to P-bodies was also evaluated as several groups have reported that viral RNA can localise to P-bodies (Chable-Bessia et al., 2009; Martin et al., 2011; Nathans et al., 2009). It is generally believed that the majority of virion assembly takes place at the plasma membrane and that Gag and gRNA must traffic to these sites in order to form particles. However, how they are directed there and whether they pass through cytoplasmic foci, such as P-bodies, beforehand is unknown. In yeast, P-bodies have been found to be associated with the plasma membrane (Beckham et al., 2007), thus linking them to sites of viral assembly. Whether the same is true in human cells remains to be determined but it is interesting to note that Ago2 was originally reported to localise to the plasma membrane (Cikaluk et al., 1999). Also, localisation of viral RNA and Gag to P-bodies would provide an opportunity for A3G to interact with these components, which is necessary for its virion encapsidation. However, it was discovered that neither HIV-1 gRNA nor Gag localised with endogenous P-body proteins using an MS2 tethering system (section 5.8). This lack of co-localisation is in

keeping with the data presented thus far in this study relating to the role of P-bodies in HIV-1 replication, and is also supported by other published reports (Abrahamyan et al., 2010; Burnett and Spearman, 2007). This is, however, in contrast to the work of both Chable-Bessia *et al* and Nathans *et al*. In the former study although they also use an MS2 tethering system, they do so in the context of a HIV-1 vector, rather than in the more biologically relevant context of a proviral plasmid, as was used here. Nathans *et al*, on the other hand, used fluorescent *in situ* hybridisation (FISH) and determined localisation with ectopic expression of an A3G-YFP construct, rather than with endogenous P-body markers. However only one representative example is shown of co-localisation at a P-body structure and therefore the generality of this finding cannot be determined. Also a FISH/IF co-analysis of HIV-1 RNA by Levesque *et al* (2006) did not produce the same punctate distribution described by Nathans *et al*. Differences in experimental procedure may account for the discrepancy in results but it is unclear why co-localisation would not be observed with an MS2 tethering system as it has been successfully used by others to track HIV-1 gRNA and Gag localisation (Jouvenet et al., 2009). Alternatively, viral RNA may be localising to other punctate foci in the cell that may potentially partially overlap with P-bodies and stress granules. Abrahamyan *et al* have reported that Staufen RNP complexes, formed in response to HIV-1 infection, contain both Gag and gRNA. They also claim that depletion of Staufen leads to a reduction in viral RNA encapsidation, hence highlighting a role for these foci in infectious particle production. The authors do note that these structures are distinct from P-bodies and stress granules but Staufen is able to localise to stress granules and A3G has been reported to partially overlap with Staufen (Martin et al., 2011). Therefore the conflicting findings relating to gRNA and Gag localisation to P-bodies may be complicated by the nature of the foci that are under observation. Various different P-body markers should therefore be used to formally verify that the foci are in fact mRNA Processing bodies and not other types of RNA granules with which P-body components may partially associate (Kedersha et al., 2005; Kulkarni et al., 2010).

The role of P-bodies and P-body components in the anti-viral action of the APOBEC3 proteins was investigated by numerous different approaches in terms of P-body depletion (shRNAs and siRNAs), virus input (transfection and infection based assays) and measure of outcome (single cycle infectivity assays and ongoing replication). Since all of these methods yielded the same conclusion, that APOBEC3 anti-viral activity was

unperturbed by P-body protein knockdown, it strongly reinforces the point that P-bodies are not necessary for this aspect of APOBEC3 function. This is supported by the work of Chable-Bessia *et al* who also found that knockdown of DDX6 and Lsm1 had no effect on A3G anti-viral activity. Here, the whole APOBEC3 family was investigated as well as specifically determining that these proteins were still packaged in the absence of P-bodies and conversely that A3G packaging defective mutants could still localise to these foci (section 5.2). This latter finding is corroborated by a recently published report (Martin et al., 2011). This refutes speculation that P-bodies are sites of APOBEC3 virion incorporation and potentially viral assembly. This is also in agreement with the work of Soros *et al*, who found that it is newly synthesised A3G that is specifically incorporated into HIV-1 particles and not that which is associated in high molecular weight RNP complexes (Soros et al., 2007). Intriguingly, another cellular protein known to regulate HIV-1 replication, Mov10, has also been found to associate with P-bodies. Mov10 is a putative RNA helicase which interacts with components of the RISC complex (Meister et al., 2005) as well as A3F and A3G in an RNA dependent manner (Gallois-Montbrun et al., 2007; Kozak et al., 2006). Its overexpression has been shown to potently inhibit wild type HIV-1, as well as SIV and MLV, by an as yet unidentified mechanism, though it has been reported to associate with viral cores and is packaged into virions (Chertova et al., 2006; Furtak et al., 2010; Wang et al., 2010). Therefore it remains to be determined why such modulaters of HIV-1, as well as other viruses, localise to these structures. The anti-viral protein Trim5α is also known to associate with cytoplasmic bodies (Stremlau et al., 2004). The nature of these bodies, which are distinct from P-bodies (Campbell et al., 2007), appears to be dependent on Trim5α oligomerisation rather than on protein-RNA complexes. Whether these bodies are important for Trim5α mediated restriction is the subject of much debate but it has been reported that pre-existing bodies are not required for this activity (Song et al., 2005). Others have shown that Trim5α aggregates form in response to viral infection (Campbell et al., 2008), which adds to the mystery surrounding the significance of foci formation for cellular restriction factors. A recent publication has claimed that A3G complex formation inhibits HIV-1 viral particle production and that dissolution of these foci, which partially overlap with P-bodies, increases virus output from these cells (Martin et al., 2011). However, these A3G 'complexes' are dependent on the presence of DDX6, which when knocked down itself can result in an increase in virus production (Figure 5.11). Therefore the distinction between A3G and DDX6 foci appears to be

strained and in the data presented in Chapter 3, section 3.4 these two proteins show significant overlap. The fact that in this study HIV-1 Gag failed to accumulate at DDX6 marked bodies further disagrees with the conclusions of Martin *et al*. Also overexpression of A3G, and more prominently other APOBEC3 proteins such as A3C (for example see Figure 5.11), is slightly inhibitory to virus production and thus is not likely the result of foci formation. In sum, the localisation of A3G and other APOBEC3 proteins does not appear to be relevant to their anti-viral phenotypes, yet the association of viral inhibitors with cytoplasmic foci is intriguing and merits further investigation.

It is conceivable that APOBEC3 localisation to these structures may be more relevant to restriction of other viruses and endogenous retroelements. Several P-body components have been implicated in the replication of a diverse array of viruses as discussed in Chapter 1, section 1.9. Significantly, in yeast, A3G localisation to P-bodies appears to be important for its packaging and hence restriction of the Ty1 retrotransposon (Dutko et al., 2010; Dutko et al., 2005; Esnault et al., 2005). However no correlation has been found in human cells between APOBEC3 inhibition of retrotransposition and P-body association for example (Niewiadomska et al., 2007). On the other hand it has been reported that A3G restricts Alu retrotransposition by sequestering these elements away in high molecular weight complexes (Chiu et al., 2006). Thus similar results may be achieved if the APOBEC3 proteins are able to recruit these transcripts to P-bodies.

Additionally P-body localisation may be a result of a more general involvement of the APOBEC3 proteins in cellular RNA regulation, rather than being related to their anti-viral activity. Other P-body components have fundamental roles in the metabolism and turnover of RNA, thus implying that the APOBEC3 proteins could also be part of such processes. As discussed in Chapter 4, though no specific role of the APOBEC3 proteins in RNAi and ARE mediated decay was revealed, description of APOBEC3 associated RNAs, both mRNA and small RNAs, including miRNAs, may provide insight into potential targets. This can be achieved through techniques such as cross-linking combined with co-immunoprecipitation (CLIP). Preliminary work by Kozak *et al* has already identified several mRNA species that interact with A3G, including its own mRNA, indicating a degree of self-regulation (Kozak et al., 2006). Several small RNAs such as Alu, 7SL and Y RNAs are also known to interact with A3G (Gallois-Montbrun et al., 2007). 7SL, for instance, has been postulated to mediate A3G virion incorporation. Thus the identification of associated RNAs can provide greater insight into A3G

activity and functional control. Further examination of the possible role of APOBEC3 proteins in the control of RNA is required to address these points and how this may impact upon their sub-cellular localisation.

Furthermore APOBEC3 localisation to P-bodies may be a means of regulating their function and preventing them from editing cellular DNA targets as proposed for A3G recruitment into high molecular weight RNP complexes (Chiu et al., 2006). Several APOBEC3 proteins may be able to target DNA viruses such as herpes viruses and human papilloma virus (Suspene et al., 2011b; Vartanian et al., 2008) as well as other types of foreign DNA (Stenglein et al., 2010). What regulates their enzymatic activities such that they do not hypermutate genomic DNA remains to be determined. Recently A3A alone has been reported to edit nuclear DNA (Stenglein et al., 2010; Suspene et al., 2011a), and it is interesting to note that it is the only APOBEC3 protein that does not associate with P-bodies (Chapter 3, section 3.4).

Finally, it has also been suggested that smaller P-body structures exist within the cell, not visible by light microscopy that can persist after the dissolution of larger visible foci by targeted protein knock down. This means that although microscopically visible P-bodies may have been eliminated, the APOBEC3 proteins may still be interacting with P-body proteins in smaller, less visible foci. This has been used as an explanation as to why the disappearance of P-bodies does not appear to impact on RNA regulatory processes such as miRNA mediated repression, siRNA silencing, NMD or AMD. However these effects can also be explained by the fact that RNA decay can occur co-translationally and thus separate from that which occurs in P-bodies (Hu et al., 2010). The existence of smaller, microscopically undetectable P-body structures is obviously difficult to verify and therefore remains undetermined at present. Whether these foci would actually be classified as P-bodies is also a matter of debate (Eulalio et al., 2007b). Overall, the relevance of APOBEC3 localisation to P-bodies in terms of functional significance requires further exploration.

In summary, P-bodies and P-body components do not appear to influence APOBEC3 anti-viral activity. They are also unlikely to be the sites of APOBEC3 virion incorporation or viral assembly as efficient packaging was maintained in the absence of these foci and HIV-1 viral components were not found to localise to them. Loss of P-bodies and associated proteins also failed to have any impact upon HIV-1 infectivity and only modestly influenced virus production in certain circumstances. This would

argue against microscopically visible P-bodies being inhibitory to HIV-1 replication. Therefore, the relevance of APOBEC3 association with P-bodies and related proteins is unresolved and may be linked to an as yet undefined cellular or regulatory role.

CHAPTER 6

DISCUSSION AND FUTURE WORK

6. DISCUSSION AND FUTURE WORK

6.1 Outstanding questions concerning the APOBEC3 family

The discovery of the antiviral protein, APOBEC3G, and its family members, nearly ten years ago, unearthed a previously unknown mechanism of host mediated innate resistance against invading pathogens. It had been well established that viruses, such as HIV-1, utilised cellular factors for their own benefit and often to the detriment of the host, but cells have evolved multiple means of limiting their replication at various stages of their life cycle. It is clear that co-evolution between host and pathogen has dramatically shaped both genomes, and in trying to understand these evolutionary pressures we have gained a better understanding not just of the biology of the pathogen, and what it must do in order to survive and propagate, but also that of the cell. Research into HIV-1 and other viruses has provided invaluable insight into processes such as reverse transcription, nuclear trafficking and oncogenesis to name a few, which has subsequently enabled targeted and effective drug development. It is well known that A3G and other APOBEC3 proteins induce mutations into the HIV-1 cDNA during reverse transcription via their cytidine deaminase capabilities. This compromises the production of replication competent progeny virions and thus impedes further replication of the virus. In defence of its own genome, the viral protein Vif has evolved to target these proteins for degradation, thereby preventing their incorporation into nascent virions and repressing their anti-viral effects. However, there is still much to be learnt and the work presented in this study aimed to further characterise the APOBEC3 family as both viral restriction factors and as cellular proteins.

The APOBEC3 proteins differentially regulate the fate of a diverse range of exogenous viruses and endogenous retroelements but the factors that contribute to their target substrate specificities have not yet been determined. The association of A3F and A3G, the two most potent anti-HIV-1 proteins, in large ribonucleoprotein complexes and their localisation to discrete cytoplasmic foci, implicates both interacting cellular proteins and sub-cellular localisation as influencing functional activity. Further, these factors have also postulated a potential cellular role for the APOBEC3 proteins, which remains largely undefined, in the regulation of RNA. However, their contribution to this process has not been fully explored. Therefore, the data presented in the preceding chapters has

sought to address some of these outstanding issues with an attempt to gain new insight into APOBEC3 activity.

6.2 Importance of cellular factors for APOBEC3 anti-viral activity

6.2.1 APOBEC3 interaction with Argonaute 2

Research is often focused on A3G, as it is the most potent anti-HIV-1 APOBEC3 protein. However, in order to better understand functional differences between the different family members, the whole family needs to be assessed in the same experimental context. This was an important and necessary feature of the work presented in this study. The APOBEC3 proteins do not all inhibit HIV-1 infectivity and neither do they do so to the same extent (Chapter 3, Figure 3.2), but their anti-HIV-1 phenotypes do positively correlate with their packaging into virions (Chapter 3, Figure 3.3). Identification of factors that regulate virion encapsidation, and hence anti-viral activity, is therefore crucial to comprehend their differential phenotypes. An important contributory factor to these differences may be their interactions with cellular components, which could potentially act as co-factors or regulators of their anti-viral activity. Although A3F and A3G associate with a diverse array of RNA binding proteins (Chiu et al., 2006; Gallois-Montbrun et al., 2008; Gallois-Montbrun et al., 2007; Kozak et al., 2006; Wichroski et al., 2006), the Argonaute proteins, in particular, make attractive candidates for this role as they are closely associated with A3F and A3G in a partially RNase insensitive manner (Gallois-Montbrun et al., 2007). Across the whole APOBEC3 family, however, interactions with Ago2 did not precisely correlate with anti-viral phenotypes, although the most inhibitory APOBEC3 proteins, A3F, A3G and A3H, did interact most strongly with Ago2 (Chapter 3, Figure 3.4). This would suggest that APOBEC3 anti-viral function is independent of Ago2. More definitive confirmation of this was obtained when it was shown that knockdown of Ago2 had no effect on APOBEC3 mediated HIV-1 inhibition (Chapter 4, Figures 4.4 and 4.5). More importantly it rules out the necessity of Ago2's endonuclease activity, which is not shared by the other Argonaute proteins, for APOBEC3 function.

An important point to note is that results from natural endogenous reverse transcription (NERT) reactions demonstrate that no target cell factors are required for A3G inhibition of HIV-1 and thus any required cellular proteins would have to be encapsidated, along

with A3G, into HIV-1 particles from virus producer cells (Bishop et al., 2008). It has been determined that it is newly synthesised A3G which is incorporated into virions and not the cellular pool that is contained within high molecular mass RNP complexes (Soros et al., 2007). This means that cellular proteins that may regulate APOBEC3 anti-viral activity are not necessarily dependent on A3G for their virion incorporation. Ago2 was originally identified as a membrane associated protein (Cikaluk et al., 1999) and recent reports have localised Ago2, and more prominently GW182, to endosomes and multi-vesicular bodies (MVBs), which appears to be important for miRNA mediated repression (Gibbings et al., 2009; Lee et al., 2009). These data indicate that Ago2 has the potential to be incorporated into viral particles. However, to date, no such reports have been published and preliminary work, not presented here, suggests that Ago2 is not packaged into virions at detectable levels. In combination this data would lead to the conclusion that Ago2, specifically, is not required for the restriction of HIV-1 as mediated by the APOBEC3 proteins.

6.2.2 APOBEC3 interaction with PIWI proteins

Whether the Argonaute proteins are required for APOBEC3 inhibition of other viruses or viral elements has not been addressed. It has been found that A3F and A3G (and potentially other APOBEC3 proteins) are highly expressed in the testis and ovary (Koning et al., 2009) and so they may act to protect the germline from the potentially deleterious effects of endogenous retroelements. The Argonuate family members, the PIWI proteins, are similarly expressed in the germline and are actively involved in inhibiting retrotransposition events by RNA silencing. Whether the APOBEC3 proteins interact with the PIWI proteins and can co-ordinate with them to defend the germline is currently unknown but would be an interesting issue to resolve, especially as several APOBEC3 proteins can very effectively restrict retrotransposition events in somatic cells. In fact, in *Drosophila*, PIWI interacting small RNAs (piRNAs) have been found in cytoplasmic foci that contain proteins normally associated with P-bodies in somatic cells, such as Dcp1a, Dcp2 and ME31B (the *Drosophila* homologue of DDX6), implying that the PIWI proteins may engage a similar set of proteins as their Argonaute counterparts (Lim et al., 2009). Similar results have also been reported in mice (Aravin et al., 2009). Alternatively the APOBEC3 and PIWI proteins may invoke distinct mechanisms of inhibition that may target different types of retrotransposons or that may

be utilised under different circumstances. Further work will be required to clarify these issues.

6.2.3 APOBEC3 interaction with other identified cellular proteins

Although Ago2 may not be involved in APOBEC3 anti-viral activity, other cellular factors may contribute to this function. One interesting candidate is the anti-viral zinc finger protein ZAP1, which has been shown to interact with A3G in a partially RNase independent manner (Kozak et al., 2006), akin to the Argonaute proteins. ZAP1 was first identified as inhibiting the replication of MLV, through depletion of viral messenger RNA from the cytoplasm of infected cells (Gao et al., 2002; Guo et al., 2004). Subsequently it has been reported that ZAP1 interacts with and utilises both the 3' - 5' and 5' - 3' mRNA degradation pathways to mediate a similar effect against HIV-1 (Guo et al., 2007; Zhu et al., 2011). Its interaction with Dcp1a, Dcp2 and Xrn1 is particularly interesting as, along with A3G, these proteins localise to P-bodies. Whether ZAP1 displays a similar subcellular localisation remains to be determined, as does the functional relevance of its interaction with A3G, with particular focus on anti-viral defence. In light of this it is important to note that the anti-viral factor Mov10 interacts and co-localises with A3G and is packaged into HIV-1 virions (Chertova et al., 2006; Gallois-Montbrun et al., 2007; Kozak et al., 2006; Wichroski et al., 2006). Yet these proteins do not work in tandem to mediate HIV-1 inhibition and instead represent independent modes of viral resistance (Burdick et al., 2010).

Upf1, which mediates NMD, is another potential candidate as it is necessary for A3G directed inhibition of the Ty1 retroelement in yeast (Dutko et al., 2010). It has been identified in A3G containing RNP complexes (Kozak et al., 2006) and localises to P-bodies but further work would be required to establish whether it is involved in the anti-HIV-1 activities of the APOBEC3 proteins.

6.3 APOBEC3 proteins and the miRNA pathway

Although the relevance of the miRNA pathway to APOBEC3 anti-viral activity was not specifically addressed in this study it is important to determine the role this pathway may play in their function. This can be achieved by targeted knockdown of essential components of this pathway, such as Dicer and GW182, or else simultaneous knockdown of all four Argonaute proteins, which has recently been reported (Roberts et al., 2011). This is of interest as there is increasing evidence to suggest that the miRNA pathway may be an important regulator in the control of virus replication in mammals, as it is in plants and invertebrates. Several groups have now shown that virally encoded miRNAs can be processed by cellular machinery to yield short noncoding RNAs that can be utilised by either the virus or the cell [reviewed in (Umbach and Cullen, 2009)]. This is especially true for DNA viruses such as herpes virus where a large number of miRNAs have now been identified (see Chapter 1, section 1.11.4). These results thus implicate miRNAs and the Argonaute proteins in the regulation of a number of different viruses, including HIV-1 although this remains controversial at present. However, the absence of an RNA dependent RNA polymerase in human cells means that the effects of individual miRNAs may be relatively inconsequential to viral replication. On the other hand, miRNAs and the Argonaute proteins can mediate the upregulation of protein expression as well as its downregulation (Vasudevan et al., 2007b). This is most evident for the replication of hepatitis C virus (HCV) which is dependent on the expression of the miR122 miRNA in liver cells for its replication (Jopling et al., 2005), and knockdown of the Argonaute proteins and/or Dicer leads to a decrease in HCV replication due to reduced HCV translation (Randall et al., 2007). These effects on HCV replication are also observed for other P-body and miRNA associated proteins (Scheller et al., 2009). This demonstrates that the miRNA pathway is not just involved in anti-viral defence but can be co-opted by viruses for their own benefit. In these cases, normally repressive translation machinery may be hijacked by the virus to instead promote translation. It has also been proposed that the subcellular localisation of Ago2 contributes to its dual functioning. Promotion of HCV replication is dependent upon recruitment to lipid droplets whereas suppression of this virus is associated with interactions with P-bodies (Berezhna et al., 2011). Whether the APOBEC3 proteins mediate a similar effect and whether they can work in conjunction or in opposition to these other proteins for HCV replication, for example, remains to be determined. An intriguing observation is that A3G expression appears to be elevated in the hepatocytes

and lymphocytes of infected HCV patients (Komohara et al., 2006). Thus it would be of relevance to determine firstly the role of the miRNA pathway in APOBEC3 function and secondly how these proteins may be involved in the restriction of other viruses, such as HCV, which appear to be heavily regulated by miRNAs and associated protein factors.

6.4 Importance of sub-cellular localisation for APOBEC3 anti-viral activity

6.4.1 P-bodies and APOBEC3 anti-viral activity

Another factor, which may influence APOBEC3 virion incorporation and hence anti-viral activity, is their subcellular localisation, and specifically localisation to P-bodies. In yeast, for example, A3G incorporation into Ty1 VLPs and hence restriction of Ty1 retrotransposition appears to be dependent upon its P-body localisation (Dutko et al., 2010). There does appear to be a positive correlation between anti-viral activity of the APOBEC3 proteins and localisation to these foci (Chapter 3, Figure 3.6). However, depletion of P-bodies through knockdown of DDX6 and Lsm1 did not substantially affect APOBEC3 virion incorporation or inhibition of HIV-1 (Chapter 5, sections 5.4 – 5.7). This indicates that microscopically visible P-bodies are not required for APOBEC3 packaging. Recently, it has also been reported that formation of A3G 'complexes', which substantially overlap with P-bodies, contribute to inhibition of HIV-1 virus production (Martin et al., 2011). Similar to the findings presented in Chapter 5, Figure 5.7, these A3G foci are dependent on the presence of DDX6 for their formation. Coupled with the fact that A3G and DDX6 foci show considerable overlap (Chapter 3, Figures 3.5 and 3.6), indicates that these A3G 'complexes' are in fact P-bodies. However, the authors conclude that it is the specific depletion of these A3G foci which mediates the effect on HIV-1 virus production. This is in opposition to what has been observed in this study as knockdown of DDX6, in a transient transfection system, consistently led to a modest increase in HIV-1 virus production regardless as to the presence or absence of A3G (Chapter 5, Figure 5.11).

6.4.2 P-bodies and APOBEC3 functional regulation

Although there did not appear to be a role for P-bodies in the antiviral activities of the APOBEC3 proteins, they may instead be required for alternative functions. An important question regarding the APOBEC3 family is whether they have other targets besides viral nucleic acid, and if so, how their function may be regulated such that they do not detrimentally mutate cellular genomic DNA, especially those proteins which localise to the nucleus. The regulation of APOBEC3 activity has already been documented in terms of high molecular weight RNP complexes and specific RNAs (Chiu et al., 2006; McDougall and Smith, 2011; Soros et al., 2007). Recently, Stenglein *et al* reported that several APOBEC3 proteins were capable of mutating foreign DNA species, thus preventing their accumulation and consequent deleterious effects. In this instance, editing of nuclear DNA was not observed, highlighting a degree of specificity in the actions of the APOBEC3 proteins (Stenglein et al., 2010). However, Suspene *et al* have since reported that A3A can deaminate nuclear DNA, particularly of genes implicated in cancers, with mutations subjected to cellular mismatch repair machinery (Suspene et al., 2011a). This demonstrates that nuclear DNA can be targeted by APOBEC3 proteins. On the other hand, only A3A has been reported to have this effect even though several APOBEC3 proteins localise to the nucleus and all have cytidine deaminase activity. With this in mind, it is especially intriguing that although A3A does localise to the cytoplasm, it is the only APOBEC3 protein which shows no association with P-bodies (Chapter 3, Figure 3.6). Therefore these foci could potentially be involved in limiting APOBEC3 enzymatic activity directed at nuclear DNA. Further work would be required to conclusively substantiate this theory.

6.4.3 APOBEC3 proteins and stress granules

As well as P-bodies, A3F and A3G are known to localise to stress granules in response to cellular stress. Other Argonaute interacting factors such as GW182, which is essential for miRNA mediated translational repression, does not relocate in this way (Kedersha et al., 2005). This demonstrates that the complex of proteins that shuttle between P-bodies and stress granules is specific and indicates that A3G may be involved in the regulation of translation related to the stress response. Stress granules are known to form in response to viral infection and thus APOBEC3 trafficking to these structures may be important for its anti-viral activity. It may be of significance that the ORF1p and ORF2p proteins of the LINE-1 retrotransposon accumulate in foci that overlap with

stress granules (Goodier et al., 2007). Thus they may be sites within which the APOBEC3 proteins interact with these retroelements. However, since viral infection stimulates the formation of stress granules, they may be more relevant to the control of exogenous viruses rather than endogenous retroelements. It would therefore be of interest to explore the movement of the APOBEC3 proteins between these foci in response to HIV-1 infection using real time imaging techniques. It has been reported that A3F can actually stabilise P-bodies and stress granules (Marin et al., 2008). Further, although several APOBEC3 proteins are resistant to Vif mediated degradation, namely A3A, A3B and A3C, their subcellular localisation appears to be altered by this viral protein (Marin et al., 2008). The reasons behind this are not clear but other groups have shown that Vif can localise to P-bodies but only when bound to an APOBEC3 protein. It may move with them to these sites before targeting them for degradation (Wichroski et al., 2005). Thus a complex interplay appears to exist between the cellular localisation of the APOBEC3 proteins, P-bodies and HIV-1 infection, which necessitates further investigation.

6.5 Cytoplasmic foci formation and anti-viral defence

6.5.1 P-bodies and HIV-1 replication

The hypothesis that P-bodies were sites of APOBEC3 virion incorporation relied on the assumption that these foci were also sites of viral assembly, or at least that viral components could traffic through them. Chable-Bessia *et al* and Nathans *et al* both reported the localisation of HIV-1 gRNA and/or Gag at P-bodies using MS2 tethering constructs and FISH respectively. It still remains unclear as to how these viral components are trafficked to the plasma membrane to initiate viral assembly and whether they may be spatially segregated within the cytoplasm. However, it seems unlikely that viral components transit through P-bodies or even that these foci are sites of viral assembly as neither Gag nor gRNA co-localised with DDX6 or Ge1, two well known P-body markers (Chapter 5, Figures 5.19 and 5.20). Other groups using slightly different experimental setups have reported similar findings (Abrahamyan et al., 2010; Burnett and Spearman, 2007). If HIV-1 viral components did not localise to P-bodies it would also have to be determined how they are protected from degradation.

An alternative possibility is that HIV-1 gRNA and/or Gag may localise to related cytoplasmic structures that may partially overlap with P-bodies. One example may be stress granules as these foci share several protein components (Kedersha et al., 2005). Also, viral RNA has been proposed to localise to Staufen containing RNP complexes, distinct from P-bodies and stress granules, which are important for its virion encapsidation (Abrahamyan et al., 2010). Therefore, from the data presented in this study, it does not appear to be the case that viral components localise to P-bodies though they may localise to related foci. Precise differentiation between these different subcellular foci is required to effectively address these issues.

6.5.2 Anti-viral proteins and cytoplasmic foci formation

An interesting point to note is the localisation of proteins, which influence viral replication, to discrete subcellular compartments. Although knockdown of the P-body proteins Ago2, DDX6 and Lsm1 did not substantially affect HIV-1 infectivity (Chapter 4, section 4.2.3 and Chapter 5, sections 5.4 – 5.7), these proteins have been more conclusively implicated in the control of other viruses, such as hepatitis C, as discussed earlier. Also, as has already been described, the recently identified antiviral factor, Mov10, which significantly compromises HIV-1 infectivity when overexpressed, localises to P-bodies and stress granules (Burdick et al., 2010; Furtak et al., 2010; Wang et al., 2010). It has also been reported that poliovirus infection causes the downregulation of both P-bodies and stress granules, with the specific degradation of key proteins (Dougherty et al., 2011; White et al., 2007). Stress granules have also been implicated in both the inhibition and promotion of a diverse range of viral life cycles, including West Nile virus, herpes simplex virus-1, Semliki Forest Virus, vesicular stomatitis virus and Sendai virus (Umbach and Cullen, 2009). Thus P-body and stress granule components may be influential in controlling the replication of certain viruses.

Aside from P-body proteins, the antiviral protein Trim5α also accumulates in cytoplasmic bodies when ectopically expressed. Although pre-existing Trim5α bodies appear to be dispensable for its inhibitory phenotype (Song et al., 2005), the use of fluorescently labelled viral particles has demonstrated the formation of these foci around viral complexes and their association in response to proteosomal inhibition (Campbell et al., 2008). Whether this is a true reflection of the localisation of the endogenous protein and the exact cellular components of these cytoplasmic bodies has yet to be determined. However, the formation of subcellular protein aggregates in

response to viral infection has also been observed for vaccinia virus, where foci with a similar but not identical protein content to stress granules, function to block virus replication (Simpson-Holley et al., 2011). Whether these and other foci act to sequester away cellular proteins required by the virus or else directly recruit antiviral proteins is unresolved at present. Thus cytoplasmic foci formation may be a significant factor in cellular antiviral defence strategies but their exact relevance and mechanism of action in most cases is unknown, representing important areas of future research.

6.6 APOBEC3 proteins and the regulation of RNA

6.6.1 APOBEC3 proteins and effects on RNA

P-body localisation of the APOBEC3 proteins may be related to an as yet unidentified cellular function. It has been speculated that the APOBEC3 family may be involved in the regulation of RNA, which would support their subcellular localisation. However, contrary to a published report, (Huang et al., 2007a), the APOBEC3 proteins were not able to specifically regulate miRNA mediated repression or siRNA mediated silencing (Chapter 4, sections 4.7 and 4.9). Nor were they involved in the related RNA regulatory pathway of AMD (subject to caveats, see Chapter 4, section 4.11). However, the APOBEC3 proteins do appear to have some influence in regulating protein expression (Chapter 4, section 4.7). An important point to resolve is the specificity of this effect against different substrates, whether cellular and/or viral, and its *in vivo* relevance. A3C, which had the dramatic phenotype, is expressed in a wide variety of different tissues and has moderate inhibitory effects against certain viruses, not including HIV-1, and retrotransposons (see Chapter 3, Table 3.1). Also, it is not induced by interferon alpha stimulation (Koning et al., 2009). From the results presented in Chapter 4 and 5 it would appear that the APOBEC3 proteins, if anything, decrease viral protein expression upon overexpression, at least for $p24^{Gag}$ (see effects of A3B, A3C and A3H). Nevertheless, as has been observed, overexpression systems in cell lines can sometimes produce artifacts or results that are not representative of endogenous function. Thus these effects of the APOBEC3 proteins would have to be more rigorously explored. To specifically address the effects of the APOBEC3 proteins on RNA translation, direct tethering assays could be utilised. Reporter constructs containing 5 BoxB hairpins in their 3'UTR are co-transfected with the protein of interest fused to a twenty-two amino acid λN peptide, which binds to the BoxB sites with high affinity (Gehring et al., 2003). Direct effects of

the protein on RNA translation can then be measured via expression of the reporter plasmid. This type of assay has successfully been used to determine that the Argonaute proteins and GW182 can repress translation of mRNAs, independently of each other and of their interactions with miRNAs (Pillai et al., 2004; Zipprich et al., 2009).

These results of an upregulation of protein expression are also somewhat contradictory to recent reports claiming that the APOBEC3 proteins are able to mediate the clearance of foreign DNA and thus reduce the expression level of co-transfected proteins, such as GFP (Stenglein et al., 2010). While this effect may be evident for certain APOBEC3 proteins in the luciferase reporter assays used in this study, it was not observed for A3A and A3C, which were both identified by Stenglein *et al* (2010) as mediating this phenotype. Therefore these discrepancies need to be addressed. As has been discovered for Ago2, which can act to both repress and enhance translation, dependent on the cellular context and potentially its cellular location (Berezhna et al., 2011; Vasudevan and Steitz, 2007a), regulatory proteins can have dual roles in the control of translation. This may make it easier for cells to rapidly respond to changing environmental circumstances and this could be the case for the APOBEC3 proteins as well.

6.6.2 Identification of APOBEC3 associated RNAs

As has already been discussed, the involvement of APOBEC3 family members in other processes relating to RNA metabolism and turnover is still a possibility. Identification of the repertoire of RNAs, both mRNA and miRNA, that associate with these proteins is of paramount importance. Several A3G associated cellular and viral RNAs have already been documented including the mRNA of A3G itself and the 7SL, Alu and Y RNAs (Kozak et al., 2006). Differential binding of certain small RNAs has been reported for A3F and A3G (Gallois-Montbrun et al., 2008), and these may potentially contribute to differences in virion encapsidation and hence the anti-viral activities of these proteins. Further, they may help elucidate other functions of the APOBEC3 family and also cellular contributions to the regulation of these proteins. The activities of APOBEC1 and AID, for example, are known to be regulated by cellular RNAs (Bransteitter et al., 2003; Sowden et al., 1996). Interaction of HIV-1 viral RNA with A3G in virus particles has been proposed to prevent its editing activity until the process of reverse transcription has been initiated in the infected target cell (Soros et al., 2007). Work is presently underway to identify these RNA species using techniques such as *in vivo* cross-linking combined with co-immunoprecipitation (CLIP). Similar studies have

already been carried out for the Argonaute proteins to identify miRNA targeted mRNAs. A comparison of CLIP data from Argonaute and APOBEC3 proteins as well as between the APOBEC3 proteins themselves, in both a cellular and viral context, will help identify shared and differential RNA interacting factors, which may yield clues as to functional activity and regulation.

6.7 Summary

In summary, it can be concluded that although several APOBEC3 proteins were able to interact and/or co-localise with Ago2, this protein did not appear to influence APOBEC3 mediated anti-viral activity. Although the role of miRNAs and miRNA mediated repression to APOBEC3 HIV-1 inhibition has not been directly addressed, the APOBEC3 proteins were not able to specifically regulate this process. The fact that the APOBEC3 family associates with a multitude of proteins related to RNA metabolism suggests that they may be involved in RNA regulatory pathways, but this would require further formal testing. Identification of the RNA components of their cellular complexes would greatly assist in this matter as well as provide insight into possible mechanisms of functional regulation. Whether any of these other associated cellular proteins have roles in APOBEC3 function, either cellular or anti-viral, remains to be seen. Finally the localisation of APOBEC3 proteins at mRNA processing bodies did not appear to be necessary for their anti-viral phenotype. The mechanisms that direct these proteins to these cytoplasmic foci as well as the relevance of this localisation to functional activity has yet to be elucidated. Further, knockdown of the P-body proteins, Ago2, DDX6 and Lsm1, did not affect HIV-1 replication indicating that this virus is neither dependent upon nor inhibited by these proteins. This highlights the complex interplay between cellular and viral factors in both the promotion and inhibition of viral replication. Greater knowledge of the latter, with regards to natural restriction factors such as the APOBEC3 proteins, is the power with which to more effectively target viruses such as HIV-1, which threaten the health and economies of some of the most vulnerable societies around the world.

REFERENCES

Abrahamyan, L.G., Chatel-Chaix, L., Ajamian, L., Milev, M.P., Monette, A., Clement, J.F., Song, R., Lehmann, M., DesGroseillers, L., Laughrea, M.*, et al.* (2010). Novel Staufen1 ribonucleoproteins prevent formation of stress granules but favour encapsidation of HIV-1 genomic RNA. J Cell Sci *123*, 369-383.

Ahluwalia, J.K., Khan, S.Z., Soni, K., Rawat, P., Gupta, A., Hariharan, M., Scaria, V., Lalwani, M., Pillai, B., Mitra, D.*, et al.* (2008). Human cellular microRNA hsa-miR-29a interferes with viral nef protein expression and HIV-1 replication. Retrovirology *5*, 117.

Alkhatib, G., Combadiere, C., Broder, C.C., Feng, Y., Kennedy, P.E., Murphy, P.M., and Berger, E.A. (1996). CC CKR5: a RANTES, MIP-1alpha, MIP-1beta receptor as a fusion cofactor for macrophage-tropic HIV-1. Science *272*, 1955-1958.

Anant, S., and Davidson, N.O. (2000). An AU-rich sequence element (UUUN[A/U]U) downstream of the edited C in apolipoprotein B mRNA is a high-affinity binding site for Apobec-1: binding of Apobec-1 to this motif in the 3' untranslated region of c-myc increases mRNA stability. Mol Cell Biol *20*, 1982-1992.

Anant, S., Murmu, N., Houchen, C.W., Mukhopadhyay, D., Riehl, T.E., Young, S.G., Morrison, A.R., Stenson, W.F., and Davidson, N.O. (2004). Apobec-1 protects intestine from radiation injury through posttranscriptional regulation of cyclooxygenase-2 expression. Gastroenterology *127*, 1139-1149.

Anderson, P., and Kedersha, N. (2006). RNA granules. J Cell Biol *172*, 803-808.

Andrei, M.A., Ingelfinger, D., Heintzmann, R., Achsel, T., Rivera-Pomar, R., and Luhrmann, R. (2005). A role for eIF4E and eIF4E-transporter in targeting mRNPs to mammalian processing bodies. RNA *11*, 717-727.

Aoki, K., Moriguchi, H., Yoshioka, T., Okawa, K., and Tabara, H. (2007). In vitro analyses of the production and activity of secondary small interfering RNAs in C. elegans. EMBO J *26*, 5007-5019.

Arakawa, H., Hauschild, J., and Buerstedde, J.M. (2002). Requirement of the activation-induced deaminase (AID) gene for immunoglobulin gene conversion. Science *295*, 1301-1306.

Aravin, A., Gaidatzis, D., Pfeffer, S., Lagos-Quintana, M., Landgraf, P., Iovino, N., Morris, P., Brownstein, M.J., Kuramochi-Miyagawa, S., Nakano, T.*, et al.* (2006). A novel class of small RNAs bind to MILI protein in mouse testes. Nature *442*, 203-207.

Aravin, A.A., Hannon, G.J., and Brennecke, J. (2007). The Piwi-piRNA pathway provides an adaptive defense in the transposon arms race. Science *318*, 761-764.

Aravin, A.A., van der Heijden, G.W., Castaneda, J., Vagin, V.V., Hannon, G.J., and Bortvin, A. (2009). Cytoplasmic compartmentalization of the fetal piRNA pathway in mice. PLoS Genet *5*, e1000764.

Ariumi, Y., Kuroki, M., Abe, K., Dansako, H., Ikeda, M., Wakita, T., and Kato, N. (2007). DDX3 DEAD-box RNA helicase is required for hepatitis C virus RNA replication. J Virol *81*, 13922-13926.

Baillat, D., and Shiekhattar, R. (2009). Functional dissection of the human TNRC6 (GW182-related) family of proteins. Mol Cell Biol *29*, 4144-4155.

Bakheet, T., Williams, B.R., and Khabar, K.S. (2006). ARED 3.0: the large and diverse AU-rich transcriptome. Nucleic Acids Res *34*, D111-114.

Balagopal, V., and Parker, R. (2009). Polysomes, P bodies and stress granules: states and fates of eukaryotic mRNAs. Curr Opin Cell Biol *21*, 403-408.

Barre-Sinoussi, F., Chermann, J.C., Rey, F., Nugeyre, M.T., Chamaret, S., Gruest, J., Dauguet, C., Axler-Blin, C., Vezinet-Brun, F., Rouzioux, C.*, et al.* (1983). Isolation of a T-lymphotropic retrovirus from a patient at risk for acquired immune deficiency syndrome (AIDS). Science *220*, 868-871.

Barreau, C., Paillard, L., and Osborne, H.B. (2005). AU-rich elements and associated factors: are there unifying principles? Nucleic Acids Res *33*, 7138-7150.

Bartee, E., McCormack, A., and Fruh, K. (2006). Quantitative membrane proteomics reveals new cellular targets of viral immune modulators. PLoS Pathog *2*, e107.

Bartel, D.P., and Chen, C.Z. (2004). Micromanagers of gene expression: the potentially widespread influence of metazoan microRNAs. Nat Rev Genet *5*, 396-400.

Bauby, H., Lopez-Verges, S., Hoeffel, G., Delcroix-Genete, D., Janvier, K., Mammano, F., Hosmalin, A., and Berlioz-Torrent, C. (2010). TIP47 is required for the production of infectious HIV-1 particles from primary macrophages. Traffic *11*, 455-467.

Beckham, C., Hilliker, A., Cziko, A.M., Noueiry, A., Ramaswami, M., and Parker, R. (2008). The DEAD-box RNA helicase Ded1p affects and accumulates in Saccharomyces cerevisiae P-bodies. Mol Biol Cell *19*, 984-993.

Beckham, C.J., Light, H.R., Nissan, T.A., Ahlquist, P., Parker, R., and Noueiry, A. (2007). Interactions between brome mosaic virus RNAs and cytoplasmic processing bodies. J Virol *81*, 9759-9768.

Beckham, C.J., and Parker, R. (2008). P bodies, stress granules, and viral life cycles. Cell Host Microbe *3*, 206-212.

Behm-Ansmant, I., Rehwinkel, J., Doerks, T., Stark, A., Bork, P., and Izaurralde, E. (2006). mRNA degradation by miRNAs and GW182 requires both CCR4:NOT deadenylase and DCP1:DCP2 decapping complexes. Genes Dev *20*, 1885-1898.

Beliakova-Bethell, N., Beckham, C., Giddings, T.H., Jr., Winey, M., Parker, R., and Sandmeyer, S. (2006). Virus-like particles of the Ty3 retrotransposon assemble in association with P-body components. RNA *12*, 94-101.

Bennasser, Y., and Jeang, K.T. (2006). HIV-1 Tat interaction with Dicer: requirement for RNA. Retrovirology *3*, 95.

Bennasser, Y., Le, S.Y., Benkirane, M., and Jeang, K.T. (2005). Evidence that HIV-1 encodes an siRNA and a suppressor of RNA silencing. Immunity *22*, 607-619.

Berezhna, S.Y., Supekova, L., Sever, M.J., Schultz, P.G., and Deniz, A.A. (2011). Dual regulation of hepatitis C viral RNA by cellular RNAi requires partitioning of Ago2 to lipid droplets and P-bodies. RNA.

Berger, G., Durand, S., Fargier, G., Nguyen, X.N., Cordeil, S., Bouaziz, S., Muriaux, D., Darlix, J.L., and Cimarelli, A. (2011). APOBEC3A is a specific inhibitor of the early phases of HIV-1 infection in myeloid cells. PLoS Pathog *7*, e1002221.

Bertrand, E., Chartrand, P., Schaefer, M., Shenoy, S.M., Singer, R.H., and Long, R.M. (1998). Localization of ASH1 mRNA particles in living yeast. Mol Cell *2*, 437-445.

Besnier, C., Takeuchi, Y., and Towers, G. (2002). Restriction of lentivirus in monkeys. Proc Natl Acad Sci U S A *99*, 11920-11925.

Bhattacharya, A., Czaplinski, K., Trifillis, P., He, F., Jacobson, A., and Peltz, S.W. (2000). Characterization of the biochemical properties of the human Upf1 gene product that is involved in nonsense-mediated mRNA decay. RNA *6*, 1226-1235.

Bhattacharyya, S.N., Habermacher, R., Martine, U., Closs, E.I., and Filipowicz, W. (2006). Relief of microRNA-mediated translational repression in human cells subjected to stress. Cell *125*, 1111-1124.

Bieniasz, P.D., and Cullen, B.R. (2000). Multiple blocks to human immunodeficiency virus type 1 replication in rodent cells. J Virol *74*, 9868-9877.

Bishop, K.N., Holmes, R.K., and Malim, M.H. (2006). Antiviral potency of APOBEC proteins does not correlate with cytidine deamination. J Virol *80*, 8450-8458.

Bishop, K.N., Holmes, R.K., Sheehy, A.M., Davidson, N.O., Cho, S.J., and Malim, M.H. (2004). Cytidine deamination of retroviral DNA by diverse APOBEC proteins. Curr Biol *14*, 1392-1396.

Bishop, K.N., Verma, M., Kim, E.Y., Wolinsky, S.M., and Malim, M.H. (2008). APOBEC3G inhibits elongation of HIV-1 reverse transcripts. PLoS Pathog *4*, e1000231.

Bogerd, H.P., and Cullen, B.R. (2008). Single-stranded RNA facilitates nucleocapsid: APOBEC3G complex formation. RNA *14*, 1228-1236.

Bogerd, H.P., Tallmadge, R.L., Oaks, J.L., Carpenter, S., and Cullen, B.R. (2008). Equine infectious anemia virus resists the antiretroviral activity of equine APOBEC3 proteins through a packaging-independent mechanism. J Virol *82*, 11889-11901.

Bogerd, H.P., Wiegand, H.L., Doehle, B.P., Lueders, K.K., and Cullen, B.R. (2006). APOBEC3A and APOBEC3B are potent inhibitors of LTR-retrotransposon function in human cells. Nucleic Acids Res *34*, 89-95.

Boissinot, S., Entezam, A., and Furano, A.V. (2001). Selection against deleterious LINE-1-containing loci in the human lineage. Mol Biol Evol *18*, 926-935.

Bour, S., and Strebel, K. (1996). The human immunodeficiency virus (HIV) type 2 envelope protein is a functional complement to HIV type 1 Vpu that enhances particle release of heterologous retroviruses. J Virol *70*, 8285-8300.

Bransteitter, R., Pham, P., Scharff, M.D., and Goodman, M.F. (2003). Activation-induced cytidine deaminase deaminates deoxycytidine on single-stranded DNA but requires the action of RNase. Proc Natl Acad Sci U S A *100*, 4102-4107.

Brass, A.L., Dykxhoorn, D.M., Benita, Y., Yan, N., Engelman, A., Xavier, R.J., Lieberman, J., and Elledge, S.J. (2008). Identification of host proteins required for HIV infection through a functional genomic screen. Science *319*, 921-926.

Brengues, M., Teixeira, D., and Parker, R. (2005). Movement of eukaryotic mRNAs between polysomes and cytoplasmic processing bodies. Science *310*, 486-489.

Briggs, J.A., Simon, M.N., Gross, I., Krausslich, H.G., Fuller, S.D., Vogt, V.M., and Johnson, M.C. (2004). The stoichiometry of Gag protein in HIV-1. Nat Struct Mol Biol *11*, 672-675.

Broderick, J.A., Salomon, W.E., Ryder, S.P., Aronin, N., and Zamore, P.D. (2011). Argonaute protein identity and pairing geometry determine cooperativity in mammalian RNA silencing. RNA.

Buchan, J.R., and Parker, R. (2009). Eukaryotic stress granules: the ins and outs of translation. Mol Cell *36*, 932-941.

Bukrinsky, M.I., Haggerty, S., Dempsey, M.P., Sharova, N., Adzhubel, A., Spitz, L., Lewis, P., Goldfarb, D., Emerman, M., and Stevenson, M. (1993). A nuclear localization signal within HIV-1 matrix protein that governs infection of non-dividing cells. Nature *365*, 666-669.

Burdick, R., Smith, J.L., Chaipan, C., Friew, Y., Chen, J., Venkatachari, N.J., Delviks-Frankenberry, K.A., Hu, W.S., and Pathak, V.K. (2010). P body-associated protein Mov10 inhibits HIV-1 replication at multiple stages. J Virol *84*, 10241-10253.

Burnett, A., and Spearman, P. (2007). APOBEC3G multimers are recruited to the plasma membrane for packaging into human immunodeficiency virus type 1 virus-like particles in an RNA-dependent process requiring the NC basic linker. J Virol *81*, 5000-5013.

Bushati, N., and Cohen, S.M. (2007). microRNA functions. Annu Rev Cell Dev Biol *23*, 175-205.

Bushman, F.D., Fujiwara, T., and Craigie, R. (1990). Retroviral DNA integration directed by HIV integration protein in vitro. Science *249*, 1555-1558.

Butsch, M., and Boris-Lawrie, K. (2002). Destiny of unspliced retroviral RNA: ribosome and/or virion? J Virol *76*, 3089-3094.

Campbell, E.M., Dodding, M.P., Yap, M.W., Wu, X., Gallois-Montbrun, S., Malim, M.H., Stoye, J.P., and Hope, T.J. (2007). TRIM5 alpha cytoplasmic bodies are highly dynamic structures. Mol Biol Cell *18*, 2102-2111.

Campbell, E.M., Perez, O., Anderson, J.L., and Hope, T.J. (2008). Visualization of a proteasome-independent intermediate during restriction of HIV-1 by rhesus TRIM5alpha. J Cell Biol *180*, 549-561.

Campbell, S.M., Crowe, S.M., and Mak, J. (2001). Lipid rafts and HIV-1: from viral entry to assembly of progeny virions. J Clin Virol *22*, 217-227.

Cao, Q., Padmanabhan, K., and Richter, J.D. (2010). Pumilio 2 controls translation by competing with eIF4E for 7-methyl guanosine cap recognition. RNA *16*, 221-227.

Carballo, E., Lai, W.S., and Blackshear, P.J. (1998). Feedback inhibition of macrophage tumor necrosis factor-alpha production by tristetraprolin. Science *281*, 1001-1005.

Carlton, J.G., and Martin-Serrano, J. (2007). Parallels between cytokinesis and retroviral budding: a role for the ESCRT machinery. Science *316*, 1908-1912.

Chable-Bessia, C., Meziane, O., Latreille, D., Triboulet, R., Zamborlini, A., Wagschal, A., Jacquet, J.M., Reynes, J., Levy, Y., Saib, A., *et al.* (2009). Suppression of HIV-1 replication by microRNA effectors. Retrovirology *6*, 26.

Charneau, P., Alizon, M., and Clavel, F. (1992). A second origin of DNA plus-strand synthesis is required for optimal human immunodeficiency virus replication. J Virol *66*, 2814-2820.

Charneau, P., and Clavel, F. (1991). A single-stranded gap in human immunodeficiency virus unintegrated linear DNA defined by a central copy of the polypurine tract. J Virol *65*, 2415-2421.

Chaudhuri, J., Khuong, C., and Alt, F.W. (2004). Replication protein A interacts with AID to promote deamination of somatic hypermutation targets. Nature *430*, 992-998.

Chaudhuri, R., Lindwasser, O.W., Smith, W.J., Hurley, J.H., and Bonifacino, J.S. (2007). Downregulation of CD4 by human immunodeficiency virus type 1 Nef is dependent on clathrin and involves direct interaction of Nef with the AP2 clathrin adaptor. J Virol *81*, 3877-3890.

Checkley, M.A., Nagashima, K., Lockett, S.J., Nyswaner, K.M., and Garfinkel, D.J. (2010). P-body components are required for Ty1 retrotransposition during assembly of retrotransposition-competent virus-like particles. Mol Cell Biol *30*, 382-398.

Cheloufi, S., Dos Santos, C.O., Chong, M.M., and Hannon, G.J. (2010). A dicer-independent miRNA biogenesis pathway that requires Ago catalysis. Nature *465*, 584-589.

Chen, C.Y., and Shyu, A.B. (1995). AU-rich elements: characterization and importance in mRNA degradation. Trends Biochem Sci *20*, 465-470.

Chen, H., and Engelman, A. (1998). The barrier-to-autointegration protein is a host factor for HIV type 1 integration. Proc Natl Acad Sci U S A *95*, 15270-15274.

Chen, H., Lilley, C.E., Yu, Q., Lee, D.V., Chou, J., Narvaiza, I., Landau, N.R., and Weitzman, M.D. (2006). APOBEC3A is a potent inhibitor of adeno-associated virus and retrotransposons. Curr Biol *16*, 480-485.

Chen, Y., Mills, J.D., and Periasamy, A. (2003). Protein localization in living cells and tissues using FRET and FLIM. Differentiation *71*, 528-541.

Chen, Y.T., Holcomb, C., and Moore, H.P. (1993). Expression and localization of two low molecular weight GTP-binding proteins, Rab8 and Rab10, by epitope tag. Proc Natl Acad Sci U S A *90*, 6508-6512.

Cheng, Z., Coller, J., Parker, R., and Song, H. (2005). Crystal structure and functional analysis of DEAD-box protein Dhh1p. RNA *11*, 1258-1270.

Chertova, E., Chertov, O., Coren, L.V., Roser, J.D., Trubey, C.M., Bess, J.W., Jr., Sowder, R.C., 2nd, Barsov, E., Hood, B.L., Fisher, R.J.*, et al.* (2006). Proteomic and biochemical analysis of purified human immunodeficiency virus type 1 produced from infected monocyte-derived macrophages. J Virol *80*, 9039-9052.

Chester, A., Somasekaram, A., Tzimina, M., Jarmuz, A., Gisbourne, J., O'Keefe, R., Scott, J., and Navaratnam, N. (2003). The apolipoprotein B mRNA editing complex performs a multifunctional cycle and suppresses nonsense-mediated decay. EMBO J *22*, 3971-3982.

Chiu, Y.L. (2011). Biochemical fractionation and purification of high-molecular-mass APOBEC3G complexes. Methods Mol Biol *718*, 185-206.

Chiu, Y.L., and Greene, W.C. (2008). The APOBEC3 cytidine deaminases: an innate defensive network opposing exogenous retroviruses and endogenous retroelements. Annu Rev Immunol *26*, 317-353.

Chiu, Y.L., Soros, V.B., Kreisberg, J.F., Stopak, K., Yonemoto, W., and Greene, W.C. (2005). Cellular APOBEC3G restricts HIV-1 infection in resting CD4+ T cells. Nature *435*, 108-114.

Chiu, Y.L., Witkowska, H.E., Hall, S.C., Santiago, M., Soros, V.B., Esnault, C., Heidmann, T., and Greene, W.C. (2006). High-molecular-mass APOBEC3G complexes restrict Alu retrotransposition. Proc Natl Acad Sci U S A *103*, 15588-15593.

Cho, P.F., Poulin, F., Cho-Park, Y.A., Cho-Park, I.B., Chicoine, J.D., Lasko, P., and Sonenberg, N. (2005). A new paradigm for translational control: inhibition via 5'-3' mRNA tethering by Bicoid and the eIF4E cognate 4EHP. Cell *121*, 411-423.

Chu, C.Y., and Rana, T.M. (2006). Translation repression in human cells by microRNA-induced gene silencing requires RCK/p54. PLoS Biol *4*, e210.

Cifuentes, D., Xue, H., Taylor, D.W., Patnode, H., Mishima, Y., Cheloufi, S., Ma, E., Mane, S., Hannon, G.J., Lawson, N.D.*, et al.* (2010). A novel miRNA processing pathway independent of Dicer requires Argonaute2 catalytic activity. Science *328*, 1694-1698.

Cikaluk, D.E., Tahbaz, N., Hendricks, L.C., DiMattia, G.E., Hansen, D., Pilgrim, D., and Hobman, T.C. (1999). GERp95, a membrane-associated protein that belongs to a family of proteins involved in stem cell differentiation. Mol Biol Cell *10*, 3357-3372.

Clapham, P.R., Blanc, D., and Weiss, R.A. (1991). Specific cell surface requirements for the infection of CD4-positive cells by human immunodeficiency virus types 1 and 2 and by Simian immunodeficiency virus. Virology *181*, 703-715.

Clavel, F., Guetard, D., Brun-Vezinet, F., Chamaret, S., Rey, M.A., Santos-Ferreira, M.O., Laurent, A.G., Dauguet, C., Katlama, C., Rouzioux, C.*, et al.* (1986). Isolation of a new human retrovirus from West African patients with AIDS. Science *233*, 343-346.

Cohen, O.J., and Fauci, A.S. (2001). Pathogenesis and Medical Aspects of HIV-1 Infection. In Fields Virology, D.H. Knipe, and P.M. Howley, eds. (Philladelphia, Lippincott Williams & Wilkins), pp. 2043-2094.

Coley, W., Van Duyne, R., Carpio, L., Guendel, I., Kehn-Hall, K., Chevalier, S., Narayanan, A., Luu, T., Lee, N., Klase, Z.*, et al.* (2010). Absence of DICER in monocytes and its regulation by HIV-1. J Biol Chem *285*, 31930-31943.

Coller, J., and Parker, R. (2005). General translational repression by activators of mRNA decapping. Cell *122*, 875-886.

Collins, K.L., Chen, B.K., Kalams, S.A., Walker, B.D., and Baltimore, D. (1998). HIV-1 Nef protein protects infected primary cells against killing by cytotoxic T lymphocytes. Nature *391*, 397-401.

Conticello, S.G., Harris, R.S., and Neuberger, M.S. (2003). The Vif protein of HIV triggers degradation of the human antiretroviral DNA deaminase APOBEC3G. Curr Biol *13*, 2009-2013.

Cordaux, R., and Batzer, M.A. (2009). The impact of retrotransposons on human genome evolution. Nat Rev Genet *10*, 691-703.

Cougot, N., Babajko, S., and Seraphin, B. (2004). Cytoplasmic foci are sites of mRNA decay in human cells. J Cell Biol *165*, 31-40.

Cowan, S., Hatziioannou, T., Cunningham, T., Muesing, M.A., Gottlinger, H.G., and Bieniasz, P.D. (2002). Cellular inhibitors with Fv1-like activity restrict human and simian immunodeficiency virus tropism. Proc Natl Acad Sci U S A *99*, 11914-11919.

Crow, Y.J., Hayward, B.E., Parmar, R., Robins, P., Leitch, A., Ali, M., Black, D.N., van Bokhoven, H., Brunner, H.G., Hamel, B.C.*, et al.* (2006). Mutations in the gene encoding the 3'-5' DNA exonuclease TREX1 cause Aicardi-Goutieres syndrome at the AGS1 locus. Nat Genet *38*, 917-920.

Cullen, B.R. (2011). Viruses and microRNAs: RISCy interactions with serious consequences. Genes Dev.

Czech, B., Malone, C.D., Zhou, R., Stark, A., Schlingeheyde, C., Dus, M., Perrimon, N., Kellis, M., Wohlschlegel, J.A., Sachidanandam, R.*, et al.* (2008). An endogenous small interfering RNA pathway in Drosophila. Nature *453*, 798-802.

Czech, B., Zhou, R., Erlich, Y., Brennecke, J., Binari, R., Villalta, C., Gordon, A., Perrimon, N., and Hannon, G.J. (2009). Hierarchical rules for Argonaute loading in Drosophila. Mol Cell *36*, 445-456.

Dang, Y., Siew, L.M., Wang, X., Han, Y., Lampen, R., and Zheng, Y.H. (2008). Human cytidine deaminase APOBEC3H restricts HIV-1 replication. J Biol Chem *283*, 11606-11614.

Dang, Y., Wang, X., Esselman, W.J., and Zheng, Y.H. (2006). Identification of APOBEC3DE as another antiretroviral factor from the human APOBEC family. J Virol *80*, 10522-10533.

David Gerecht, P.S., Taylor, M.A., and Port, J.D. (2010). Intracellular localization and interaction of mRNA binding proteins as detected by FRET. BMC Cell Biol *11*, 69.

Deacon, N.J., Tsykin, A., Solomon, A., Smith, K., Ludford-Menting, M., Hooker, D.J., McPhee, D.A., Greenway, A.L., Ellett, A., Chatfield, C.*, et al.* (1995). Genomic structure of an attenuated quasi species of HIV-1 from a blood transfusion donor and recipients. Science *270*, 988-991.

Deneka, M., Pelchen-Matthews, A., Byland, R., Ruiz-Mateos, E., and Marsh, M. (2007). In macrophages, HIV-1 assembles into an intracellular plasma membrane domain containing the tetraspanins CD81, CD9, and CD53. J Cell Biol *177*, 329-341.

Deng, H., Liu, R., Ellmeier, W., Choe, S., Unutmaz, D., Burkhart, M., Di Marzio, P., Marmon, S., Sutton, R.E., Hill, C.M.*, et al.* (1996). Identification of a major co-receptor for primary isolates of HIV-1. Nature *381*, 661-666.

Depienne, C., Roques, P., Creminon, C., Fritsch, L., Casseron, R., Dormont, D., Dargemont, C., and Benichou, S. (2000). Cellular distribution and karyophilic properties of matrix, integrase, and Vpr proteins from the human and simian immunodeficiency viruses. Exp Cell Res *260*, 387-395.

Diaz-Pendon, J.A., Li, F., Li, W.X., and Ding, S.W. (2007). Suppression of antiviral silencing by cucumber mosaic virus 2b protein in Arabidopsis is associated with drastically reduced accumulation of three classes of viral small interfering RNAs. Plant Cell *19*, 2053-2063.

Doehle, B.P., Schafer, A., and Cullen, B.R. (2005). Human APOBEC3B is a potent inhibitor of HIV-1 infectivity and is resistant to HIV-1 Vif. Virology *339*, 281-288.

Dorfman, T., Bukovsky, A., Ohagen, A., Hoglund, S., and Gottlinger, H.G. (1994). Functional domains of the capsid protein of human immunodeficiency virus type 1. J Virol *68*, 8180-8187.

Doucet, A.J., Hulme, A.E., Sahinovic, E., Kulpa, D.A., Moldovan, J.B., Kopera, H.C., Athanikar, J.N., Hasnaoui, M., Bucheton, A., Moran, J.V.*, et al.* (2010). Characterization of LINE-1 ribonucleoprotein particles. PLoS Genet *6*.

Dougherty, J.D., White, J.P., and Lloyd, R.E. (2011). Poliovirus-mediated disruption of cytoplasmic processing bodies. J Virol *85*, 64-75.

Douglas, J.L., Gustin, J.K., Viswanathan, K., Mansouri, M., Moses, A.V., and Fruh, K. (2010). The great escape: viral strategies to counter BST-2/tetherin. PLoS Pathog *6*, e1000913.

Dragic, T., Litwin, V., Allaway, G.P., Martin, S.R., Huang, Y., Nagashima, K.A., Cayanan, C., Maddon, P.J., Koup, R.A., Moore, J.P.*, et al.* (1996). HIV-1 entry into CD4+ cells is mediated by the chemokine receptor CC-CKR-5. Nature *381*, 667-673.

Dube, M., Roy, B.B., Guiot-Guillain, P., Binette, J., Mercier, J., Chiasson, A., and Cohen, E.A. (2010). Antagonism of tetherin restriction of HIV-1 release by Vpu involves binding and sequestration of the restriction factor in a perinuclear compartment. PLoS Pathog *6*, e1000856.

Dube, M., Roy, B.B., Guiot-Guillain, P., Mercier, J., Binette, J., Leung, G., and Cohen, E.A. (2009). Suppression of Tetherin-restricting activity upon human immunodeficiency virus type 1 particle release correlates with localization of Vpu in the trans-Golgi network. J Virol *83*, 4574-4590.

Duggal, N.K., Malik, H.S., and Emerman, M. (2011). Positive selection of Apobec3DE in chimpanzees has driven breadth in anti-viral activity. J Virol.

Dutko, J.A., Kenny, A.E., Gamache, E.R., and Curcio, M.J. (2010). 5' to 3' mRNA decay factors colocalize with Ty1 gag and human APOBEC3G and promote Ty1 retrotransposition. J Virol *84*, 5052-5066.

Dutko, J.A., Schafer, A., Kenny, A.E., Cullen, B.R., and Curcio, M.J. (2005). Inhibition of a yeast LTR retrotransposon by human APOBEC3 cytidine deaminases. Curr Biol *15*, 661-666.

Esnault, C., Heidmann, O., Delebecque, F., Dewannieux, M., Ribet, D., Hance, A.J., Heidmann, T., and Schwartz, O. (2005). APOBEC3G cytidine deaminase inhibits retrotransposition of endogenous retroviruses. Nature *433*, 430-433.

Eulalio, A., Behm-Ansmant, I., and Izaurralde, E. (2007a). P bodies: at the crossroads of post-transcriptional pathways. Nat Rev Mol Cell Biol *8*, 9-22.

Eulalio, A., Behm-Ansmant, I., Schweizer, D., and Izaurralde, E. (2007b). P-body formation is a consequence, not the cause, of RNA-mediated gene silencing. Mol Cell Biol *27*, 3970-3981.

Eulalio, A., Huntzinger, E., and Izaurralde, E. (2008a). Getting to the root of miRNA-mediated gene silencing. Cell *132*, 9-14.

Eulalio, A., Huntzinger, E., and Izaurralde, E. (2008b). GW182 interaction with Argonaute is essential for miRNA-mediated translational repression and mRNA decay. Nat Struct Mol Biol *15*, 346-353.

Evan, G.I., Lewis, G.K., Ramsay, G., and Bishop, J.M. (1985). Isolation of monoclonal antibodies specific for human c-myc proto-oncogene product. Mol Cell Biol *5*, 3610-3616.

Eystathioy, T., Jakymiw, A., Chan, E.K., Seraphin, B., Cougot, N., and Fritzler, M.J. (2003). The GW182 protein colocalizes with mRNA degradation associated proteins hDcp1 and hLSm4 in cytoplasmic GW bodies. RNA *9*, 1171-1173.

Fan, X.C., and Steitz, J.A. (1998). Overexpression of HuR, a nuclear-cytoplasmic shuttling protein, increases the in vivo stability of ARE-containing mRNAs. EMBO J *17*, 3448-3460.

Farazi, T.A., Spitzer, J.I., Morozov, P., and Tuschl, T. (2011). miRNAs in human cancer. J Pathol *223*, 102-115.

Fassati, A., and Goff, S.P. (2001). Characterization of intracellular reverse transcription complexes of human immunodeficiency virus type 1. J Virol *75*, 3626-3635.

Feng, Q., Moran, J.V., Kazazian, H.H., Jr., and Boeke, J.D. (1996a). Human L1 retrotransposon encodes a conserved endonuclease required for retrotransposition. Cell *87*, 905-916.

Feng, Y., Broder, C.C., Kennedy, P.E., and Berger, E.A. (1996b). HIV-1 entry cofactor: functional cDNA cloning of a seven-transmembrane, G protein-coupled receptor. Science *272*, 872-877.

Fields, S., and Song, O. (1989). A novel genetic system to detect protein-protein interactions. Nature *340*, 245-246.

Fisher, A.G., Ensoli, B., Ivanoff, L., Chamberlain, M., Petteway, S., Ratner, L., Gallo, R.C., and Wong-Staal, F. (1987). The sor gene of HIV-1 is required for efficient virus transmission in vitro. Science *237*, 888-893.

Fornerod, M., Ohno, M., Yoshida, M., and Mattaj, I.W. (1997). CRM1 is an export receptor for leucine-rich nuclear export signals. Cell *90*, 1051-1060.

Forstemann, K., Horwich, M.D., Wee, L., Tomari, Y., and Zamore, P.D. (2007). Drosophila microRNAs are sorted into functionally distinct argonaute complexes after production by dicer-1. Cell *130*, 287-297.

Fouchier, R.A., Meyer, B.E., Simon, J.H., Fischer, U., and Malim, M.H. (1997). HIV-1 infection of non-dividing cells: evidence that the amino-terminal basic region of the viral matrix protein is important for Gag processing but not for post-entry nuclear import. EMBO J *16*, 4531-4539.

Frankel, A.D., and Young, J.A. (1998). HIV-1: fifteen proteins and an RNA. Annu Rev Biochem *67*, 1-25.

Franks, T.M., and Lykke-Andersen, J. (2007). TTP and BRF proteins nucleate processing body formation to silence mRNAs with AU-rich elements. Genes Dev *21*, 719-735.

Freed, E.O., and Martin, M.A. (2001). HIVs and their Replication. In Fields Viriology, D.H. Knipe, and P.M. Howley, eds. (Philladelphia, Lippincott Williams & Wilkins), pp. 1971-2041.

Furtak, V., Mulky, A., Rawlings, S.A., Kozhaya, L., Lee, K., Kewalramani, V.N., and Unutmaz, D. (2010). Perturbation of the P-body component Mov10 inhibits HIV-1 infectivity. PLoS One *5*, e9081.

Gabuzda, D.H., Lawrence, K., Langhoff, E., Terwilliger, E., Dorfman, T., Haseltine, W.A., and Sodroski, J. (1992). Role of vif in replication of human immunodeficiency virus type 1 in CD4+ T lymphocytes. J Virol *66*, 6489-6495.

Galao, R.P., Chari, A., Alves-Rodrigues, I., Lobao, D., Mas, A., Kambach, C., Fischer, U., and Diez, J. (2010). LSm1-7 complexes bind to specific sites in viral RNA genomes and regulate their translation and replication. RNA *16*, 817-827.

Gallay, P., Hope, T., Chin, D., and Trono, D. (1997). HIV-1 infection of nondividing cells through the recognition of integrase by the importin/karyopherin pathway. Proc Natl Acad Sci U S A *94*, 9825-9830.

Gallo, R.C., Salahuddin, S.Z., Popovic, M., Shearer, G.M., Kaplan, M., Haynes, B.F., Palker, T.J., Redfield, R., Oleske, J., Safai, B.*, et al.* (1984). Frequent detection and isolation of cytopathic retroviruses (HTLV-III) from patients with AIDS and at risk for AIDS. Science *224*, 500-503.

Gallois-Montbrun, S., Holmes, R.K., Swanson, C.M., Fernandez-Ocana, M., Byers, H.L., Ward, M.A., and Malim, M.H. (2008). Comparison of cellular ribonucleoprotein complexes associated with the APOBEC3F and APOBEC3G antiviral proteins. J Virol *82*, 5636-5642.

Gallois-Montbrun, S., Kramer, B., Swanson, C.M., Byers, H., Lynham, S., Ward, M., and Malim, M.H. (2007). Antiviral protein APOBEC3G localizes to ribonucleoprotein complexes found in P bodies and stress granules. J Virol *81*, 2165-2178.

Gao, F., Bailes, E., Robertson, D.L., Chen, Y., Rodenburg, C.M., Michael, S.F., Cummins, L.B., Arthur, L.O., Peeters, M., Shaw, G.M., *et al.* (1999). Origin of HIV-1 in the chimpanzee Pan troglodytes troglodytes. Nature *397*, 436-441.

Gao, G., Guo, X., and Goff, S.P. (2002). Inhibition of retroviral RNA production by ZAP, a CCCH-type zinc finger protein. Science *297*, 1703-1706.

Garrus, J.E., von Schwedler, U.K., Pornillos, O.W., Morham, S.G., Zavitz, K.H., Wang, H.E., Wettstein, D.A., Stray, K.M., Cote, M., Rich, R.L., *et al.* (2001). Tsg101 and the vacuolar protein sorting pathway are essential for HIV-1 budding. Cell *107*, 55-65.

Gehring, N.H., Neu-Yilik, G., Schell, T., Hentze, M.W., and Kulozik, A.E. (2003). Y14 and hUpf3b form an NMD-activating complex. Mol Cell *11*, 939-949.

Ghildiyal, M., Seitz, H., Horwich, M.D., Li, C., Du, T., Lee, S., Xu, J., Kittler, E.L., Zapp, M.L., Weng, Z., *et al.* (2008). Endogenous siRNAs derived from transposons and mRNAs in Drosophila somatic cells. Science *320*, 1077-1081.

Ghildiyal, M., Xu, J., Seitz, H., Weng, Z., and Zamore, P.D. (2010). Sorting of Drosophila small silencing RNAs partitions microRNA* strands into the RNA interference pathway. RNA *16*, 43-56.

Gibbings, D.J., Ciaudo, C., Erhardt, M., and Voinnet, O. (2009). Multivesicular bodies associate with components of miRNA effector complexes and modulate miRNA activity. Nat Cell Biol *11*, 1143-1149.

Gilboa, E., Mitra, S.W., Goff, S., and Baltimore, D. (1979). A detailed model of reverse transcription and tests of crucial aspects. Cell *18*, 93-100.

Gilks, N., Kedersha, N., Ayodele, M., Shen, L., Stoecklin, G., Dember, L.M., and Anderson, P. (2004). Stress granule assembly is mediated by prion-like aggregation of TIA-1. Mol Biol Cell *15*, 5383-5398.

Girard, A., Sachidanandam, R., Hannon, G.J., and Carmell, M.A. (2006). A germline-specific class of small RNAs binds mammalian Piwi proteins. Nature *442*, 199-202.

Glass, W.G., McDermott, D.H., Lim, J.K., Lekhong, S., Yu, S.F., Frank, W.A., Pape, J., Cheshier, R.C., and Murphy, P.M. (2006). CCR5 deficiency increases risk of symptomatic West Nile virus infection. J Exp Med *203*, 35-40.

Goff (2001). The Retroviruses and their Replication. In Fields Virology, D.H. Knipe, and P.M. Howley, eds. (Philladelphia, Lippincott Williams & Wilkins), pp. 1871-1940.

Goh, W.C., Rogel, M.E., Kinsey, C.M., Michael, S.F., Fultz, P.N., Nowak, M.A., Hahn, B.H., and Emerman, M. (1998). HIV-1 Vpr increases viral expression by manipulation of the cell cycle: a mechanism for selection of Vpr in vivo. Nat Med *4*, 65-71.

Goila-Gaur, R., Khan, M.A., Miyagi, E., Kao, S., and Strebel, K. (2007). Targeting APOBEC3A to the viral nucleoprotein complex confers antiviral activity. Retrovirology *4*, 61.

Goldstrohm, A.C., Hook, B.A., Seay, D.J., and Wickens, M. (2006). PUF proteins bind Pop2p to regulate messenger RNAs. Nat Struct Mol Biol *13*, 533-539.

Goodier, J.L., Zhang, L., Vetter, M.R., and Kazazian, H.H., Jr. (2007). LINE-1 ORF1 protein localizes in stress granules with other RNA-binding proteins, including components of RNA interference RNA-induced silencing complex. Mol Cell Biol *27*, 6469-6483.

Gottlinger, H.G., Dorfman, T., Sodroski, J.G., and Haseltine, W.A. (1991). Effect of mutations affecting the p6 gag protein on human immunodeficiency virus particle release. Proc Natl Acad Sci U S A *88*, 3195-3199.

Goujon, C., Riviere, L., Jarrosson-Wuilleme, L., Bernaud, J., Rigal, D., Darlix, J.L., and Cimarelli, A. (2007). SIVSM/HIV-2 Vpx proteins promote retroviral escape from a proteasome-dependent restriction pathway present in human dendritic cells. Retrovirology *4*, 2.

Gregory, R.I., Chendrimada, T.P., Cooch, N., and Shiekhattar, R. (2005). Human RISC couples microRNA biogenesis and posttranscriptional gene silencing. Cell *123*, 631-640.

Grivna, S.T., Beyret, E., Wang, Z., and Lin, H. (2006). A novel class of small RNAs in mouse spermatogenic cells. Genes Dev *20*, 1709-1714.

Grossman, Z., Meier-Schellersheim, M., Paul, W.E., and Picker, L.J. (2006). Pathogenesis of HIV infection: what the virus spares is as important as what it destroys. Nat Med *12*, 289-295.

Grundhoff, A., and Sullivan, C.S. (2011). Virus-encoded microRNAs. Virology *411*, 325-343.

Guo, X., Carroll, J.W., Macdonald, M.R., Goff, S.P., and Gao, G. (2004). The zinc finger antiviral protein directly binds to specific viral mRNAs through the CCCH zinc finger motifs. J Virol *78*, 12781-12787.

Guo, X., Ma, J., Sun, J., and Gao, G. (2007). The zinc-finger antiviral protein recruits the RNA processing exosome to degrade the target mRNA. Proc Natl Acad Sci U S A *104*, 151-156.

Gupta, R.K., Mlcochova, P., Pelchen-Matthews, A., Petit, S.J., Mattiuzzo, G., Pillay, D., Takeuchi, Y., Marsh, M., and Towers, G.J. (2009). Simian immunodeficiency virus envelope glycoprotein counteracts tetherin/BST-2/CD317 by intracellular sequestration. Proc Natl Acad Sci U S A *106*, 20889-20894.

Hammond, S.M., Boettcher, S., Caudy, A.A., Kobayashi, R., and Hannon, G.J. (2001). Argonaute2, a link between genetic and biochemical analyses of RNAi. Science *293*, 1146-1150.

Hammonds, J., Wang, J.J., Yi, H., and Spearman, P. (2010). Immunoelectron microscopic evidence for Tetherin/BST2 as the physical bridge between HIV-1 virions and the plasma membrane. PLoS Pathog *6*, e1000749.

Harris, R.S., Bishop, K.N., Sheehy, A.M., Craig, H.M., Petersen-Mahrt, S.K., Watt, I.N., Neuberger, M.S., and Malim, M.H. (2003a). DNA deamination mediates innate immunity to retroviral infection. Cell *113*, 803-809.

Harris, R.S., and Liddament, M.T. (2004). Retroviral restriction by APOBEC proteins. Nat Rev Immunol *4*, 868-877.

Harris, R.S., Petersen-Mahrt, S.K., and Neuberger, M.S. (2002a). RNA editing enzyme APOBEC1 and some of its homologs can act as DNA mutators. Mol Cell *10*, 1247-1253.

Harris, R.S., Sale, J.E., Petersen-Mahrt, S.K., and Neuberger, M.S. (2002b). AID is essential for immunoglobulin V gene conversion in a cultured B cell line. Curr Biol *12*, 435-438.

Harris, R.S., Sheehy, A.M., Craig, H.M., Malim, M.H., and Neuberger, M.S. (2003b). DNA deamination: not just a trigger for antibody diversification but also a mechanism for defense against retroviruses. Nat Immunol *4*, 641-643.

Hata, K., and Sakaki, Y. (1997). Identification of critical CpG sites for repression of L1 transcription by DNA methylation. Gene *189*, 227-234.

Hatziioannou, T., Perez-Caballero, D., Yang, A., Cowan, S., and Bieniasz, P.D. (2004). Retrovirus resistance factors Ref1 and Lv1 are species-specific variants of TRIM5alpha. Proc Natl Acad Sci U S A *101*, 10774-10779.

Hayes, A.M., Qian, S., Yu, L., and Boris-Lawrie, K. (2011). Tat RNA silencing suppressor activity contributes to perturbation of lymphocyte miRNA by HIV-1. Retrovirology *8*, 36.

Hilleren, P., and Parker, R. (1999). mRNA surveillance in eukaryotes: kinetic proofreading of proper translation termination as assessed by mRNP domain organization? RNA *5*, 711-719.

Hock, J., Weinmann, L., Ender, C., Rudel, S., Kremmer, E., Raabe, M., Urlaub, H., and Meister, G. (2007). Proteomic and functional analysis of Argonaute-containing mRNA-protein complexes in human cells. EMBO Rep *8*, 1052-1060.

Hogg, J.R., and Goff, S.P. (2010). Upf1 senses 3'UTR length to potentiate mRNA decay. Cell *143*, 379-389.

Holmes, R.K., Koning, F.A., Bishop, K.N., and Malim, M.H. (2007a). APOBEC3F can inhibit the accumulation of HIV-1 reverse transcription products in the absence of hypermutation. Comparisons with APOBEC3G. J Biol Chem *282*, 2587-2595.

Holmes, R.K., Malim, M.H., and Bishop, K.N. (2007b). APOBEC-mediated viral restriction: not simply editing? Trends Biochem Sci *32*, 118-128.

Houzet, L., and Jeang, K.T. (2011). MicroRNAs and human retroviruses. Biochim Biophys Acta.

Houzet, L., Yeung, M.L., de Lame, V., Desai, D., Smith, S.M., and Jeang, K.T. (2008). MicroRNA profile changes in human immunodeficiency virus type 1 (HIV-1) seropositive individuals. Retrovirology *5*, 118.

Hrecka, K., Gierszewska, M., Srivastava, S., Kozaczkiewicz, L., Swanson, S.K., Florens, L., Washburn, M.P., and Skowronski, J. (2007). Lentiviral Vpr usurps Cul4-DDB1[VprBP] E3 ubiquitin ligase to modulate cell cycle. Proc Natl Acad Sci U S A *104*, 11778-11783.

Hrecka, K., Hao, C., Gierszewska, M., Swanson, S.K., Kesik-Brodacka, M., Srivastava, S., Florens, L., Washburn, M.P., and Skowronski, J. (2011). Vpx relieves inhibition of HIV-1 infection of macrophages mediated by the SAMHD1 protein. Nature *474*, 658-661.

Hu, W., Petzold, C., Coller, J., and Baker, K.E. (2010). Nonsense-mediated mRNA decapping occurs on polyribosomes in Saccharomyces cerevisiae. Nat Struct Mol Biol *17*, 244-247.

Hu, W., Sweet, T.J., Chamnongpol, S., Baker, K.E., and Coller, J. (2009). Co-translational mRNA decay in Saccharomyces cerevisiae. Nature *461*, 225-229.

Huang, J., Liang, Z., Yang, B., Tian, H., Ma, J., and Zhang, H. (2007a). Derepression of microRNA-mediated protein translation inhibition by apolipoprotein B mRNA-editing enzyme catalytic polypeptide-like 3G (APOBEC3G) and its family members. J Biol Chem *282*, 33632-33640.

Huang, J., Wang, F., Argyris, E., Chen, K., Liang, Z., Tian, H., Huang, W., Squires, K., Verlinghieri, G., and Zhang, H. (2007b). Cellular microRNAs contribute to HIV-1 latency in resting primary CD4+ T lymphocytes. Nat Med *13*, 1241-1247.

Hultquist, J.F., Lengyel, J.A., Refsland, E.W., Larue, R.S., Lackey, L., Brown, W.L., and Harris, R.S. (2011). Human and Rhesus APOBEC3D, APOBEC3F, APOBEC3G, and APOBEC3H Demonstrate a Conserved Capacity to Restrict Vif-deficient HIV-1. J Virol.

Huthoff, H., Autore, F., Gallois-Montbrun, S., Fraternali, F., and Malim, M.H. (2009). RNA-dependent oligomerization of APOBEC3G is required for restriction of HIV-1. PLoS Pathog *5*, e1000330.

Huthoff, H., and Malim, M.H. (2007). Identification of amino acid residues in APOBEC3G required for regulation by human immunodeficiency virus type 1 Vif and Virion encapsidation. J Virol *81*, 3807-3815.

Hutvagner, G., McLachlan, J., Pasquinelli, A.E., Balint, E., Tuschl, T., and Zamore, P.D. (2001). A cellular function for the RNA-interference enzyme Dicer in the maturation of the let-7 small temporal RNA. Science *293*, 834-838.

Hutvagner, G., and Zamore, P.D. (2002). A microRNA in a multiple-turnover RNAi enzyme complex. Science *297*, 2056-2060.

Ingelfinger, D., Arndt-Jovin, D.J., Luhrmann, R., and Achsel, T. (2002). The human LSm1-7 proteins colocalize with the mRNA-degrading enzymes Dcp1/2 and Xrnl in distinct cytoplasmic foci. RNA *8*, 1489-1501.

Jakymiw, A., Lian, S., Eystathioy, T., Li, S., Satoh, M., Hamel, J.C., Fritzler, M.J., and Chan, E.K. (2005). Disruption of GW bodies impairs mammalian RNA interference. Nat Cell Biol *7*, 1267-1274.

Jangra, R.K., Yi, M., and Lemon, S.M. (2010). DDX6 (Rck/p54) is required for efficient hepatitis C virus replication but not for internal ribosome entry site-directed translation. J Virol *84*, 6810-6824.

Janini, M., Rogers, M., Birx, D.R., and McCutchan, F.E. (2001). Human immunodeficiency virus type 1 DNA sequences genetically damaged by hypermutation are often abundant in patient peripheral blood mononuclear cells and may be generated during near-simultaneous infection and activation of CD4(+) T cells. J Virol *75*, 7973-7986.

Janvier, K., Pelchen-Matthews, A., Renaud, J.B., Caillet, M., Marsh, M., and Berlioz-Torrent, C. (2011). The ESCRT-0 component HRS is required for HIV-1 Vpu-mediated BST-2/tetherin down-regulation. PLoS Pathog *7*, e1001265.

Jarmuz, A., Chester, A., Bayliss, J., Gisbourne, J., Dunham, I., Scott, J., and Navaratnam, N. (2002). An anthropoid-specific locus of orphan C to U RNA-editing enzymes on chromosome 22. Genomics *79*, 285-296.

Jern, P., Russell, R.A., Pathak, V.K., and Coffin, J.M. (2009). Likely role of APOBEC3G-mediated G-to-A mutations in HIV-1 evolution and drug resistance. PLoS Pathog *5*, e1000367.

Jia, B., Serra-Moreno, R., Neidermyer, W., Rahmberg, A., Mackey, J., Fofana, I.B., Johnson, W.E., Westmoreland, S., and Evans, D.T. (2009). Species-specific activity of SIV Nef and HIV-1 Vpu in overcoming restriction by tetherin/BST2. PLoS Pathog *5*, e1000429.

Jing, Q., Huang, S., Guth, S., Zarubin, T., Motoyama, A., Chen, J., Di Padova, F., Lin, S.C., Gram, H., and Han, J. (2005). Involvement of microRNA in AU-rich element-mediated mRNA instability. Cell *120*, 623-634.

Jopling, C.L., Yi, M., Lancaster, A.M., Lemon, S.M., and Sarnow, P. (2005). Modulation of hepatitis C virus RNA abundance by a liver-specific MicroRNA. Science *309*, 1577-1581.

Jouvenet, N., Simon, S.M., and Bieniasz, P.D. (2009). Imaging the interaction of HIV-1 genomes and Gag during assembly of individual viral particles. Proc Natl Acad Sci U S A *106*, 19114-19119.

Kaiser, S.M., and Emerman, M. (2006). Uracil DNA glycosylase is dispensable for human immunodeficiency virus type 1 replication and does not contribute to the antiviral effects of the cytidine deaminase Apobec3G. J Virol *80*, 875-882.

Kaletsky, R.L., Francica, J.R., Agrawal-Gamse, C., and Bates, P. (2009). Tetherin-mediated restriction of filovirus budding is antagonized by the Ebola glycoprotein. Proc Natl Acad Sci U S A *106*, 2886-2891.

Kawamura, Y., Saito, K., Kin, T., Ono, Y., Asai, K., Sunohara, T., Okada, T.N., Siomi, M.C., and Siomi, H. (2008). Drosophila endogenous small RNAs bind to Argonaute 2 in somatic cells. Nature *453*, 793-797.

Kazazian, H.H., Jr. (2004). Mobile elements: drivers of genome evolution. Science *303*, 1626-1632.

Kedersha, N., and Anderson, P. (2002). Stress granules: sites of mRNA triage that regulate mRNA stability and translatability. Biochem Soc Trans *30*, 963-969.

Kedersha, N., and Anderson, P. (2007). Mammalian stress granules and processing bodies. Methods Enzymol *431*, 61-81.

Kedersha, N., Stoecklin, G., Ayodele, M., Yacono, P., Lykke-Andersen, J., Fritzler, M.J., Scheuner, D., Kaufman, R.J., Golan, D.E., and Anderson, P. (2005). Stress granules and processing bodies are dynamically linked sites of mRNP remodeling. J Cell Biol *169*, 871-884.

Kedersha, N.L., Gupta, M., Li, W., Miller, I., and Anderson, P. (1999). RNA-binding proteins TIA-1 and TIAR link the phosphorylation of eIF-2 alpha to the assembly of mammalian stress granules. J Cell Biol *147*, 1431-1442.

Keegan, L.P., Gallo, A., and O'Connell, M.A. (2001). The many roles of an RNA editor. Nat Rev Genet *2*, 869-878.

Keele, B.F., Jones, J.H., Terio, K.A., Estes, J.D., Rudicell, R.S., Wilson, M.L., Li, Y., Learn, G.H., Beasley, T.M., Schumacher-Stankey, J.*, et al.* (2009). Increased mortality and AIDS-like immunopathology in wild chimpanzees infected with SIVcpz. Nature *460*, 515-519.

Keele, B.F., Van Heuverswyn, F., Li, Y., Bailes, E., Takehisa, J., Santiago, M.L., Bibollet-Ruche, F., Chen, Y., Wain, L.V., Liegeois, F*., et al.* (2006). Chimpanzee reservoirs of pandemic and nonpandemic HIV-1. Science *313*, 523-526.

Khan, M.A., Goila-Gaur, R., Kao, S., Miyagi, E., Walker, R.C., Jr., and Strebel, K. (2009). Encapsidation of APOBEC3G into HIV-1 virions involves lipid raft association and does not correlate with APOBEC3G oligomerization. Retrovirology *6*, 99.

Khan, M.A., Kao, S., Miyagi, E., Takeuchi, H., Goila-Gaur, R., Opi, S., Gipson, C.L., Parslow, T.G., Ly, H., and Strebel, K. (2005). Viral RNA is required for the association of APOBEC3G with human immunodeficiency virus type 1 nucleoprotein complexes. J Virol *79*, 5870-5874.

Kieffer, T.L., Kwon, P., Nettles, R.E., Han, Y., Ray, S.C., and Siliciano, R.F. (2005). G-->A hypermutation in protease and reverse transcriptase regions of human immunodeficiency virus type 1 residing in resting CD4+ T cells in vivo. J Virol *79*, 1975-1980.

Kim, V.N., Han, J., and Siomi, M.C. (2009). Biogenesis of small RNAs in animals. Nat Rev Mol Cell Biol *10*, 126-139.

Kimball, S.R., Horetsky, R.L., Ron, D., Jefferson, L.S., and Harding, H.P. (2003). Mammalian stress granules represent sites of accumulation of stalled translation initiation complexes. Am J Physiol Cell Physiol *284*, C273-284.

Kiriakidou, M., Tan, G.S., Lamprinaki, S., De Planell-Saguer, M., Nelson, P.T., and Mourelatos, Z. (2007). An mRNA m7G cap binding-like motif within human Ago2 represses translation. Cell *129*, 1141-1151.

Klase, Z., Kale, P., Winograd, R., Gupta, M.V., Heydarian, M., Berro, R., McCaffrey, T., and Kashanchi, F. (2007). HIV-1 TAR element is processed by Dicer to yield a viral micro-RNA involved in chromatin remodeling of the viral LTR. BMC Mol Biol *8*, 63.

Klase, Z., Winograd, R., Davis, J., Carpio, L., Hildreth, R., Heydarian, M., Fu, S., McCaffrey, T., Meiri, E., Ayash-Rashkovsky, M*., et al.* (2009). HIV-1 TAR miRNA protects against apoptosis by altering cellular gene expression. Retrovirology *6*, 18.

Klattenhoff, C., and Theurkauf, W. (2008). Biogenesis and germline functions of piRNAs. Development *135*, 3-9.

Klimkait, T., Strebel, K., Hoggan, M.D., Martin, M.A., and Orenstein, J.M. (1990). The human immunodeficiency virus type 1-specific protein vpu is required for efficient virus maturation and release. J Virol *64*, 621-629.

Komohara, Y., Yano, H., Shichijo, S., Shimotohno, K., Itoh, K., and Yamada, A. (2006). High expression of APOBEC3G in patients infected with hepatitis C virus. J Mol Histol *37*, 327-332.

Konig, R., Zhou, Y., Elleder, D., Diamond, T.L., Bonamy, G.M., Irelan, J.T., Chiang, C.Y., Tu, B.P., De Jesus, P.D., Lilley, C.E*., et al.* (2008). Global analysis of host-pathogen interactions that regulate early-stage HIV-1 replication. Cell *135*, 49-60.

Koning, F.A., Newman, E.N., Kim, E.Y., Kunstman, K.J., Wolinsky, S.M., and Malim, M.H. (2009). Defining APOBEC3 expression patterns in human tissues and hematopoietic cell subsets. J Virol *83*, 9474-9485.

Kozak, S.L., Marin, M., Rose, K.M., Bystrom, C., and Kabat, D. (2006). The anti-HIV-1 editing enzyme APOBEC3G binds HIV-1 RNA and messenger RNAs that shuttle between polysomes and stress granules. J Biol Chem *281*, 29105-29119.

Krausslich, H.G., Facke, M., Heuser, A.M., Konvalinka, J., and Zentgraf, H. (1995). The spacer peptide between human immunodeficiency virus capsid and nucleocapsid proteins is essential for ordered assembly and viral infectivity. J Virol *69*, 3407-3419.

Kulkarni, M., Ozgur, S., and Stoecklin, G. (2010). On track with P-bodies. Biochem Soc Trans *38*, 242-251.

Kulpa, D.A., and Moran, J.V. (2005). Ribonucleoprotein particle formation is necessary but not sufficient for LINE-1 retrotransposition. Hum Mol Genet *14*, 3237-3248.

Laguette, N., Sobhian, B., Casartelli, N., Ringeard, M., Chable-Bessia, C., Segeral, E., Yatim, A., Emiliani, S., Schwartz, O., and Benkirane, M. (2011). SAMHD1 is the dendritic- and myeloid-cell-specific HIV-1 restriction factor counteracted by Vpx. Nature.

Lama, J., Mangasarian, A., and Trono, D. (1999). Cell-surface expression of CD4 reduces HIV-1 infectivity by blocking Env incorporation in a Nef- and Vpu-inhibitable manner. Curr Biol *9*, 622-631.

Landthaler, M., Gaidatzis, D., Rothballer, A., Chen, P.Y., Soll, S.J., Dinic, L., Ojo, T., Hafner, M., Zavolan, M., and Tuschl, T. (2008). Molecular characterization of human Argonaute-containing ribonucleoprotein complexes and their bound target mRNAs. RNA *14*, 2580-2596.

Langlois, M.A., Beale, R.C., Conticello, S.G., and Neuberger, M.S. (2005). Mutational comparison of the single-domained APOBEC3C and double-domained APOBEC3F/G anti-retroviral cytidine deaminases provides insight into their DNA target site specificities. Nucleic Acids Res *33*, 1913-1923.

Langlois, M.A., and Neuberger, M.S. (2008). Human APOBEC3G can restrict retroviral infection in avian cells and acts independently of both UNG and SMUG1. J Virol *82*, 4660-4664.

Lau, N.C., Seto, A.G., Kim, J., Kuramochi-Miyagawa, S., Nakano, T., Bartel, D.P., and Kingston, R.E. (2006). Characterization of the piRNA complex from rat testes. Science *313*, 363-367.

Le Hir, H., Moore, M.J., and Maquat, L.E. (2000). Pre-mRNA splicing alters mRNP composition: evidence for stable association of proteins at exon-exon junctions. Genes Dev *14*, 1098-1108.

Le Tortorec, A., and Neil, S.J. (2009). Antagonism to and intracellular sequestration of human tetherin by the human immunodeficiency virus type 2 envelope glycoprotein. J Virol *83*, 11966-11978.

Lecellier, C.H., Dunoyer, P., Arar, K., Lehmann-Che, J., Eyquem, S., Himber, C., Saib, A., and Voinnet, O. (2005). A cellular microRNA mediates antiviral defense in human cells. Science *308*, 557-560.

Lee, Y., Ahn, C., Han, J., Choi, H., Kim, J., Yim, J., Lee, J., Provost, P., Radmark, O., Kim, S.*, et al.* (2003). The nuclear RNase III Drosha initiates microRNA processing. Nature *425*, 415-419.

Lee, Y., Jeon, K., Lee, J.T., Kim, S., and Kim, V.N. (2002). MicroRNA maturation: stepwise processing and subcellular localization. EMBO J *21*, 4663-4670.

Lee, Y.S., Pressman, S., Andress, A.P., Kim, K., White, J.L., Cassidy, J.J., Li, X., Lubell, K., Lim do, H., Cho, I.S.*, et al.* (2009). Silencing by small RNAs is linked to endosomal trafficking. Nat Cell Biol *11*, 1150-1156.

Lejeune, F., Li, X., and Maquat, L.E. (2003). Nonsense-mediated mRNA decay in mammalian cells involves decapping, deadenylating, and exonucleolytic activities. Mol Cell *12*, 675-687.

Lellek, H., Kirsten, R., Diehl, I., Apostel, F., Buck, F., and Greeve, J. (2000). Purification and molecular cloning of a novel essential component of the apolipoprotein B mRNA editing enzyme-complex. J Biol Chem *275*, 19848-19856.

Leung, A.K., Calabrese, J.M., and Sharp, P.A. (2006). Quantitative analysis of Argonaute protein reveals microRNA-dependent localization to stress granules. Proc Natl Acad Sci U S A *103*, 18125-18130.

Lewinski, M.K., Yamashita, M., Emerman, M., Ciuffi, A., Marshall, H., Crawford, G., Collins, F., Shinn, P., Leipzig, J., Hannenhalli, S.*, et al.* (2006). Retroviral DNA integration: viral and cellular determinants of target-site selection. PLoS Pathog *2*, e60.

Lewis, P., Hensel, M., and Emerman, M. (1992). Human immunodeficiency virus infection of cells arrested in the cell cycle. EMBO J *11*, 3053-3058.

Li, S., Lian, S.L., Moser, J.J., Fritzler, M.L., Fritzler, M.J., Satoh, M., and Chan, E.K. (2008). Identification of GW182 and its novel isoform TNGW1 as translational repressors in Ago2-mediated silencing. J Cell Sci *121*, 4134-4144.

Lian, S., Fritzler, M.J., Katz, J., Hamazaki, T., Terada, N., Satoh, M., and Chan, E.K. (2007). Small interfering RNA-mediated silencing induces target-dependent assembly of GW/P bodies. Mol Biol Cell *18*, 3375-3387.

Liao, W., Hong, S.H., Chan, B.H., Rudolph, F.B., Clark, S.C., and Chan, L. (1999). APOBEC-2, a cardiac- and skeletal muscle-specific member of the cytidine deaminase supergene family. Biochem Biophys Res Commun *260*, 398-404.

Liddament, M.T., Brown, W.L., Schumacher, A.J., and Harris, R.S. (2004). APOBEC3F properties and hypermutation preferences indicate activity against HIV-1 in vivo. Curr Biol *14*, 1385-1391.

Lim, A.K., Tao, L., and Kai, T. (2009). piRNAs mediate posttranscriptional retroelement silencing and localization to pi-bodies in the Drosophila germline. J Cell Biol *186*, 333-342.

Limon, A., Nakajima, N., Lu, R., Ghory, H.Z., and Engelman, A. (2002). Wild-type levels of nuclear localization and human immunodeficiency virus type 1 replication in the absence of the central DNA flap. J Virol *76*, 12078-12086.

Lin, J., and Cullen, B.R. (2007). Analysis of the interaction of primate retroviruses with the human RNA interference machinery. J Virol *81*, 12218-12226.

Lingel, A., Simon, B., Izaurralde, E., and Sattler, M. (2003). Structure and nucleic-acid binding of the Drosophila Argonaute 2 PAZ domain. Nature *426*, 465-469.

Liu, J., Carmell, M.A., Rivas, F.V., Marsden, C.G., Thomson, J.M., Song, J.J., Hammond, S.M., Joshua-Tor, L., and Hannon, G.J. (2004). Argonaute2 is the catalytic engine of mammalian RNAi. Science *305*, 1437-1441.

Liu, J., Rivas, F.V., Wohlschlegel, J., Yates, J.R., 3rd, Parker, R., and Hannon, G.J. (2005a). A role for the P-body component GW182 in microRNA function. Nat Cell Biol *7*, 1261-1266.

Liu, J., Valencia-Sanchez, M.A., Hannon, G.J., and Parker, R. (2005b). MicroRNA-dependent localization of targeted mRNAs to mammalian P-bodies. Nat Cell Biol *7*, 719-723.

Liu, R., Paxton, W.A., Choe, S., Ceradini, D., Martin, S.R., Horuk, R., MacDonald, M.E., Stuhlmann, H., Koup, R.A., and Landau, N.R. (1996). Homozygous defect in HIV-1 coreceptor accounts for resistance of some multiply-exposed individuals to HIV-1 infection. Cell *86*, 367-377.

Llano, M., Saenz, D.T., Meehan, A., Wongthida, P., Peretz, M., Walker, W.H., Teo, W., and Poeschla, E.M. (2006). An essential role for LEDGF/p75 in HIV integration. Science *314*, 461-464.

Lleres, D., Swift, S., and Lamond, A.I. (2007). Detecting protein-protein interactions in vivo with FRET using multiphoton fluorescence lifetime imaging microscopy (FLIM). Curr Protoc Cytom *Chapter 12*, Unit12 10.

Lu, C., Contreras, X., and Peterlin, B.M. (2011). P bodies inhibit retrotransposition of endogenous Intracisternal A Particles. J Virol.

Lu, S., and Cullen, B.R. (2004). Adenovirus VA1 noncoding RNA can inhibit small interfering RNA and MicroRNA biogenesis. J Virol *78*, 12868-12876.

Lund, E., Guttinger, S., Calado, A., Dahlberg, J.E., and Kutay, U. (2004). Nuclear export of microRNA precursors. Science *303*, 95-98.

Luo, K., Liu, B., Xiao, Z., Yu, Y., Yu, X., Gorelick, R., and Yu, X.F. (2004). Amino-terminal region of the human immunodeficiency virus type 1 nucleocapsid is required for human APOBEC3G packaging. J Virol *78*, 11841-11852.

Lytle, J.R., Yario, T.A., and Steitz, J.A. (2007). Target mRNAs are repressed as efficiently by microRNA-binding sites in the 5' UTR as in the 3' UTR. Proc Natl Acad Sci U S A *104*, 9667-9672.

Madani, N., and Kabat, D. (1998). An endogenous inhibitor of human immunodeficiency virus in human lymphocytes is overcome by the viral Vif protein. J Virol *72*, 10251-10255.

Maddon, P.J., Dalgleish, A.G., McDougal, J.S., Clapham, P.R., Weiss, R.A., and Axel, R. (1986). The T4 gene encodes the AIDS virus receptor and is expressed in the immune system and the brain. Cell *47*, 333-348.

Malim, M.H., and Cullen, B.R. (1991). HIV-1 structural gene expression requires the binding of multiple Rev monomers to the viral RRE: implications for HIV-1 latency. Cell *65*, 241-248.

Malim, M.H., and Emerman, M. (2008). HIV-1 accessory proteins--ensuring viral survival in a hostile environment. Cell Host Microbe *3*, 388-398.

Malim, M.H., Hauber, J., Le, S.Y., Maizel, J.V., and Cullen, B.R. (1989). The HIV-1 rev trans-activator acts through a structured target sequence to activate nuclear export of unspliced viral mRNA. Nature *338*, 254-257.

Mancebo, H.S., Lee, G., Flygare, J., Tomassini, J., Luu, P., Zhu, Y., Peng, J., Blau, C., Hazuda, D., Price, D.*, et al.* (1997). P-TEFb kinase is required for HIV Tat transcriptional activation in vivo and in vitro. Genes Dev *11*, 2633-2644.

Mangeat, B., Turelli, P., Caron, G., Friedli, M., Perrin, L., and Trono, D. (2003). Broad antiretroviral defence by human APOBEC3G through lethal editing of nascent reverse transcripts. Nature *424*, 99-103.

Mansharamani, M., Graham, D.R., Monie, D., Lee, K.K., Hildreth, J.E., Siliciano, R.F., and Wilson, K.L. (2003). Barrier-to-autointegration factor BAF binds p55 Gag and matrix and is a host component of human immunodeficiency virus type 1 virions. J Virol *77*, 13084-13092.

Margottin, F., Bour, S.P., Durand, H., Selig, L., Benichou, S., Richard, V., Thomas, D., Strebel, K., and Benarous, R. (1998). A novel human WD protein, h-beta TrCp, that interacts with HIV-1 Vpu connects CD4 to the ER degradation pathway through an F-box motif. Mol Cell *1*, 565-574.

Mariani, R., Chen, D., Schrofelbauer, B., Navarro, F., Konig, R., Bollman, B., Munk, C., Nymark-McMahon, H., and Landau, N.R. (2003). Species-specific exclusion of APOBEC3G from HIV-1 virions by Vif. Cell *114*, 21-31.

Marin, M., Golem, S., Rose, K.M., Kozak, S.L., and Kabat, D. (2008). Human immunodeficiency virus type 1 Vif functionally interacts with diverse APOBEC3 cytidine deaminases and moves with them between cytoplasmic sites of mRNA metabolism. J Virol *82*, 987-998.

Marin, M., Rose, K.M., Kozak, S.L., and Kabat, D. (2003). HIV-1 Vif protein binds the editing enzyme APOBEC3G and induces its degradation. Nat Med *9*, 1398-1403.

Martin, A., Bardwell, P.D., Woo, C.J., Fan, M., Shulman, M.J., and Scharff, M.D. (2002). Activation-induced cytidine deaminase turns on somatic hypermutation in hybridomas. Nature *415*, 802-806.

Martin, K.L., Johnson, M., and D'Aquila, R.T. (2011). APOBEC3G Complexes Decrease Human Immunodeficiency Virus Type 1 (HIV-1) Production. J Virol.

Martin, S.L., Cruceanu, M., Branciforte, D., Wai-Lun Li, P., Kwok, S.C., Hodges, R.S., and Williams, M.C. (2005). LINE-1 retrotransposition requires the nucleic acid chaperone activity of the ORF1 protein. J Mol Biol *348*, 549-561.

Martin-Serrano, J., and Neil, S.J. (2011). Host factors involved in retroviral budding and release. Nat Rev Microbiol *9*, 519-531.

Martin-Serrano, J., Zang, T., and Bieniasz, P.D. (2001). HIV-1 and Ebola virus encode small peptide motifs that recruit Tsg101 to sites of particle assembly to facilitate egress. Nat Med *7*, 1313-1319.

Martinez, J., and Tuschl, T. (2004). RISC is a 5' phosphomonoester-producing RNA endonuclease. Genes Dev *18*, 975-980.

Mas, A., Alves-Rodrigues, I., Noueiry, A., Ahlquist, P., and Diez, J. (2006). Host deadenylation-dependent mRNA decapping factors are required for a key step in brome mosaic virus RNA replication. J Virol *80*, 246-251.

Mbisa, J.L., Barr, R., Thomas, J.A., Vandegraaff, N., Dorweiler, I.J., Svarovskaia, E.S., Brown, W.L., Mansky, L.M., Gorelick, R.J., Harris, R.S.*, et al.* (2007). Human immunodeficiency virus type 1 cDNAs produced in the presence of APOBEC3G exhibit defects in plus-strand DNA transfer and integration. J Virol *81*, 7099-7110.

McDougall, W.M., and Smith, H.C. (2011). Direct evidence that RNA inhibits APOBEC3G ssDNA cytidine deaminase activity. Biochem Biophys Res Commun.

Mehle, A., Strack, B., Ancuta, P., Zhang, C., McPike, M., and Gabuzda, D. (2004). Vif overcomes the innate antiviral activity of APOBEC3G by promoting its degradation in the ubiquitin-proteasome pathway. J Biol Chem *279*, 7792-7798.

Mehta, A., Kinter, M.T., Sherman, N.E., and Driscoll, D.M. (2000). Molecular cloning of apobec-1 complementation factor, a novel RNA-binding protein involved in the editing of apolipoprotein B mRNA. Mol Cell Biol *20*, 1846-1854.

Meister, G., Landthaler, M., Patkaniowska, A., Dorsett, Y., Teng, G., and Tuschl, T. (2004). Human Argonaute 2 mediates RNA cleavage targeted by miRNAs and siRNAs Molecular Cell *15*, 185-197.

Meister, G., Landthaler, M., Peters, L., Chen, P.Y., Urlaub, H., Luhrmann, R., and Tuschl, T. (2005). Identification of novel argonaute-associated proteins. Curr Biol *15*, 2149-2155.

Mikl, M.C., Watt, I.N., Lu, M., Reik, W., Davies, S.L., Neuberger, M.S., and Rada, C. (2005). Mice deficient in APOBEC2 and APOBEC3. Mol Cell Biol *25*, 7270-7277.

Mili, S., and Steitz, J.A. (2004). Evidence for reassociation of RNA-binding proteins after cell lysis: implications for the interpretation of immunoprecipitation analyses. RNA *10*, 1692-1694.

Minshall, N., Kress, M., Weil, D., and Standart, N. (2009). Role of p54 RNA helicase activity and its C-terminal domain in translational repression, P-body localization and assembly. Mol Biol Cell *20*, 2464-2472.

Mitchell, R.S., Katsura, C., Skasko, M.A., Fitzpatrick, K., Lau, D., Ruiz, A., Stephens, E.B., Margottin-Goguet, F., Benarous, R., and Guatelli, J.C. (2009). Vpu antagonizes BST-2-mediated restriction of HIV-1 release via beta-TrCP and endo-lysosomal trafficking. PLoS Pathog *5*, e1000450.

Miyagi, E., Brown, C.R., Opi, S., Khan, M., Goila-Gaur, R., Kao, S., Walker, R.C., Jr., Hirsch, V., and Strebel, K. (2010). Stably expressed APOBEC3F has negligible antiviral activity. J Virol *84*, 11067-11075.

Moran, J.V., Holmes, S.E., Naas, T.P., DeBerardinis, R.J., Boeke, J.D., and Kazazian, H.H., Jr. (1996). High frequency retrotransposition in cultured mammalian cells. Cell *87*, 917-927.

Moulard, M., and Decroly, E. (2000). Maturation of HIV envelope glycoprotein precursors by cellular endoproteases. Biochim Biophys Acta *1469*, 121-132.

Muckenfuss, H., Hamdorf, M., Held, U., Perkovic, M., Lower, J., Cichutek, K., Flory, E., Schumann, G.G., and Munk, C. (2006). APOBEC3 proteins inhibit human LINE-1 retrotransposition. J Biol Chem *281*, 22161-22172.

Mukherjee, D., Gao, M., O'Connor, J.P., Raijmakers, R., Pruijn, G., Lutz, C.S., and Wilusz, J. (2002). The mammalian exosome mediates the efficient degradation of mRNAs that contain AU-rich elements. EMBO J *21*, 165-174.

Mulder, L.C., Harari, A., and Simon, V. (2008). Cytidine deamination induced HIV-1 drug resistance. Proc Natl Acad Sci U S A *105*, 5501-5506.

Mulder, L.C., Ooms, M., Majdak, S., Smedresman, J., Linscheid, C., Harari, A., Kunz, A., and Simon, V. (2010). Moderate influence of human APOBEC3F on HIV-1 replication in primary lymphocytes. J Virol *84*, 9613-9617.

Muramatsu, M., Kinoshita, K., Fagarasan, S., Yamada, S., Shinkai, Y., and Honjo, T. (2000). Class switch recombination and hypermutation require activation-induced cytidine deaminase (AID), a potential RNA editing enzyme. Cell *102*, 553-563.

Nachmani, D., Stern-Ginossar, N., Sarid, R., and Mandelboim, O. (2009). Diverse herpesvirus microRNAs target the stress-induced immune ligand MICB to escape recognition by natural killer cells. Cell Host Microbe *5*, 376-385.

Nathans, R., Chu, C.Y., Serquina, A.K., Lu, C.C., Cao, H., and Rana, T.M. (2009). Cellular microRNA and P bodies modulate host-HIV-1 interactions. Mol Cell *34*, 696-709.

Navarro, F., Bollman, B., Chen, H., Konig, R., Yu, Q., Chiles, K., and Landau, N.R. (2005). Complementary function of the two catalytic domains of APOBEC3G. Virology *333*, 374-386.

Neil, S.J., Eastman, S.W., Jouvenet, N., and Bieniasz, P.D. (2006). HIV-1 Vpu promotes release and prevents endocytosis of nascent retrovirus particles from the plasma membrane. PLoS Pathog *2*, e39.

Neil, S.J., Sandrin, V., Sundquist, W.I., and Bieniasz, P.D. (2007). An interferon-alpha-induced tethering mechanism inhibits HIV-1 and Ebola virus particle release but is counteracted by the HIV-1 Vpu protein. Cell Host Microbe *2*, 193-203.

Neil, S.J., Zang, T., and Bieniasz, P.D. (2008). Tetherin inhibits retrovirus release and is antagonized by HIV-1 Vpu. Nature *451*, 425-430.

Newman, E.N., Holmes, R.K., Craig, H.M., Klein, K.C., Lingappa, J.R., Malim, M.H., and Sheehy, A.M. (2005). Antiviral function of APOBEC3G can be dissociated from cytidine deaminase activity. Curr Biol *15*, 166-170.

Nguyen, D.H., Gummuluru, S., and Hu, J. (2007). Deamination-independent inhibition of hepatitis B virus reverse transcription by APOBEC3G. J Virol *81*, 4465-4472.

Nguyen, D.H., and Hildreth, J.E. (2000). Evidence for budding of human immunodeficiency virus type 1 selectively from glycolipid-enriched membrane lipid rafts. J Virol *74*, 3264-3272.

Niewiadomska, A.M., Tian, C., Tan, L., Wang, T., Sarkis, P.T., and Yu, X.F. (2007). Differential inhibition of long interspersed element 1 by APOBEC3 does not correlate with high-molecular-mass-complex formation or P-body association. J Virol *81*, 9577-9583.

Niranjanakumari, S., Lasda, E., Brazas, R., and Garcia-Blanco, M.A. (2002). Reversible cross-linking combined with immunoprecipitation to study RNA-protein interactions in vivo. Methods *26*, 182-190.

Nitahara-Kasahara, Y., Kamata, M., Yamamoto, T., Zhang, X., Miyamoto, Y., Muneta, K., Iijima, S., Yoneda, Y., Tsunetsugu-Yokota, Y., and Aida, Y. (2007). Novel nuclear import of Vpr promoted by importin alpha is crucial for human immunodeficiency virus type 1 replication in macrophages. J Virol *81*, 5284-5293.

Noueiry, A.O., Diez, J., Falk, S.P., Chen, J., and Ahlquist, P. (2003). Yeast Lsm1p-7p/Pat1p deadenylation-dependent mRNA-decapping factors are required for brome mosaic virus genomic RNA translation. Mol Cell Biol *23*, 4094-4106.

OhAinle, M., Kerns, J.A., Li, M.M., Malik, H.S., and Emerman, M. (2008). Antiretroelement activity of APOBEC3H was lost twice in recent human evolution. Cell Host Microbe *4*, 249-259.

OhAinle, M., Kerns, J.A., Malik, H.S., and Emerman, M. (2006). Adaptive evolution and antiviral activity of the conserved mammalian cytidine deaminase APOBEC3H. J Virol *80*, 3853-3862.

Okamura, K., Chung, W.J., Ruby, J.G., Guo, H., Bartel, D.P., and Lai, E.C. (2008). The Drosophila hairpin RNA pathway generates endogenous short interfering RNAs. Nature *453*, 803-806.

Okamura, K., Liu, N., and Lai, E.C. (2009). Distinct mechanisms for microRNA strand selection by Drosophila Argonautes. Mol Cell *36*, 431-444.

Ono, A., Ablan, S.D., Lockett, S.J., Nagashima, K., and Freed, E.O. (2004). Phosphatidylinositol (4,5) bisphosphate regulates HIV-1 Gag targeting to the plasma membrane. Proc Natl Acad Sci U S A *101*, 14889-14894.

Ostertag, E.M., and Kazazian, H.H., Jr. (2001). Biology of mammalian L1 retrotransposons. Annu Rev Genet *35*, 501-538.

Ott, D.E. (2008). Cellular proteins detected in HIV-1. Rev Med Virol *18*, 159-175.

Ouellet, D.L., Plante, I., Landry, P., Barat, C., Janelle, M.E., Flamand, L., Tremblay, M.J., and Provost, P. (2008). Identification of functional microRNAs released through asymmetrical processing of HIV-1 TAR element. Nucleic Acids Res *36*, 2353-2365.

Owsianka, A.M., and Patel, A.H. (1999). Hepatitis C virus core protein interacts with a human DEAD box protein DDX3. Virology *257*, 330-340.

Pache, L., Konig, R., and Chanda, S.K. (2011). Identifying HIV-1 host cell factors by genome-scale RNAi screening. Methods *53*, 3-12.

Parent, L.J., Bennett, R.P., Craven, R.C., Nelle, T.D., Krishna, N.K., Bowzard, J.B., Wilson, C.B., Puffer, B.A., Montelaro, R.C., and Wills, J.W. (1995). Positionally

independent and exchangeable late budding functions of the Rous sarcoma virus and human immunodeficiency virus Gag proteins. J Virol *69*, 5455-5460.

Parker, R., and Sheth, U. (2007). P bodies and the control of mRNA translation and degradation. Mol Cell *25*, 635-646.

Parker, R., and Song, H. (2004). The enzymes and control of eukaryotic mRNA turnover. Nat Struct Mol Biol *11*, 121-127.

Peng, G., Greenwell-Wild, T., Nares, S., Jin, W., Lei, K.J., Rangel, Z.G., Munson, P.J., and Wahl, S.M. (2007). Myeloid differentiation and susceptibility to HIV-1 are linked to APOBEC3 expression. Blood *110*, 393-400.

Pfeffer, S., Zavolan, M., Grasser, F.A., Chien, M., Russo, J.J., Ju, J., John, B., Enright, A.J., Marks, D., Sander, C., *et al.* (2004). Identification of virus-encoded microRNAs. Science *304*, 734-736.

Pillai, R.S., Artus, C.G., and Filipowicz, W. (2004). Tethering of human Ago proteins to mRNA mimics the miRNA-mediated repression of protein synthesis. RNA *10*, 1518-1525.

Pillai, R.S., Bhattacharyya, S.N., Artus, C.G., Zoller, T., Cougot, N., Basyuk, E., Bertrand, E., and Filipowicz, W. (2005). Inhibition of translational initiation by Let-7 MicroRNA in human cells. Science *309*, 1573-1576.

Qian, S., Zhong, X., Yu, L., Ding, B., de Haan, P., and Boris-Lawrie, K. (2009). HIV-1 Tat RNA silencing suppressor activity is conserved across kingdoms and counteracts translational repression of HIV-1. Proc Natl Acad Sci U S A *106*, 605-610.

Quenault, T., Lithgow, T., and Traven, A. (2011). PUF proteins: repression, activation and mRNA localization. Trends Cell Biol *21*, 104-112.

Randall, G., Panis, M., Cooper, J.D., Tellinghuisen, T.L., Sukhodolets, K.E., Pfeffer, S., Landthaler, M., Landgraf, P., Kan, S., Lindenbach, B.D., *et al.* (2007). Cellular cofactors affecting hepatitis C virus infection and replication. Proc Natl Acad Sci U S A *104*, 12884-12889.

Refsland, E.W., Stenglein, M.D., Shindo, K., Albin, J.S., Brown, W.L., and Harris, R.S. (2010). Quantitative profiling of the full APOBEC3 mRNA repertoire in lymphocytes and tissues: implications for HIV-1 restriction. Nucleic Acids Res *38*, 4274-4284.

Reijns, M.A., Alexander, R.D., Spiller, M.P., and Beggs, J.D. (2008). A role for Q/N-rich aggregation-prone regions in P-body localization. J Cell Sci *121*, 2463-2472.

Reil, H., Bukovsky, A.A., Gelderblom, H.R., and Gottlinger, H.G. (1998). Efficient HIV-1 replication can occur in the absence of the viral matrix protein. EMBO J *17*, 2699-2708.

Rice, G.I., Bond, J., Asipu, A., Brunette, R.L., Manfield, I.W., Carr, I.M., Fuller, J.C., Jackson, R.M., Lamb, T., Briggs, T.A*., et al.* (2009). Mutations involved in Aicardi-Goutieres syndrome implicate SAMHD1 as regulator of the innate immune response. Nat Genet *41*, 829-832.

Ritter, G.D., Jr., Yamshchikov, G., Cohen, S.J., and Mulligan, M.J. (1996). Human immunodeficiency virus type 2 glycoprotein enhancement of particle budding: role of the cytoplasmic domain. J Virol *70*, 2669-2673.

Roberts, A.P., Lewis, A.P., and Jopling, C.L. (2011). miR-122 activates hepatitis C virus translation by a specialized mechanism requiring particular RNA components. Nucleic Acids Res.

Roe, T., Reynolds, T.C., Yu, G., and Brown, P.O. (1993). Integration of murine leukemia virus DNA depends on mitosis. EMBO J *12*, 2099-2108.

Rogozin, I.B., Basu, M.K., Jordan, I.K., Pavlov, Y.I., and Koonin, E.V. (2005). APOBEC4, a new member of the AID/APOBEC family of polynucleotide (deoxy)cytidine deaminases predicted by computational analysis. Cell Cycle *4*, 1281-1285.

Rose, K.M., Marin, M., Kozak, S.L., and Kabat, D. (2005). Regulated production and anti-HIV type 1 activities of cytidine deaminases APOBEC3B, 3F, and 3G. AIDS Res Hum Retroviruses *21*, 611-619.

Rosenberg, B.R., Hamilton, C.E., Mwangi, M.M., Dewell, S., and Papavasiliou, F.N. (2011). Transcriptome-wide sequencing reveals numerous APOBEC1 mRNA-editing targets in transcript 3' UTRs. Nat Struct Mol Biol *18*, 230-236.

Rowe, P.M. (1996). CKR-5 deletion heterozygotes progress slower to AIDS. Lancet *348*, 947.

Rudel, S., Flatley, A., Weinmann, L., Kremmer, E., and Meister, G. (2008). A multifunctional human Argonaute2-specific monoclonal antibody. RNA *14*, 1244-1253.

Russell, R.A., Wiegand, H.L., Moore, M.D., Schafer, A., McClure, M.O., and Cullen, B.R. (2005). Foamy virus Bet proteins function as novel inhibitors of the APOBEC3 family of innate antiretroviral defense factors. J Virol *79*, 8724-8731.

Rybak, A., Fuchs, H., Hadian, K., Smirnova, L., Wulczyn, E.A., Michel, G., Nitsch, R., Krappmann, D., and Wulczyn, F.G. (2009). The let-7 target gene mouse lin-41 is a stem cell specific E3 ubiquitin ligase for the miRNA pathway protein Ago2. Nat Cell Biol *11*, 1411-1420.

Saad, J.S., Miller, J., Tai, J., Kim, A., Ghanam, R.H., and Summers, M.F. (2006). Structural basis for targeting HIV-1 Gag proteins to the plasma membrane for virus assembly. Proc Natl Acad Sci U S A *103*, 11364-11369.

Sadler, H.A., Stenglein, M.D., Harris, R.S., and Mansky, L.M. (2010). APOBEC3G contributes to HIV-1 variation through sublethal mutagenesis. J Virol *84*, 7396-7404.

Samson, M., Libert, F., Doranz, B.J., Rucker, J., Liesnard, C., Farber, C.M., Saragosti, S., Lapoumeroulie, C., Cognaux, J., Forceille, C.*, et al.* (1996). Resistance to HIV-1 infection in caucasian individuals bearing mutant alleles of the CCR-5 chemokine receptor gene. Nature *382*, 722-725.

Sanghvi, V.R., and Steel, L.F. (2011). A re-examination of global suppression of RNA interference by HIV-1. PLoS One *6*, e17246.

Sasada, A., Takaori-Kondo, A., Shirakawa, K., Kobayashi, M., Abudu, A., Hishizawa, M., Imada, K., Tanaka, Y., and Uchiyama, T. (2005). APOBEC3G targets human T-cell leukemia virus type 1. Retrovirology *2*, 32.

Sasaki, T., Shiohama, A., Minoshima, S., and Shimizu, N. (2003). Identification of eight members of the Argonaute family in the human genome small star, filled. Genomics *82*, 323-330.

Sassaman, D.M., Dombroski, B.A., Moran, J.V., Kimberland, M.L., Naas, T.P., DeBerardinis, R.J., Gabriel, A., Swergold, G.D., and Kazazian, H.H., Jr. (1997). Many human L1 elements are capable of retrotransposition. Nat Genet *16*, 37-43.

Sawyer, S.L., Emerman, M., and Malik, H.S. (2004). Ancient adaptive evolution of the primate antiviral DNA-editing enzyme APOBEC3G. PLoS Biol *2*, E275.

Sayah, D.M., Sokolskaja, E., Berthoux, L., and Luban, J. (2004). Cyclophilin A retrotransposition into TRIM5 explains owl monkey resistance to HIV-1. Nature *430*, 569-573.

Sayed, D., and Abdellatif, M. (2011). MicroRNAs in development and disease. Physiol Rev *91*, 827-887.

Schafer, A., Bogerd, H.P., and Cullen, B.R. (2004). Specific packaging of APOBEC3G into HIV-1 virions is mediated by the nucleocapsid domain of the gag polyprotein precursor. Virology *328*, 163-168.

Scheller, N., Mina, L.B., Galao, R.P., Chari, A., Gimenez-Barcons, M., Noueiry, A., Fischer, U., Meyerhans, A., and Diez, J. (2009). Translation and replication of hepatitis C virus genomic RNA depends on ancient cellular proteins that control mRNA fates. Proc Natl Acad Sci U S A *106*, 13517-13522.

Schmitter, D., Filkowski, J., Sewer, A., Pillai, R.S., Oakeley, E.J., Zavolan, M., Svoboda, P., and Filipowicz, W. (2006). Effects of Dicer and Argonaute down-regulation on mRNA levels in human HEK293 cells. Nucleic Acids Res *34*, 4801-4815.

Schrofelbauer, B., Chen, D., and Landau, N.R. (2004). A single amino acid of APOBEC3G controls its species-specific interaction with virion infectivity factor (Vif). Proc Natl Acad Sci U S A *101*, 3927-3932.

Schrofelbauer, B., Hakata, Y., and Landau, N.R. (2007). HIV-1 Vpr function is mediated by interaction with the damage-specific DNA-binding protein DDB1. Proc Natl Acad Sci U S A *104*, 4130-4135.

Schwarz, D.S., Hutvagner, G., Du, T., Xu, Z., Aronin, N., and Zamore, P.D. (2003). Asymmetry in the assembly of the RNAi enzyme complex. Cell *115*, 199-208.

Sen, G.L., and Blau, H.M. (2005). Argonaute 2/RISC resides in sites of mammalian mRNA decay known as cytoplasmic bodies. Nat Cell Biol *7*, 633-636.

Serman, A., Le Roy, F., Aigueperse, C., Kress, M., Dautry, F., and Weil, D. (2007). GW body disassembly triggered by siRNAs independently of their silencing activity. Nucleic Acids Res *35*, 4715-4727.

Seto, E., Moosmann, A., Gromminger, S., Walz, N., Grundhoff, A., and Hammerschmidt, W. (2010). Micro RNAs of Epstein-Barr virus promote cell cycle progression and prevent apoptosis of primary human B cells. PLoS Pathog *6*.

Shah, R.R., Knott, T.J., Legros, J.E., Navaratnam, N., Greeve, J.C., and Scott, J. (1991). Sequence requirements for the editing of apolipoprotein B mRNA. J Biol Chem *266*, 16301-16304.

Sheehy, A.M., Gaddis, N.C., Choi, J.D., and Malim, M.H. (2002). Isolation of a human gene that inhibits HIV-1 infection and is suppressed by the viral Vif protein. Nature *418*, 646-650.

Sheehy, A.M., Gaddis, N.C., and Malim, M.H. (2003). The antiretroviral enzyme APOBEC3G is degraded by the proteasome in response to HIV-1 Vif. Nat Med *9*, 1404-1407.

Sheth, U., and Parker, R. (2003). Decapping and decay of messenger RNA occur in cytoplasmic processing bodies. Science *300*, 805-808.

Sheth, U., and Parker, R. (2006). Targeting of aberrant mRNAs to cytoplasmic processing bodies. Cell *125*, 1095-1109.

Shun, M.C., Raghavendra, N.K., Vandegraaff, N., Daigle, J.E., Hughes, S., Kellam, P., Cherepanov, P., and Engelman, A. (2007). LEDGF/p75 functions downstream from preintegration complex formation to effect gene-specific HIV-1 integration. Genes Dev *21*, 1767-1778.

Shyu, A.B., Wilkinson, M.F., and van Hoof, A. (2008). Messenger RNA regulation: to translate or to degrade. EMBO J *27*, 471-481.

Simon, J.H., Fouchier, R.A., Southerling, T.E., Guerra, C.B., Grant, C.K., and Malim, M.H. (1997). The Vif and Gag proteins of human immunodeficiency virus type 1 colocalize in infected human T cells. J Virol *71*, 5259-5267.

Simon, J.H., Gaddis, N.C., Fouchier, R.A., and Malim, M.H. (1998). Evidence for a newly discovered cellular anti-HIV-1 phenotype. Nat Med *4*, 1397-1400.

Simpson-Holley, M., Kedersha, N., Dower, K., Rubins, K.H., Anderson, P., Hensley, L.E., and Connor, J.H. (2011). Formation of antiviral cytoplasmic granules during orthopoxvirus infection. J Virol *85*, 1581-1593.

Sokolskaja, E., Berthoux, L., and Luban, J. (2006). Cyclophilin A and TRIM5alpha independently regulate human immunodeficiency virus type 1 infectivity in human cells. J Virol *80*, 2855-2862.

Sokolskaja, E., and Luban, J. (2006). Cyclophilin, TRIM5, and innate immunity to HIV-1. Curr Opin Microbiol *9*, 404-408.

Song, B., Diaz-Griffero, F., Park, D.H., Rogers, T., Stremlau, M., and Sodroski, J. (2005). TRIM5alpha association with cytoplasmic bodies is not required for antiretroviral activity. Virology *343*, 201-211.

Song, J.J., Liu, J., Tolia, N.H., Schneiderman, J., Smith, S.K., Martienssen, R.A., Hannon, G.J., and Joshua-Tor, L. (2003). The crystal structure of the Argonaute2 PAZ domain reveals an RNA binding motif in RNAi effector complexes. Nat Struct Biol *10*, 1026-1032.

Song, J.J., Smith, S.K., Hannon, G.J., and Joshua-Tor, L. (2004). Crystal structure of Argonaute and its implications for RISC slicer activity. Science *305*, 1434-1437.

Song, L., Liu, H., Gao, S., Jiang, W., and Huang, W. (2010). Cellular microRNAs inhibit replication of the H1N1 influenza A virus in infected cells. J Virol *84*, 8849-8860.

Soros, V.B., Yonemoto, W., and Greene, W.C. (2007). Newly synthesized APOBEC3G is incorporated into HIV virions, inhibited by HIV RNA, and subsequently activated by RNase H. PLoS Pathog *3*, e15.

Sova, P., and Volsky, D.J. (1993). Efficiency of viral DNA synthesis during infection of permissive and nonpermissive cells with vif-negative human immunodeficiency virus type 1. J Virol *67*, 6322-6326.

Sowden, M., Hamm, J.K., and Smith, H.C. (1996). Overexpression of APOBEC-1 results in mooring sequence-dependent promiscuous RNA editing. J Biol Chem *271*, 3011-3017.

Stalder, L., and Muhlemann, O. (2009). Processing bodies are not required for mammalian nonsense-mediated mRNA decay. RNA *15*, 1265-1273.

Stenglein, M.D., Burns, M.B., Li, M., Lengyel, J., and Harris, R.S. (2010). APOBEC3 proteins mediate the clearance of foreign DNA from human cells. Nat Struct Mol Biol *17*, 222-229.

Stenglein, M.D., and Harris, R.S. (2006). APOBEC3B and APOBEC3F inhibit L1 retrotransposition by a DNA deamination-independent mechanism. J Biol Chem *281*, 16837-16841.

Stern-Ginossar, N., Elefant, N., Zimmermann, A., Wolf, D.G., Saleh, N., Biton, M., Horwitz, E., Prokocimer, Z., Prichard, M., Hahn, G., *et al.* (2007). Host immune system gene targeting by a viral miRNA. Science *317*, 376-381.

Stoecklin, G., Mayo, T., and Anderson, P. (2006). ARE-mRNA degradation requires the 5'-3' decay pathway. EMBO Rep *7*, 72-77.

Stopak, K., de Noronha, C., Yonemoto, W., and Greene, W.C. (2003). HIV-1 Vif blocks the antiviral activity of APOBEC3G by impairing both its translation and intracellular stability. Mol Cell *12*, 591-601.

Strack, B., Calistri, A., Craig, S., Popova, E., and Gottlinger, H.G. (2003). AIP1/ALIX is a binding partner for HIV-1 p6 and EIAV p9 functioning in virus budding. Cell *114*, 689-699.

Strebel, K., Daugherty, D., Clouse, K., Cohen, D., Folks, T., and Martin, M.A. (1987). The HIV 'A' (sor) gene product is essential for virus infectivity. Nature *328*, 728-730.

Stremlau, M., Owens, C.M., Perron, M.J., Kiessling, M., Autissier, P., and Sodroski, J. (2004). The cytoplasmic body component TRIM5alpha restricts HIV-1 infection in Old World monkeys. Nature *427*, 848-853.

Suspene, R., Aynaud, M.M., Guetard, D., Henry, M., Eckhoff, G., Marchio, A., Pineau, P., Dejean, A., Vartanian, J.P., and Wain-Hobson, S. (2011a). Somatic hypermutation of human mitochondrial and nuclear DNA by APOBEC3 cytidine deaminases, a pathway for DNA catabolism. Proc Natl Acad Sci U S A *108*, 4858-4863.

Suspene, R., Aynaud, M.M., Koch, S., Pasdeloup, D., Labetoulle, M., Gaertner, B., Vartanian, J.P., Meyerhans, A., and Wain-Hobson, S. (2011b). Genetic editing of herpes simplex virus 1 and Epstein-Barr herpesvirus genomes by human APOBEC3 cytidine deaminases in culture and in vivo. J Virol *85*, 7594-7602.

Suspene, R., Guetard, D., Henry, M., Sommer, P., Wain-Hobson, S., and Vartanian, J.P. (2005). Extensive editing of both hepatitis B virus DNA strands by APOBEC3 cytidine deaminases in vitro and in vivo. Proc Natl Acad Sci U S A *102*, 8321-8326.

Suspene, R., Sommer, P., Henry, M., Ferris, S., Guetard, D., Pochet, S., Chester, A., Navaratnam, N., Wain-Hobson, S., and Vartanian, J.P. (2004). APOBEC3G is a single-stranded DNA cytidine deaminase and functions independently of HIV reverse transcriptase. Nucleic Acids Res *32*, 2421-2429.

Svarovskaia, E.S., Xu, H., Mbisa, J.L., Barr, R., Gorelick, R.J., Ono, A., Freed, E.O., Hu, W.S., and Pathak, V.K. (2004). Human apolipoprotein B mRNA-editing enzyme-catalytic polypeptide-like 3G (APOBEC3G) is incorporated into HIV-1 virions through interactions with viral and nonviral RNAs. J Biol Chem *279*, 35822-35828.

Svoboda, P., Stein, P., Anger, M., Bernstein, E., Hannon, G.J., and Schultz, R.M. (2004). RNAi and expression of retrotransposons MuERV-L and IAP in preimplantation mouse embryos. Dev Biol *269*, 276-285.

Swanson, C.M., and Malim, M.H. (2006). Retrovirus RNA trafficking: from chromatin to invasive genomes. Traffic *7*, 1440-1450.

Swanson, C.M., and Malim, M.H. (2008). SnapShot: HIV-1 proteins. Cell *133*, 742, 742 e741.

Swanson, C.M., Sherer, N.M., and Malim, M.H. (2010). SRp40 and SRp55 promote the translation of unspliced human immunodeficiency virus type 1 RNA. J Virol *84*, 6748-6759.

Tam, O.H., Aravin, A.A., Stein, P., Girard, A., Murchison, E.P., Cheloufi, S., Hodges, E., Anger, M., Sachidanandam, R., Schultz, R.M.*, et al.* (2008). Pseudogene-derived small interfering RNAs regulate gene expression in mouse oocytes. Nature *453*, 534-538.

Teixeira, D., and Parker, R. (2007). Analysis of P-body assembly in Saccharomyces cerevisiae. Mol Biol Cell *18*, 2274-2287.

Teixeira, D., Sheth, U., Valencia-Sanchez, M.A., Brengues, M., and Parker, R. (2005). Processing bodies require RNA for assembly and contain nontranslating mRNAs. RNA *11*, 371-382.

Tolia, N.H., and Joshua-Tor, L. (2007). Slicer and the argonautes. Nat Chem Biol *3*, 36-43.

Towers, G., Bock, M., Martin, S., Takeuchi, Y., Stoye, J.P., and Danos, O. (2000). A conserved mechanism of retrovirus restriction in mammals. Proc Natl Acad Sci U S A *97*, 12295-12299.

Towers, G.J. (2007). The control of viral infection by tripartite motif proteins and cyclophilin A. Retrovirology *4*, 40.

Triboulet, R., Mari, B., Lin, Y.L., Chable-Bessia, C., Bennasser, Y., Lebrigand, K., Cardinaud, B., Maurin, T., Barbry, P., Baillat, V.*, et al.* (2007). Suppression of microRNA-silencing pathway by HIV-1 during virus replication. Science *315*, 1579-1582.

Turelli, P., Mangeat, B., Jost, S., Vianin, S., and Trono, D. (2004). Inhibition of hepatitis B virus replication by APOBEC3G. Science *303*, 1829.

Umbach, J.L., and Cullen, B.R. (2009). The role of RNAi and microRNAs in animal virus replication and antiviral immunity. Genes Dev *23*, 1151-1164.

UNAIDS (2009). AIDS Epidemic Update, Global Facts and Figures (World Health Organisation).

Vagin, V.V., Sigova, A., Li, C., Seitz, H., Gvozdev, V., and Zamore, P.D. (2006). A distinct small RNA pathway silences selfish genetic elements in the germline. Science *313*, 320-324.

Van Damme, N., Goff, D., Katsura, C., Jorgenson, R.L., Mitchell, R., Johnson, M.C., Stephens, E.B., and Guatelli, J. (2008). The interferon-induced protein BST-2 restricts HIV-1 release and is downregulated from the cell surface by the viral Vpu protein. Cell Host Microbe *3*, 245-252.

Van Heuverswyn, F., Li, Y., Neel, C., Bailes, E., Keele, B.F., Liu, W., Loul, S., Butel, C., Liegeois, F., Bienvenue, Y., *et al.* (2006). Human immunodeficiency viruses: SIV infection in wild gorillas. Nature *444*, 164.

Vartanian, J.P., Guetard, D., Henry, M., and Wain-Hobson, S. (2008). Evidence for editing of human papillomavirus DNA by APOBEC3 in benign and precancerous lesions. Science *320*, 230-233.

Vartanian, J.P., Meyerhans, A., Asjo, B., and Wain-Hobson, S. (1991). Selection, recombination, and G----A hypermutation of human immunodeficiency virus type 1 genomes. J Virol *65*, 1779-1788.

Vasudevan, S., and Steitz, J.A. (2007a). AU-rich-element-mediated upregulation of translation by FXR1 and Argonaute 2. Cell *128*, 1105-1118.

Vasudevan, S., Tong, Y., and Steitz, J.A. (2007b). Switching from repression to activation: microRNAs can up-regulate translation. Science *318*, 1931-1934.

Vasudevan, S., Tong, Y., and Steitz, J.A. (2008). Cell-cycle control of microRNA-mediated translation regulation. Cell Cycle *7*, 1545-1549.

Voinnet, O., Pinto, Y.M., and Baulcombe, D.C. (1999). Suppression of gene silencing: a general strategy used by diverse DNA and RNA viruses of plants. Proc Natl Acad Sci U S A *96*, 14147-14152.

von Schwedler, U., Song, J., Aiken, C., and Trono, D. (1993). Vif is crucial for human immunodeficiency virus type 1 proviral DNA synthesis in infected cells. J Virol *67*, 4945-4955.

Wang, T., Tian, C., Zhang, W., Luo, K., Sarkis, P.T., Yu, L., Liu, B., Yu, Y., and Yu, X.F. (2007). 7SL RNA mediates virion packaging of the antiviral cytidine deaminase APOBEC3G. J Virol *81*, 13112-13124.

Wang, T., Tian, C., Zhang, W., Sarkis, P.T., and Yu, X.F. (2008). Interaction with 7SL RNA but not with HIV-1 genomic RNA or P bodies is required for APOBEC3F virion packaging. J Mol Biol *375*, 1098-1112.

Wang, X., Han, Y., Dang, Y., Fu, W., Zhou, T., Ptak, R.G., and Zheng, Y.H. (2010). Moloney leukemia virus 10 (MOV10) protein inhibits retrovirus replication. J Biol Chem *285*, 14346-14355.

Watanabe, T., Totoki, Y., Toyoda, A., Kaneda, M., Kuramochi-Miyagawa, S., Obata, Y., Chiba, H., Kohara, Y., Kono, T., Nakano, T., *et al.* (2008). Endogenous siRNAs from naturally formed dsRNAs regulate transcripts in mouse oocytes. Nature *453*, 539-543.

Wei, P., Garber, M.E., Fang, S.M., Fischer, W.H., and Jones, K.A. (1998). A novel CDK9-associated C-type cyclin interacts directly with HIV-1 Tat and mediates its high-affinity, loop-specific binding to TAR RNA. Cell *92*, 451-462.

Wei, X., Decker, J.M., Liu, H., Zhang, Z., Arani, R.B., Kilby, J.M., Saag, M.S., Wu, X., Shaw, G.M., and Kappes, J.C. (2002). Emergence of resistant human immunodeficiency virus type 1 in patients receiving fusion inhibitor (T-20) monotherapy. Antimicrob Agents Chemother *46*, 1896-1905.

Weinberg, J.B., Matthews, T.J., Cullen, B.R., and Malim, M.H. (1991). Productive human immunodeficiency virus type 1 (HIV-1) infection of nonproliferating human monocytes. J Exp Med *174*, 1477-1482.

Weinmann, L., Hock, J., Ivacevic, T., Ohrt, T., Mutze, J., Schwille, P., Kremmer, E., Benes, V., Urlaub, H., and Meister, G. (2009). Importin 8 is a gene silencing factor that targets argonaute proteins to distinct mRNAs. Cell *136*, 496-507.

Wharton, R.P., and Aggarwal, A.K. (2006). mRNA regulation by Puf domain proteins. Sci STKE *2006*, pe37.

White, J.P., Cardenas, A.M., Marissen, W.E., and Lloyd, R.E. (2007). Inhibition of cytoplasmic mRNA stress granule formation by a viral proteinase. Cell Host Microbe *2*, 295-305.

Wichroski, M.J., Ichiyama, K., and Rana, T.M. (2005). Analysis of HIV-1 viral infectivity factor-mediated proteasome-dependent depletion of APOBEC3G: correlating function and subcellular localization. J Biol Chem *280*, 8387-8396.

Wichroski, M.J., Robb, G.B., and Rana, T.M. (2006). Human retroviral host restriction factors APOBEC3G and APOBEC3F localize to mRNA processing bodies. PLoS Pathog *2*, e41.

Wickens, M., Bernstein, D.S., Kimble, J., and Parker, R. (2002). A PUF family portrait: 3'UTR regulation as a way of life. Trends Genet *18*, 150-157.

Wiegand, H.L., Doehle, B.P., Bogerd, H.P., and Cullen, B.R. (2004). A second human antiretroviral factor, APOBEC3F, is suppressed by the HIV-1 and HIV-2 Vif proteins. EMBO J *23*, 2451-2458.

Wilson, J.A., Zhang, C., Huys, A., and Richardson, C.D. (2011). Human Ago2 is required for efficient microRNA 122 regulation of hepatitis C virus RNA accumulation and translation. J Virol *85*, 2342-2350.

Wu, X., Li, Y., Crise, B., and Burgess, S.M. (2003). Transcription start regions in the human genome are favored targets for MLV integration. Science *300*, 1749-1751.

Wu, Y., and Marsh, J.W. (2001). Selective transcription and modulation of resting T cell activity by preintegrated HIV DNA. Science *293*, 1503-1506.

Xu, X.N., Laffert, B., Screaton, G.R., Kraft, M., Wolf, D., Kolanus, W., Mongkolsapay, J., McMichael, A.J., and Baur, A.S. (1999). Induction of Fas ligand expression by HIV involves the interaction of Nef with the T cell receptor zeta chain. J Exp Med *189*, 1489-1496.

Yamashita, M., and Emerman, M. (2005). The cell cycle independence of HIV infections is not determined by known karyophilic viral elements. PLoS Pathog *1*, e18.

Yamashita, M., Perez, O., Hope, T.J., and Emerman, M. (2007). Evidence for direct involvement of the capsid protein in HIV infection of nondividing cells. PLoS Pathog *3*, 1502-1510.

Yan, K.S., Yan, S., Farooq, A., Han, A., Zeng, L., and Zhou, M.M. (2003). Structure and conserved RNA binding of the PAZ domain. Nature *426*, 468-474.

Yan, N., Regalado-Magdos, A.D., Stiggelbout, B., Lee-Kirsch, M.A., and Lieberman, J. (2010). The cytosolic exonuclease TREX1 inhibits the innate immune response to human immunodeficiency virus type 1. Nat Immunol *11*, 1005-1013.

Yang, N., and Kazazian, H.H., Jr. (2006). L1 retrotransposition is suppressed by endogenously encoded small interfering RNAs in human cultured cells. Nat Struct Mol Biol *13*, 763-771.

Yang, Z., Jakymiw, A., Wood, M.R., Eystathioy, T., Rubin, R.L., Fritzler, M.J., and Chan, E.K. (2004). GW182 is critical for the stability of GW bodies expressed during the cell cycle and cell proliferation. J Cell Sci *117*, 5567-5578.

Yedavalli, V.S., Neuveut, C., Chi, Y.H., Kleiman, L., and Jeang, K.T. (2004). Requirement of DDX3 DEAD box RNA helicase for HIV-1 Rev-RRE export function. Cell *119*, 381-392.

Yeung, M.L., Bennasser, Y., Myers, T.G., Jiang, G., Benkirane, M., and Jeang, K.T. (2005). Changes in microRNA expression profiles in HIV-1-transfected human cells. Retrovirology *2*, 81.

Yeung, M.L., Houzet, L., Yedavalli, V.S., and Jeang, K.T. (2009). A genome-wide short hairpin RNA screening of jurkat T-cells for human proteins contributing to productive HIV-1 replication. J Biol Chem *284*, 19463-19473.

Yi, R., Qin, Y., Macara, I.G., and Cullen, B.R. (2003). Exportin-5 mediates the nuclear export of pre-microRNAs and short hairpin RNAs. Genes Dev *17*, 3011-3016.

Yu, J.H., Yang, W.H., Gulick, T., Bloch, K.D., and Bloch, D.B. (2005). Ge-1 is a central component of the mammalian cytoplasmic mRNA processing body. RNA *11*, 1795-1802.

Yu, Q., Chen, D., Konig, R., Mariani, R., Unutmaz, D., and Landau, N.R. (2004a). APOBEC3B and APOBEC3C are potent inhibitors of simian immunodeficiency virus replication. J Biol Chem *279*, 53379-53386.

Yu, Q., Konig, R., Pillai, S., Chiles, K., Kearney, M., Palmer, S., Richman, D., Coffin, J.M., and Landau, N.R. (2004b). Single-strand specificity of APOBEC3G accounts for minus-strand deamination of the HIV genome. Nat Struct Mol Biol *11*, 435-442.

Yu, X., Yu, Y., Liu, B., Luo, K., Kong, W., Mao, P., and Yu, X.F. (2003). Induction of APOBEC3G ubiquitination and degradation by an HIV-1 Vif-Cul5-SCF complex. Science *302*, 1056-1060.

Zekri, L., Huntzinger, E., Heimstadt, S., and Izaurralde, E. (2009). The silencing domain of GW182 interacts with PABPC1 to promote translational repression and degradation of microRNA targets and is required for target release. Mol Cell Biol *29*, 6220-6231.

Zennou, V., and Bieniasz, P.D. (2006). Comparative analysis of the antiretroviral activity of APOBEC3G and APOBEC3F from primates. Virology *349*, 31-40.

Zennou, V., Perez-Caballero, D., Gottlinger, H., and Bieniasz, P.D. (2004). APOBEC3G incorporation into human immunodeficiency virus type 1 particles. J Virol *78*, 12058-12061.

Zennou, V., Petit, C., Guetard, D., Nerhbass, U., Montagnier, L., and Charneau, P. (2000). HIV-1 genome nuclear import is mediated by a central DNA flap. Cell *101*, 173-185.

Zhang, F., Wilson, S.J., Landford, W.C., Virgen, B., Gregory, D., Johnson, M.C., Munch, J., Kirchhoff, F., Bieniasz, P.D., and Hatziioannou, T. (2009). Nef proteins from simian immunodeficiency viruses are tetherin antagonists. Cell Host Microbe *6*, 54-67.

Zhang, H., Yang, B., Pomerantz, R.J., Zhang, C., Arunachalam, S.C., and Gao, L. (2003). The cytidine deaminase CEM15 induces hypermutation in newly synthesized HIV-1 DNA. Nature *424*, 94-98.

Zhang, W., Wagner, B.J., Ehrenman, K., Schaefer, A.W., DeMaria, C.T., Crater, D., DeHaven, K., Long, L., and Brewer, G. (1993). Purification, characterization, and cDNA cloning of an AU-rich element RNA-binding protein, AUF1. Mol Cell Biol *13*, 7652-7665.

Zheng, D., Chen, C.Y., and Shyu, A.B. (2011). Unraveling regulation and new components of human P-bodies through a protein interaction framework and experimental validation. RNA *17*, 1619-1634.

Zheng, D., Ezzeddine, N., Chen, C.Y., Zhu, W., He, X., and Shyu, A.B. (2008). Deadenylation is prerequisite for P-body formation and mRNA decay in mammalian cells. J Cell Biol *182*, 89-101.

Zheng, Y.H., Irwin, D., Kurosu, T., Tokunaga, K., Sata, T., and Peterlin, B.M. (2004). Human APOBEC3F is another host factor that blocks human immunodeficiency virus type 1 replication. J Virol *78*, 6073-6076.

Zhou, H., Xu, M., Huang, Q., Gates, A.T., Zhang, X.D., Castle, J.C., Stec, E., Ferrer, M., Strulovici, B., Hazuda, D.J.*, et al.* (2008). Genome-scale RNAi screen for host factors required for HIV replication. Cell Host Microbe *4*, 495-504.

Zhou, L., Sokolskaja, E., Jolly, C., James, W., Cowley, S.A., and Fassati, A. (2011). Transportin 3 Promotes a Nuclear Maturation Step Required for Efficient HIV-1 Integration. PLoS Pathog *7*, e1002194.

Zhu, Y., Chen, G., Lv, F., Wang, X., Ji, X., Xu, Y., Sun, J., Wu, L., Zheng, Y.T., and Gao, G. (2011). Zinc-finger antiviral protein inhibits HIV-1 infection by selectively targeting multiply spliced viral mRNAs for degradation. Proc Natl Acad Sci U S A.

Zielonka, J., Bravo, I.G., Marino, D., Conrad, E., Perkovic, M., Battenberg, M., Cichutek, K., and Munk, C. (2009). Restriction of equine infectious anemia virus by equine APOBEC3 cytidine deaminases. J Virol *83*, 7547-7559.

Zimmerman, E.S., Sherman, M.P., Blackett, J.L., Neidleman, J.A., Kreis, C., Mundt, P., Williams, S.A., Warmerdam, M., Kahn, J., Hecht, F.M.*, et al.* (2006). Human immunodeficiency virus type 1 Vpr induces DNA replication stress in vitro and in vivo. J Virol *80*, 10407-10418.

Zipprich, J.T., Bhattacharyya, S., Mathys, H., and Filipowicz, W. (2009). Importance of the C-terminal domain of the human GW182 protein TNRC6C for translational repression. RNA *15*, 781-793.

APPENDIX

Name	Sequence	Vector	Gene	Restriction Site
Opp24	GATCGGATCCATGTACTCGGGAGCCGG	pCMV4.HA	Ago2	BamH1 (3')
Opp25	GATCTCTAGAAGCAAAGTACATGGTGC	pCMV4.HA	Ago2	Xba1 (5')
Opp26	GATCGAATTCATGGAAGCGGGACCCTC	KT7/HB18	Ago1	EcoR1 (3')
Opp27	GATCCTGCAGTCAAGCGAAGTACATGGT GC	KT7/HB18	Ago1	Xho1 (5')
Opp28	GATCGAATTCATGTACTCGGGAGCCGGC CCCG	KT7/HB18	Ago2	EcoR1 (3')
Opp29	GATCGTCGACTCAAGCAAAGTACATGGT GC	KT7/HB18	Ago2	Sal1 (5')
Opp48	GATCGAATTCATGTACTCGGGAGCCGGC CCCG	pCMV2B-Cherry	Ago2	EcoR1 (3')
Opp49	GATCGTCGACTCAAGCAAAGTACATGGT GC	pCMV2B-Cherry	Ago2	Sal1 (5')
Opp71	GATCAAGCTATGGTGAGCAAGGGCGAG GAGC	pCMV4.HA	GFP	HindIII (3')
Opp72	GATCTCTAGACTTGTACAGCTCGTCCAT GCCG	pCMV4.HA	GFP	Xba1 (5')
Opp89	GATCCTCGAGTTAAGGTTTCTCATCTTCT AC	pCMS28-YFP	DDX6 (wt, dms)	Xho1 (5')
Opp90	CTGGTAGGGATATCTTAGCT**GCA**GCA**GC** **C**AATGGAACAGGCAAGAGCGG		DDX6-A	(3')
Opp91	CCGCTCTTGCCTGTTCCATT**GGC**TGC**TG** **C**AGCTAAGATATCCCTACCAG		DDX6-A	(5')
Opp92	GATCTGTTTACCCGA**GCA**ATTGATATAC AAGC		DDX6-B	(3')
Opp93	GCTTGTATATCAA**TTG**CTCGGGTAAACA GATC		DDX6-B	(5')
Opp135	GATCAAGCTTACCATGGCTCTGTTAACA GCCG	pCMV4.HA	A3H	HindIII (3')
Opp136	GATCTCTAGACTGCTTTATCCTCTCAAG	pCMV4.HA	A3H	Xba1 (5')
Opp181	GATCGCGGCCGCAGCACGGCCAGAACA GAGAAC	pCMS28-YFP	DDX6 (wt, dms)	Not1 (3')
Opp185	GATCCTCGAGTCAGTTTTCCTGATTCTG	pNG72	A3G	Xho1 (5')
Opp190	GATCCCTATCTCCATCGTATTGGA**CAA**T CAGGT CGCTTTGGTCATCTTG		DDX6-C	(3')
Opp191	GATCCAAGATGACCAAAGCGACCTGA**TT** **G**TCCAAT ACGATGGAGATAGG		DDX6-C	(5')
Opp194	GATCAAGCTTATGAGCACGGCCAGAACA GAG	pCMV4.HA	DDX6 (wt, dms)	HindIII (3')
Opp195	GATCTCTAGAAGGTTTCTCATCTTCTACA GG	pCMV4.HA	DDX6 (wt, dms)	Xba1 (5')
Opp199	GATCACCGGTACATGGAGTGTATTATGA CCCATC	pCMS309	Vif	Age1 (3')
Opp200	GATCGAATTCTTATTATGGCTTCCACTCC TG	pCMS309	Vif	EcoR1 (5')
Opp201	GATCCACATGGAAAAGATTAGTA**TAATA** **G**CATATGTTATTTCAAGG	NL43	Δ*vif*	
Opp202	GATCCCTTGAAATATACATATG**CTATTA** TACTAATCT TTTCCATGTG	NL43	Δ*vif*	

Opp203	GATCAAGCTT**CTATTA**CACGGCGATCTTTCCGCCCTTC	pCMV4.HA	Luc + STOP	HindIII (5')
Opp222	GATCAAGCTTATGGAAGACGCCAAAAACATAAAG	p3xFLAG	Luc	HindIII (3')
Opp223	GATCGGATCCTTACACGGCGATCTTTCCGCCCTTC	p3xFLAG	Luc	BamH1 (5')
Opp224	GATCGGATCCTTAAGGTTTCTCATCTTCTAC	p3xFLAG	DDX6	HindIII (3')
Opp233	GATCGAATTCATGAAGCCTCACTTCAGAAAC	pNG72	A3G	EcoR1 (3')

Mutations and insertions are highlighted in bold